IMPROVEMENT OF PHOTOSYNTHESIS THROUGH PHOTOPROTECTION IN WHEAT AND RICE

CHUAN CHING FOO

BSc Biotechnology, Monash University

MSc Crop Improvement, University of Nottingham

Thesis submitted to the University of Nottingham for the degree of Doctor of Philosophy

December 2019

Abstract

Photosynthesis is the light-driven process fundamental to life. Although widely studied, this process is still not well understood and there is a need to address the gap in the photosynthetic response of crop canopies towards the fluctuating light environment. Wheat and rice are the top two important cereal crops feeding the global population. The manipulation of a Photosystem II subunit S photoprotective gene, *PsbS*, in these crops would allow further understanding of how they respond to the canopy light environment in terms of non-photochemical quenching (NPQ). Spring wheat (cv 'Fielder') was transformed successfully to overexpress rice *PsbS* (Os01g64960). However, they failed to maintain the phenotype to T_2 generation and no wheat plant homozygous for rice *PsbS* was obtained for further studies. Wheat canopy NPQ studies were made on a subset of genetically diverse (PSTails) wheat population. NPQ capacity and variations were greater at the bottom of the wheat canopy. In the screening of large wheat populations, a new parameter $NPQ_{(T)}$ proved useful as $NPQ_{(T)}$ midday measurements correlated negatively to total radiation use efficiency and biomass, and to some extent, correlated positively to grain yield. NPQ and its protective ability were studied at a rice canopy scale using established rice (cv 'Kaybonnet') *PsbS* overexpressor and RNAi lines. *PsbS* levels in rice can be overexpressed to benefit the crop canopies by reducing the risk of photoinactivation. Consistent with the results from wheat canopy study, the bottom of rice canopies also showed higher NPQ capacity and phototolerance. *PsbS* is known to play a photoprotective role but was recently suggested to control stomatal pore opening in tobacco (Głowacka *et al.*, 2018). An experiment carried out under controlled environment showed that *PsbS* is not involved in stomatal regulation. However, there was some evidence that under a mild water deficit, rice

overexpressing *PsbS* have slightly improved water use efficiency. Another study using nitrogen-fixing bacteria in rice (cv ‘Valencia) showed that under no nitrogen treatment, there was some indication of improved photosynthesis (not significant). It was the first time that a 100% colonization of rice seedlings with Gd was observed.

Publications

S., Hubbart. I.R.A., Smillie, M., Heatley, R., Swarup, **C.C., Foo**, L., Zhao and E.H., Murchie (2018). Enhanced thylakoid photoprotection can increase yield and canopy radiation use efficiency in rice. *Communications Biology*, **1**(1), pp. 22.

Dedication

I would like to dedicate this thesis my late grandmother. You left me a lifetime lesson on how a woman can also be strong and independent yet kind and selfless. I miss you.

Acknowledgment

This PhD journey is not the easiest and I would not have come this far without the help and support of many. It is a pleasure to have the chance to acknowledge and thank them here. Foremost, I am forever grateful to Prof. Erik Murchie for allowing me to complete this PhD under his guidance, encouragement and support; including securing scholarship and financial aid.

Thank you to Alex and Lorna for their comments on my thesis drafts. My sincere thanks to Murchie group, Plant Science & South Lab technical teams and SB Glasshouse team. They have definitely made things easier for me throughout my PhD! I am extremely grateful to the University of Nottingham for awarding me the Vice-Chancellor's Scholarship for Research Excellence (International). Without the scholarship, this PhD will not be possible.

I am blessed to have my ever-supportive family, believing and reassuring me that I can pursue this PhD. Thank you for always keeping me in check and making sure I am happy with what I am doing. Last but not least, I would like to extend my gratitude and thanks to my awesome possum friends. Thank you for the hugs, support and encouraging words when I am lost and feeling down, especially during the writing period.

Table of Contents

Abstract i

Publications iii

Dedication iv

Abbreviations xii

Table of Figures xv

Table of Tables xxviii

Table of Equations xxxi

Chapter 1 Introduction 1

1.1 Feeding the world 1

1.2 Global wheat and rice productions 5

1.3 Photosynthesis in plants 7

1.3.1 Overview 7

1.3.2 Chloroplasts 8

1.3.3 Light and dark reactions 11

1.3.4 Photorespiration in plants 12

1.3.5 Photoinhibition 14

1.3.6 Photoprotective mechanisms in plants 17

1.3.7 Non-photochemical quenching (NPQ) 20

1.3.8 Xanthophyll cycle in plants 21

1.3.9 *PsbS* in plants 23

1.4 Using chlorophyll fluorescence in assessing plant physiology quantitatively 25

1.4.1 Photosynthetic Units (PSU) 25

1.4.2 Chlorophyll fluorescence in plants 26

1.4.3 Chlorophyll fluorescence yield parameters 26

1.5 Improving photosynthesis in plants 28

1.5.1 Target sites of improving photosynthesis 30
1.5.2 Dynamic photosynthesis 33
1.5.3 Using biostimulants to enhance plants 34
1.6 Objectives of the thesis 36
Chapter 2 Assessing Non-Photochemical Quenching (NPQ) Capacity of Transgenic Spring Wheat Overexpressing Rice *PsbS* Transgene 39
2.1 Abstract 40
2.2 Introduction 41
2.3 Materials and methods 44
2.3.1 Plant material 44
2.3.1.1 Gene cloning and wheat transformation 44
2.3.1.2 Selection of putative *PsbS* transformant lines at T_0 generation 48
2.3.1.3 Selection for homozygous *PsbS* transformant lines at T_1 and T_2 generations 49
2.3.2 Plant growth and maintenance: University of Nottingham 51
2.3.3 Characterisation of the *PsbS* transformant lines: University of Nottingham 52
2.3.3.1 Molecular analysis for confirmation of presence of transgene and gene copy number 52
2.3.3.1.1 gDNA extraction 52
2.3.3.1.2 Polymerase chain reaction (PCR) amplification of rice *PsbS* gene 52
2.3.3.1.3 Gel electrophoresis analysis 54
2.3.3.2 Non-photochemical quenching (NPQ) characterisation of the T_1 plants 54
2.3.4 Statistical analysis 55
2.4 Results 55

2.4.1 Physiological characterisation T_o generation *PsbS* transformant lines 55
2.4.2 NPQ expression and gene copy number of the rice transgene in the T_o generation *PsbS* transformant lines 60
2.4.3 Selection of homozygous *PsbS* transformant lines from T_1 generation of CW10_17 and CW10_23 61
2.4.4 Screening for homozygous *PsbS* transformant lines in T_2 generation 67
2.5 Discussion 69
2.6 Summary 71
Supplementary Material 72
Chapter 3 Investigating non-photochemical quenching dynamics and radiation use efficiency in wheat canopies in the field 76
3.1 Abstract 77
3.2 Introduction 78
3.3 Materials and methods 81
3.3.1 Plant material 81
3.3.2 Physiological measurements 83
3.3.2.1 Chlorophyll fluorescence and gas exchange measurements 84
3.3.2.2 Rapid $NPQ_{(T)}$ measurements 85
3.3.3 Statistical analysis 86
3.4 Results 86
3.4.1 Light environment in the canopy 86
3.4.2 Chlorophyll fluorescence and gas exchange 89
3.4.3 Non-photochemical quenching measured under ambient light ($NPQ_{(T)}$) as a screening tool 95
3.5 Discussion 103

3.6 Summary 107

Chapter 4 Canopy architecture and protective energy dissipation in rice canopy with altered levels of *PsbS* 110

4.1 Abstract 111

4.2 Introduction 112

4.3 Materials and methods 116

4.3.1 Plant material, experimental design and plant maintenance 116

4.3.2 Physiological Measurements 117

4.3.2.1 Plant physiological data 117

4.3.2.2 Chlorophyll fluorescence measurements 117

4.3.2.2.1 Theory behind pNPQ protocol 121

4.3.3 Canopy imaging, reconstruction and ray tracing 122

4.3.4 Modelling 123

4.3.5 Statistical analysis 124

4.4 Results 124

4.4.1 Canopy architecture 124

4.5 Discussion 136

4.6 Summary 139

Supplementary Material 140

Chapter 5 Overexpression of *PsbS* could Improve Water Use Efficiency (WUE) in Rice 153

5.1 Abstract 154

5.2 Introduction 155

5.3 Materials and methods 159

5.3.1 Plant material 159

5.3.2 Growth conditions 159

5.3.3 Water restriction regime 160

5.3.4 Chlorophyll fluorescence and gas exchange 161

5.3.5 Relative water content (RWC) 162
5.3.6 Statistical analysis 163
5.4 Results 163
5.4.1 Comparison between rice overexpressing *PsbS* (OE99) and wildtype (WT) rice 163
5.4.2 Comparison between rice overexpressing *PsbS* (OE74 and OE99) and wildtype (WT) rice under water deficit 167
5.5 Discussion 170
5.6 Summary 172
Supplementary material 173
Chapter 6 Improving Photosynthesis in Rice Using Nitrogen-Fixing Bacteria 176
6.1 Abstract 177
6.2 Introduction 178
6.2.1 Importance of nitrogen 178
6.2.2 Nitrogen-fixing bacteria 180
6.2.3 *Gluconacetobacter diaztrophicus* (Gd) in crops 182
6.3 Materials and methods 185
6.3.1 Plant material 185
6.3.2 Plant growth conditions 186
6.3.3 Seed inoculation with Gd 186
6.3.4 Nitrogen treatment 187
6.3.5 Experimental design 187
6.3.6 *Gluconacetobacter diazotrophicus* (Gd) colonization analysis 188
6.3.7 Experimental measurements 189
6.3.7.1 Physiological measurements 189
6.3.7.2 Chlorophyll fluorescence and gas exchange measurements

..... 190
6.3.7.3 Dry weights 190
6.3.8 Statistical analysis 191
6.4 Results 191
6.4.1 Successful colonization of Gd in GdN rice seedlings 191
6.4.2 The effect of GdN and GdW at different nitrogen treatment levels 192
6.4.3 Nitrogen content of seeds 200
6.4.4 GdN treatment at no nitrogen supplementation 201
6.5 Discussion 204
6.5.1 Successful Gd colonization does not translate to yield 204
6.5.2 Photosynthesis and nitrogen fixing bacteria 206
6.5.3 The prospect of using Gd in Spanish rice 209
6.6 Summary 211
Chapter 7 General Discussion 212
7.1 Physiological studies should be made at canopy level 212
7.2 Photoprotection is a key trait in crop breeding 213
7.3 Improving non-photochemical quenching (NPQ) response outweighs cost of photoinhibition 214
7.4 Dynamic stomatal response to light at canopy level 215
7.5 Improvement of photoprotection via biological methods 216
7.6 Concluding remarks 217
References 220

Abbreviations

2-PG	2-phosphoglycolate
3D	Three dimensional
3-PGA	3-phosphoglycerate
AL	Actinic light
ANOVA	Analysis of variance
ATP	Adenosine triphosphate
CAM	Crassulacean acid metabolism
cDNA	Complementary deoxyribonucleic acid
cLAI	Cumulative leaf area index
CIMMYT	International Maize and Wheat Improvement Centre
CO_2	Carbon dioxide
CRWT	Community resource for wheat transformation
DAT	Days after transplanting
DNA	Deoxyribonucleic acid
DW	Dry weight
ET	Electron transport
FBP-ase	Fructose 1, 6-bisphosphatase
FR	Far-red light
F_v/F_m	Maximum photochemical quantum yield of PSII
FW	Fresh weight
G3P	Glyceraldehyde 3-phosphate
Gd	*Gluconacetobacter diaztrophicus*
g_s	Stomatal conductance
GS	Growth stage
IRGA	Infra-red gas analyser
LAI	Leaf area index
LED	Light-emitting diode

LHC	Light harvesting complexes
MJ	Megajoule
mRNA	messenger ribonucleic acid
N_2O	Nitrous oxide
$NADPH_2$	Nicotinamide adenine dinucleotide phosphate
nGMs	New genetic modification techniques
NIAB	National Institute of Agricultural Botany
NO_3^-	Nitrate
NPQ	Non-photochemical quenching
OE	Overexpressor
PAM	Pulse amplitude modulation
PAR	Photosynthetically active radiation
PCR	Polymerase chain reaction
PEPc	Phosphoenolpyruvate carboxylase
PGPR	Plant growth promoting Rhizobacteria
pNPQ	Protective non-photochemical quenching
PPFD	Photosynthetic photon flux density
ppm	Parts per million
PsbS	Photosystem II subunit S
PSI	Photosystem I
PSII	Photosystem II
PSU	Photosynthetic unit
Q_A	Primary quinone acceptor
qP	Photochemical quenching
qRT-PCR	Quantitative real time polymerase chain reaction
qP_d	Coefficient of photochemistry in the dark
RC	Reaction centres
RCII	Reaction centres of Photosystem II

RNA	Ribonucleic acid
RNAi	RNA interference
ROS	Reactive oxygen species
RT-PCR	Reverse transcriptase-polymerase chain reaction
Rubisco	Ribulose 1,5-biphosphate carboxylase/oxygenase
RuBP	Ribulose-1,5-biphosphate
RUE	Radiation use efficiency
RWC	Relative water content
SBP-ase	Sedoheptulose-1, 7-bisphosphatase
SP	Saturating pulse
TBE	Tris-Borate-EDTA
TIC	Translocon on the inner chloroplast membrane
TK	Transketolase
TOC	Translocon on the outer chloroplast membrane
TW	Turgid weight
VDE	Violaxanthin de-epoxidase
WT	Wildtype
WUE	Water use efficiency
WUE_i	Intrinsic water use efficiency
ZE	Zeaxanthin epoxidase
ΦPSII	Quantum yield of Photosystem II

Table of Figures

Figure 1-1. The rate of population growth and global population growth trend and forecast (Ourworldindata, 2019a; United Nations, 2019). 2

Figure 1-2. A general overview of global land used for food production (Ourworldindata, 2019b). 3

Figure 1-3. The crop losses due to dry weather resulted in reduced cereal production (orange line) and could threaten the availability of cereal (yellow dashed line). The global cereal inventories (grey bars, right axis) have also been forecasted to reduce (FAO, 2019). 4

Figure 1-4. A highly schematic diagram of the light-driven photosynthesis in plants showing the principle of interaction between thylakoid and stroma (Yamori, 2015). 7

Figure 1-5. Structure of a chloroplast (Nature, 2010). 8

Figure 1-6. A schematic diagram of the major photosynthetic processes within the chloroplast of a typical C3 plant (Yamori and Shikanai, 2016). 9

Figure 1-7. (A) Under normal light level, LHCII function to harvest light energy to allow photosynthesis to take place. (B) At saturating light level, LHCII would switch into quenching mode to remove the excess light energy, thereby preventing photodamage (Barros and Kühlbrandt, 2009). 10

Figure 1-8. (**A**) An illustration of the principle of photoprotection whereby the light absorbed for photosynthesis exceeds a threshold and results in excess excitation energy that needs to be removed to protect the plant from damage. (**B**) An illustration depicting the varying effect of photoinhibition on the quantum yield and light-saturated photosynthetic rate (A_{max}) Note: A dashed line was used to illustrate the severe photoinhibition as photoinhibition is not necessarily due to a reduction in A_{max} (Murchie and Niyogi, 2011). 15

Figure 1-9. A chart of photoprotection molecular to leaf levels (Takahashi and Badger, 2011). 17

Figure 1-10. A diagram showing the different states contributing to NPQ (Malnoë, 2018). 20

Figure 1-11. A schematic diagram of the reversible xanthophyll cycle dependant on light levels (Adapted from Demmig-Adams, Gilmore and Adams, 1996). 22

Figure 1-12. A schematic of the electron flow (blue arrows) and proton flux (brown arrows) in the thylakoid membrane leading to acidification of the thylakoid lumen. This resulted in the activation of the violaxanthin de-epoxidase (VDE) and protonation of *PsbS*, triggering the formation of qE (Harbinson, 2012; Zaks *et al.*, 2012). 24

Figure 1-13. Plot showing the idealistic plant state: having the ability to maximize productivity yet be able to counter the photoinhibitory effects (Hubbart *et al.*, 2012). 25

Figure 1-14. Chlorophyll fluorescence yield parameters used during modulated fluorescence whereby a dark-adapted leaf is exposed to different light treatments (Murchie and Lawson, 2013)..... 27

Figure 1-15. A wheat canopy model succinctly identifying the physiological traits relating grain yield and biomass. Biomass could be expressed as a function of radiation use efficiency (RUE) and light interception ($I_{incident}$) throughout the whole canopy (Furbank, Quick and Sirault, 2015). 31

Figure 1-16. (a) Plants do not respond instantaneously to environmental conditions resulting in a loss of productivity. (b) This showed an ideal situation where plants could track and respond to environmental changes immediately (Ruban, 2017a). 33

Figure 2-1. An overview of gene cloning and wheat transformation carried out by Dr. R. Swarup (University of Nottingham, UK) and NIAB, Cambridge respectively. 45

Figure 2-2. Final gene construct employed in transformation of wheat using Gateway cloning. 46

Figure 2-3. Rice *PsbS* gene (Os*PsbS*) was inserted between *EcoRI*, flanked by specific attL recombination sites (attL1 and attL2) cloned into pCR8. 46

Figure 2-4. Non-photochemical quenching (NPQ) capacity was significantly higher in the T_0 generation *PsbS* overexpressors (white bars) compared to

the control (grey bars) plants (t(19) = 2.01, P = 0.030). The numbers above each bar show the corresponding rice *PsbS* transgene copy number of each transformed line. The lines marked with asterisk (*) were used in T_1 generation experiment (Foo, 2014). 56

Figure 2-5. A comparison of the F_v/F_m values of T_0 generation wheat plants overexpressing rice *PsbS* with **(A)** maximum carbon assimilation, A_{max} and **(B)** non-photochemical quenching, NPQ. Control plants were included in the plots as $_X$. Regression analysis using GenStat (VSN International Ltd., Hemel Hempstead, UK) was applied (Foo, 2014). 58

Figure 2-6. A comparison of the stomatal conductance (g_s) of T_0 generation wheat plants overexpressing rice *PsbS* with **(A)** maximum carbon assimilation, A_{max} and **(B)** non-photochemical quenching, NPQ. Control plants were included in the plots as $_X$. Regression analysis using GenStat (VSN International Ltd., Hemel Hempstead, UK) was applied (Foo, 2014). 58

Figure 2-7. A correlation of the non-photochemical quenching, NPQ, of T_0 generation wheat plants overexpressing rice *PsbS* with maximum carbon assimilation, A_{max}. Control plants were included in the plots as $_X$. Regression analysis using GenStat (VSN International Ltd., Hemel Hempstead, UK) was applied (Foo, 2014). 59

Figure 2-8. A selective comparison of the chlorophyll fluorescence parameters, quantum efficiency of the Photosystem II, ΦPSII and the parameter denoting “openness” of the reaction centers, photochemical quenching, qP against maximum carbon assimilation, A_{max} (**A** and **C** respectively) and non-photochemical quenching, NPQ (**B** and **D** respectively). Control plants were included in the plots as $_X$. Regression analysis using GenStat (VSN International Ltd., Hemel Hempstead, UK) was applied (Foo, 2014). 59

Figure 2-9.A plot between NPQ capacity and minimum number of rice *PsbS* transgene copy in the *PsbS* transformant lines. Control plants were included in the plot as $_X$. T-test using GenStat (VSN International Ltd., Hemel Hempstead, UK) was applied (Foo, 2014). 60

Figure 2-10. A colour-coded diagram of the qRT-PCR results of T_1 generation of CW10_17 (B) and CW10_23 (A). All germinated plantlets leaf gDNA were

sent for qRT-PCR analysis. “Empty” refers to seeds that did not germinate. Plants with ambiguous qRT-PCR and/or PCR analyses results (strikethrough) were discarded. Boxes left uncoloured refers to plants that are confirmed to be heterozygous. Purple colour coded boxes refer to plants with no transgene detected (Azygous), green colour boxes coded for plants that are possibly homozygous for rice *PsbS* transgene (two gene copy number), red colour boxes are plants with at least one rice *PsbS* transgene present. For T_1 of CW10_17, B-25, B-47 and B-57 (lettered in red) were found to have one transgene only. Blue and yellow lettered refer to plants with three or more than four transgene copies respectively. 63

Figure 2-11. PCR results on a screen of the T_1 generation *PsbS* transformant line CW10_23. Gel electrophoresis run of PCR products using rice primers (*PSBS*-F and NOST-Rev) with expected band size of 1046bp. From left to right: **L**: HyperLadder™ (Bioline, London, UK) 1kB DNA ladder, **1**: A-6, **2**: A-27, **3**: A-11, **4**: A-13, **5**: A-22, **6**: A-20, **7**: A-10, **8**: A-8, **9**: A-18, **10**: A-12, **11**: A-26, **12**: A-30, **13**: A-31, **14**: A-1 and **15**: Plasmid containing rice *PsbS* gene. 64

Figure 2-12. T_1 generation *PsbS* transformant line, CW10_23 showed presence of rice *PsbS* gene that was not present in ayzgous controls. Gel electrophoresis run of PCR products using rice primers (RP6 and RP7) with expected band size of 530bp. From left to right: **1**: Plasmid containing rice *PsbS* gene, **2**: Rice (Nipponbare) gDNA, **L**: HyperLadder™ (Bioline, London, UK) 1kB DNA ladder **3**: A-27, **4**: A-13, **5**: A-8, **6**: A-26, **7**: A-30 and **8**: A-1. .. 65

Figure 2-13. A comparison of the average NPQ (n=3) between azygous control (grey bars) and homozygous (black bars) plants of T_1 generation of *PsbS* transformed line, CW10_23. Error bars showed the standard deviation between the last three NPQ values. No statistical difference was observed. 65

Figure 3-1. Camas sowing system involved two subplots within a plot. Each plot is 400 cm long and 160 cm wide. Within each 80 cm subplot, plants are tightly sown in two rows 20 cm apart from one another leaving a 30 cm gap on the outer sides. Each plot is 100 cm apart from one another from either side. 83

Figure 3-2. A simple two-dimensional illustration of the side view of a canopy.

The canopy was divided into two layers based on the midpoint of its height. 'A' is the point at the top of the canopy, 'B' is the mid-point of the canopy while 'C' is the bottom of the canopy which corresponds to ground level. 84

Figure 3-3. The average light intensity measured using a ceptometer (Decagon Devices, Washington, USA) at points A, B and C (Figure 3-2) of the canopy for Lines 1 to 4 (Table 3-1) over three days. The right inset magnified the differences between the light intensity at Point B and Point C of the canopy. The error bars showed standard error of mean amongst the replicates over three days (n=9). Significant differences at 5% are denoted by alphabets a, b etc..... 87

Figure 3-4. A comparison of light intensity measured at the leaf measurement points at the **(A)** top and **(B)** bottom layers of the canopies for Lines 1 to 4 (Table 3-1). The measurements were made using MultiSpeQ (PhotoSynQ, Michigan, USA). The error bars showed standard error of mean amongst the replicates over three days (n=9). Significant differences are denoted by alphabets a, b etc..... 88

Figure 3-5. A comparison of the **(A)** fractional interception, F and **(B)** maximum quantum efficiency, F_v/F_m values at the top (white) and bottom (black) of the canopies for Lines 1 to 4 (Table 3-1). The error bars showed standard error of mean for measurements over three days (n=9). Significant differences are denoted by alphabets a, b etc..... 89

Figure 3-6. Plots of **(A)** carbon dioxide assimilation rate (A), **(B)** stomatal conductance (g_s) and **(C)** non-photochemical quenching (NPQ) of the top and bottom of the canopies for Lines 1 to 4 (Table 3-1) induced at 1800µmol $m^{-2}s^{-1}$ for fifteen minutes followed by 100µmol $m^{-2}s^{-1}$ for five minutes. Measurements for gas exchange were logged every 10 seconds and fluorescence measurements were logged every minute. Solid lines represent the measurements on top of the canopy whereas dashed lines represent the measurements made on the bottom of the canopy. The error bars denote the standard error of mean between the replicates (n=3). 90

Figure 3-7. The averages of the **(A)** maximum carbon assimilation rate (A_{max}), **(B)** quantum efficiency of PSII (ΦPSII) and **(C)** the parameter denoting the "openness" of the reaction centres, photochemical quenching (qP) between

Lines 1 to 4 (Table 3-1) at the top (white) and bottom (black) of the canopies after 15 minutes induction at 1800µmol $m^{-2}s^{-1}$ (left) and 5 minutes relaxation at 100µmol $m^{-2}s^{-1}$ (right). The error bars showed standard error of mean for the replicates (n=3). Significant differences are denoted by alphabets a, b etc. 92

Figure 3-8. The **(A)** carbon assimilation rate (A) recovery and **(B)** non-photochemical quenching (NPQ) recovery of the top and bottom of the canopies for Lines 1 to 4 (Table 3-1) after light intensity was reduced from 1800µmol $m^{-2}s^{-1}$ to 100µmol $m^{-2}s^{-1}$. Values have been normalized against the final value at 1800µmol $m^{-2}s^{-1}$. Measurements for gas exchange was logged every 10 seconds and fluorescence measurements was logged every minute. Solid lines represent the measurements on top of the canopy whereas dashed lines represent the measurements made on the bottom of the canopy. The error bars denote the standard error of mean between the replicates (n=3). 94

Figure 3-9. The averages of the non-photochemical quenching, NPQ **(A)** induction half-time and **(B)** relaxation half-time for the top (white) and bottom (black) of the canopies for Lines 1 to 4 (Table 3-1). NPQ induction and relaxation data was fitted to an exponential model using MATLAB (Mathworks, version 2019b). The error bars denote the standard error of mean between the replicates (n=3). The significance differences are denoted with the alphabets a, b etc. 95

Figure 3-10. The average of the **(A**) non-photochemical quenching, NPQ capacity measured under constant light (1800µ$m^{-2}s^{-1}$) and the **(B)** NPQ measured under ambient light in the field, $NPQ_{(T)}$ at the top (white) and bottom (black) canopy layers of Lines 1 to 4 (Table 3-1). The error bars for NPQ capacity denote the standard error of mean between the replicates (n=3) whereas the error bars for $NPQ_{(T)}$ denote the standard error of mean between the replicates over three days of measurements (n=9). The significance differences are denoted with the alphabets a, b etc. 96

Figure 3-11. A correlation between the NPQ measured under constant light (1800µ$m^{-2}s^{-1}$) and $NPQ_{(T)}$ measured under ambient light in the field at the top (black dots) and the bottom (white dots) canopy layers for all the 20 lines tabulated in Table 3-1. Regression analysis (Genstat, VSN International Ltd.,

Hemel Hempstead, UK) on the data showed no significant correlation between NPQ and $NPQ_{(T)}$. 97

Figure 3-12. A correlation between the light intensity measured and the $NPQ_{(T)}$ measurements made using the MultiSpeQ (PhotosynQ, Michigan, USA) at the **(A)** top canopy layer and **(B)** bottom canopy layer for all the 20 lines tabulated in Table 3-1. Regression analysis (Genstat, VSN International Ltd., Hemel Hempstead, UK) on the data showed a significant correlation of $NPQ_{(T)}$ to light at top canopy layer but not the bottom canopy layer. 98

Figure 3-13. A selective presentation of the averages of the chlorophyll fluorescence data measured using MultiSpeQ (PhotosynQ, Michigan, USA); **(A**) quantum efficiency of PSII (ΦPSII), **(B)** ratio of incoming light directed to non-photochemical quenching (ΦNPQ), **(C)** maximum efficiency of PSII photochemistry in light given all reaction centres were open (F_v'/F_m') and **(D)** photochemical quenching (qP) at the top (white) and bottom (black) canopy layers of Lines 1 to 4 (Table 3-1) measured under field ambient midday light conditions. The error bars denote the standard error of mean between the measurements (n=9). The significance differences are denoted with the alphabets a, b etc..... 99

Figure 3-14. A correlation between the radiation use efficiencies (RUE) on 2016/7 crop cycle and rate of induction (**A**, **B** and **C**) and relaxation (**D**, **E** and **F**) of non-photochemical quenching (NPQ) at the top canopy layer; **(A)**, **(D)** RUE recorded from initiation of booting to 7-days post anthesis (RUE1; Table 3-1), **(B)**, **(E)** during grain filling (RUE2; Table 3-1) and **(C)**, **(D)** total RUE recorded during the whole crop cycle (RUET; Table 3-1). Regression analysis (Genstat, VSN International Ltd., Hemel Hempstead, UK) on the data set showed no correlation between rate of NPQ relaxation and RUEs. 100

Figure 3-15. A correlation between the radiation use efficiencies (RUE) on 2016/7 crop cycle and non-photochemical quenching measured under ambient light ($NPQ_{(T)}$); **(A)** RUE recorded from initiation of booting to 7-days post anthesis (RUE1; Table 3-1), **(B)** during grain filling (RUE2; Table 3-1) and **(C)** total RUE recorded during the whole crop cycle (RUET; Table 3-1). Regression analysis (Genstat, VSN International Ltd., Hemel Hempstead, UK) showed significance between $NPT_{(T)}$ and RUET only..... 101

Figure 3-16. A correlation between the non-photochemical quenching measured under ambient light conditions ($NPQ_{(T)}$) and **(A)** Yield of the respective lines from crop cycle 2016/7 (Table 3-1) and **(B)** maximum carbon assimilation (A_{max}) at the top canopy layer. Regression analysis (Genstat, VSN International Ltd., Hemel Hempstead, UK) showed marginal significance between $NPT_{(T)}$ and yield only..... 101

Figure 3-17. A correlation between the non-photochemical quenching measured under ambient light conditions ($NPQ_{(T)}$) and **(A)** Biomass of the respective lines from crop cycle 2017/8 and **(B)** total RUE recorded during the whole crop cycle of 2017/8 (RUET) at the top canopy layer. Regression analysis (Genstat, VSN International Ltd., Hemel Hempstead, UK) showed significant correlations between $NPT_{(T)}$ and biomass and RUET..... 102

Figure 4-1. Example scheme of induction of chlorophyll fluorescence programme with an eight-step actinic light (AL) routine made on a Junior-PAM (Heinz Walz GmbH, Effeltrich, Germany). For a detailed explanation of the routine development, see Ruban and Belgio (2014). **Inset**: The gradually increasing AL routine induces photoinactivation which can be readily observed as a divergence between $F_o'_{act.}$ and $F_o'_{calc.}$ and be seen as a decrease in the qP_d parameter..... 120

Figure 4-2. Fractional interception, F was measured within the plots of rice overexpressing *PsbS* (OE), rice with downregulated *PsbS* (RNAi) and wildtype (WT) at the three growth stages (GS) at GS1, GS2 and GS3. At GS1, F was measured for the whole canopy as one (grey). At GS2 and GS3, F was measured at the top layer (white) and bottom layer (black) of the canopies. Error bars denote the standard error between the plots (n=4). Significant differences are denoted by alphabets a, b etc..... 125

Figure 4-3. The **(A)** tiller number and **(B)** plant height in cm recorded for rice overexpressing *PsbS* (OE), rice with downregulated *PsbS* (RNAi) and wildtype (WT) at the three growth stages (GS) at GS1 (white), GS2 (grey) and GS3 (black). Five plants per plot were sampled. Error bars denote the standard error between the plots (n=4). Significant differences are denoted by alphabets a, b etc..... 126

Figure 4-4. Dry weights of three plants per plot were measured for for rice

overexpressing *PsbS* (OE), rice with downregulated *PsbS* (RNAi) and wildtype (WT) at GS2 (grey) and GS3 (black). Error bars denote the standard error between the plots (n=4). Significant differences are denoted by alphabets a, b etc..... 126

Figure 4-5. **(A)** The modelled cumulative leaf area index (cLAI); the area of leaf material (or mesh area) per unit ground as a function of the height from the top of the canopy between rice overexpressing *PsbS* (OE; black solid line), rice with downregulated *PsbS* (RNAi; black dashed line) and wildtype (WT; grey solid line) at GS1, GS2 and GS3. The steepness of the curve indicates how much leaf material is present at each layer. **(B)** The reconstructed 3D canopies of WT, OE and RNAi rice lines at GS1, GS2 and GS3 following the imaging methodology described. Main figure shows the side-on view whilst the inset shows the top-down view. 127

Figure 4-6. A selective comparison of maximum carbon assimilation (Amax), stomatal conductance (gs) and non-photochemical quenching (NPQ) measured at 2000 µmol $m^{-2}s^{-1}$ at the top (white) and bottom (black) of the canopies of rice overexpressing *PsbS* (OE), rice with downregulated *PsbS* (RNAi) and wildtype (WT). Data from the three growth stages (GS), GS1, GS2 and GS3 are shown. Error bars denote the standard error between the plots (n=4). Significant differences at 5% based on ANOVA are denoted by alphabets a, b, c etc. 129

Figure 4-7. F_v/F_m values were measured at the top (white) and bottom (black) of the canopies of rice overexpressing *PsbS* (OE), rice with downregulated *PsbS* (RNAi) and wildtype (WT) at the three growth stages (GS), GS1, GS2 and GS3. Five plants per plot per canopy layer were sampled. Error bars denote the standard error between the plots (n=4). Significant differences at 5% based on ANOVA are denoted by alphabets a, b, c etc. 130

Figure 4-8. A comparison of the light intensities at which 50% of the leaves within the canopy layer are photoinactivated ($I_{50\%}$) at the top (white) and bottom (black) layers of the canopy of rice overexpressing *PsbS* (OE), rice with downregulated *PsbS* (RNAi) and wildtype (WT) at the three growth stages (GS), GS1, GS2 and GS3. No statistical analysis was possible. 131

Figure 4-9. Frequency of PPFD values according to the fraction of surface

received at 1200H in the **A**, **C** and **E**. top of the canopy and **B**, **D** and **F.** bottom of the canopy where **A**, **B**. GS1, **C**, **D**. GS2 and **E**, **F**. GS3 and the grey, green and red arrows indicate the average PPFD value for wildtype (WT) rice, rice overexpressing *PsbS* (OE) and rice with downregulated *PsbS* (RNAi) respectively. 133

Figure 4-10. Light tolerance curves combined with canopy light profiles enable the visualisation of photoinactivation according to canopy position **A**. Wildtype (WT) rice population tolerance curve calculated using the fluorescence routine on the Junior-PAM (Heinz Walz GmbH, Effeltrich, Germany). The photosynthetic photon flux density (PPFD) ranges that correspond to a set photoinactivation per canopy top or bottom are colour coded. **B**. A representative reconstructed WT rice canopy at GS3 with a single plant in bold. Right panel showed the colour-coded photoinactivation range. **C**. The PPFD during the course of a day at four representative canopy positions, with the height of each canopy location from the ground given the top left corner of each graph, calculated using ray-tracing technique. 134

Figure 4-11. Profiles of photoinactivation (expressed in terms of percentage of leaves photoinactivated) according to the total surface area of leaves (expressed in percentage) and the time of the day (between 0600H and 1800H) for rice overexpressing *PsbS* (OE), rice with downregulated *PsbS* (RNAi) and wildtype (WT) at the three growth stages (GS), GS1, GS2 and GS3. 135

Figure 5-1. A hypothetical schematic of a proposed Q_A redox signal initiated from plastoquinone derived signalling resulting in control of stomata when there *PsbS* expression is modified (Głowacka *et al.*, 2018). 157

Figure 5-2. A comparison of the induction (left) and light response (right) curves for **(A)** non-photochemical quenching (NPQ), **(B)** carbon assimilation rate (A) and **(C)** stomatal conductance (g_s) between rice line overexpressing *PsbS* (OE99; black ●) and the wildtype rice (WT; white △) at 1500 µmol $m^{-2}s^{-1}$ for fifteen minutes followed by 200 µmol $m^{-2}s^{-1}$ for six minutes. Gas exchange measurements were logged every 30 seconds but data at every minute is shown. Error bars denote the standard error of mean between replicates (n=4). No significant differences in NPQ, carbon assimilation rate and stomatal conductance were observed between OE99 and WT. 165

Figure 5-3. A comparison of the **(A)** photochemical quenching (qP) and **(B)** Q_A redox state (1-qL) between rice line overexpressing *PsbS* (OE99; black ●) and the wildtype rice (WT; white △) at 1500 µmol $m^{-2}s^{-1}$ for fifteen minutes followed by 200 µmol $m^{-2}s^{-1}$ for six minutes. Error bars denote the standard error of mean between replicates (n=8). Statistical significance is denoted with alphabets a, b etc. 166

Figure 5-4. **(A)** A comparison of the intrinsic water use efficiency (WUE_i) between rice line overexpressing *PsbS* (OE99; black ●) and the wildtype rice (WT; white △) at 1500 µmol $m^{-2}s^{-1}$ for fifteen minutes followed by 200 µmol $m^{-2}s^{-1}$ for six minutes. Error bars denote the standard error of mean between replicates (n=8). **(B)** A comparison of the leaf relative water content (RWC) between *PsbS* overexpressor lines, OE74 and OE99 (black bars) and wildtype (WT) rice. Error bar denotes standard error of mean (three leaf discs per plant, n=6). Statistical significance is denoted with alphabets a, b etc.. 166

Figure 5-5. A comparison between **(A)** soil moisture content (SMC) measured using thetaprobe, **(B)** stomatal conductance (g_s) and **(C)** the dark-adapted quantum efficiency of Photosystem II (F_v/F_m) of the rice plants before (white bars) and after (black) stable water restriction for a minimum of three days for the first experiment. OE74 and OE99 are rice plants overexpressing *PsbS* and WT refers to wildtype Kaybonnet rice. Error bars denotes the standard error of mean (n=8). Statistical significance is denoted by alphabets a, b etc. 167

Figure 5-6. A comparison between **(A)** maximum carbon assimilation (A_{max}), **(B)** non-photochemical quenching (NPQ), **(C)** quantum yield of Photosystem II (ΦPSII), **(D)** intrinsic water use efficiency (WUE_i), **(E)** photochemical quenching (qP) and **(F)** plastoquinone redox state (Q_A redox state, =1-qL) of the rice plants before (white bars) and after (black) stable water restriction for a minimum of three days. OE74 and OE99 are rice plants overexpressing *PsbS* and WT refers to wildtype Kaybonnet rice. Error bars denotes the standard error of mean (n=8). Statistical significance is denoted by alphabets a, b etc. 169

Figure 6-1. A simple depiction of the nitrogen cycle (Vitousek *et al.*, 1997).178

Figure 6-2. A schematic diagram of the diazotrophs and their associations

with host plants (Mus *et al.*, 2016)..... 180

Figure 6-3. The principle of Gd inoculation that could be applied to all crops. This inoculant is proposed to allow the induction of Gd into host plant in an intracellular manner, replacing half of the plant's nitrogen demand (Azotic Technologies Ltd, 2018)..... 183

Figure 6-4. Each 20L tub was filled with up to the brim with standard rice compost, mixed by SB glasshouse team. Each tub was flooded with tap water and allowed to settle before sowing of treated seeds (left). Red circles showed the positioning of eight seeds in each tub (right). 188

Figure 6-5. GdN rice seedling was separated into five sections for Gd detection and analysis. Colonization of Gd was highly successful with 100% colonization of Gd bacteria in all five parts of the seedling tested..... 192

Figure 6-6. A selected comparison of the SPAD (proxy for chlorophyll content), leaf area index and dry weight per plant between GdW (white) and GdN (black) at 0%, 50% and 100% nitrogen treatments at stem elongation (week 6), booting (week 7), anthesis (week 8) and full maturity. Growth stages are noted at the top of each graph. The error bars denote the standard error between the replicates (n=5). 196

Figure 6-7. A selected comparison of the maximum photosynthetic rate (A_{max}), quantum yield of PSII (ΦPSII), photochemical quenching (qP) and electron transport rate (ETR) between GdW (white) and GdN (black) at 0%, 50% and 100% nitrogen treatments at stem elongation (week 6), booting (week 7) and anthesis (week 8). Growth stages are noted at the very top. The error bars denote the standard error between the replicates (n=5). 199

Figure 6-8. A comparison of the protein content (w/w%) between GdW (white) and GdN (black) at different nitrogen treatment levels. Protein content was converted from nitrogen content analysis based on specific (Jones) factor provided by Food and Agriculture Organization. No statistical analysis was carried out on the data. 200

Figure 6-9. A comparison of the general growth trends between GdW (white circles) and GdN (black circles) rice plants during from the Week 3 to Week 8, in terms of average leaf number, tiller number and plant height per plant and

the average SPAD value (proxy for chlorophyll content). Week 6, 7 and 8 correspond to the growth stages stem elongation, booting and anthesis respectively. Error bars show standard deviation (n=5). 201

Figure 6-10. A comparison of the average fertile shoot per plant, ear weight per plant, seed number per plant, seed weight per plant and thousand grain weight (TGW) between GdW (white) and GdN (black) rice plants, under zero nitrogen supplementation at full maturity. Error bars showed standard error between the replicates (n=5) 203

Figure 6-11. Yield increase were observed with Gd treatment and nitrogen supplementation in Vietnamese rice fields, either through direct sowing or transplanting of rice seedlings (Azotic Technologies, 2017). 208

Table of Tables

Table 1-1. Some photoprotective mechanisms found in plants (Demmig-Adams and Adams, 1996; Müller, Li and Niyogi, 2001; Külheim *et al.*, 2002; Jung and Niyogi, 2009; Ruban, 2009; Nilkens *et al.*, 2010; Murchie and Niyogi, 2011; Peter Jahns and Holzwarth, 2012; Nauš, Šmecko and Špundová, 2016)..... 19

Table 2-1. Optimized PCR protocol for the amplification of rice *PsbS* gene sequence for one reaction tube..... 53

Table 2-2. A collation of the qRT-PCR and PCR results for the T_1 generation of *PsbS* transformant wheat line CW10_17. Some qRT-PCR results are ambiguous or unsuccessful (N/A) and no PCR analysis was made on them (marked with -). PCR using *PSBS*-F and NOST-Rev is labelled as PCR1 whereas PCR using RP6 and RP7 is labelled as PCR2. ✓ and X denote the presence or absence of rice *PsbS* gene respectively and '–' denotes that no analysis was done. Shaded in grey are putative homozygous *PsbS* transformant lines and shaded in red are azygous control plants. The plant codes correspond to those in Figure 2-10..... 62

Table 2-3. A comparison of the molecular and physiological characterisation results for the T_1 generation of *PsbS* transformed line, CW10_23. Green coded lines were the lines triple confirmed to be either homozygous or azygous. qRT-PCR results showed whether the line was azygous or homozygous. PCR1 referred to PCR analysis using *PSBS*-F and NOST-Rev whereas PCR2 referred to the PCR analysis using RP6 and RP7. ✓ denotes the presence of rice *PsbS* gene, X denotes the absence of rice *PsbS* gene and – denotes that no analysis was done. The red F_v/F_m values highlighted the F_v/F_m value lower than 0.78 (cut-off point for acceptance of NPQ value). Shaded in grey are putative homozygous *PsbS* transformant lines and shaded in red are azygous control plants..... 66

Table 2-4. A summary of the number of seeds sown and subsequently sampled for qRT-PCR analysis for the T_2 generation selection of homozygous *PsbS* transformant lines based on T_0 generation parents CW10_17 and CW10_23. The number of plants based on the rice *PsbS* gene copy number is also tabulated..... 68

Table 3-1. 20 out of the 80 PSTails used in the experiment. The top four lines were selected based on 2016/7 yield category and radiation use efficiency (RUE) data. RUE1, RUE2 and RUET are the RUE recorded from initiation of booting to 7-days post anthesis, during grain filling and the total RUE recorded during the whole crop cycle respectively. Maximum photosynthesis (P_{max}) was measured during 7-days post anthesis. Unpublished confidential data provided by G Molero and C Robles (CIMMYT, Mexico). 82

Table 3-2. The P-values of the ANOVA analysis for the averages of the last three logged values of chlorophyll fluorescence and gas exchange parameters during induction phase of Lines 1 to 4 (Table 3-1; Line) at the two canopy layers (Layer). The interaction between the lines and canopy layers (Line*Layer) was also analysed. Red P-values showed significance at 5% level. Blue P-values showed significance at 10% level. 93

Table 3-3. The P-values of the ANOVA analysis for the averages of the last three logged values of chlorophyll fluorescence and gas exchange parameters during relaxation phase of Lines 1 to 4 (Table 3-1; Line) at the two canopy layers (Layer). The interaction between the lines and canopy layers (Line*Layer) was also analysed. Red P-values showed significance at 5% level. 93

Table 4-1. The individual light levels for each maximum light level setting on the Junior PAM. 119

Table 5-1. Environmental factors that affect the opening and closing of the stomatal pore. 156

Table 6-1. Summary of the P-values of the ANOVA analysis for morphological and yield parameters between Gd treated (GdN) rice plants and non-Gd treated (GdW) rice plants at both the Gd treatment (Gd) and the three nitrogen treatments at 0%, 50% and 100% of the field recommended 150kg N per hectare (nitrogen) levels at the different key growth stages (stem elongation, booting, anthesis and at full maturity). The interaction between the treatments were also analysed (Gd*Nitrogen). In cases where no measurement was made are shaded in grey. At instances where P-values (at 5% or 10%) showed significance, the significance was inconsistent between GdN and GdW throughout the growth stages. The comparison of differences

of each parameter between growth stages were significant (P<0.05)..... 194

Table 6-2. Summary of the P-values of the ANOVA analysis for chlorophyll fluorescence and gas exchange parameters between Gd treated (GdN) rice plants and non-Gd treated (GdW) rice plants at both the Gd treatment (Gd) and the three nitrogen treatments at 0%, 50% and 100% of the field recommended 150kg N per hectare (nitrogen) levels at the different key growth stages (stem elongation, booting, anthesis and at full maturity). The interaction between the treatments were also analysed (Gd*Nitrogen). At instances where P-values (at 5% or 10%) showed significance, the significance was inconsistent between GdN and GdW throughout the growth stages. The comparison of differences of each parameter between growth stages were significant (P<0.05). 198

Table of Equations

Equation 3-1: $A = g_{sc}.(C_a - C_i)$ 103

Equation 3-2: $E = g_{sw}.(W_i - W_a)$ 103

Equation 4-1: $\phi PSII = qPd.FvFm[1 + 1 - FvFm.NPQ]$ 121

Equation 4-2: $qPd = (Fm' - Fo' act.)(Fm' - Fo' calc.)$ 121

Equation 4-3: $Fo' calc. = 11Fo - 1Fm + 1Fm'$ 121

Equation 4-4: $fL = a - a - b1 + expcL - de$ 123

Equation 4-5: $Lp = c\ d - \log 1a - ba - p1/e - 1c$ 123

Equation 5-1: RWC (%) = [(FW – DW)/(TW – DW)] X 100% 163

Chapter 1 Introduction

1.1 Feeding the world

In the next few decades and beyond, global food security will remain under threat (Rosegrant and Cline, 2003). The overall annual global population growth rate is declining, but population is still expected to rise to 10.9 billion in 2100 (Figure 1-1). Analysis showed that the global population would not cease to grow without achieving replacement-level fertility rates (Gerland *et al.*, 2014) or sufficient food supply (Holt, 2014). However, there were also reports that the global population will stabilize and stop increasing by the end of the century (Lutz, Sanderson and Scherbov, 1997, 2001; Lutz *et al.*, 2014). This is apparent in the fact that the global population projection has now been revised from 11.2 billion to 10.9 billion in 2100. However, the annual population growth rate is predicted to remain at 0.1%, which is 2.5 times greater than the annual population growth rate before 1700 (United Nations, 2019). This implied that effort to improve global food security must continue (Beddington *et al.*, 2012).

It has been reported that current food production would meet the future demand of the projected 9.7 billion population in 2050 (Holt-Giménez *et al.*, 2012; Berners-Lee *et al.*, 2018). However, progress in crop yield per annum in terms of tonnes per hectare are insufficient and crop productivity is stagnating in many regions. FAO (2019) recently reported huge crop losses due to climate change resulting in constant revision of the global cereal production forecast. The dry weather had affected crop production in many parts of the world including Thailand, Japan, Australia and Kazakhstan. This resulted in a lower forecasted global cereal production (Figure 1-3).

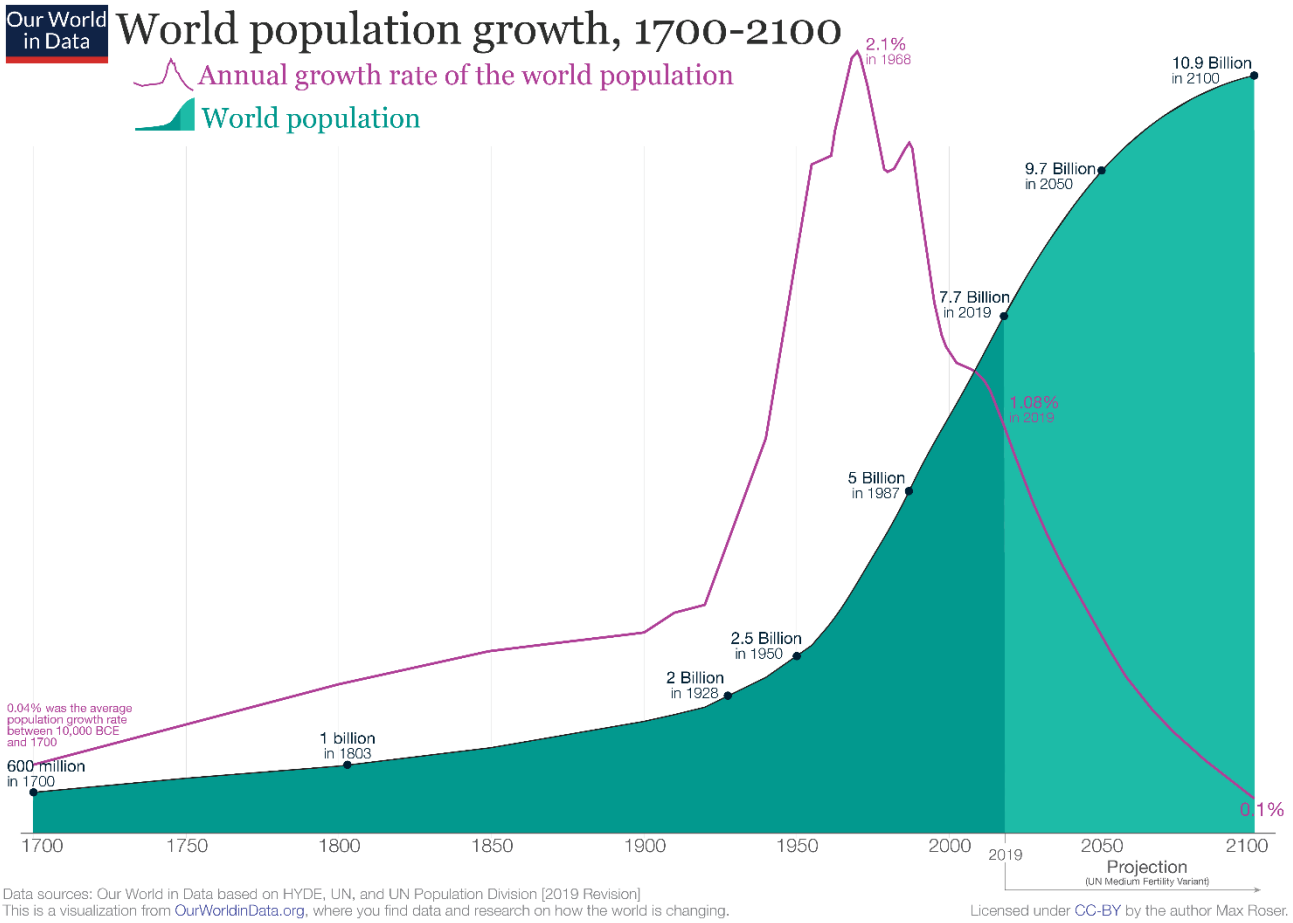


Figure 1-1. The rate of population growth and global population growth trend and forecast (Ourworldindata, 2019a; United Nations, 2019).

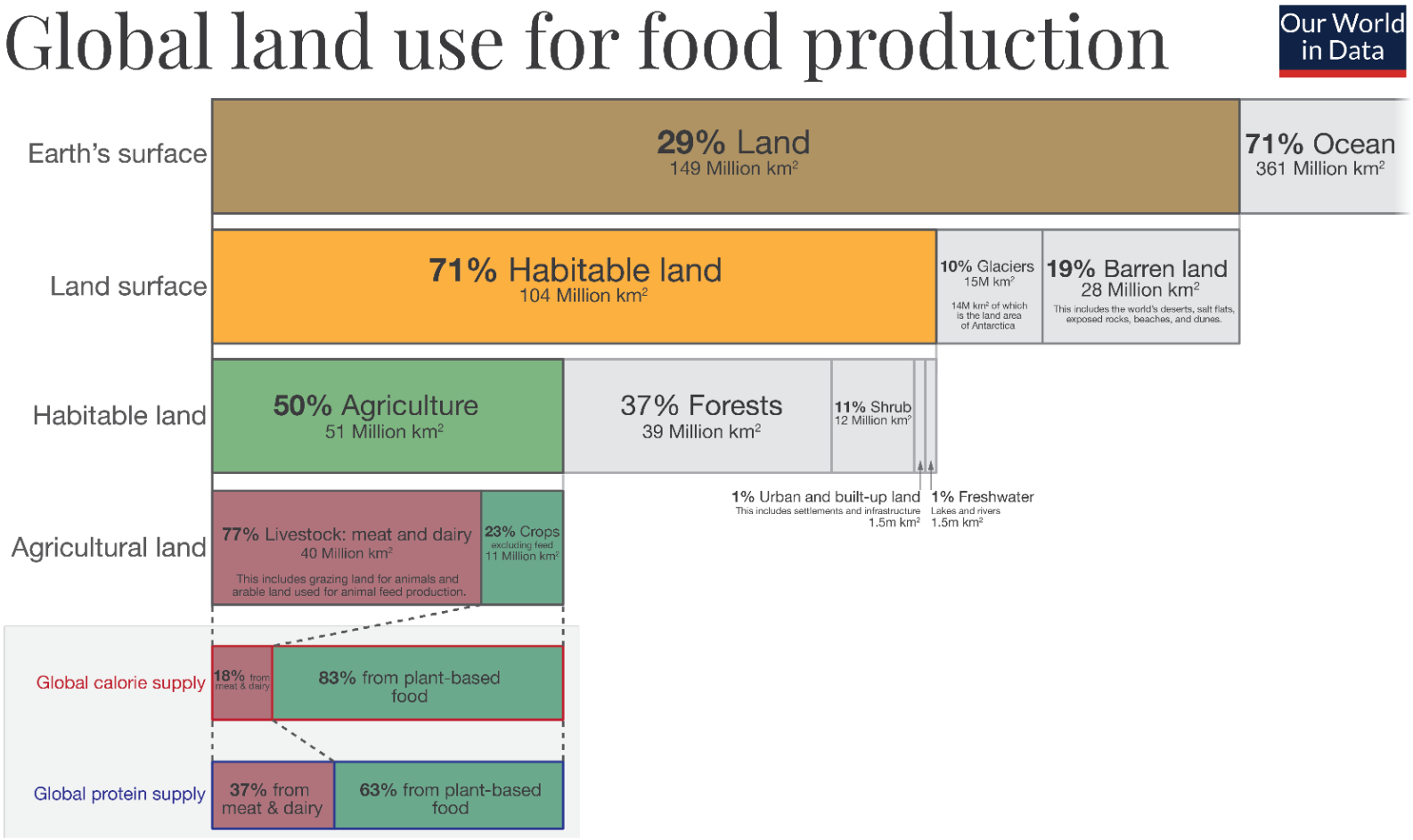


Figure 1-2. A general overview of global land used for food production (Ourworldindata, 2019b).

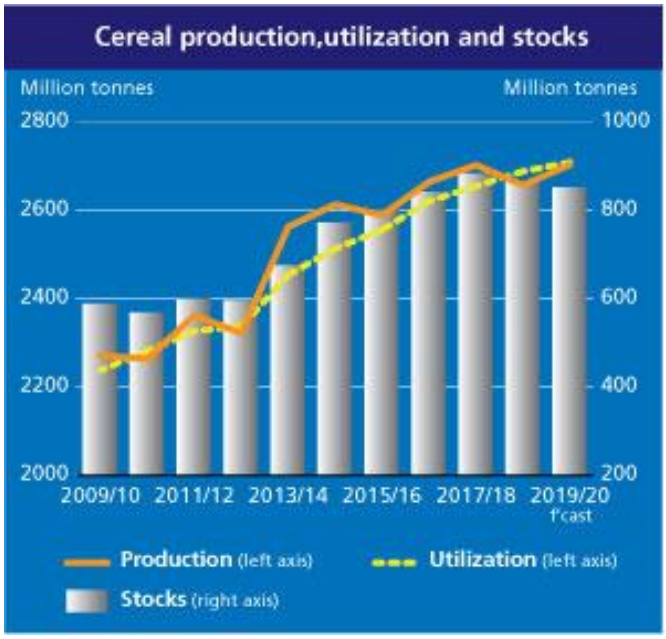


Figure 1-3. The crop losses due to dry weather resulted in reduced cereal production (orange line) and could threaten the availability of cereal (yellow dashed line). The global cereal inventories (grey bars, right axis) have also been forecasted to reduce (FAO, 2019).

Current crop productivity coupled with the threats from climate change mean more efforts should be made to not only stabilize but also to increase global food production taking into account different climate change scenarios (Edgerton, 2009; Ray *et al.*, 2012; Challinor *et al.*, 2014; Rötter, 2014; Walker *et al.*, 2016). Currently, half of the habitable lands are already occupied by agriculture (Ellis *et al.*, 2010). Although only 23% of these agricultural lands are used for cropping, they account for a significant supply of calories and protein in human diet (Figure 1-2). We cannot solely rely on re-appropriating or rehabilitating land for agriculture due to constant demand from other aspects for land use (growing population, wildlife conservation, etc). Hence, for crop yield to be improved, we must focus on raising crop productivity resulting in higher yield per land area (Ewert *et al.*, 2005).

Other than that, a plethora of issues such as pest and diseases which could potentially remove a crop species (e.g. banana, papaya, etc.), socio-

economic issues, resource competition with biofuels, urbanization, reduction in agricultural population and water scarcity also come into spotlight in terms of satisfying global food demand. It is important to continue to invest in agriculture research due to its broad and significant global impact. There is a strong argument that all efforts incorporating diverse technologies including agro-ecological approaches and biotechnological innovations must be incorporated into agriculture continuously to pre-empt global food insecurity after 2050 (Pingali and Heisey, 1999; Oerke and Dehne, 2004; Battisti and Naylor, 2009; Ericksen, Ingram and Liverman, 2009; Ray *et al.*, 2012; Challinor *et al.*, 2014; Rosenzweig *et al.*, 2014; Bagley *et al.*, 2015; Rötter *et al.*, 2015).

1.2 Global wheat and rice productions

It is expected that global food security would be achieved by having sufficient supply of the main staple food crops; namely wheat, rice and maize (Rötter *et al.*, 2015). These three cereal grains contribute to more than 50% of the global calories intake (Awika, 2011). Wheat and rice are the top two most important cereals in the human diet globally with rice mostly consumed by people directly while wheat is milled into flour and turned into pasta, bread, biscuits etc. The by-product of wheat milling is also pelleted as animal feed. Globally, wheat is a staple food, including in regions where wheat is not grown (Shewry, 2009; Shiferaw *et al.*, 2013; Mason, Jayne and Shiferaw, 2015). Wheat is also the most widely grown crop globally in terms of cropping acreage. This is attributed to the fact that wheat has a greater environmental adaptability compared to rice which can only be grown in hot and humid conditions and its distribution limited by low temperatures (Makino, 2011).

Maize is the third most widely grown cereal but differs because a substantial proportion is directed to animal feed (Awika, 2011).

A study by Ray et al. (2012) found that significant wheat and rice growing areas showed yield stagnation globally with a small percentage experiencing yield collapse. It was observed that wheat yield has increased steadily between 0.7% to 1.1% per year since 1950 (Waddington *et al.*, 1986; Lopes *et al.*, 2012; Manès *et al.*, 2012). However, since last decade, it has been observed to slow down (Aisawi *et al.*, 2015). This translated to insufficient wheat and rice production to meet the future global demands. It is often stated that cereals underwent genetic bottlenecks during domestication and breeding which may have reduced diversity.

Additionally, the key traits used for physiological breeding (e.g. harvest index, canopy structure, leaf area, leaf duration) have been optimised and may have reached their maximum biological potential (Furbank, Quick and Sirault, 2015). Cereal crops were not selected directly for high photosynthetic capability and a study in winter wheat showed that improved photosynthesis during heading resulted in improved grain yield (Xiao *et al.*, 2012). However, there is limited evidence that photosynthesis per unit leaf area has been improved by breeding but rather it has resulted in higher photosynthesis per unit land area (Hay, 1995; Murchie, Pinto and Horton, 2009; Zhou *et al.*, 2014; Furbank, Quick and Sirault, 2015; Kromdijk and Long, 2016). Leaf photosynthesis and consequently, canopy radiation use efficiency (mass accumulated per unit radiation intercepted) are great potential areas to exploit to increase biomass (Parry *et al.*, 2011; Xiao *et al.*, 2012).

1.3 Photosynthesis in plants

1.3.1 Overview

Photosynthesis is the basic biological process sustaining life on earth. This light-driven mechanism is not only of utmost importance for plant survival but also helps in removal of atmospheric carbon dioxide and replenishing atmospheric oxygen. In crops, photosynthesis is the main driver of crop productivity (Cheng and Fleming, 2009; Chmeliov *et al.*, 2016; Yamori *et al.*, 2016). Photosynthesis is defined as a light driven process by which plants fix atmospheric carbon dioxide into sugar (carbohydrates) in the plant chloroplasts, allowing the conversion or transduction of solar energy into chemical energy (Figure 1-4). It is driven by visible light within the photosynthetically active radiation (PAR) region (between 400 nm and 700 nm).

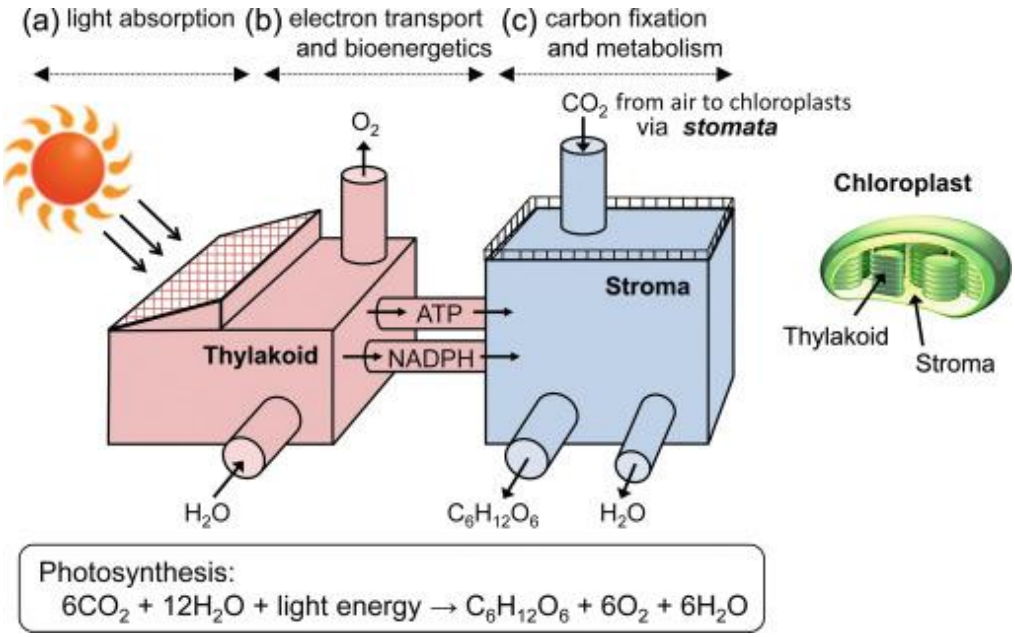


Figure 1-4. A highly schematic diagram of the light-driven photosynthesis in plants showing the principle of interaction between thylakoid and stroma (Yamori, 2015).

Within the chloroplasts, light is “harvested” in a series of redox reactions in the thylakoids, producing adenosine triphosphate (ATP) and reduced nicotinamide adenine dinucleotide phosphate ($NADPH_2$). These are fed into the Calvin-Benson cycle to power the fixation of atmospheric carbon dioxide which enter the plant through openings called stomata. The stomatal aperture is controlled by a pair of guard cells which reacts to environmental cues such as light and humidity. Hence, effective harvesting of light by the plant is crucial for maintaining efficient photosynthesis rate.

1.3.2 Chloroplasts

The photosynthetic pathway and many other assimilatory pathways are housed in the chloroplast. Amino acids, fatty acids and photosynthetic pigments are also synthesized in the chloroplasts. The chloroplast is an important organelle for the maintenance of plant growth and development. It responds dynamically to the environmental light cues. The three main parts of chloroplasts are the chloroplast envelope, stroma and thylakoid (Figure 1-5).

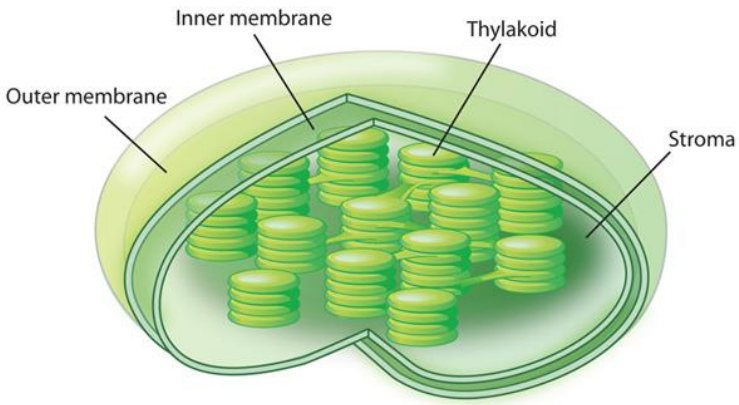


Figure 1-5. Structure of a chloroplast (Nature, 2010).

The chloroplast envelope consists of the outer membrane and the inner membrane separated by an intermembrane space. The outer membrane is

impermeable to large proteins but semi-porous allowing small molecules and ions to move freely. Large proteins travel through the double membrane via the TOC (translocon on the outer chloroplast membrane) and TIC (translocon on the inner chloroplast membrane) complexes (Soll and Schleiff, 2004; Jensen and Leister, 2014). The inner membrane encloses the stroma and grana. The stroma contains important enzymes for Calvin-Benson cycle and ions essential for photosynthesis. Grana are stacks of thylakoids linked together by stromal lamellae which keeps the integrity of the grana and allows efficient light harvesting (Anderson, 1986).

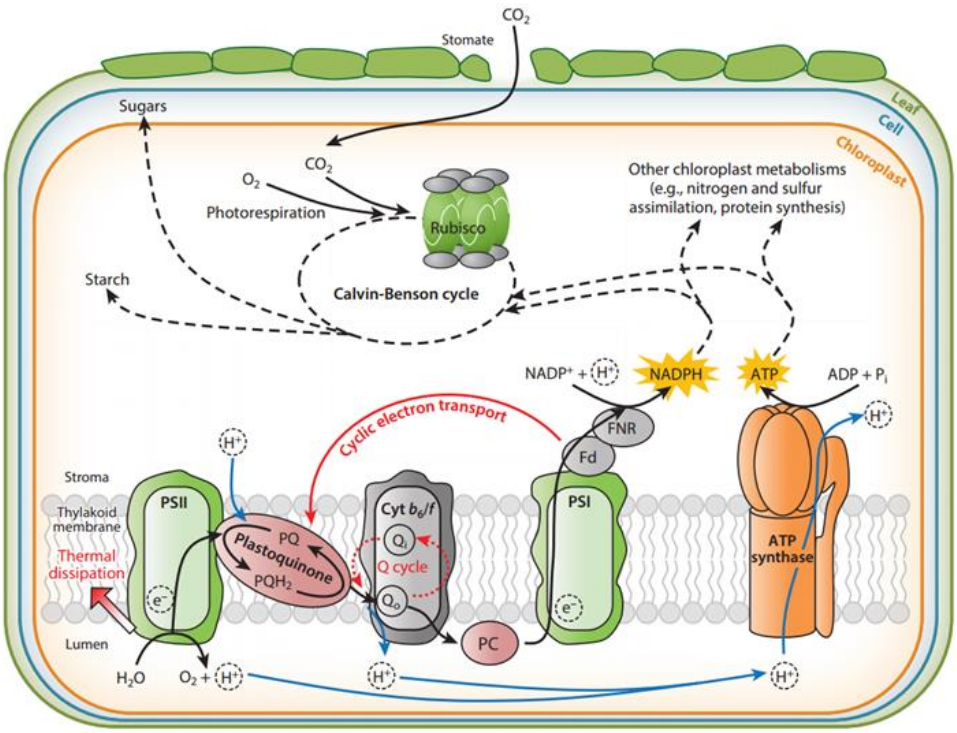


Figure 1-6. A schematic diagram of the major photosynthetic processes within the chloroplast of a typical C3 plant (Yamori and Shikanai, 2016).

The thylakoid membrane holds in place four major protein complexes; namely Photosystem I (540 kDa), Photosystem II (250 kDa), ATP synthase (520 kDa) and Cytochrome b6f complex (260 kDa) which sit within the thylakoid membrane (Figure 1-6; Kawaguchi *et al.*, 1992; Thidholm *et al.*, 2002; Yamori and Shikanai, 2016). They are involved in the transportation of electrons

across the membrane to create a proton gradient which in turn drives ATP synthesis. Of the four major complexes, Photosystem II is the smallest yet plays a large role in overall photosynthesis (Durchan, Vácha and Krieger-Liszkay, 2001; Thidholm *et al.*, 2002).

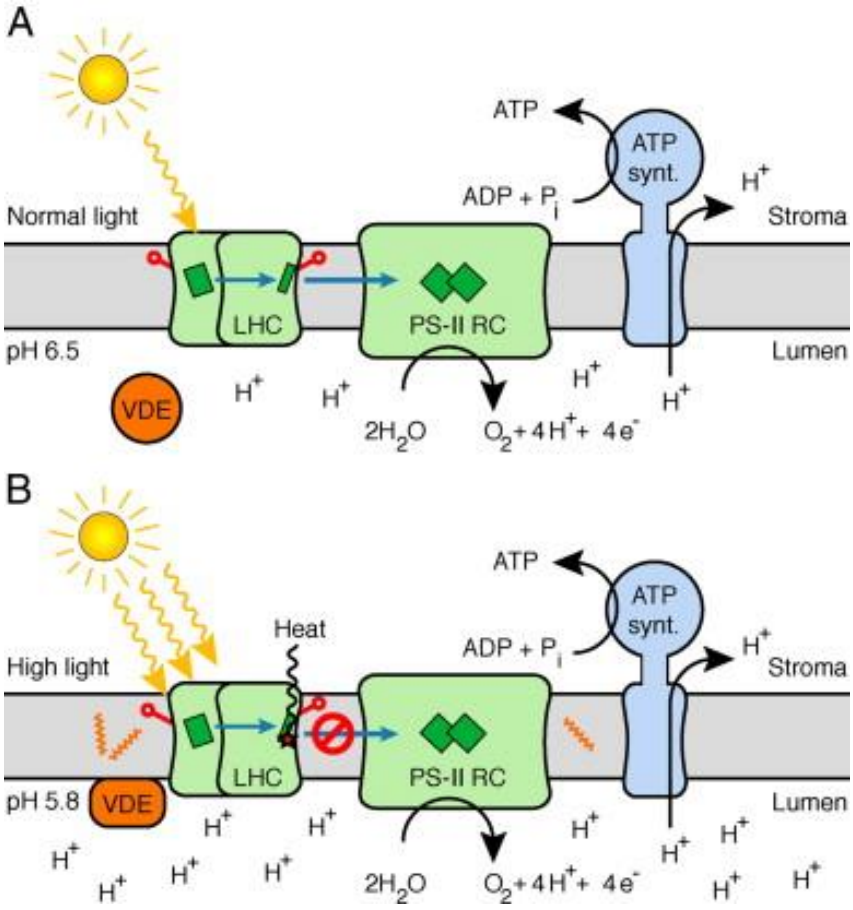


Figure 1-7. (A) Under normal light level, LHCII function to harvest light energy to allow photosynthesis to take place. (B) At saturating light level, LHCII would switch into quenching mode to remove the excess light energy, thereby preventing photodamage (Barros and Kühlbrandt, 2009).

Photosystem II is also known as the water/plastoquinone oxidoreductase as it has the ability to absorb photons and transfer the excess electrons produced from water molecule to plastoquinone (Kawaguchi *et al.*, 1992; Nelson and Yocum, 2006). This results in the proton-motive force (pmf), driving photosynthesis. The photosystems also contain light harvesting complexes (LHCs) which are spread around a reaction centre which encloses P700

chlorophyll (Photosystem I) and P680 chlorophyll (Photosystem II). The light harvesting complexes (LHCs) in the photosystems channel the excitation energy to the reaction centres for an efficient photosynthesis (Figure 1-7A). However, under saturating light conditions, Photosystem II would quench the excess electrons to prevent photodamage (Figure 1-7B; Barros and Kühlbrandt, 2009).

1.3.3 Light and dark reactions

Photosynthesis comprises of two main stages; namely the thylakoid reactions and Calvin-Benson cycle. Thylakoid reactions, or sometimes known as light reactions, refers to the electron transport (ET) chain reactions occurring within the grana, which are stacks of thylakoids. ET is a complex set of redox reactions by which harvested light (recognised as electrons) are transported across membranes to result in an electrochemical gradient facilitating photosynthesis. The light energy absorbed is used to breakdown water molecules and produce high energy molecules adenosine triphosphate (ATP) and nicotinamide-adenine dinucleotide phosphate (NADPH) and oxygen. The Calvin-Benson cycle occurs in the stroma, whereby the carbon dioxide absorbed is converted to sugar using the ATP and NADPH produced during the thylakoid reactions. Ribulose-1,5-biphosphate (RuBP) fixes one carbon dioxide to form two three-carbon molecules, 3-phosphoglycerate (3-PGA). This reaction is catalysed by the enzyme Ribulose 1,5-biphosphate carboxylase/oxygenase (Rubisco). It is then converted into two three-carbon molecules, glyceraldehyde 3-phosphate (G3P) before the substrate RuBP is regenerated in a series of reactions, G3P is removed from the Calvin cycle to synthesize hexose sugars.

1.3.4 Photorespiration in plants

Rubisco is one of the largest plant proteins which is abundant in nature but highly inefficient due to slow enzymatic activity and dual substrate specificity, resulting in energy-consuming photorespiration (Sharkey, 1985; Portis and Parry, 2007). When RuBP is oxygenated by Rubisco (instead of carboxylated), photorespiration occurs resulting in one molecule of 3-PGA and one molecule of 2-phosphoglycolate (2-PG) (Parry *et al.*, 1999; Betti *et al.*, 2016). The resulting 3-PGA will follow the metabolic pathway as described above while the 'toxic' 2-PG will be recycled through the C_2 cycle. The 2-PG cannot be utilized in the biosynthetic pathways for biosynthesis in plants and it can also inhibit proper functioning of chloroplast (Anderson, 1971). Two molecules of 2-PG are required for the recovery of one 3-PGA, with one molecule of CO_2 released as a by-product. The complex details of the C_2 cycle are reviewed by Bauwe, Hagemann and Fernie (2010). In short, although photorespiration is important for recycling of 2-PG into 3-PGA, it is a wasteful yet cost-intensive process (Gerbaud and André, 1980; Parry *et al.*, 2008; Bauwe, Hagemann and Fernie, 2010; Peterhansel and Maurino, 2011; South *et al.*, 2018).

Most plants utilize the C_3 photosynthetic pathway where carbon dioxide is directly assimilated to produce 3-PGA. Due to competition with oxygen, photorespiration in C_3 plants is unavoidable. It was not an issue during early evolutionary era where oxygen levels were negligible. Over geological timespans, increased oxygen in the atmosphere and lowered atmospheric carbon dioxide resulted in the evolutionary pressure for plants to make use of carbon dioxide efficiently in terms of photosynthesis. In the 1970s, ambient conditions (light level at 390 µmol photons.$m^{-2}s^{1}$ and 350ppm atmospheric

carbon dioxide) proved to boost photorespiration by about 25%. A study also showed that under current conditions, photorespiration resulted in a carbon loss of up to 30% (Zhu, Portis and Long, 2004). Under hot and dry conditions, photorespiration could be aggravated resulting in greater loss of plant productivity (Gerbaud and André, 1980; Tourneux and Peltier, 1995; Peterhansel and Maurino, 2011; South *et al.*, 2018).

There exist other systems such C_4 and Crassulacean acid metabolism (CAM) carbon metabolism pathways where photorespiration is reduced or eliminated. There is also a wide range of C_3-C_4 intermediate variants, which involve C_2 photosynthesis whereby the resulting carbon dioxide from photorespiration is recycled (Sage, Sage and Kocacinar, 2012). C_4 plants are capable of compartmentalizing Rubisco allowing the concentration of carbon dioxide for the production of a four-carbon molecule, oxaloacetate. This reduces the chances for oxygenation of RuBP and thus prevents photorespiration (Rawsthorne, 1992; Ehleringer and Cerling, 2002; Sage, 2004; Bauwe, Hagemann and Fernie, 2010; Peterhansel and Maurino, 2011; Sage and Stata, 2015). On the other hand, CAM plants go through dark acidification; they fix carbon at night in a similar way as C_4 plants and convert it to an organic acid. During daylight, the organic acid is broken down to release carbon dioxide. This thus results in a high carbon dioxide concentration environment around Rubisco for effective photosynthesis (Ranson and Thomas, 1960; Ting, 1985).

Despite the increase in global atmospheric CO_2, it was shown that the rate of increase is not sufficient to suppress photorespiration (Bravdo and Canvin, 1979; Betti *et al.*, 2016). However, Osmond and Bjorkman (1972) controversially suggested that photorespiration could be a major photoprotective mechanism (Guan *et al.*, 2004). Studies found that

photorespiration played a role in protecting plants from the damaging effects of photoinhibition during drought stress by acting as an electron sink (Kozaki and Takeba, 1996 - tobacco; Wingler *et al.* - barley, 1999; Haupt-Herting and Fock, 2000 - tomato; Guan *et al.*, 2004 - grapevine). However, this is difficult to determine experimentally and is not clear-cut due to the multiple photoprotective mechanisms in plants. Brestic *et al.* (1995) found photorespiration did not protect bean plants from the damaging effects of high light conditions. Similarly, Nogués and Alegre (2002) found that photorespiration did not play any key role in photoprotection in lavender and rosemary.

1.3.5 Photoinhibition

In natural field conditions, light saturation is very common and typically happens around midday. In theory, high light conditions would allow plants to photosynthesize at their maximal capacity. In fact, at increasing high light levels where excessive amount of light is absorbed, the photosynthetic apparatus can be damaged. At excessive light conditions, net photosynthesis is reduced and eventually plateaus, resulting in excessive excitation energy in pigment protein complexes (Figure 1-8A). The excess energy would ‘harm’ the reaction centres, inactivating the Photosystem II, resulting in a condition called photoinhibition (Horton, 2000; Takahashi and Badger, 2011; Matloobi, 2012). Photoinhibition is often defined as the inactivation of and subsequent repairing of the Photosystem II. When the light available in the environment surpasses the need of the plants, there would be excess excitation energy present in the chlorophyll within plant cells. If this remained in excess and unremoved, it would result in the inactivation of the Photosystem II. This

process occurs regardless of the light environment in which the plant is exposed to (Sonoike, 1996; Horton, 2000; Takahashi and Murata, 2005; Takahashi and Badger, 2011; Matloobi, 2012; Murata, Allakhverdiev and Nishiyama, 2012). However, specific conditions could change the relative rates of damage and repair, resulting in higher proportions of inactivated centres.

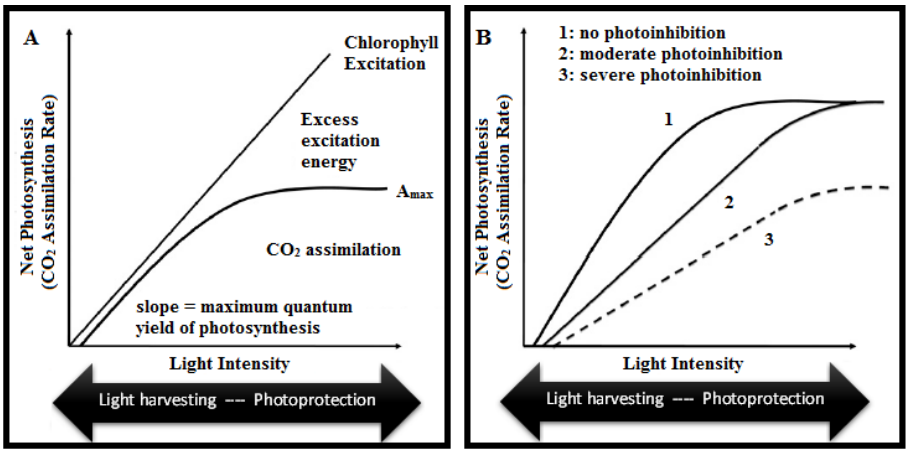


Figure 1-8. (**A**) An illustration of the principle of photoprotection whereby the light absorbed for photosynthesis exceeds a threshold and results in excess excitation energy that needs to be removed to protect the plant from damage. (**B**) An illustration depicting the varying effect of photoinhibition on the quantum yield and light-saturated photosynthetic rate (A_{max}) Note: A dashed line was used to illustrate the severe photoinhibition as photoinhibition is not necessarily due to a reduction in A_{max} (Murchie and Niyogi, 2011).

Environmental conditions such as light, temperature, water and carbon dioxide concentration etc. contribute to photoinhibition by lowering photosynthetic capacity and increasing the proportion of excess excitation energy (Figure 1-8B). Some processes such as stomatal closure or inactivation of Rubisco at high temperatures could also result in photoinhibition (Aro, Virgin and Andersson, 1993; Murchie and Niyogi, 2011; Demmig-Adams *et al.*, 2012). This constant damage is repaired by the constant breakdown and synthesis of a 32kDa protein known as D1-polypeptide (Barber and Andersson, 1992; Keren *et al.*, 1997; Niyogi, 1999).

Photoinhibition can also occur in Photosystem I due to the presence of excessive reactive oxygen species (ROS). Relative to Photosystem II, Photosystem I takes longer to recover from the damage of photoinhibition (Mellis, 1999; Sonoike, 2011; Pinnola and Bassi, 2018). ROS are usually generated in Photosystem I and Photosystem II reaction centres from the photoreduction of oxygen. Oxygen is reduced to hydrogen peroxide in a process called Mehler's reaction. Oxygen is reduced by electrons from ferredoxin of Photosystem I resulting in superoxide. Superoxide is then reduced by superoxide dismutase to form ROS, hydrogen peroxide. Hydrogen peroxide is toxic to biological systems as it can damage the proteins, lipid membrane and pigments. Hydrogen peroxide is further reduced by ascorbate peroxidase to result in the formation of water (Badger, 1985). Hence, Mehler's reaction is also known as water-water cycle. In higher plants, Mehler's reaction contributed to higher proportion of superoxide than photorespiration (Badger *et al.*, 2000).

Early studies showed that plants acclimated to low light conditions are more susceptible to photoinhibition (Barber and Andersson, 1992). The level of photoinhibition varies in both intraspecies and interspecies (Barber and Andersson, 1992). The quantum yield of carbon dioxide assimilation would definitely be affected by photoinhibition resulting in a long term damage and lowered photosynthetic efficiency (Niyogi, 1999). Hence, even with increased resources, productivity could be limited by photosynthesis if the reaction centres are impaired. Photoinhibition is not only damaging but also very costly to the plants. As such, plants require photoprotection, particularly non-photochemical quenching (NPQ) which could offer a relatively "cheaper" alternative to protect plants from excessive light.

1.3.6 Photoprotective mechanisms in plants

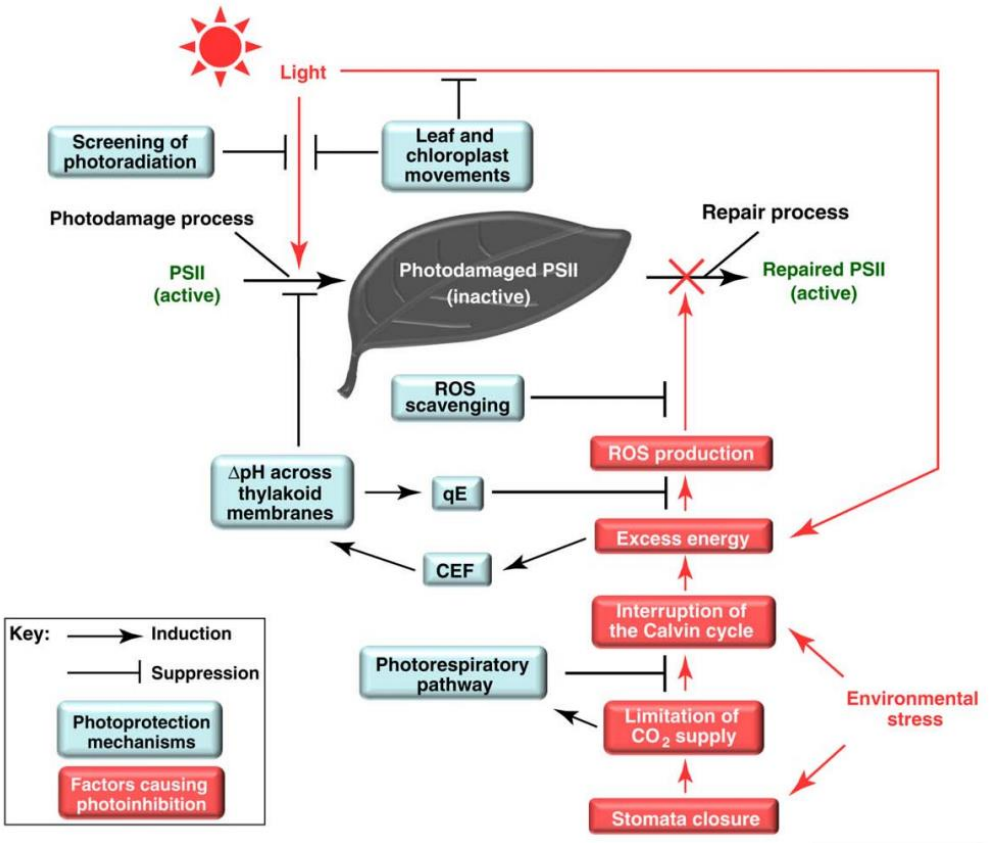


Figure 1-9. A chart of photoprotection molecular to leaf levels (Takahashi and Badger, 2011).

Plants have evolved a wide range of sophisticated protective mechanisms from cell to leaf levels (Figure 1-9). However, many of the mechanisms "avoid" light to prevent absorption of excessive light rather than removing any excessive excitation energy (Demmig-Adams and Adams, 1992; Ruban, 2009; Murchie and Niyogi, 2011; Takahashi and Badger, 2011; Murchie, 2017). Plants are immobile and appear to be physically passive when it comes to self-protection. Their leaves and stems do, to an extent, move towards light or shy away from high light conditions to adjust to their light environment and maximize the light absorbed for photosynthesis. These are rather slow and generally insufficient for crop plants grown under field conditions, especially during midday. Chloroplasts within the leaves help

strengthen the photoprotective mechanisms by movement within the mesophyll cell, to avoid high light conditions (chlorophyll fluorescence quenching due to movement is termed qM). However, they are restricted by the presence of large organelles within the cell thus making it rather inefficient (Ruban, 2009).

Photoprotection describes the adaptations that plant employs to quench excessive energy in their system under excessive light environment. Plants have various photoprotection mechanisms functioning within different timeframes (Table 1-1). It occurs at cell level and is usually initiated in the LHCs where excitation energy is concentrated (Müller, Li and Niyogi, 2001; Zhu *et al.*, 2004; Murchie and Niyogi, 2011). Due to the short lifespan of reactive singlet oxygen, photodamage is largely restricted to photosystem II only (Keren *et al.*, 1997). Hence, only Photosystem II removes any excessive excitation energy as part of the photoprotection mechanism (Ahn *et al.*, 2008; Murchie and Niyogi, 2011; Takahashi and Badger, 2011; Yamori and Shikanai, 2016).

Plants remove excitation energy via three main pathways; photosynthesis, chlorophyll fluorescence and thermal dissipation. Only thermal dissipation is considered photoprotection as the excessive electrons are removed via a harmless non-photochemical pathway, termed as non-photochemical quenching or NPQ (Maxwell and Johnson, 2000; Müller, Li and Niyogi, 2001; Murchie and Niyogi, 2011; Murchie and Lawson, 2013). Although NPQ also lowers quantum yield temporarily, it prevents the permanent damage on plants potentially resulting from photoinhibition. Hence, it is important to exploit NPQ to prevent long term damage of reactive centres. For this PhD, focus will be on NPQ as it is the major photoprotective component (Müller, Li and Niyogi, 2001; Murchie and Niyogi, 2011).

Table 1-1. Some photoprotective mechanisms found in plants (Demmig-Adams and Adams, 1996; Müller, Li and Niyogi, 2001; Külheim *et al.*, 2002; Jung and Niyogi, 2009; Ruban, 2009; Nilkens *et al.*, 2010; Murchie and Niyogi, 2011; Jahns and Holzwarth, 2012; Nauš, Šmecko and Špundová, 2016).

Photoprotection	**Response Period**	**General Mechanism**
Non-photochemical quenching (NPQ)	Seconds to hours depending on each of the components	Thermal dissipation of excess excited electrons via a non-photochemical pathway.
Chloroplast movement	Within minutes	Chloroplast relocate to avoid high light absorption. However, only protecting the photosynthetic apparatus from 10-20% of excessive energy.
D_1 protein	Hours or more	Inactivation of the Photosystem II by the degradation of damaged D_1 protein and partially disassembly of Photosystem II, followed by re-synthesis of D_1 protein and re-assembling of Photosystem II.
Photoacclimation	Days	"Constant" changing of amounts of photosynthetic components within cells to adjust to the long-term light conditions.
Photochemical pathways	Variable	Reactions that remove the excessive electrons such as photorespiration, cyclic electron transport, Mehler reaction etc.
Xanthophyll cycle (part of NPQ)	Minutes	The conversion of violaxanthin to intermediate an antheraxanthin and to zeaxanthin to help dissipate excess excitation energy. This process is reversible at light limiting conditions.

1.3.7 Non-photochemical quenching (NPQ)

NPQ is an inherent protective mechanism found in plants protecting them from any potential damage caused by over-excitation of photosystem II when exposed to high light conditions (Xiao Ping Li *et al.*, 2002; Bonente *et al.*, 2008; Kasajima *et al.*, 2011; Roach and Krieger-Liszkay, 2012). NPQ varies greatly across plants, whether it is intraspecies or interspecies and can vary from 0.5 to 3.5, with higher values indicating better photoprotection and calculated as in Chapter 2 of this thesis (Maxwell and Johnson, 2000; Jung and Niyogi, 2009; Kasajima *et al.*, 2011).

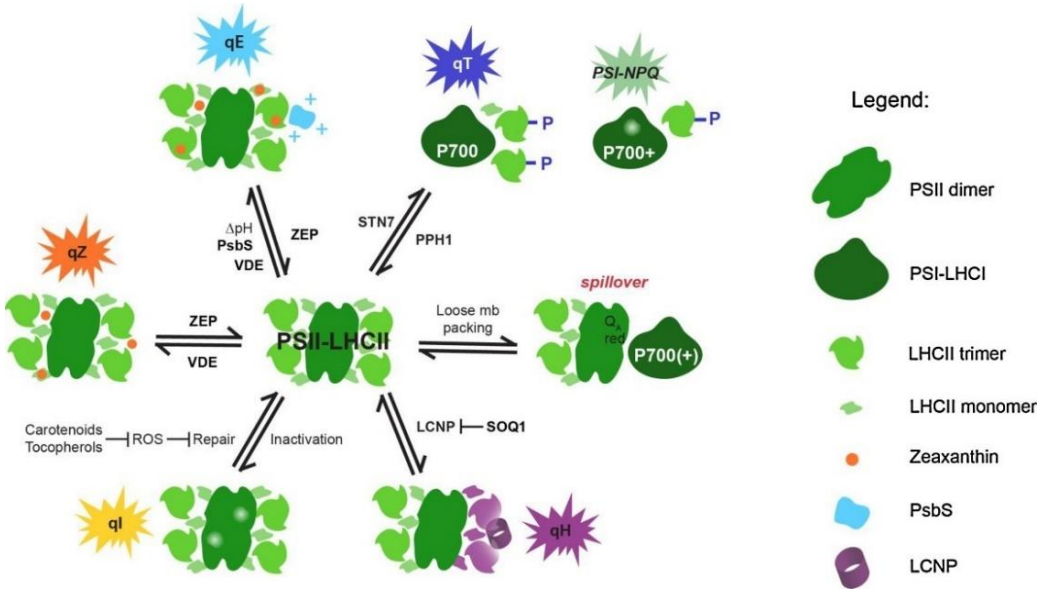


Figure 1-10. A diagram showing the different states contributing to NPQ (Malnoë, 2018).

NPQ is determined and regulated by a few components (Figure 1-10): the four major components are feedback de-excitation (qE), zeaxanthin-dependant quenching (qZ), state transitions quenching (qT) and photoinhibitory quenching (qI). These components confer photoprotection over various timeframe ranging from seconds to days. In terms of NPQ, qE and qZ contribute to protection while qI often represents damage. In terms of

timeframe, qI gives the slowest response while qE gives the fastest and most significant response *in vivo* (Li *et al.*, 2000; Müller, Li and Niyogi, 2001; Külheim *et al.*, 2002; Zulfugarov *et al.*, 2007; Nilkens *et al.*, 2010; Murchie and Niyogi, 2011; Hubbart *et al.*, 2012; Roach and Krieger-Liszkay, 2012; Ruban, Johnson and Duffy, 2012; Brooks *et al.*, 2013). Meanwhile, qT is a reduction in fluorescence when energy is re-distributed between the photosystems. It is not thought to affect NPQ measurements at saturating light levels in higher plants (Nilkens *et al.*, 2010; Malnoë, 2018).

qE is regulated by the proton gradient between thylakoid and lumen (ΔpH across thylakoid membrane), carotenoid and zeaxanthin in xanthophyll cycle and the Photosystem II subunit S photoprotective protein, *PsbS* (Krause, 1974; Horton, Wentworth and Ruban, 2005; Zulfugarov *et al.*, 2007). The rate of formation and the capacity for NPQ is under control of the protein *PsbS* and xanthophyll cycle. Both carotenoid zeaxanthin (in xanthophyll cycle) and *PsbS* protein (in Photosystem II) are inherent in plants. They are the two most well-characterized regulators of qE (Demmig *et al.*, 1987; Külheim *et al.*, 2002; Niyogi *et al.*, 2005; Johnson and Ruban, 2010, 2011; Kereiche *et al.*, 2010; Murchie and Niyogi, 2011; Goral *et al.*, 2012; Ruban, 2012; Zaks *et al.*, 2012; Harbinson, 2012; Roach and Krieger-Liszkay, 2012; Sacharz *et al.*, 2017).

1.3.8 Xanthophyll cycle in plants

The xanthophyll cycle is a light-controlled and pH-dependant reversible process whereby violaxanthin is converted to an intermediate, antheraxanthin and then to zeaxanthin (Figure 1-11). In high light, de-epoxidation will occur to

remove the excessive energy, converting violaxanthin to zeaxanthin by violaxanthin de-epoxidase (VDE). This then results in the temporary accumulation of zeaxanthin. At low light conditions, the accumulated zeaxanthin will be reconverted to violaxanthin by zeaxanthin epoxidase (Demmig-Adams and Adams, 1992, 1996; Choudhury and Behera, 2001; Harbinson, 2012).

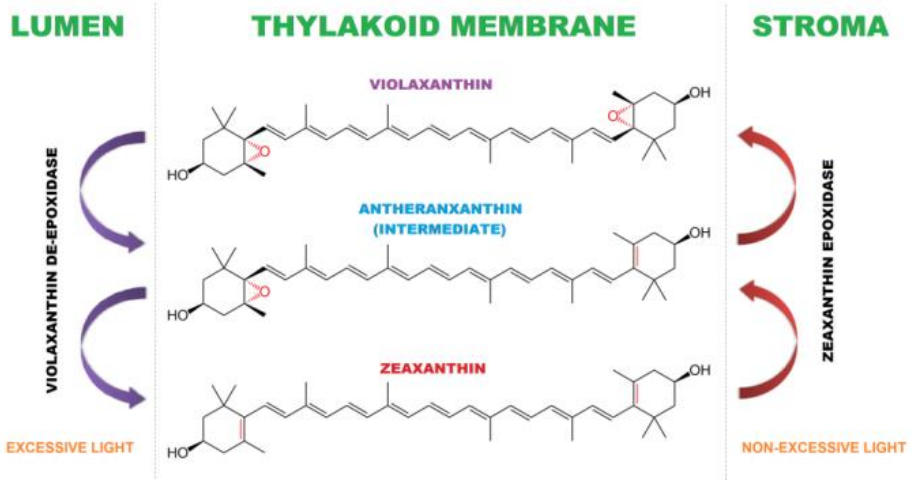


Figure 1-11. A schematic diagram of the reversible xanthophyll cycle dependant on light levels (Adapted from Demmig-Adams, Gilmore and Adams, 1996).

Roles of xanthophyll cycle in photoprotection were relatively well studied in a diverse range of plants (Hieber, Bugos and Yamamoto, 2000); particularly various algae, Arabidopsis and tobacco (Demmig-Adams, Gilmore and Adams, 1996; Niyogi, 1999; Niyogi *et al.*, 2001; Külheim *et al.*, 2002). In most cases, studies were related to violaxanthin de-epoxidase (e.g. Külheim et al. 2002) instead of zeaxanthin epoxidase. Few in-depth studies on the xanthophyll cycle in crops has been made except some on rice (Xu *et al.*, 1998, 1999, 2000; Yang *et al.*, 2013) and wheat (Tambussi *et al.*, 2002; Lu *et al.*, 2003). However, the role of xanthophyll cycle in NPQ is still highly debatable (Li *et al.*, 2000; Murchie and Niyogi, 2011). In this thesis, the focus will be placed on *PsbS*.

1.3.9 *PsbS* in plants

PsbS was first observed in spinach by Berthold *et al.* in 1981 (Kim *et al.*, 1992). It is a 22 kDa chloroplastic Photosystem II protein found in the thylakoid membrane (Ljungberg, Åkerlund and Andersson, 1986; Kim *et al.*, 1992). It is encoded by *NPQ4* gene and determines the rate and capacity of NPQ by regulating qE (Kim *et al.*, 1992; Li *et al.*, 2000). Although *PsbS* is structurally homologous to one of the LHC proteins, it does not bind to photosynthetic pigments and it is also not involved in light harvesting (Li *et al.*, 2000; Dominici *et al.*, 2002; Xiao Ping Li *et al.*, 2002). Furthermore, this highly hydrophobic protein has four instead of three transmembrane α helices (Funk *et al.*, 1994).

PsbS plays a key role in protecting plants from photodamage by inducing quick qE response (within few seconds) in fluctuating lights. *PsbS* expression level within the plant is considered a key factor to determine the extent of qE capacity of the plant, which in turn dictates the NPQ level (Li *et al.*, 2000; Xiao Ping Li *et al.*, 2002; Niyogi *et al.*, 2005; Kereiche *et al.*, 2010). This quick NPQ response is derived from its high sensitivity in high light (Thidholm *et al.*, 2002; Bergantino *et al.*, 2003). However, Johnson and Ruban (2010) suggested that *PsbS* does not modulate qE formation because plants lacking this protein can be induced to form qE. Previously, Li *et al.* (2000) suggested that *PsbS* could have acted as a binding protein which maintained the integrity of LHC resulting in the activation of qE and thus promoting quicker NPQ response. Later studies further showed that acidification of the thylakoid lumen is the key point in the activation of qE (Figure 1-12). When there is an influx of excessive electrons in the thylakoid lumen, a great pH difference between the lumen and stroma acidifies the thylakoid lumen resulting in a

structural change in thylakoid membrane which then quenches the light harvesting centres in Photosystem II (Harbinson, 2012; Zaks *et al.*, 2012).

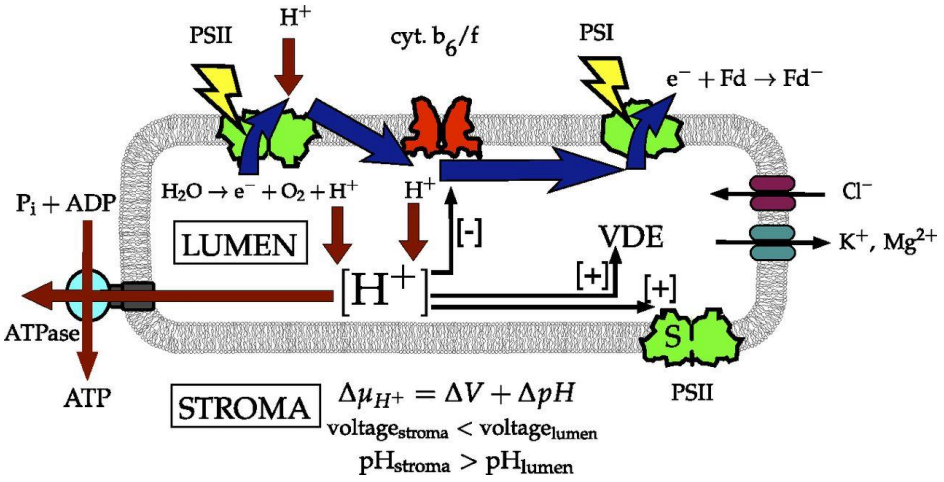


Figure 1-12. A schematic of the electron flow (blue arrows) and proton flux (brown arrows) in the thylakoid membrane leading to acidification of the thylakoid lumen. This resulted in the activation of the violaxanthin de-epoxidase (VDE) and protonation of *PsbS*, triggering the formation of qE (Harbinson, 2012; Zaks *et al.*, 2012).

NPQ studies on *Arabidopsis thaliana* showed that they were better protected from highly reactive singlet oxygen molecules in Photosystem II resulting in photodamage (Roach and Krieger-Liszkay, 2012). However, studies of *PsbS* in *Arabidopsis* are deemed not ideal and insufficient due to its small size and small NPQ capacity (Hubbart *et al.*, 2012). The *PsbS* studies were then brought to crop level (Ishida *et al.*, 2011; Kasajima *et al.*, 2011; Hubbart *et al.*, 2012, 2018; Morita *et al.*, 2013; Kromdijk *et al.*, 2016; Głowacka *et al.*, 2018). Ideally, plants should be able to function at maximum productivity yet be able to counter the increased photoinhibitory effects (Figure 1-13; Hubbart *et al.*, 2012). NPQ reduces quantum yield which can be a problem in fluctuating light environments. Therefore, it is not clear whether there existed a trade-off between photoprotection and productivity. It was only recently that empirical links were found between improved photoprotection response under fluctuating lights and enhanced resource use efficiency and improved plant

productivity (Kromdijk *et al.*, 2016; Głowacka *et al.*, 2018; Hubbart *et al.*, 2018).

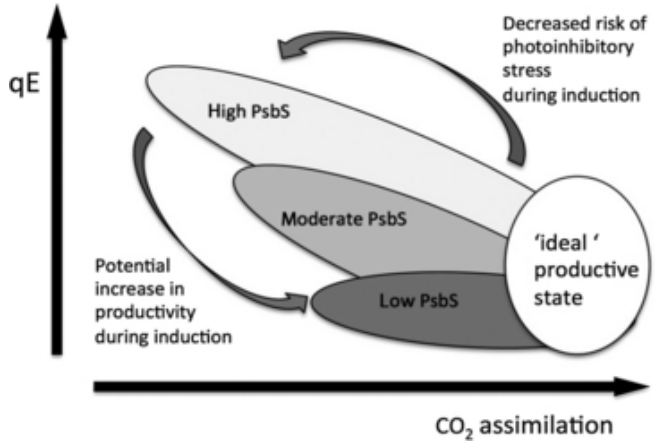


Figure 1-13. Plot showing the idealistic plant state: having the ability to maximize productivity yet be able to counter the photoinhibitory effects (Hubbart *et al.*, 2012).

1.4 Using chlorophyll fluorescence in assessing plant physiology quantitatively

1.4.1 Photosynthetic Units (PSU)

The exact molecular mechanism of light harvesting component in plant is not fully understood. Currently, there are two models as to how the photosynthetic units (PSU) are arranged and interacting within plant cells. Initially, the Photosystem II reaction centres were considered to run as a single body which is linked to a single antenna. This separate PSU was termed as the puddle model. In the other model, known as lake model, the Photosystem II reaction centres are assumed to be perfectly linked PSUs within a reservoir of antennas (Trissl, Gao and Wulf, 1993; Lazár, 1999). Quenching parameters were first studied based on the puddle model.

1.4.2 Chlorophyll fluorescence in plants

Chlorophyll fluorescence allowed in-depth plant physiology studies to be made. It is non-destructive, sensitive, fast and easy method to study photosynthesis in plants. Chlorophyll absorbs best at red and blue parts of the light spectrum. Under white light, they are observed as green while at blue light, they are observed as pink. As aforementioned, the light absorbed by chlorophyll is constant and will either be quenched during photosynthesis or dissipated as heat or re-emitted as a longer wavelength, lower energy state fluorescence. Any changes in photosynthesis or NPQ could be visualised in fluorescence. As the energy absorbed cannot be destroyed, the variability and intensity of the re-emitted chlorophyll fluorescence could then be studied. At room temperature, chlorophyll fluorescence of Photosystem I is negligible and rather constant, hence measuring the chlorophyll fluorescence re-emitted could give an insight into photosynthetic capacity and NPQ of Photosystem II. This led to the development of quenching parameters used to study plant physiology (Genty, Briantais and Baker, 1989; Lazár, 1999; Roháček, 2002; Baker, 2008; Murchie and Lawson, 2013).

1.4.3 Chlorophyll fluorescence yield parameters

Chlorophyll fluorescence measurements can be made to derive both quenched and unquenched parameters. Quenched parameters are made on dark-adapted leaves whereas unquenched parameters can be obtained from light-adapted leaves. Unquenched parameters are usually denoted the same as quenched parameter, but followed by a prime (‘) to indicate the light-adapted state (Baker, 2008; Murchie and Lawson, 2013). Figure 1-14 shows

the chlorophyll fluorescence parameters made on a dark-adapted leaf material. When a 'measuring light' of an intensity that is incapable to drive photosynthesis (non-actinic light) is projected on a dark-adapted leaf, a chlorophyll fluorescence minimum (F_o) is derived. Its equivalent in light-adapted state (F_o') is then measured after a short actinic light pulse. A far-red (FR) light can ensure a better estimate of the F_o' as it stimulates the Photosystem I to draw the electrons away from Photosystem II.

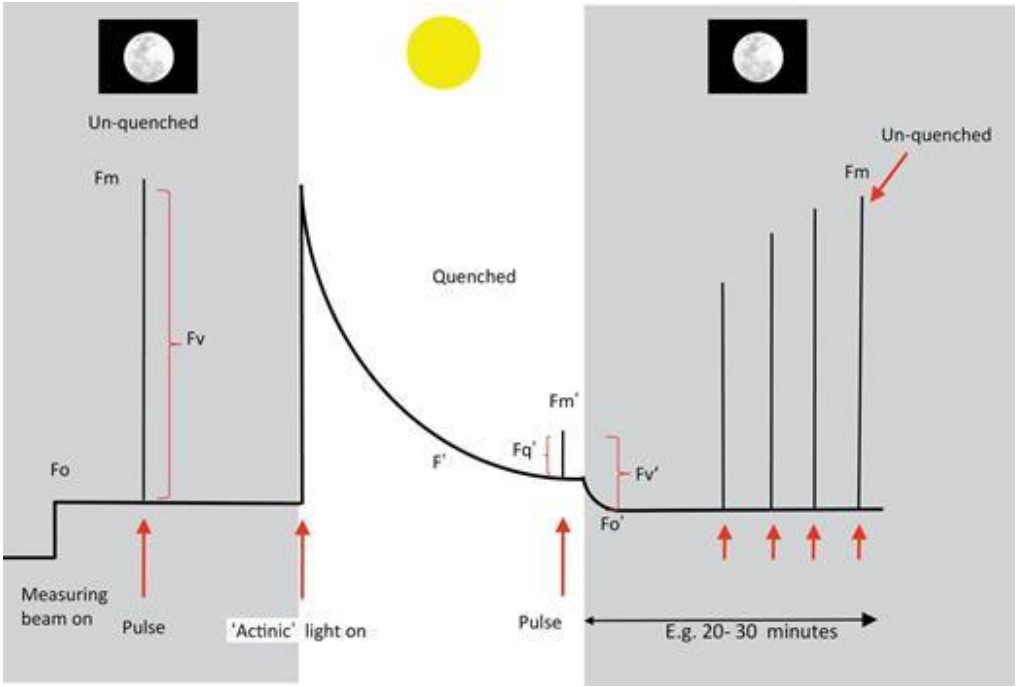


Figure 1-14. Chlorophyll fluorescence yield parameters used during modulated fluorescence whereby a dark-adapted leaf is exposed to different light treatments (Murchie and Lawson, 2013).

A saturating pulse applied after the FR pulse would close all the reaction centres and allow the derivation of the chlorophyll fluorescence maxima (F_m), without the influence of NPQ. The difference between F_o and F_m would give the variable fluorescence, F_v. The ratio of variable to maximum fluorescence (F_v/F_m) is usually 0.83 but can vary between species (Björkman and Demmig, 1987; Johnson *et al.*, 1993). It is a widely applied indicator for the maximum quantum yield of Photosystem II. A decrease in the quantum yield is often a

result of the presence of some stress such as photoinhibition. This dark-adapted parameter is often used as a “stress indicator” (Murchie and Lawson, 2013).

Under a strong actinic light, fluorescence increases transiently and would take a few minutes or more to reach steady-state (F’). If the leaf material was fully dark-adapted, it would take much longer to achieve F’. During this light step, application of a saturating pulse would result in the closing of all reaction centres transiently. This light state fluorescence value reaches its maxima to give F_m’. These two fluorescence measurements would allow the derivation of the most commonly used light-adapted parameter, the operating efficiency of Photosystem II photochemistry, F_q'/F_m' whereby $F_q' = F_m' – F'$ (Genty, Briantais and Baker, 1989).

All these fluorescence measurements also allow the derivation of the photochemical quenching parameter, qP and NPQ. qP is the proportion of Photosystem II reaction centres and is calculate from F_q'/F_v' whereby $F_v' = F_m' – F_o'$. When qP is equivalent to 1, all the Photosystem II reaction centres are open and when qP is zero, they are fully closed. NPQ is derived from $(F_m-F_m')/F_m'$ and can vary between 0.5 to 3.5. A higher NPQ value indicates better photoprotection (Maxwell and Johnson, 2000; Jung and Niyogi, 2009; Kasajima *et al.*, 2011).

1.5 Improving photosynthesis in plants

Natural selection is based on survival of the fittest but the “Green Revolution” hastened the selection of the “assumingly” more productive plants, especially under the surplus of nitrogen fertilizer, irrigation system, allocation of fund to

research pertinent to agriculture (Pingali, 2012; Long, Marshall-Colon and Zhu, 2015). Photosynthesis and photoprotection were not kept in the loop of selection and would be hard to do so (Zhu, De Sturler and Long, 2007; Sinclair, Rufty and Lewis, 2019). For many years, there was a lack of experimental proof linking successful yield increments as a result of improved leaf photosynthesis. Hence, there have always been questions on whether the efforts placed into improving photosynthesis are essential and worthwhile (Sinclair, Purcell and Sneller, 2004; von Caemmerer and Evans, 2010; Murchie, Ali and Herman, 2015; Sinclair, Rufty and Lewis, 2019).

Regardless of the doubts on value of improving photosynthesis, huge effort is continuously made to further improve the C_3 photosynthetic machinery in crops (as reviewed in Photosynthesis is said to account for 90% of plant biomass (Makino, 2011). Singh *et al.* (2014)). Improving photosynthesis and photoprotection is commonly accepted as the key pathway to advancing crop productivity and yield (Hibberd, Sheehy and Langdale, 2008; Peterhansel, Niessen and Kebeish, 2008; von Caemmerer and Evans, 2010; Long, Marshall-Colon and Zhu, 2015; Wu *et al.*, 2019). Photosynthesis and photoprotective mechanisms are highly complex and difficult to segregate singly for studies (Murchie, Pinto and Horton, 2009; Murchie, Ali and Herman, 2015). Recently, some studies showed an empirical link between photosynthesis, photoprotection and yield under fluctuating light (Hubbart *et al.*, 2012, 2018; Kromdijk *et al.*, 2016). However, there could be huge trade-offs with “simple” genetic improvements (Denison, 2011). Thus, more work has to be done for these plants to be realised in commercial fields (Peterhansel, Niessen and Kebeish, 2008).

1.5.1 Target sites of improving photosynthesis

Plants can be genetically modified from cell level to whole canopy in order to improve various components which would in turn improve photosynthesis (Figure 1-15). Structures such as mesophyll cell and chloroplast membranes and leaf anatomy could be bioengineered to improve photosynthesis (von Caemmerer and Evans, 2010; Singh *et al.*, 2014; Furbank, Quick and Sirault, 2015; Long, Marshall-Colon and Zhu, 2015). Carbon dioxide is transported through lipid membranes or aquaporins. Hence, increasing aquaporins could essentially improve the carbon dioxide transport and permeability of the membranes, resulting in more efficient photosynthesis (Uehlein *et al.*, 2003, 2008, 2012). In terms of canopy architecture, canopy with more erect leaves were associated with better radiation use efficiency (biomass per unit light intercepted; Yunusa *et al.*, 1993). There is a natural genetic variation in terms of leaf angle present in wheat and rice populations which could be exploited in future breeding programmes to create “smart” canopies (Furbank, Quick and Sirault, 2015).

Metabolic enhancements can be made to circumvent the C_3 photosynthesis limitations. These changes could possibly present a small-scale improvement which are generally tested at leaf level but should not be disregarded until more complex and inclusive canopy modelling could be applied to disprove them (Sinclair, Purcell and Sneller, 2004; Furbank, Quick and Sirault, 2015). A study suggested that the allocation and partitioning of the resources between the enzymes in the Calvin-Benson cycle are not fully maximizing plant productivity. The modelling results concluded that if proper partitioning of resources was made, it could provide significant improvements to photosynthesis (Zhu, De Sturler and Long, 2007).

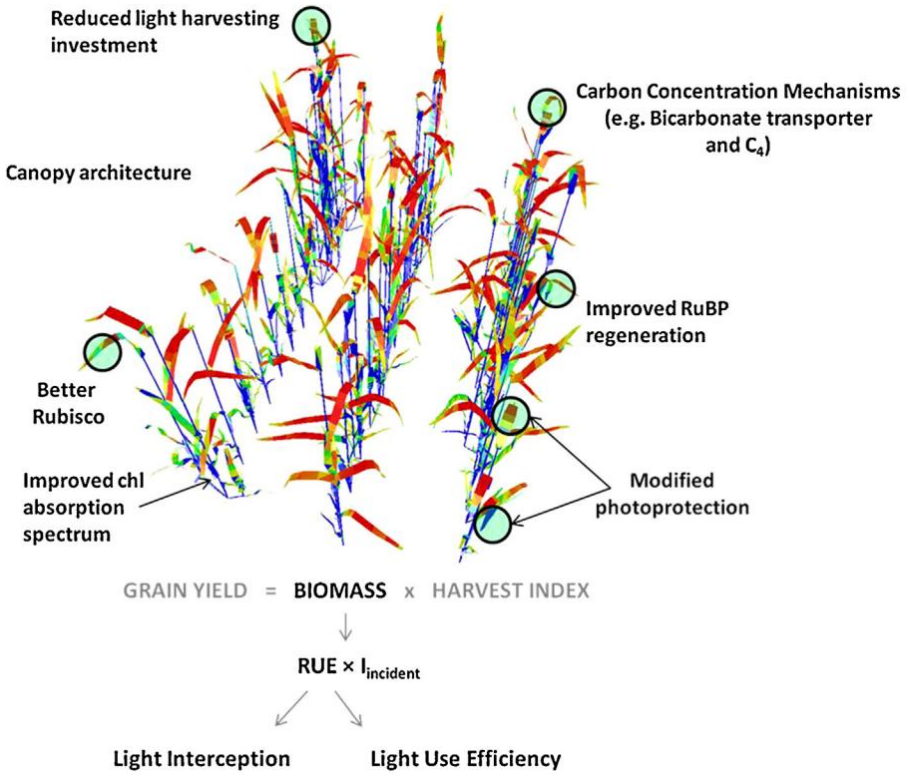


Figure 1-15. A wheat canopy model succinctly identifying the physiological traits relating grain yield and biomass. Biomass could be expressed as a function of radiation use efficiency (RUE) and light interception ($I_{incident}$) throughout the whole canopy (Furbank, Quick and Sirault, 2015).

RuBP regeneration is a known to limit photosynthesis under low light level or high carbon dioxide concentrations. Hence, enzymes involving RuBP regeneration such as transketolase (TK), fructose 1, 6-bisphosphatase (FBP-ase) and sedoheptulose-1, 7-bisphosphatase (SBP-ase) could be overexpressed. TK was identified as a key enzyme to overexpress in order to improve RuBP regeneration as a reduction in TK could inhibit RuBP regeneration and photosynthesis (Henkes *et al.*, 2001). Overexpression of FBP-ase or SBP-ase was found to improve RuBP regeneration and consequently enhance photosynthesis and biomass accumulation in tobacco and potato (Haake *et al.*, 1999; Raines *et al.*, 2000; Lefebvre *et al.*, 2005). It was also found that SBP-ase overexpression could lead to better growth during heat stress in rice (Feng *et al.*, 2007).

It was postulated that the abundance of Rubisco in plants compensated for its inefficiency but the effect is largely negated as atmospheric oxygen is much more concentrated than atmospheric carbon dioxide (Mann, 1999). Although there is a possibility to further increase Rubisco, there is no need to further overexpress incompetent Rubisco, especially when it adds on to an increased requirement for nitrogen (Spreitzer and Salvucci, 2002; Murchie, Pinto and Horton, 2009). However, the competence of Rubisco can either be increased by improving its carboxylation efficiency or reducing its oxygenase efficiency (Raines, 2006; Peterhansel, Niessen and Kebeish, 2008). Another method would be to improve the carbon concentration around Rubisco via introducing C_4 pathway.

Most of our crops work based on a C_3 photosynthetic machinery, which involved photorespiration (Chapter 1.3.4). C_4 photosynthetic machinery could realise more efficient photosynthetic pathways in current C_3 crops. This is not unachievable as the C_4 photosynthetic machinery had independently evolved at least 66 times, with either functional or biochemical variations, from the C_3 photosynthetic machinery (Sage, 2004; Hibberd, Sheehy and Langdale, 2008; Sage, Sage and Kocacinar, 2012). There is a huge consortium dedicated to introducing C_4 pathway into rice, creating “climate-ready” rice (Von Caemmerer, Quick and Furbank, 2012; Karki, Rizal and Quick, 2013).

Many works are ongoing to introduce the C_4 pathway into C_3 crops, by either introducing the Kranz anatomy or building biochemical carbon dioxide pumps. In a C_4 leaf, the fixation of carbon dioxide starts in the mesophyll cells, allowing the concentration of carbon dioxide into the bundle sheath cells whereas in the C_3 leaf, the process occurs in a single cell. This Kranz anatomy adaptation allowed C_4 plants to contribute about a fifth of the earth’s primary productivity (Lloyd and Farquhar, 1994). Carbon dioxide can also be

accumulated using phosphoenolpyruvate carboxylase (PEPc) as a biochemical carbon dioxide pump. This is regarded as an easier way than to create the Kranz anatomy in C_3 plants (Furbank, Quick and Sirault, 2015; Long, Marshall-Colon and Zhu, 2015).

1.5.2 Dynamic photosynthesis

Enhancing photosynthesis and photoprotection under fluctuating conditions which mimic field conditions would be another ideal focus. Zulfugarov *et al.* (2007) pointed out that higher plants have evolved to possess complex yet flexible photoprotective mechanisms in response to their varying environmental settings. Plants are sessile yet slow to respond to environmental cues (Figure 1-16). This equate to a loss in potential plant productivity (Ruban, 2017a; Slattery *et al.*, 2018). Alteration towards the formation and relaxation of the kinetics of NPQ would be required to improve the efficiency and productivity of the plants.

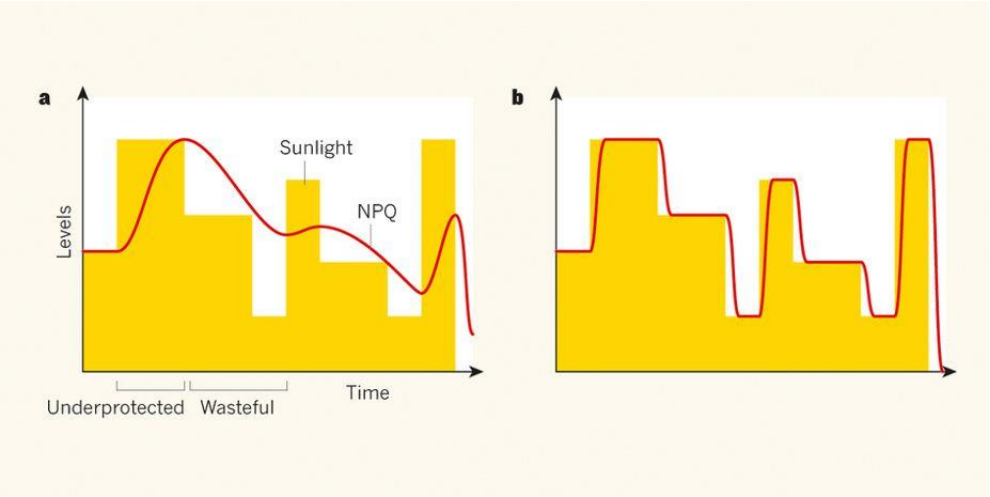


Figure 1-16. (a) Plants do not respond instantaneously to environmental conditions resulting in a loss of productivity. (b) This showed an ideal situation where plants could track and respond to environmental changes immediately (Ruban, 2017a).

It was also suggested that NPQ studies would be beneficial to crop breeding programmes, especially under the pressure of the uncertainty of climate change (Horton, 2000; Zhu *et al.*, 2004). Such early speculation has been corroborated by recent modelling and transgenic work showing a 'proof of concept' that altering both the level of NPQ and the dynamics of change of NPQ in the field can directly determine productivity and yield in tobacco and rice (Kromdijk and Long, 2016; Hubbart *et al.*, 2018). Such approaches could ensure crop varieties introduced through these breeding programmes would also select varieties that can track and react to surrounding light dynamically (Kromdijk *et al.*, 2016; Ruban, 2017a).

A modelling analysis by Zhu *et al.* (2004) showed that plants have higher photosynthesis potential when photoprotection responses (in this case kinetics) are improved. This model prediction was validated experimentally by Kromdijk *et al.* (2016) who showed that an improved NPQ response under fluctuating light environment could improve crop productivity by 15%. In another study by Hubbart *et al.* (2018), it was found that overexpressing *PsbS* in rice resulted in improved canopy radiation use efficiency under fluctuating light. The resulting rice plants also showed a 26% increase in grain yield (Hubbart *et al.*, 2018). Hence, plants should effectively track the light environment and respond to the changes instantaneously. This could lead to an increase in photoprotection response will result in reduced photoinhibition and thus, increased photosynthesis.

1.5.3 Using biostimulants to enhance plants

Most of the aforementioned improvements would involve genetic engineering

techniques made possible through recombinant DNA technology such as agrobacterium-mediated transformation (e.g. spring wheat transformed studied in Chapter 1) or newer genetic modification techniques (nGMs), such as genome editing techniques (e.g. clustered regularly interspaced short palindromic repeat (CRISPR)-directed nucleases or synthetic oligonucleotides-directed mutagenesis), transgrafting using genetically modified rootstocks and creation of double haploids for acceleration breeding. However, it would still be difficult for actual realisation of genetically modified organisms in the field due to the existing biosafety frameworks and legislations (Eckerstorfer *et al.*, 2019).

Another method would be to apply biostimulants to enhance plant growth. This would be subjected to less scrutinization than genetically modified organisms. Biostimulants are classed as substances or microorganisms that could be used on plants to improve nutrient uptake, confer improved abiotic stress tolerance or improve a certain crop quality, regardless of its nutrients content. Some major biostimulants include, (1) algal extracts, (2) protein hydrolysates and nitrogen-containing compounds which are usually derived as agricultural by-products, (3) humic and fulvic acids and (4) microorganisms such as fungi, nitrogen-fixing bacteria (Chapter 6) to improve nutrient uptake by plants could prove useful in improving yield. Application of these biostimulants, unlike herbicides and plant growth regulators, provide various agriculture functions but do not affect the life processes of the plant yield. They usually allow the plants to have establishment advantage and make them more resilient under harsh field conditions. Currently biostimulants are used on a wide range of crops ranging from citrus trees to vegetables, fruits and crops (du Jardin, 2015; Van Oosten *et al.*, 2017).

1.6 Objectives of the thesis

Arabidopsis plants which lacked qE components were found to perform badly compared to wildtype (Külheim *et al.*, 2002). Jung and Niyogi (2009) carried out quantitative trait loci (QTL) analysis of NPQ variation in Arabidopsis and concluded (perhaps surprisingly) that *PsbS* is not genetically linked to NPQ variation. On the contrary, another QTL study on rice by Kasajima *et al.* (2011) found that rice has two *PsbS* homologues (*OsPsbS1* and *OsPsbS2*) which regulate NPQ. These indicated that the factors determining the NPQ expression could be complex. Studies have shown that improved photoprotection through *PsbS* overexpression and/or upregulation of zeaxanthin epoxidase could enhance photosynthesis, improve water use efficiency and increase yield (Hubbart *et al.*, 2012, 2018; Kromdijk *et al.*, 2016; Głowacka *et al.*, 2018).

Leaf and canopy levels NPQ studies can divulge quantitative information, particularly on improving photosynthesis, which will be useful for crop improvement, especially with respect to unfavourable conditions of the impending climate change (Horton, 2000; Zhu *et al.*, 2004). Some NPQ studies have been made in rice but not much in wheat. Moreover, no studies to date have been made on how *PsbS* and NPQ are different in different canopy levels. Hence, the main aim of this PhD project is to study NPQ and how protective NPQ (pNPQ) is in wheat (*Triticum aestivum* L.) and rice (*Oryza sativa*) at different canopy levels. Li *et al.* (2002) suggested the overexpression of *PsbS* in crops could result in them being more resilient to the harsh fluctuating lights in the field and improve carbon gain (Külheim *et al.*, 2002; Li *et al.*, 2002; Zhu *et al.*, 2004). This is very important as not much is known about NPQ expression under the harsh ever-changing field

conditions (Murchie *et al.*, 2002).

This thesis addresses these gaps in our understanding of NPQ in rice and wheat plants. In an ideal situation, a plant will overexpress both *PsbS* and zeaxanthin epoxidase to improve photoprotection without having any negative effect on photosynthesis. We hypothesise that an increase in *PsbS* expression would result in greater NPQ capacity and improved photoprotection response to fluctuating light conditions. This would in turn (hopefully) increase photosynthesis which would translate to higher yield. The first part of the thesis addresses NPQ manipulation in wheat. In Chapter 2, spring wheat transformed to overexpress rice *PsbS* was used to investigate the role of photoprotection in wheat. It was hypothesised that an overexpression of rice *PsbS* in transgenic wheat would result in an increase in NPQ. On successful selection of wheat plants overexpressing *PsbS*, NPQ studies in wheat could be extended to canopy level. Canopy level NPQ variations present in current wheat population was also assessed. This was studied in a subset of selected genetically diverse wheat grown in the field (Chapter 3). It was hypothesised that due to photoacclimation, the top of the canopy would have greater NPQ whereas the bottom of the canopy would have higher NPQ capacity to accommodate to fluctuating light conditions within the canopy.

In the second part of the thesis, photoprotection was also studied in established rice lines overexpressing *PsbS* at canopy level. Chapter 4 aimed to quantify the protective ability of NPQ at the top and bottom of the rice canopies. It was expected that an overexpression of *PsbS* would be consistent throughout the whole canopy and the bottom of the canopy would show greater phototolerance, consistent with the previous hypothesis that the bottom of the crop canopy would have higher NPQ capacity. Water use

efficiency of these transgenic rice lines overexpressing *PsbS* was also studied. A study on tobacco overexpressing *PsbS* showed improved stomatal conductance under a light transition (Głowacka *et al.*, 2018) but this was not previously observed in transgenic rice lines overexpressing *PsbS*. Chapter 5 analysed the water use efficiency in two established transgenic rice lines overexpressing *PsbS* by under light transitions and water restriction regimes. Improved nitrogen content was also implicated to result in improved photosynthesis and photoprotection in plants (Verhoeven, Demmig-Adams and Adams, 1997). Chapter 6 hypothesised that photosynthesis could be improved in rice by colonisation with nitrogen-fixing bacteria.

Chapter 2 Assessing Non-Photochemical Quenching (NPQ) Capacity of Transgenic Spring Wheat Overexpressing Rice *PsbS* Transgene

C.C. Foo[1], R. Swarup[1], R. Howells[2], E. Wallington[2] and E. H. Murchie[1]

[1] Plant and Crop Science Division, School of Biosciences, University of Nottingham, Sutton Bonington LE12 5RD UK

[2] NIAB, Huntingdon Road, Cambridge CB3 0LE UK

Author contribution:

Experiment conceived by EH Murchie and CC Foo

Project supervision performed by EH Murchie and R Swarup

Gene cloning performed by R Swarup

Wheat transformation and qRT-PCR analysis by R. Howells and E.

Wallington (NIAB)

All other experimental work by CC Foo

Chapter written by CC Foo

2.1 Abstract

Rice *PsbS* was overexpressed in spring wheat (*Triticum aestivum* cv 'Fielder'). Molecular and physiological characterization of the T_0 generation of the *PsbS* transformant lines showed that overexpression of rice *PsbS* in wheat resulted in higher non-photochemical quenching (NPQ) capacity. Based on the T_0 generation NPQ level and rice *PsbS* gene copy number results, wheat plants were selected to be homozygous for rice *PsbS* transgene. Selection was carried out using PCR and qRT-PCR. Putative wheat plants homozygous for *PsbS* were further characterised for their NPQ. However, wheat plants homozygous for rice *PsbS* transgene were not attained and we did not see increased NPQ expression in the subsequent generations.

2.2 Introduction

Wheat is often hailed as a “miracle crop” due to its role in sustaining food production and contribution to reducing hunger in the last century. As one of the three major cereal crops, there is a need to constantly improve yield for higher productivity to meet global food security demands caused by population increase, changes in dietary habits and changes in land use (Ray *et al.*, 2015). Wheat can grow over a wide range of climatic zones and is the most cultivated cereal crop globally in terms of land area (Shewry, 2009). Wheat is a substantial part of human daily diet, including in many regions where it is not grown. It makes up about 20% of the daily calorie intake and protein consumed, making it an important crop for global food security (Ladha *et al.*, 2003; Shiferaw *et al.*, 2013). However, data has shown that about 38% of the wheat areas showed either stagnant or collapsed productivity since the mid-1990s. In scenarios where there were yield improvements, the rate of productivity is insufficient to meet future demands (Calderini and Slafer, 1998; Ladha *et al.*, 2003; Lobell *et al.*, 2005; Peltonen-Sainio, Jauhiainen and Laurila, 2009; Brisson *et al.*, 2010; Finger, 2010; Ray *et al.*, 2012, 2015, 2019).

One way to improve productivity is to increase the resilience of wheat to environmental change. Wheat grows over a wide range of environment, from temperate to tropical regions. Wheat in tropical regions would experience similar conditions as rice whereas in temperate regions, photoprotection could also be as important, if not more important. A study by Demmig-Adams, Gilmore and Adams (1996) pointed out that during winter season, plants have a greater photoprotection need than during summer season. During winter, the unfavourable conditions such as low temperature result in lower metabolic

rate and hence there would be a greater proportion of excess energy that requires dissipation. In addition, wheat also faces photoinhibition during sunny conditions. It is apparent that regardless of the conditions, photoprotection is crucial in maximizing the photosynthetic capacity of wheat (Zhu *et al.*, 2004; Hubbart *et al.*, 2012, 2018; Kromdijk *et al.*, 2016).

As the key driver of all yield production, the efficient capture and use of light energy in photosynthesis is critical for underpinning yield improvement. However, the photosynthetic apparatus can often capture more energy than can be utilised in the subsequent energy transfer and redox reactions. This disparity can create a bottleneck leading to a build-up of excitation energy and the formation of reactive oxygen species leading to photoinhibition; the light induced reduction of photosynthetic capacity (Sonoike, 1996; Horton, 2000; Takahashi and Murata, 2005; Takahashi and Badger, 2011; Matloobi, 2012; Murata, Allakhverdiev and Nishiyama, 2012). This excess energy and resultant damage must be dealt with, either through dissipative processes to prevent energy accumulation or through the repair of damage to the photosynthetic machinery. The fastest process employed by plants to relieve excitation pressure and prevent damage is non-photochemical quenching (NPQ) of chlorophyll fluorescence, where excess energy is dissipated harmlessly as heat via chlorophyll-chlorophyll and/or chlorophyll-carotenoid interactions (Jahns and Holzwarth, 2012; Ruban, 2012, 2016).

NPQ consists of a number of components, however the fastest acting component is energy-dependent quenching (qE), and is triggered by the generation of a pH gradient across the thylakoid membrane (Δ pH; Krause, 1974; Horton, Wentworth and Ruban, 2005). qE is also known to be modulated by the carotenoid zeaxanthin and the protein PSII subunit S (*PsbS*), which act as allosteric regulators to alter the structure of the

membrane and antenna conformation in order to enhance its affinity for protons, thus facilitating qE formation and relaxation (Horton and Ruban, 1992; Li *et al.*, 2000; Horton, Wentworth and Ruban, 2005; Johnson and Ruban, 2011; Goral *et al.*, 2012; Ruban, 2012, 2016; Sacharz *et al.*, 2017). Many studies have shown that alterations to NPQ, and in particular qE, can contribute to improved photosynthesis and thus increased productivity in crops (Ishida *et al.*, 2011; Kasajima *et al.*, 2011; Hubbart *et al.*, 2012, 2018; Morita *et al.*, 2013; Kromdijk *et al.*, 2016; Głowacka *et al.*, 2018). This effect is particularly pronounced under dynamic conditions. This is crucial as NPQ dynamics under field conditions is not fully understood (Murchie *et al.*, 2002). In a crop canopy, photosynthetic tissue can pass rapidly from saturating light to low light due to clouds and leaf self-shading. In this scenario photosynthetic tissue is transferred from light saturation to light limitation, and dissipation, i.e. the protection, of absorbed light energy as heat will lower the efficiency of photosynthesis. Modelling of the dynamics of these light fluctuations shows that this could cost up to 20-30% of the potential CO_2 assimilation (Zhu *et al.*, 2004).

Contrary to a steady light, altering the key component of NPQ under fluctuating light showed improved photoprotection leading to improved photosynthesis. For example, an improved NPQ response in tobacco, resulting from overexpression in two genes involved the reversible conversion of zeaxanthin to violaxanthin and one gene determining *PsbS* levels showed up to 20% increase in yield of field grown plants (Kromdijk *et al.*, 2016). Rice canopies with an improved NPQ response were also found to have better canopy radiation use efficiency, which was also reflected in a 26% increased grain yield (Hubbart *et al.*, 2018). However, NPQ response has not been fully explored in wheat possibly due to the complexity of not only the *PsbS* gene

but also wheat being a hexaploid. As a comparison, the wheat genome is five times that of a human genome and also 35 times larger than a rice genome (Jones, 2005). Wheat also has three different set of chromosomes (A, B and D) with more than 80% repetitive genes (Flavell *et al.*, 1974). This resulted in technical difficulties for gene cloning and alignment due to identical sequences within the large genome (Treangen and Salzberg, 2012).

Here we take the same approach adopted in rice (Hubbart *et al.*, 2018) to analyse the effect of overexpression in *PsbS* in spring wheat. This project, in collaboration with Emma Wallington and Rhian Howells of NIAB (Cambridge, UK) as part of the Community Resource for Wheat Transformation (CRWT) project, aimed to overexpress the rice *PsbS* gene in spring wheat to investigate if NPQ capacity could be elevated and thus, help to prevent photoinhibition, indirectly improving photosynthesis. Successful selection of stable homozygous lines would allow the study of wheat canopies overexpressing *PsbS*.

2.3 Materials and methods

2.3.1 Plant material

2.3.1.1 Gene cloning and wheat transformation

Gene cloning (Figure 2-1: Steps 1 to 5) using rice (*Oryza sativa*) *PsbS* sequence (Os01g64960; refer to Supplementary material S2.1 for gene sequence) was carried out by Dr. R. Swarup (University of Nottingham, UK). Ribonucleic acid (RNA) was extracted from rice leaf for reverse transcriptase-polymerase chain reaction (RT-PCR), resulting in complementary

deoxyribonucleic acid (cDNA) which was used to clone into an entry vector (Figure 2-2). Rice *PsbS* gene was polymerase chain reaction (PCR) amplified using Rp1b and Rp3 primers (See Supplementary material S2.2 for primers sequence). It was then recombined into a Gateway destination vector, pCR8, between Gateway aatL1 and aatL2 sites, so that it could be driven by a strong Actin promoter (Figure 2-3). PCR analysis and gene mapping with restriction enzymes were also carried out to confirm the incorporation of the rice *PsbS* gene in the correct orientation (Full detail can be found in Supplementary material S2.3).

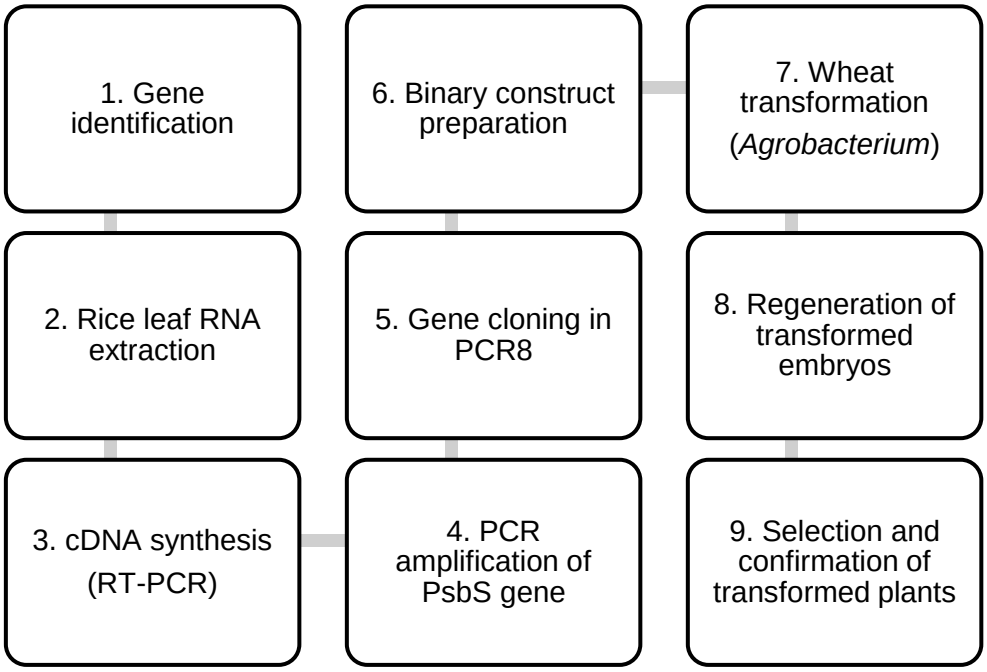


Figure 2-1. An overview of gene cloning and wheat transformation carried out by Dr. R. Swarup (University of Nottingham, UK) and NIAB, Cambridge respectively.

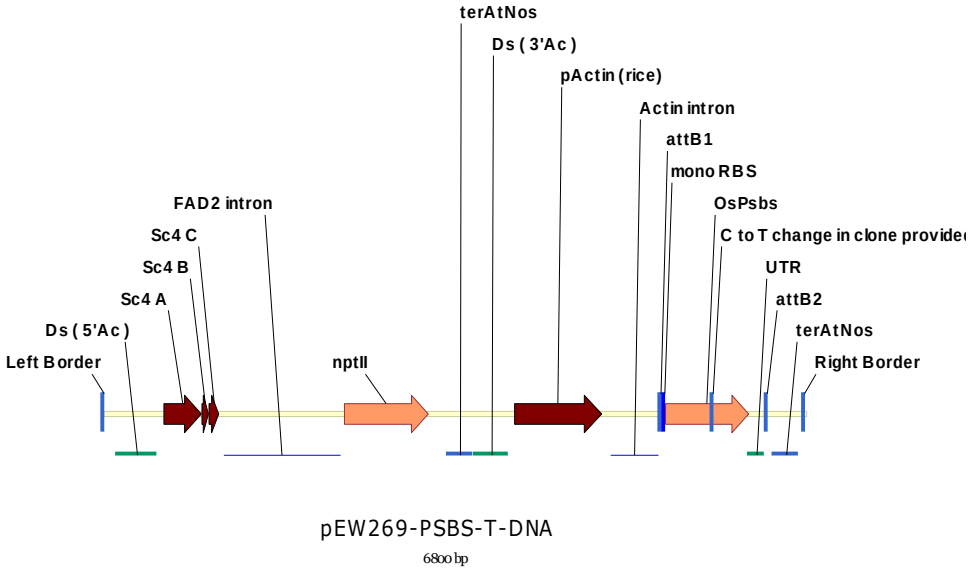


Figure 2-2. Final gene construct employed in transformation of wheat using Gateway cloning.

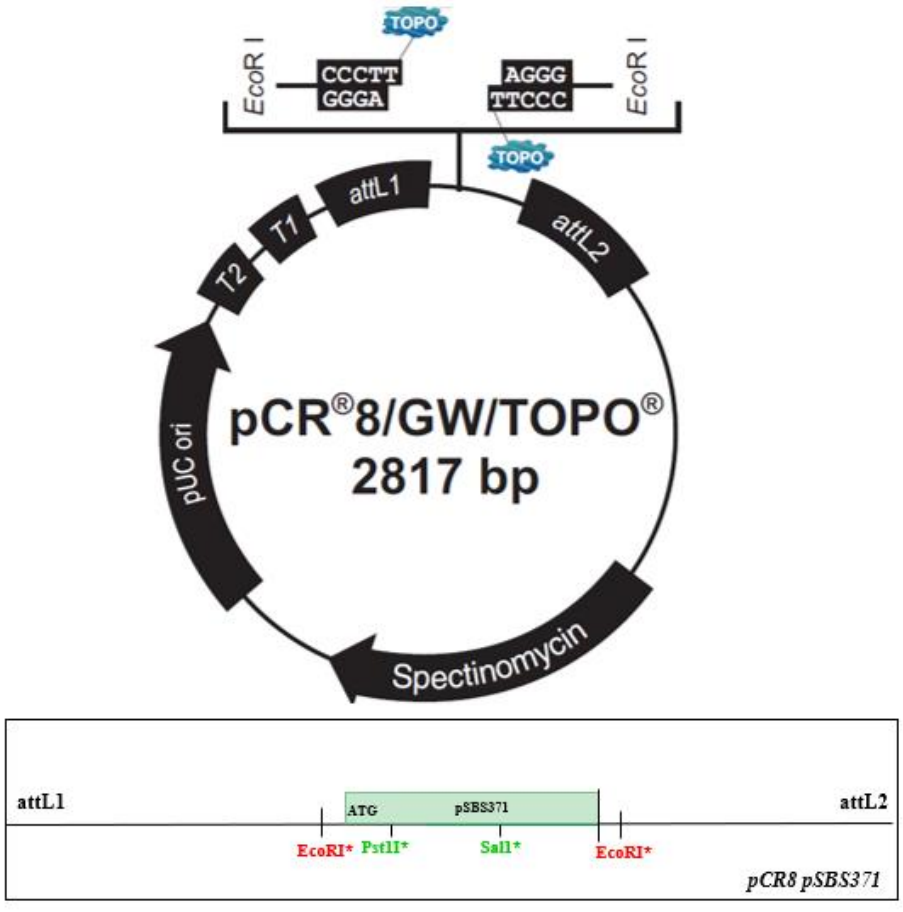


Figure 2-3. Rice *PsbS* gene (Os*PsbS*) was inserted between *EcoRI*, flanked by specific attL recombination sites (attL1 and attL2) cloned into pCR8.

The final construct was sent to National Institute of Agricultural Botany (NIAB), Cambridge for transformation into wheat (Figure 2-1: Steps 6 to 9). E. Wallington (NIAB, Cambridge) recombined the inserts using a Gateway Clonase II kit (Invitrogen; California, USA) into a binary vector, pSC4-ActR1R2-SCV containing Gateway aatR1 and aatR2 sites. This is a super clean vector (Firek *et al.*, 1993), containing the *NPTII* (*neomycin phosphotransferase II*) gene under the control of the *subterranean clover stunt virus* Sc4 promoter (Schünmann *et al.*, 2003) and *Arabidopsis thaliana FAD2* intron (Okuley *et al.*, 1994) for selection on Geneticin G418 in tissue culture (Figure 2-2). After transfer into wheat the *PsbS* would be expressed from the rice Actin promoter (McElroy *et al.*, 1990). The resultant plasmid, pEW269-*PSBS*, was electrotransformed into *Agrobacterium* strain EHA105-U1. Plasmids were isolated from *Agrobacterium* and verified by restriction.

M. Craze and S. Bowden performed the wheat transformation experiments at NIAB, Cambridge. Immature donor wheat seeds (US spring variety, *Triticum aestivum* cv 'Fielder') were collected 14 to 16 days after anthesis and surface sterilized as per Risacher *et al.* (2009). Before *Agrobacterium* infection, isolated embryos were pre-treated with a centrifugation step essentially as detailed in Ishida *et al.* (2015). Treated embryos were co-cultivated with the *Agrobacterium* strains described above at 23°C in the dark for two days. Following removal of the embryonic axis, subsequent tissue culture of the plant material was performed essentially as described in Risacher *et al.* (2009). Regenerated plants were grown in a growth chamber (Conviron; Winnipeg, Canada) operated on a 16-hour photoperiod at 20°C/15°C day/night temperature, irradiance maintained between 350 to 500 µmol quanta m^{-2} s^{-1}.

R. Howells (NIAB, Cambridge) analysed the wheat plantlets by quantitative

PCR (qPCR) for the copy number of the *nptII* selectable marker gene, the presence of the gene of interest was confirmed by PCR amplification with *PSBS*-F and NosT-rev primers (Refer to Supplementary material S2.2 for primers sequences), PCR amplification performed in a 10µL reaction with 1µL reaction buffer, 2µL CG-RICH solution, 0.4U Faststart Taq DNA polymerase (Roche Molecular Biochemicals; Indianapolis, USA) and 1µL of each primer. The PCR reaction was operated under the following conditions: 40 cycles of 30 seconds annealing at 65 °C and extension of 90 seconds.

Wheat transformation and analysis details were provided by R. Howells (NIAB, Cambridge) and included with permission. Control plants did not show the presence of the transgene. Out of the 33 successful transformed lines, 30 of them showed positive for transgene presence. The list of T_o generation of these successful *PsbS* transformant lines and their PCR and qRT-PCR results are tabulated in Supplementary material S2.4.

2.3.1.2 Selection of putative *PsbS* transformant lines at T_0 generation

The T_o generation of the successfully transformed and regenerated putative spring wheat overexpressing rice *PsbS* were characterized and analysed at the NIAB laboratories described in Foo (2014). For the ease of referring to these lines, they will be termed as "*PsbS* transformant lines" here. A total of 37 independent wheat lines were regenerated; 33 putative lines overexpressing rice *PsbS* and four control (without the rice *PsbS* transgene) wheat plants obtained from the same transformation event. Leaf samples were collected from the *PsbS* transformant lines for molecular characterisation and confirmation of the presence of the rice *PsbS* gene.

During post-anthesis (approximately within two weeks of anthesis) stage, dark-adapted gas-exchange and chlorophyll fluorescence measurements were carried out on the healthiest flag leaf of each wheat plant. Physiological measurements for the *PsbS* transformant lines were made in the free space outside the growth chamber. A LI-COR 6400XT photosynthesis analyser (LI-COR Biosciences, Nebraska, USA) was used with the fluorescence attachment. An automated programme was set in place to determine NPQ during a 15 photosynthetic induction phases. First, dark-adapted chlorophyll fluorescence parameters (F_o, F_m and F_v) were measured. Following this, photosynthesis was induced with photosynthetically active radiation (PAR) supplied at 1500 µmol $m^{-2}s^{-1}$. Throughout the whole programme, the ambient carbon dioxide concentration in the cuvette was kept at 400 ppm. Block temperature was maintained at 20°C. Flow rate was set at 500 mL min^{-1}. The measurements of gas exchange (main parameters of interest were net carbon dioxide assimilation rate and stomatal conductance) were recorded over a period of 14 minutes at every two minutes intervals. Following the gas exchange measurement, a saturating flash was applied every two minutes to measure F_s', F_m', F_v' and F_o' which permitted the determination NPQ, photochemical quenching (qP) and the operational PSII efficiency in the light (ϕPSII). For an explanation of these parameters, see Murchie and Lawson (2013).

2.3.1.3 Selection for homozygous *PsbS* transformant lines at T_1 and T_2 generations

All the lines derived from T_0 generation are heterozygous for rice *PsbS* transgene and will segregate in the next generation. Hence, the seeds from

T_0 generation was grown to select for wheat plants with the introgressed rice *PsbS* transgene. The selected wheat plants carrying the rice *PsbS* transgene can then be brought into next generation(s) to select for plants homozygous (two copies of the identical gene at the same gene locus) for rice *PsbS* transgene. They need to be in a homozygous state in order for the rice *PsbS* transgene to stably inherited to the next generation.

Based on the NPQ results and gene copy number of the T_o generation, the seeds from two *PsbS* transformant lines (CW10_17, 3 or 4 rice *PsbS* gene copy number and CW10_23, one rice *PsbS* gene copy number) were selected (T_1 generation) for subsequent experiments in order to select for homozygous lines. Based on Mendelian inheritance genetics and on the assumption that the gene copies (if there are multiple copies) are not on the same locus, they would segregate in a 3:1 manner (Two gene copies, 15:1; three gene copies, 63:1, four gene copies, 255:1, etc.). Working with higher gene copy number would be more difficult as more seeds need to be sown in order to obtain a plant with the transgene present in it.

Method and material for molecular characterisation detailed in Chapter 2.3.3.1. Leaf gDNA of samples were extracted and sent to R. Howell (NIAB, UK) for qRT-PCR analysis. PCR analyses were run on the plant samples that had returned with qRT-PCR result (including those without the presence of the rice *PsbS* gene). Two sets of PCR analyses were run simultaneously to detect the presence of rice *PsbS* gene. The two primer pairs used were 1. *PSBS*-F and NOST-Rev and 2. RP6 and RP7 (Primer sequence can be found Supplementary material S2.2). Not only were *PsbS* transformant lines with the rice *PsbS* transgene selected but also azygous plants were also retained as controls. Azygous plants are plants selected from the same generation and found to not contain the rice *PsbS* transgene. These control plants would

have the same genetic background as the homozygous *PsbS* transformant lines selected.

2.3.2 Plant growth and maintenance: University of Nottingham

The experiments were carried out in a walk in Conviron (Controlled Environments Ltd., Manitoba, Canada) LED growth room (South Lab Annexe, University of Nottingham, Sutton Bonington campus). The experiments used a completely randomized block design with a minimum of four replicates. For all experiments, seeds were germinated in modular trays before transplanting into 2L pots containing John Innes No. 2 compost after genotyping analysis. Plants were grown under high light conditions of 800 µmol $m^{-2}s^{-1}$ with a 16H photoperiod, 22/16°C day/night temperature and 50% RH. Plants were kept well-watered and fed with liquid nutrients after they started to tiller. All wheat plants that were grown and brought to full maturity had their ears carefully bagged before anthesis to avoid cross-pollination or cross-contamination.

For the T_1 generation selection of *PsbS* transformant lines, 64 seeds were sown for CW10_17 (3 or 4 gene copies based on the parent) and 32 seeds were sown for CW10_23 (1 gene copy based on the parent) from their T_0 generation were sown on 2nd December 2016. Germinated seedlings were transplanting into 2L pots on 16th January 2017. The T_2 generation of CW10_17 and CW10_23 were subsequently sown on 4th May 2017 based on presence of rice *PsbS* transgene and gene copy number analyses of the T_1 generation experiment. The seedlings from T_2 generation were transplanted into 2L pots on 16th June 2017.

2.3.3 Characterisation of the *PsbS* transformant lines: University of Nottingham

2.3.3.1 Molecular analysis for confirmation of presence of transgene and gene copy number

2.3.3.1.1 gDNA extraction

A quick DNA extraction method adapted from Klimyuk *et al.* (1993) was used to extract gDNA from the wheat leaf samples. Leaf samples were collected and flash frozen in liquid nitrogen and ground to fine powder. 50 μL of 0.25 M sodium hydroxide was added to the sample and homogenised by vortex to ensure the whole sample had been re-suspended in sodium hydroxide. The mixture was heated to 96°C on a heat block for 30 seconds. Subsequently, 50 μL of 0.25 M hydrochloric acid (Sigma-Aldrich, Darmstadt, Germany), 25 μL of 0.5 M Tris; pH8.0 (Thermo Fisher Scientific, Massachusetts, USA) and 0.25% IGEPAL® CA-630 (Sigma-Aldrich, Darmstadt, Germany) were added to the mixture. The mixture was homogenised and heated at 96°C again for three minutes.

2.3.3.1.2 Polymerase chain reaction (PCR) amplification of rice *PsbS* gene

PCR amplification of the rice *PsbS* transgene was adapted from a protocol provided by NIAB (Cambridge, UK). Roche FastStart™ Taq DNA polymerase (Sigma-Aldrich, Darmstadt, Germany) was used. The PCR master mix was made as tabulated in Table 2-1, with the appropriate forward and reverse primers (See Supplementary material S2.2 for a complete list of primers). The PCR master mix was then pipetted into each of PCR tube. Positive controls

using rice gDNA (*Orzya sativa* cv. 'Nipponbare') and/or plasmid carrying rice *PsbS* gene (used for gene cloning – Chapter 2.3.1.1) were used. PCR reaction was carried out in the final volume of 20 µL

Table 2-1. Optimized PCR protocol for the amplification of rice *PsbS* gene sequence for one reaction tube.

Component	**Volume (µL)**
Sample DNA	2.00
10X standard PCR buffer	2.00
10X GC-rich buffer	2.00
$MgCl_2$ (50mM)	0.60
dNTP (10mM)	0.40
Forward primers	1.00
Reverse primers	1.00
Taq polymerase	0.16
Sterile distilled water	10.84
Total volume	**20.00**

The PCR tubes were placed into a thermocycler GeneAmp® PCR System 9700 (Applied Biosystems; California, USA) for PCR amplification under the following optimized conditions: Initial denaturation of one cycle at 94 °C for 2 minutes, 40 cycles of denaturation at 94 °C for 30 seconds (strand separation), 60°C for 30 seconds (annealing) and 72 °C for 1 minute (extension) and one cycle of final extension at 72 °C for ten minutes. Finally, the reaction was held at 4 °C.

After the whole reaction was completed, the PCR tubes were removed and kept on ice. After PCR amplification, DNA gel electrophoresis analysis was carried out to resolve the PCR products. The PCR tubes were kept on ice at all times.

2.3.3.1.3 Gel electrophoresis analysis

DNA samples were analysed by gel electrophoresis. A 1.0% agarose gel in Tris-Borate-EDTA (TBE) buffer was used for gel electrophoresis. DNA loading dye was added to each sample before loaded into each well. The gel was run at 100V for a minimum of 30 minutes, up to 60 minutes. The gel was visualized with ethidium bromide using a gel imaging system (Syngene; Bangalore, India).

2.3.3.2 Non-photochemical quenching (NPQ) characterisation of the T_1 plants

Physiological characterisation of the T_1 generation of the *PsbS* transformant lines were measured at six-leaf stage or older. Measurements were made in a dark lab with minimal light from either the computer screen or safe light. Induction curves were made primarily using Junior-PAM chlorophyll fluorometer (Heinz Walz GmbH, Effeltrich, Germany). A 50 cm fibre-optic connecting the Junior-PAM (Heinz Walz GmbH, Effeltrich, Germany) and a magnetic leaf clip were used for the induction curve measurements. The light level emitted from the fibre optic was calibrated using a mini quantum sensor (MQS-B/A; Heinz Walz GmbH, Effeltrich, Germany) attached to the universal light meter (ULM-500; Heinz Walz GmbH, Effeltrich, Germany) every morning of the measurements. Leaf sections were dark-adapted with aluminium foil for an hour prior to measurements. An induction curve program was set to run at 1500 µmol m^{-2} s^{-1} for 14 minutes with a saturating light administered every two minutes. Dark-adapted F_o and F_m values were recorded before the start of the induction curve. Chlorophyll fluorescence parameters (in particular NPQ) were calculated and recorded within the WinControl-3 window.

2.3.4 Statistical analysis

Analysis of variance (ANOVA) and regression analyses were carried out on the data collected using the statistical package, *Genstat* (19th Edition) for Windows (VSN International Ltd., Hemel Hempstead, UK). They were analysed based on the probability generated by *Genstat* whereby a P value of less than 0.05 ($P<0.05$) shows significant interactions and P value greater than 0.05 ($P>0.05$) shows insignificance. Data were checked to have met the assumption of constant variance and normal distribution of residuals.

2.4 Results

2.4.1 Physiological characterisation T_o generation *PsbS* transformant lines

The results for T_0 generation of the transformant lines were first included in Foo (2014). The *PsbS* transformant T_o lines showed greater NPQ expressions than the control plants (Figure 2-4), showing that the transformation with *PsbS* transgene had worked. The ratio of variable to maximum fluorescence (F_v/F_m) is an easy measurement that gives great indication of the PSII photochemistry (Bjorkmann and Demmig, 1987). On average, healthy plants should have F_v/F_m value around 0.83 (Björkman and Demmig, 1987; Johnson *et al.*, 1993; Maxwell and Johnson, 2000; Murchie and Lawson, 2013). However, the Fv/Fm values for healthy and unstressed plants could vary from 0.78 to 0.86 (Björkman and Demmig, 1987). A F_v/F_m value of 0.79 was used as the cut-off point for the selection and analysis of T_0 generation *PsbS* transformant lines.

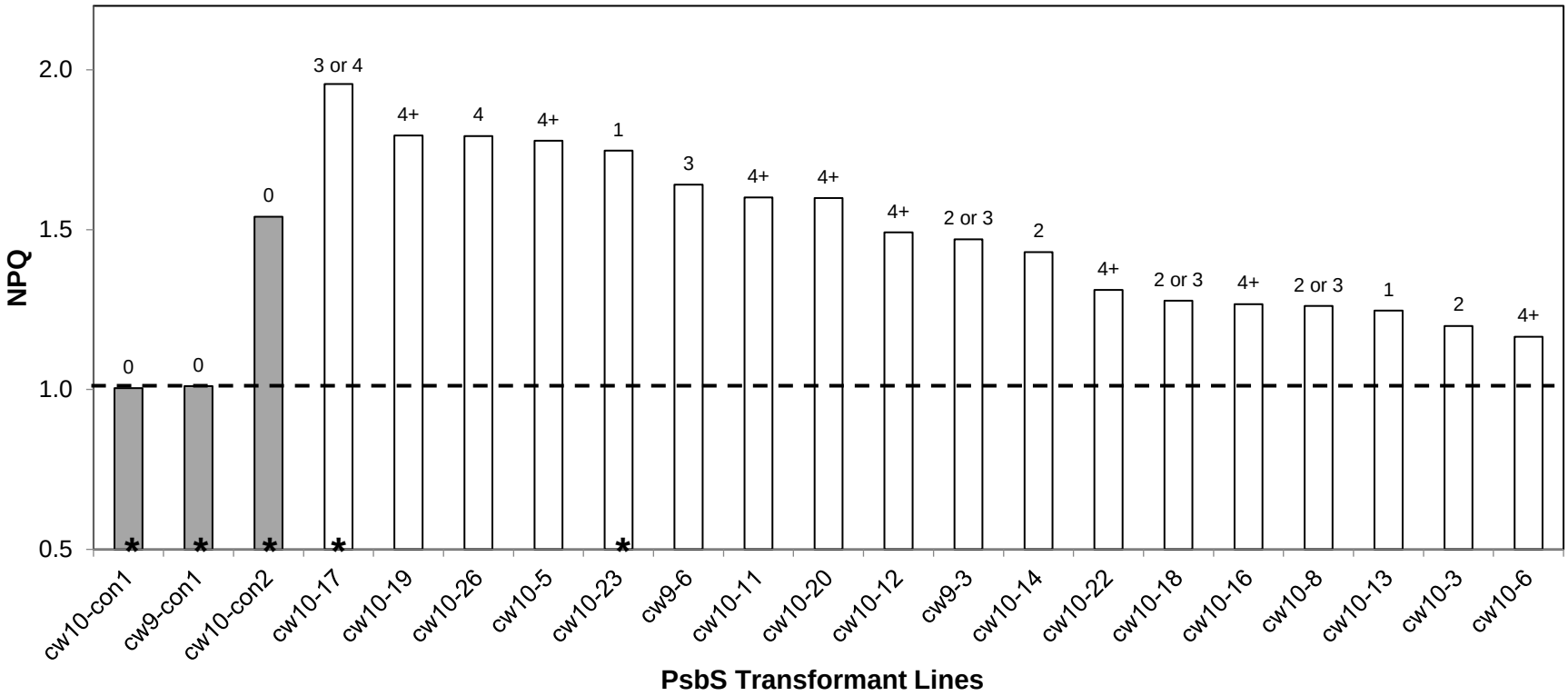


Figure 2-4. Non-photochemical quenching (NPQ) capacity was significantly higher in the T_0 generation *PsbS* overexpressors (white bars) compared to the control (grey bars) plants ($t(19) = 2.01$, $P = 0.030$). The numbers above each bar show the corresponding rice *PsbS* transgene copy number of each transformed line. The lines marked with asterisk (*) were used in T_1 generation experiment (Foo, 2014).

The F_v/F_m values are correlated with photosynthetic capacity and NPQ to give an overall picture of how the *PsbS* transformant lines were performing (Figure 2-5). The selected *PsbS* transformant lines showed no correlation between F_v/F_m values with photosynthetic capacity ($F(1, 19)=1.56$, $P=0.227$; Figure 2-5A) and better NPQ expression ($F(1, 19)=10.93$, $P=0.004$; Figure 2-5B). As expected, photosynthetic capacity correlated positively to stomatal conductance ($F(1, 19)=7.44$, $P=0.013$; Figure 2-6A) but not NPQ ($F(1, 19)=0.12$, $P=0.732$; Figure 2-6B).

There was no significant correlation between NPQ expression and maximum photosynthetic capacity in these *PsbS* transformant lines grown under controlled conditions ($F(1, 19)=0.08$, $P=0.788$; Figure 2-7). The variation in NPQ observed did not result in any change of the photosynthetic machinery of the *PsbS* transformant lines and was attributed to the introduction of the rice *PsbS* transgene. Photosynthetic capacity was positively correlated to ΦPSII ($F(1, 19)=21.27$, $P<0.001$; Figure 2-8A) and qP. ($F(1, 19)=12.73$, $P=0.002$; Figure 2-8C).The chlorophyll fluorescence parameters, quantum efficiency of the Photosystem II, ΦPSII and the parameter denoting "openness" of the reaction centers, photochemical quenching, qP are relevant to the studies of photochemical quenching, and hence are expected to show positive correlation to photosynthetic capacity but not have any significant effect on NPQ. However, a significant but weak correlation could be observed between NPQ and qP ($F(1, 19)=5.67$, $P=0.028$; Figure 2-8D). Both NPQ and qP can occur simultaneously to dissipate excitation energy. There was no correlation between NPQ and ΦPSII ($F(1, 19)=0.57$, $P=0.459$; Figure 2-8B).

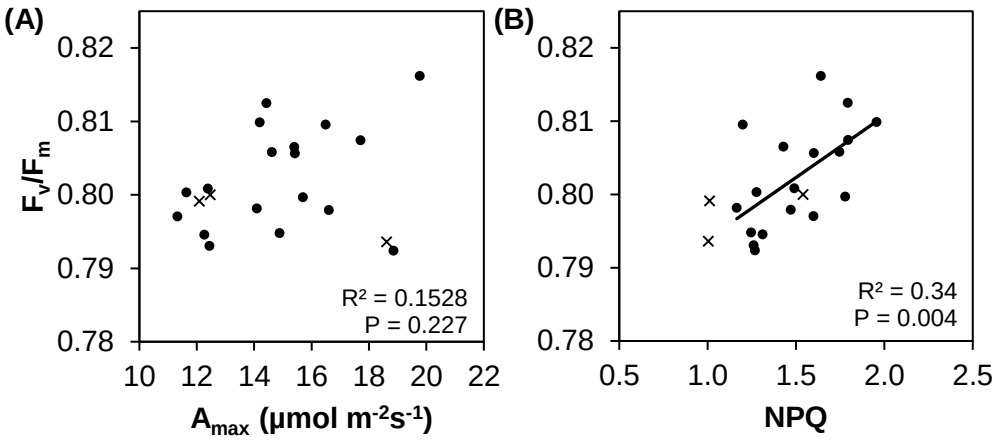


Figure 2-5. A comparison of the F_v/F_m values of T_0 generation wheat plants overexpressing rice *PsbS* with **(A)** maximum carbon assimilation, A_{max} and **(B)** non-photochemical quenching, NPQ. Control plants were included in the plots as $_X$. Regression analysis using GenStat (VSN International Ltd., Hemel Hempstead, UK) was applied (Foo, 2014).

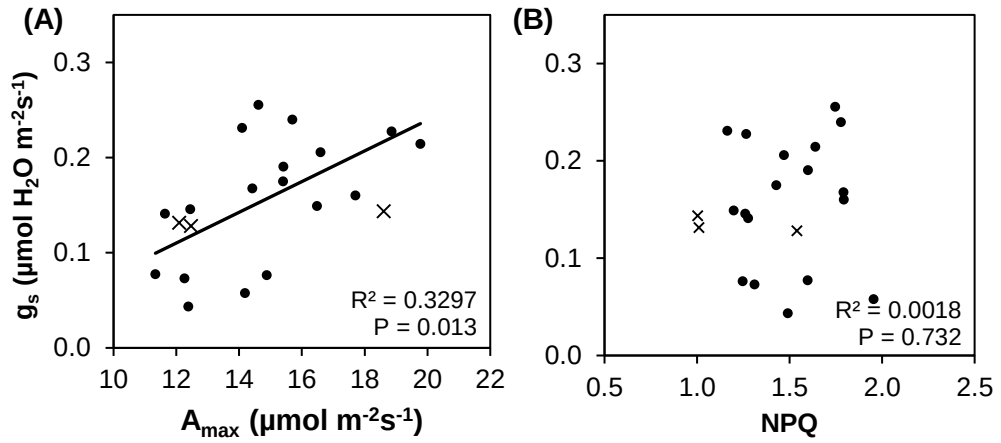


Figure 2-6. A comparison of the stomatal conductance (g_s) of T_0 generation wheat plants overexpressing rice *PsbS* with **(A)** maximum carbon assimilation, A_{max} and **(B)** non-photochemical quenching, NPQ. Control plants were included in the plots as $_X$. Regression analysis using GenStat (VSN International Ltd., Hemel Hempstead, UK) was applied (Foo, 2014).

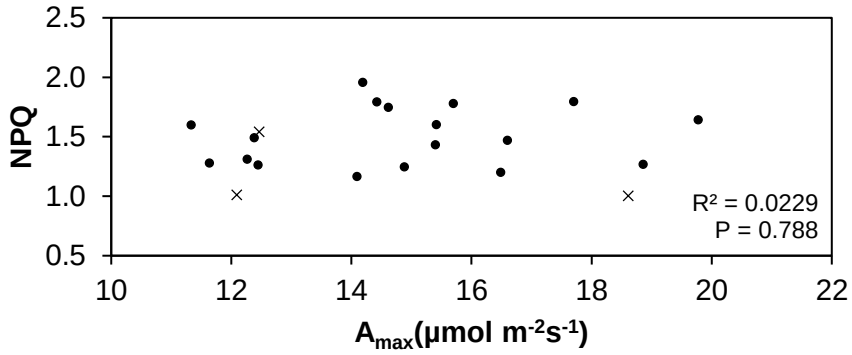


Figure 2-7. A correlation of the non-photochemical quenching, NPQ, of T_0 generation wheat plants overexpressing rice *PsbS* with maximum carbon assimilation, A_{max}. Control plants were included in the plots as X. Regression analysis using GenStat (VSN International Ltd., Hemel Hempstead, UK) was applied (Foo, 2014).

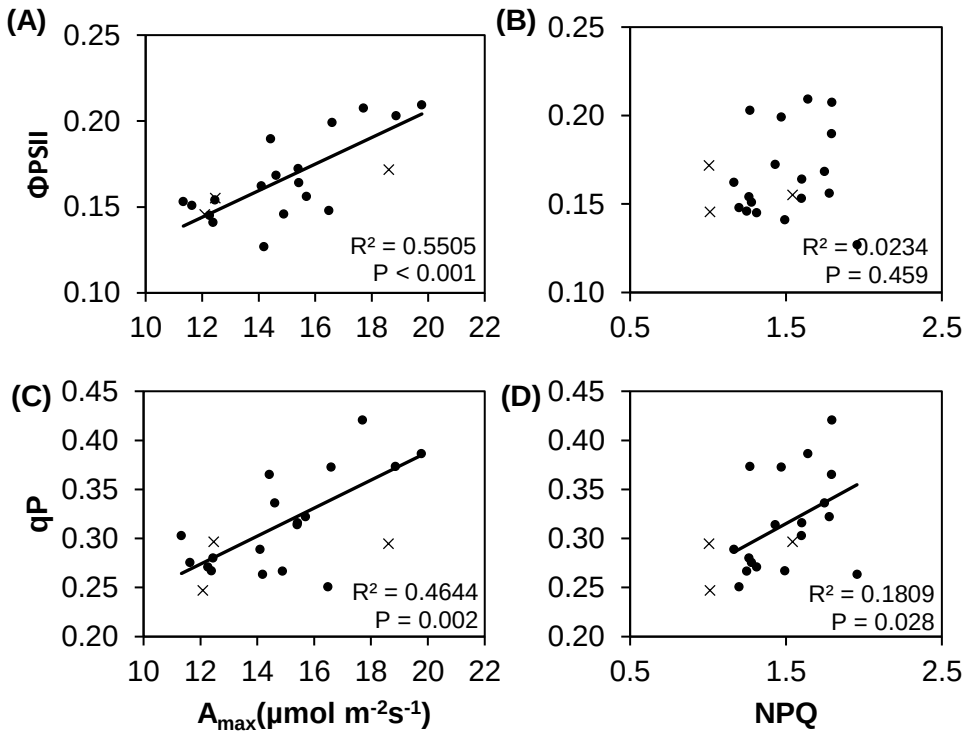


Figure 2-8. A selective comparison of the chlorophyll fluorescence parameters, quantum efficiency of the Photosystem II, ΦPSII and the parameter denoting "openness" of the reaction centers, photochemical quenching, qP against maximum carbon assimilation, A_{max} (**A** and **C** respectively) and non-photochemical quenching, NPQ (**B** and **D** respectively). Control plants were included in the plots as X. Regression analysis using GenStat (VSN International Ltd., Hemel Hempstead, UK) was applied (Foo, 2014).

2.4.2 NPQ expression and gene copy number of the rice transgene in the T_o generation *PsbS* transformant lines

There is a significant but weak correlation between the minimum number of transgene copy in the transgenic plants with the NPQ expression ($F_{(1,19)}$=4.65, P=0.030; Figure 2-9). A one-tailed t-test was conducted to compare the NPQ expression relative to the minimum gene copy number between control plants and *PsbS* transformed lines. There was a difference in NPQ between the control plants which carried no *PsbS* transgene (Mean=1.185; Standard deviation=0.3077; N=3) and *PsbS* transformed lines which carried a minimum of one copy of *PsbS* transgene (Mean=1.502; Standard deviation=0.2458; N=18). The transgenic plants showed significantly higher NPQ levels than the control plants (t(19)=2.01, P=0.030). The variation in NPQ capacity of the *PsbS* transformant lines can be attributed to the natural variation in *PsbS* expression or due to "positional effects whereby the rice *PsbS* transgene could be inserted in a transcriptionally active region resulting in high expression of the rice *PsbS* or in a transcriptionally inactive region resulting in the expression of the "background" wheat *PsbS*.

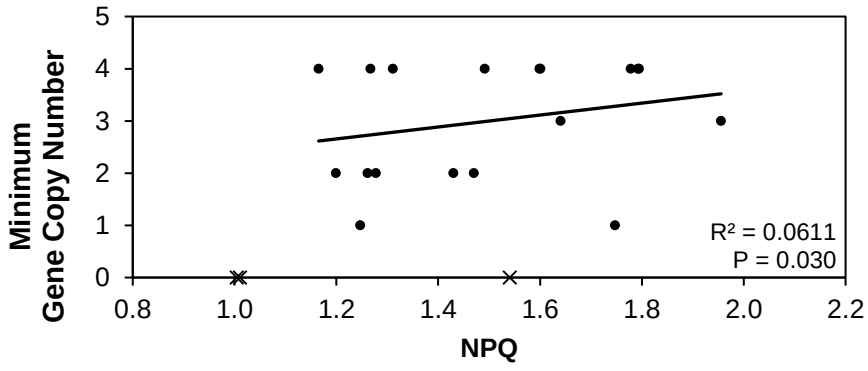


Figure 2-9.A plot between NPQ capacity and minimum number of rice *PsbS* transgene copy in the *PsbS* transformant lines. Control plants were included in the plot as $_X$. T-test using GenStat (VSN International Ltd., Hemel Hempstead, UK) was applied (Foo, 2014).

2.4.3 Selection of homozygous *PsbS* transformant lines from T_1 generation of CW10_17 and CW10_23

Only results where all the PCR analyses using different primer pairs and qRT-PCR analysis matched up were considered reliable. For the ease of reference, the T_1 generation plants for both CW10_17 and CW10_23 are referred to using the code as given in Figure 2-10. In the screening of the T_1 generation of *PsbS* transformant wheat line CW10_17, it was expected there would be low number of plants with the rice *PsbS* transgene as the parent line has 3 or 4 gene copies of the rice *PsbS* gene. Table 2-2 shows the results for the qRT-PCR side by side with the two sets of PCR analyses. Out of all the 60 successfully germinated T_1 generation *PsbS* transformant plants, only six plants were confirmed to have an even number of rice *PsbS* gene (either 2 copies or 4 copies); B-42 and B-53 were the only two plants with two rice *PsbS* gene copies and B-12, B-13, B-16 and B-20 were the only four plants with four rice *PsbS* gene copies. There were eight confirmed azygous control plants (B-14, B-17, B-18, B-36, B-43, B-49, B-56 and B-59). No physiological measurement was carried out on these lines as they were expected to continue segregating. Based on a combination of presence of rice *PsbS* transgene presence and rice *PsbS* gene copy number results, the T_2 generation of CW10_17 was subsequently sown. Plants with an even gene copy number were selected as they have higher chances of being homozygous.

Table 2-2. A collation of the qRT-PCR and PCR results for the T_1 generation of *PsbS* transformant wheat line CW10_17. Some qRT-PCR results (showing transgene copy number) are ambiguous or unsuccessful (N/A) and no PCR analysis was made on them (marked with -). PCR using *PSBS*-F and NOST-Rev is labelled as PCR1 whereas PCR using RP6 and RP7 is labelled as PCR2. ✓ and X denote the presence or absence of rice *PsbS* gene respectively and '–' denotes that no analysis was done. Shaded in grey are putative homozygous *PsbS* transformant lines and shaded in red are azygous control plants. The plant codes correspond to those in Figure 2-10.

Plant	qRT-PCR	PCR1	PCR2	Plant	qRT-PCR	PCR1	PCR2
B-1	N/A	-	-	**B-33**	0	✓	✓
B-2	N/A	-	-	**B-34**	N/A	-	-
B-3	4+	X	✓	**B-35**	0	✓	✓
B-4	4+	X	✓	**B-36**	0	X	X
B-5	N/A	-	-	**B-37**	4	X	✓
B-6	2	?	?	**B-38**	N/A	-	-
B-7	2	X	X	**B-39**	N/A	-	-
B-9	2	X	✓	**B-40**	N/A	-	-
B-10	N/A	-	-	**B-41**	N/A	-	-
B-12	4	✓	✓	**B-42**	2	✓	✓
B-13	4	✓	✓	**B-43**	0	X	X
B-14	0	X	X	**B-45**	0	?	?
B-15	2	X	X	**B-46**	2	X	✓
B-16	4	✓	✓	**B-47**	1	X	✓
B-17	0	X	X	**B-48**	N/A	-	-
B-18	0	X	X	**B-49**	0	X	X
B-19	4	X	X	**B-51**	N/A	-	-
B-20	4	✓	✓	**B-52**	0	X	✓
B-21	2	X	✓	**B-53**	2	✓	✓
B-22	N/A	-	-	**B-54**	N/A	-	-
B-23	N/A	-	-	**B-55**	4	X	X
B-24	N/A	-	-	**B-56**	0	X	X
B-25	1	X	✓	**B-57**	1	X	✓
B-26	2	?	?	**B-58**	2	?	?
B-27	N/A	-	-	**B-59**	0	X	X
B-28	N/A	-	-	**B-60**	N/A	-	-
B-29	0	✓	✓	**B-61**	N/A	-	-
B-30	4	X	X	**B-62**	4	X	✓
B-31	N/A	-	-	**B-63**	N/A	-	-
B-32	N/A	-	-	**B-64**	2	X	X

CW10_17 T_1 Generation				CW10_23 T_1 Generation							
A-1	A-9	~~A-17~~	A-25	~~B-1~~	B-9	B-17	**B-25**	B-33	~~B-41~~	B-49	**B-57**
A-2	A-10	A-18	A-26	~~B-2~~	**B-10**	B-18	B-26	~~B-34~~	B-42	Empty	B-58
Empty	A-11	Empty	A-27	**B-3**	Empty	B-19	~~B-27~~	B-35	B-43	B-51	B-59
A-4	A-12	A-20	Empty	**B-4**	B-12	B-20	~~B-28~~	B-36	Empty	B-52	~~B-60~~
~~A-5~~	A-13	A-21	A-29	~~B-5~~	B-13	B-21	B-29	B-37	B-45	B-53	~~B-61~~
A-6	A-14	A-22	A-30	B-6	B-14	~~B-22~~	B-30	~~B-38~~	B-46	**B-54**	B-62
A-7	Empty	A-23	A-31	B-7	B-15	**B-23**	~~B-31~~	~~B-39~~	**B-47**	B-55	~~B-63~~
A-8	A-16	A-24	Empty	Empty	B-16	~~B-24~~	~~B-32~~	**B-40**	~~B-48~~	B-56	B-64

Figure 2-10. A colour-coded diagram of the qRT-PCR results of T_1 generation of CW10_17 (B) and CW10_23 (A). All germinated plantlets leaf gDNA were sent for qRT-PCR analysis. “Empty” refers to seeds that did not germinate. Plants with ambiguous qRT-PCR and/or PCR analyses results (strikethrough) were discarded. Boxes left uncoloured refers to plants that are confirmed to be heterozygous. Purple colour coded boxes refer to plants with no transgene detected (Azygous), green colour boxes coded for plants that are possibly homozygous for rice *PsbS* transgene (two gene copy number), red colour boxes are plants with at least one rice *PsbS* transgene present. For T_1 of CW10_17, B-25, B-47 and B-57 (lettered in red) were found to have one transgene only. Blue and yellow lettered refer to plants with three or more than four transgene copies respectively.

Selection of homozygous plants from T_1 generation of CW10_23 was easier than that of CW10_17 as the parent has only one rice *PsbS* transgene. Similar to the selection method for T_1 generation of CW10_17, only when all three molecular analyses results were consistent, would the plant be further analysed. The PCR analysis using *PSBS*-F and NOST-Rev primer pairs (Figure 2-11) were compared to the qRT-PCR analysis results (Figure 2-10) to select best matched lines. A-27, A-13, A-26 and A-30 showed positive bands of 1046bp on the electrophoresis gel run and matched up well to the qRT-PCR analysis. A1 and A8 were also selected as the azygous controls as the electrophoresis gel run did not show any band, also matching with the result from the qRT-PCR results.

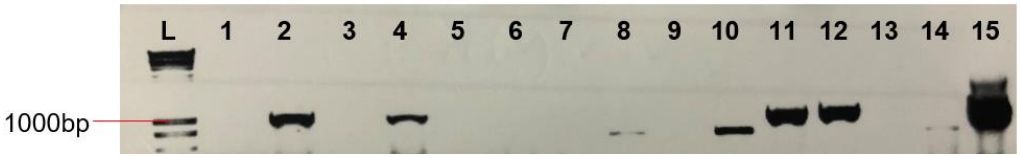


Figure 2-11. PCR results on a screen of the T_1 generation *PsbS* transformant line CW10_23. Gel electrophoresis run of PCR products using rice primers (*PSBS*-F and NOST-Rev) with expected band size of 1046bp. From left to right: **L**: HyperLadder™ (Bioline, London, UK) 1kB DNA ladder, **1**: A-6, **2**: A-27, **3**: A-11, **4**: A-13, **5**: A-22, **6**: A-20, **7**: A-10, **8**: A-8, **9**: A-18, **10**: A-12, **11**: A-26, **12**: A-30, **13**: A-31, **14**: A-1 and **15**: Plasmid containing rice *PsbS* gene.

Those lines which showed positive for both the first PCR analysis and matched with qRT-PCR were further confirmed for gene presence through PCR rice primers (RP6 and RP7) to triple confirm the homozygosity of the lines and also to keep confident azygous controls (Figure 2-12). An expected PCR product band size of 530 bp was observed for the plasmid carrying the rice *PsbS*, rice (Nipponbare) gDNA and the lines with homozygous rice *PsbS*. No band was observed for the azygous control lines, showing that the resulting band observed was due to the presence of rice *PsbS* transgene.

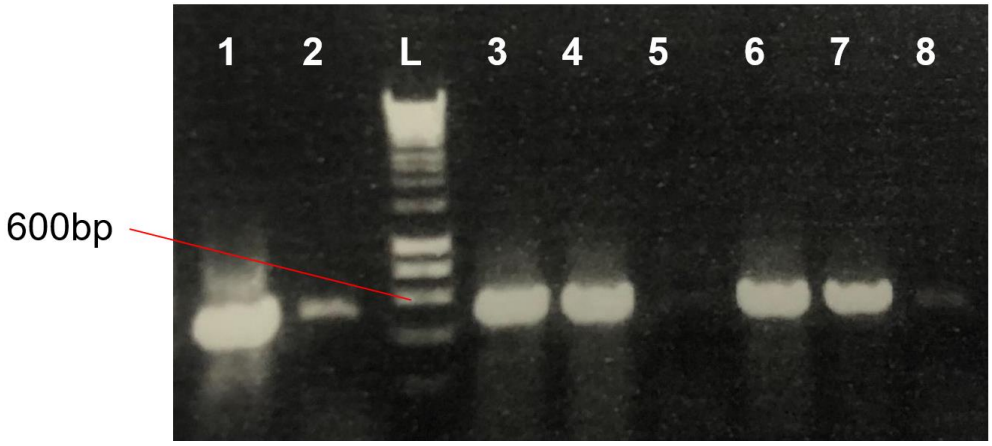


Figure 2-12. T_1 generation *PsbS* transformant line, CW10_23 showed presence of rice *PsbS* gene that was not present in ayzgous controls. Gel electrophoresis run of PCR products using rice primers (RP6 and RP7) with expected band size of 530bp. From left to right: **1**: Plasmid containing rice *PsbS* gene, **2**: Rice (Nipponbare) gDNA, **L**: HyperLadder™ (Bioline, London, UK) 1kB DNA ladder **3**: A-27, **4**: A-13, **5**: A-8, **6**: A-26, **7**: A-30 and **8**: A-1.

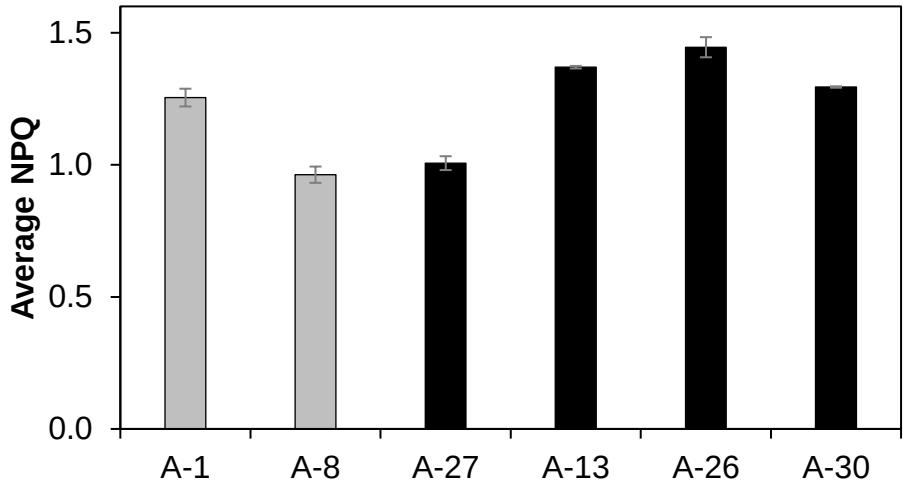


Figure 2-13. A comparison of the average NPQ (n=3) between azygous control (grey bars) and homozygous (black bars) plants of T_1 generation of *PsbS* transformed line, CW10_23. Error bars showed the standard deviation between the last three NPQ values. No statistical difference was observed.

Induction curves were also made using Junior-PAM following the protocol described in Chapter 2.3.3.2. All the wheat plants were measured and one plant, A-18 had a F_v/F_m value lower than 0.78 (measurement done twice, second measurement marked with an asterisk, in Table 2-3). A one-tailed t-

test was conducted to compare the average NPQ expression between the azygous control plants (Mean=1.109, Standard deviation=0.2065, N=2) and homozygous plants (Mean=1.279, Standard deviation=1.279, N=4). There was no statistically significant difference in NPQ expression between them (t(4)=-1.01, P=0.372; Figure 2-13).

Table 2-3. A comparison of the molecular and physiological characterisation results for the T_1 generation of *PsbS* transformed line, CW10_23. Green coded lines were the lines triple confirmed to be either homozygous or azygous. qRT-PCR results showed whether the line was azygous or homozygous. PCR1 referred to PCR analysis using *PSBS*-F and NOST-Rev whereas PCR2 referred to the PCR analysis using RP6 and RP7. ✓ denotes the presence of rice *PsbS* gene, X denotes the absence of rice *PsbS* gene and – denotes that no analysis was done. The red F_v/F_m values highlighted the F_v/F_m value lower than 0.78 (cut-off point for acceptance of NPQ value). Shaded in grey are putative homozygous *PsbS* transformant lines and shaded in red are azygous control plants. No statistically significant differences in NPQ was observed between the azygous and homozygous transgenic plants.

Line name	qRT-PCR	PCR1	PCR2	Fv/Fm	Average NPQ
A-6	Azygous	X	-	0.799	1.690
A-27	Homozygous	✓	✓	0.782	1.006
A-11	Homozygous	X	-	0.803	1.777
A-13	Homozygous	✓	✓	0.800	1.370
A-22	Homozygous	X	-	0.799	1.048
A-20	Azygous	X	-	0.795	1.091
A-10	Azygous	X	-	0.804	1.367
A-8	Azygous	X	X	0.790	0.963
A-18	Homozygous	X	-	0.754	1.049
A-18*	Homozygous	X	-	0.773	1.010
A-12	Azygous	X	-	0.785	1.042
A-26	Homozygous	✓	✓	0.792	1.445
A-30	Homozygous	✓	✓	0.798	1.295
A-31	Homozygous	X	-	0.799	0.883
A-1	Azygous	X	X	0.807	1.255

2.4.4 Screening for homozygous *PsbS* transformant lines in T_2 generation

For the confirmation and further characterization of stable homozygous *PsbS* transformant lines of CW10_17 in T_2 generation, 32 seeds from each of these lines B-16, B-20 and B-53 were sown. In consideration of the ease to work with one rice *PsbS* transgene copy, 24 seeds each from two lines with one rice *PsbS* gene copy (B-25 and B-57) were also sown. Twelve seeds from B-36 were sown as azygous controls. For the T_2 generation selection of homozygous *PsbS* transformant lines of CW10_23, 12 seeds each of A-13, A-26, A-27 and A-30 were sown to further study the putative homozygous *PsbS* transformant lines. Twelve seeds from A-8 were also sown as azygous controls.

The qRT-PCR on the samples were made independently twice. All the qRT-PCR analyses results came back with low reliability (Table 2-4). The qRT-PCR analysis for confirmed homozygous lines (from T_1 generation of CW10_23) showed that the lines continued to segregate resulting in a segregating generation where some progenies had three or more gene copy number. There were also seeds from plants with only one gene copy number resulting in progenies with more than one gene copy number. However, the qRT-PCR results for all azygous controls showed zero rice *PsbS* transgene. The T_2 generation *PsbS* transformant plants also grew poorly and were stunted with very short leaves. Hence, no physiological data were collected on the T_2 generation *PsbS* transformant plants.

Table 2-4. A summary of the number of seeds sown and subsequently sampled for qRT-PCR analysis for the T_2 generation selection of homozygous *PsbS* transformant lines based on T_0 generation parents CW10_17 and CW10_23. The number of plants based on the rice *PsbS* gene copy number is also tabulated.

Parent (T_0)	Plant (T_1)	Rice *PsbS* gene number	Number of seeds		Number of rice *PsbS* gene copy				
			Seeds sown	Sampled	0	1	1 or 2	2 or 3	3 or more
CW10_23	A-8	0 - Azygous	12	9	3	-	-	-	-
	A-13	2 - Homozygous	12	8	-	-	2	-	2
	A-26	2 - Homozygous	12	12	-	-	-	-	-
	A-27	2 - Homozygous	12	11	1	4	1	1	
	A-30	2 - Homozygous	12	8	-	2	1		
CW10-17	B-36	0 - Azygous	12	9	3	-	-	-	-
	B-16	4	32	24	1	-	-	1	1
	B-20	4	32	27	-	4	2	-	-
	B-25	1	24	24	3	2	1	2	2
	B-53	2	32	23	1	2	1	-	3
	B-57	1	24	21	2	6	2	3	1

2.5 Discussion

NPQ studies based on overexpressing *PsbS* have been made in rice, tobacco and Arabidopsis (Hubbart *et al.*, 2012, 2018; Ruban, Johnson and Duffy, 2012; Kromdijk *et al.*, 2016). This is the first instance that a foreign *PsbS* gene has been overexpressed in wheat successfully (Foo, 2014). The higher NPQ expression in wheat lines overexpressing rice *PsbS* observed in T_0 generation prompted further studies. Although higher NPQ expression was observed in these *PsbS* transformant lines, they were relatively low. This could have been due to the growth of the T_0 generation under ambient (400-500 µmol $m^{-2}s^{-1}$) light condition within a growth chamber. Hence, for the subsequent studies, the selection for wheat homozygous for rice *PsbS* transgene was carried out under high light (800 µmol $m^{-2}s^{-1}$). Studies in rice overexpressing *PsbS* showed promising results of enhanced photosynthesis and yield under fluctuating lights (Hubbart *et al.*, 2012, 2018). It would be ideal to select and study the *PsbS* transformant lines under fluctuating lights. However, the capacity to carry this out did not exist at the time.

In order for in-depth characterization of *PsbS* in wheat, wheat plants homozygous for the rice *PsbS* transgene has to be produced. If the *PsbS* transformant lines are not homozygous, they will continue to segregate in the next generation and the progenies would not be similar in genetic background. For example, in the study of wheat canopies, identical wheat plants of the same genetic background and rice *PsbS* transgene insertion is required. Hence, the study proceeded with the selection of homozygous wheat plants overexpressing rice *PsbS* transgene. The earliest instance of obtaining a homozygous wheat line overexpressing rice *PsbS* transgene, this would require at least two subsequent wheat generations from a putative

wheat overexpressing rice *PsbS*.

Ideally, in order to confirm high *PsbS* expression, protein level expression should be investigated. Difficulty working with *PsbS* protein extraction is not new (Foo, 2014). *PsbS* is low in abundance and highly hydrophobic. Hence, it would require working with thylakoid membranes in order to study its expression. Other than labour intensive, a large number of leaves (20 to 40 leaf blades) per plant is required for thylakoid membrane extractions. This also meant that expression studies could not be made during selection of the lines as it would require destruction of the whole plant. Hence, it was easier to first identify wheat plants homozygous for rice *PsbS* transgene and bulk up the seeds for studies. After two generations of selection, we failed to generate homozygous lines and, crucially, did not observe higher NPQ expression in the subsequent generations of the *PsbS* transformant lines. It is assumed that complications arising from the complexity of the wheat genome meant that it was difficult to obtain homozygous lines (Jones, 2005), particularly within the time limitations of the project. It took 18 months to optimize the PCR of rice *PsbS* gene in wheat.

There are numerous reasons that could explain the lack of observation of increased NPQ expression in these wheat *PsbS* transformant lines. The introduction of a foreign promoter and genes into a complex wheat genome could result in poor recognition of the promoter elements and result in a discrepancy in transcription efficiency (McElroy and Brettell, 1994). It was also reported that at a particular locus (sometimes, multiple loci), transgene inserted is capable of self-rearrangement or total elimination of the transgene. These could also be facilitated by DNA repair mechanism of the plant itself (Stoger *et al.*, 1998; Jones, 2005). Coding regions could also be interrupted by the non-coding regions resulting in splicing of genes (Callis, Fromm and

Walbot, 1987). These could interfere the normal growth of the plants; though this was not observed in T_0 and T_1 generations, the introduction of rice *PsbS* gene could have been unstable and resulted in interference in T_2 generation resulting in stunted plants. There were also reports that transgene introduced into cereals did not segregate according to Mendelian inheritance ratios (McElroy and Brettell, 1994; Demeke *et al.*, 1999; Jones, 2005). It was suggested that the ability to introduce the transgene specifically at a known location within the genome would allow more stable inheritance of the transgene in cereal (Callis, Fromm and Walbot, 1987).

2.6 Summary

Studying of NPQ in wheat through overexpression of *PsbS* would divulge useful information pertaining to *PsbS* expression in a complex hexaploid genome. Rice *PsbS* gene was successfully overexpressed in wheat. However, the selection for stable homozygous wheat plants overexpressing rice *PsbS* was unsuccessful and no higher NPQ expression was observed in the subsequent generations. Efforts continued in this direction would allow the study of overexpression of *PsbS* in wheat canopy and potentially, in the field.

Supplementary Material

Supplementary material S2.1

Rice *PsbS* Gene (Os01g64960) Sequence

CGAGGTCATTCATATGCTTGAGAAGAGAGTCGGGATAGTCCAAAATAAAACAAA
GGTAAGATTACCTGGTCAAAAGTGAAAACATCAGTTAAAAGGTGGTATAAAGTAA
AATATCGGTAATAAAAGGTGGCCCAAAGTGAAATTTACTCTTTTCTACTATTATAA
AAATTGAGGATGTTTTTGTCGGTACTTTGATACGTCATTTTTGTATGAATTGGTTT
TTAAGTTTATTCGCTTTTGGAAATGCATATCTGTATTTGAGTCGGGTTTTAAGTTC
GTTTGCTTTTGTAAATACAGAGGGATTTGTATAAGAAATATCTTTAAAAAAACCCA
TATGCTAATTTGACATAATTTTTGAGAAAAATATATATTCAGGCGAATTCTCACAA
TGAACAATAATAAGATTAAAATAGCTTTCCCCCGTTGCAGCGCATGGGTATTTTTT
TCTAGTAAAAATAAAAGATAAACTTAGACTCAAAACATTTACAAAAACAACCCCTA
AAGTTCCTAAAGCCCAAAGTGCTATCCACGATCCATAGCAAGCCCAGCCCAACC
CAACCCAACCCAACCCACCCCAGTCCAGCCAACTGGACAATAGTCTCCACACCC
CCCCACTATCACCGTGAGTTGTCCGCACGCACCGCACGTCTCGCAGCCAAAAAA
AAAAAAAGAAAGAAAAAAAAGAAAAAGAAAAACAGCAGGTGGGTCCGGGTCGTG
GGGGCCGGAAACGCGAGGAGGATCGCGAGCCAGCGACGAGGCCGGCCCTCC
CTCCGCTTCCAAAGAAACGCCCCCCATCGCCACTATATACATACCCCCCCCTCT
CCTCCCATCCCCCCAACCCTACCACCACCACCACCACCACCTCCACCTCCTCCC
CCCTCGCTGCCGGACGACGAGCTCCTCCCCCCTCCCCCTCCGCCGCCGCCGC
GCCGGTAACCACCCCGCCCCTCTCCTCTTTCTTTCTCCGTTTTTTTTTTCCGTCT
CGGTCTCGATCTTTGGCCTTGGTAGTTTGGGTGGGCGAGAGGCGGCTTCGTGC
GCGCCCAGATCGGTGCGCGGGAGGGGCGGGATCTCGCGGCTGGGGCTCTCG
CCGGCGTGGATCCGGCCCGGATCTCGCGGGGAATGGGGCTCTCGGATGTAGA
TCTGCGATCCGCCGTTGTTGGGGGAGATGATGGGGGGTTTAAAATTTCCGCCAT
GCTAAACAAGATCAGGAAGAGGGGAAAAGGGCACTATGGTTTATATTTTTATATA
TTTCTGCTGCTTCGTCAGGCTTAGATGTGCTAGATCTTTCTTTCTTCTTTTTGTGG
GTAGAATTTGAATCCCTCAGCATTGTTCATCGGTAGTTTTTCTTTTCATGATTTGT
GACAAATGCAGCCTCGTGCGGAGCTTTTTTGTAGGTAGACGATAAGCTTGATAT
CACAAGTTTGTACAAAAAAGCAGGCTCCGAATTCGCCCTTCCACCATGGCGCAG
TCGATGCTGGTGTCGGGAGCCAATGGCACGGTGGCCGCCGCGAGCACCAGCA
GGCTGCAGCCCGTGCGGCCGACGCCGTTCTCGCGGCTCGTGCTGTCGCAGCC
GTCGTCGTCGCTGGGGCGCGCGGTGTCCGTCAAGACGGTGGCGCTGTTCGGC
AGGTCCAAGACCAAGGCCGCGCCCGCAAGAAAGGCTGAGCCGAAGCCAAAGTT
CAAGACCGAGGACGGCATCTTCGGCACGTCCGGTGGGATCGGTTTCACCAAGG
AGAACGAGCTGTTCGTCGGGCGTGTCGCCATGCTCGGGTTTGCCGCGTCGATC
CTGGGTGAGGCCATCACCGGGAAGGGAATCCTGGCGCAGCTGAACCTGGAGA
CGGGGATCCCGATCTACGAGGCGGAGCCCCTCCTCCTCTTCTTCATCCTCTTCA
CCCTCCTCGGCGCCATCGGCGCGCTCGGCGACCGTGGCAGCTTCGTCGACGA
CCAGCCGGTGACGGGCCTCGACAAGGCCGTCATCGCCCCGGGCAAGGGCTTC
CGCTCCGCGCTGGGCCTCAGCGAGGGCGGCCCGCTGTTCGGCTTCACCAAGG
CCAACGAGCTGTTCGTCGGCCGGCTCGCGCAGCTCGGCATCGCCTTCTCCATC
ATCGGCGAGATCATCACCGGCAAGGGCGCCCTCGCGCAGCTCAACATCGAGAC
CGGCGTCCCCATCAACGAGATCGAGCCGCTCGTCCTCTTCAACGTCGTCTTCTT
CTTCATCGCCGCCATCAACCCCGGCACCGGCAAGTTCGTCAGCGACGACGACG
AAGAGTAGAATTACGAGGATCGATCGATCTACCGAGGTTTCGCCGCCATTGTTG
TGCTTGCGCATCATTGAGACTTTCTTTCAAGTGTATATGTACTGTGTACGTGTAG
GTGTAAAGACGTACCTTGTTTAATTAGTTGTTAATTAATGCCCATGGAGAAAATTA
ACGTGAAGGGCGAATTCGACCCAGCTTTCTTGTACAAAGTGG

Legend:

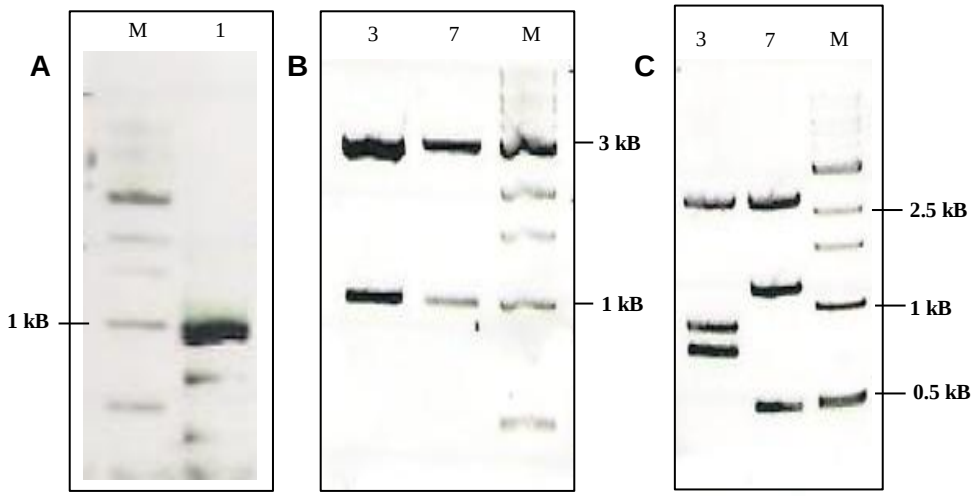
Rice actin Promoter *PsbS* gene with RBS *Attb* cloning sites

Supplementary material S2.2

Supplementary Table S 2-1. Primer pairs list used in genotyping of putative wheat lines overexpressing rice *PsbS*

Primer	Direction	Sequence
RP1	Forward	5'-ATG GCG CAG TCG ATG CTG GTG-3'
RP1B	Forward	5'-CCA CCA TGG CGC AGT CGA TGC TGG TG-3'
RP2	Reverse	5'-CTA CTC TTC GTC GTC GTC GCT G-3'
RP3	Reverse	5'-CAC GTT AAT TTT CTC CAT GGG C-3'
ACTIN PRO F1	Forward	5'-CCC AAA GTG CTA TCC ACG AT-3'
RP5	Forward	5'-CCC CTC CTC CTC TTC TTC AT-3'
RP6	Reverse	5'-CGG CTC GAT CTC GTT GAT-3'
RP7	Forward	5'-CAA GAA AGG CTG AGC CGA AG-3'
RP8	Reverse	5'-CTT GTC GAG GCC CGT CAC C-3'
PSBS-F	Forward	5’- AGT CGA TGC TGG TGT CGG GAG-3’
NosT-rev	Reverse	5’- CGA TCG GGT GAA ATT CGG ATC C-3’
Wheat TaActinF	Forward	5’-CCT CTC TGC GCC AAT CGT-3’
Wheat TaActinR	Reverse	5’-TCA GCC GAG CGG GAA ATT GT-3’

Supplementary material S2.3



Supplementary Figure S 2-1. Results showing successful gene cloning of rice *PsbS* using PCR amplification and restriction mapping. (**A**) PCR amplification of *PsbS* using rice primers (RP1 and RP3) showed a successful amplicon of 1kB band size (Lane 2), matching with the size of *PsbS* sequence (**B**) Restriction of two different colonies (3 and 7) with *EcoRI* showed two bands; 3kB which is approximately the size of pCR8 cloning vector and 1kB which is an approximate size of *PsbS* sequence (**C**) Fragments result from restriction mapping by sequential digestion with *EcoRI* followed by *PvuII*. When the entry vector was restricted in a sequential digestion manner with *EcoRI*, followed by *PvuII*, three fragment sizes of approximately 2.4kB, 0.85kB and 0.8kB were observed as expected for 3 but not for 7. This showed that the gene was inserted in the correct position and orientation for 3. Sequencing data for 3 showed a one base mismatch but the mismatch did not result in any amino acid change after transcription. M denotes NEB 1kB DNA ladder.

Supplementary material S2.4

Supplementary Table S 2-2. PCR and qPCR result of T_o generation *PsbS* transformant lines carried out by NIAB, Cambridge. PCR verified the presence of *PsbS*; '+' denotes presence and '–' denotes absence of transgene. qPCR results showed the number of copies of *PsbS* transgene; '✓' meant the plant was re-potted whereas '×' meant it was not re-potted. Asterisk (*) denotes control plants without *PsbS*.

	Plant Code	*PsbS*	Gene Copy Number	Re-Potted
1	CW9-1	+	4+	✓
2	CW9-2	+	4+	✓
3	CW9-3	+	2 or 3	✓
4	CW9-4	+	4+	✓
5	CW9-5	+	4+	✓
6	CW9-6	+	3	✓
7	CW9-7	+	4+	✓
8	CW9-Con1*	–	0	✓
9	CW9-Con2*	–	0	✓
10	CW10-1	+	4+	✓
11	CW10-2	+	2	✓
12	CW10-3	–	2	✓
13	CW10-4	–	1	✓
14	CW10-5	+	4+	✓
15	CW10-6	+	4+	✓
16	CW10-7	–	0	×
17	CW10-8	+	2 or 3	✓
18	CW10-9	+	4+	✓
19	CW10-10	+	4+	✓
20	CW10-11	+	4+	✓
21	CW10-12	+	4+	✓
22	CW10-13	+	1	✓
23	CW10-14	+	2	✓
24	CW10-15	+	4+	✓
25	CW10-16	+	4+	✓
26	CW10-17	+	3 or 4	✓
27	CW10-18	+	2 or 3	✓
28	CW10-19	+	4+	✓
29	CW10-20	+	4+	✓
30	CW10-21	+	4+	✓
31	CW10-22	+	4+	✓
32	CW10-23	+	1	✓
33	CW10-24	+	4+	✓
34	CW10-25	+	4+	✓
35	CW10-26	+	4	✓
36	CW10-Con1*	–	0	✓
37	CW10-Con2*	–	0	✓

Chapter 3 Investigating non-photochemical quenching dynamics and radiation use efficiency in wheat canopies in the field

C.C. Foo[1], C.R. Zazueta[1,2], G. Molero[2], M. Reynolds[2] and E.H. Murchie[1]

[1] Plant and Crop Science Division, School of Bioscience, University of Nottingham, Sutton Bonington LE12 5RD UK

[2] CIMMYT Carretera Mexico-Veracruz, Km. 45, El Batan, Texcoco 56237 Mexico

Author contribution:

Experiment conceived by EH Murchie and CC Foo

Project supervision performed by EH Murchie, M Reynolds and G Molero

Experimental work by CC Foo

Additional data from CR Zazueta and G Molero

Written by CC Foo

3.1 Abstract

This experiment studied the non-photochemical quenching (NPQ) dynamics within the canopies of four wheat lines with varied radiation use efficiency (RUE) selected from a genetically diverse wheat population in the field in the International Maize and Wheat Improvement Centre (CIMMYT), Obregon, Mexico. The capacity for NPQ was measured at saturating light and compared to the *in situ* at ambient light according to canopy position. It was found that NPQ capacity was higher at the lower portions of the canopy compared to the top. Moreover, the NPQ capacity showed greater variation at the bottom than the top of the canopies. No correlation was found between NPQ capacity and field midday light conditions $NPQ_{(T)}$ measurements. However, $NPQ_{(T)}$ was found to correlate negatively to total RUE and biomass. Selection for a better wheat lines should focus on selection under fluctuating lights and at different canopy levels instead of the youngest fully expanded leaf under the most optimal light level.

3.2 Introduction

Light plays an important role in feeding the world, through photosynthesis in plants (Souza *et al.*, 2009). Canopy radiation use efficiency (RUE) is measured as the amount of dry weight (biomass) generated per unit radiation intercepted by the canopy (Arkebauer *et al.*, 1994; Hammer and Wright, 1994; Dreccer *et al.*, 2000; Morales-Ruiz *et al.*, 2016). RUE is a parameter closely associated with crop productivity under optimal conditions; light can be a limiting factor for field crops due to reliance on canopy photosynthesis rate (Sinclair and Muchow, 1999). Two physiological parameters capable of affecting RUE significantly are quantum efficiency and the maximum leaf photosynthetic rate of the plant (Sinclair and Muchow, 1999). RUE is found to be higher when plants are growing under optimal conditions and not under abiotic (including high light) stress (Hatfield and Dold, 2019a). In wheat, biomass accumulation (RUE) during pre-anthesis and anthesis is crucial for the final yield (Fischer, 1985). Thus, studying photoprotective processes such as non-photochemical quenching (NPQ; see Chapter 1.3.7) and its association with variation in RUE would divulge important information for breeding programs.

In any given light environment, plants would increase the rate of photosynthesis until one or more components within the photosynthetic machinery becomes limiting. Recent research has made it clear that the disposal of the excessive energy, i.e. NPQ is a key limiting factor in photosynthesis in fluctuating light. This is reflected in the shift of photosynthetic research from photosynthesis to photoprotection (Papageorgiou and Govindjee, 2014). In realisation of the importance of photoprotection mechanisms in plants, studies have been made to improve

photoprotection in crops to ensure greater productivity (Murchie and Niyogi, 2011; Hubbart *et al.*, 2012, 2018; Murchie, Ali and Herman, 2015; Kromdijk *et al.*, 2016). However, many studies on photoprotection in crops were carried out under controlled and optimal conditions and, critically did not measure canopy RUE (see Hubbart *et al.*, 2018). Hence for the large part the link between canopy RUE and photoprotection has not been made.

Studies of useful crop traits are usually made under controlled glasshouse conditions with the consideration of eliminating any other co-variations or possible conditions that could affect the traits being studied. More often than not, successful selection of favourable traits under controlled conditions does not translate to the field conditions (Castiglioni *et al.*, 2008; Poorter *et al.*, 2009; Pierre *et al.*, 2012; Araus, Serret and Lopes, 2019). Photosynthetic traits are complex and the genes underlying the regulation of photosynthetic responses are not completely understood. The highly variable and constantly fluctuating field conditions such as cloud movement, windiness, precipitation, etc., could add to this complexity (Burgess *et al.*, 2016). Hence, screening of crops should be carried out under field conditions where feasible or under realistic controlled environments. Furthermore, crops such as cereals are generally cultivated in a whole canopy form which adds more complexity to experimental studies (Murchie *et al.*, 2002; Hubbart *et al.*, 2012).

A fully formed cereal canopy such as wheat consists of a complex three-dimensional (3D) arrangement in which light is extinguished exponentially from the top to bottom but each leaf is commonly exposed to complex fluctuating light patterns, commonly shifting between light saturation and light limitation within seconds. Within such an environment, photoprotective mechanisms such as NPQ will play an important role, however they have not been studied extensively due to the difficulty of characterising and describing

such an environment and linking the data to photosynthetic measurements. However, with the incorporation of 3D modelling and mathematical predictions into actual data collected, highly reliable predictions could be achieved within a crop canopy (Burgess *et al.*, 2015, 2017; Pound *et al.*, 2017). This is essential for progress in terms of realistic prediction of future crop canopy productivity.

In collaboration with International Maize and Wheat Improvement Centre (CIMMYT), Mexico, photoprotection dynamics in field-grown PSTails wheat canopies are studied here. PSTails is an elite panel of wheat varieties selected from High Biomass Association Mapping Panel (HiBAP; Molero *et al.*, 2019) and Bread Wheat Diversity Panel (BWDiv; Smale *et al.*, 2002) based on genetic diversity, contrasting RUE, photosynthesis (P) and respiration (S) data; hence the name PSTails. The main aim of the experiment was to investigate the NPQ variation within the wheat canopies under the rigorous field conditions. The dynamics of non-photochemical quenching (NPQ) were studied and compared to the light levels within wheat canopies in the field. Rapid $NPQ_{(T)}$ (Tietz *et al.*, 2017) measurements were also used to screen a random subset of the PSTails. $NPQ_{(T)}$ is a relatively new parameter derived as a variation of the NPQ parameter using the Stern-Volmer approximation. Measurements for NPQ require dark-adaptation of the plant material to ensure full relaxation of the PSII reaction centres, resulting in a time-consuming protocol for each measurement. However, it allows a good estimation of NPQ capacity at saturating light levels. On the contrary, $NPQ_{(T)}$ allows rapid measurements of NPQ in dynamic (fluctuating) light conditions since no pre dark adaptation or actinic treatment is required but may present inaccuracies when comparing absolute values of NPQ one variety against another (Murchie *et al.*, 2018). It was suggested that $NPQ_{(T)}$ correlates to

NPQ in a linear manner if measured under the same conditions. Therefore, this should be a good parameter for screening of large crop populations, something that has not been achieved so far. In this study, we compare the induction and relaxation rates of photosynthesis and photoprotection at different canopy positions in wheat lines with varied RUE values. We hypothesize that wheat canopies with greater NPQ and/or faster induction or relaxation rates of NPQ will be associated with higher RUE. We also hypothesize that NPQ capacity and dynamics will vary according to canopy depth.

3.3 Materials and methods

3.3.1 Plant material

A total of 80 different genotypes of PSTails were sown on the 5th of December 2017 in a “camas” style where plants are sown in tight rows at a high density in the field in CIMMYT station in Obregon, NW Mexico (Figure 3-1). Four contrasting wheat lines from PSTails were selected based on previous year RUE and yield data for in-depth NPQ dynamics study. An additional randomly selected 16 lines were included for rapid $NPQ_{(T)}$ measurements (Details on $NPQ_{(T)}$ measurements to follow in Chapter 3.3.2.2). All the 20 lines used for this experimental study and their yield, RUE and photosynthesis data are tabulated in Table 3-1. Four replicates were sown but only three were used due to mechanical error during sowing of the fourth replicate. A randomized block design was used for the field experiments. All the experimental plots were managed and flood-irrigated by CIMMYT as and when required.

Table 3-1. 20 out of the 80 PSTails used in the experiment. The top four lines were selected based on 2016/7 yield category and radiation use efficiency (RUE) data. RUE1, RUE2 and RUET are the RUE recorded from initiation of booting to 7-days post anthesis, during grain filling and the total RUE recorded during the whole crop cycle respectively. Maximum photosynthesis (P_{max}) was measured during 7-days post anthesis. Unpublished confidential data provided by G Molero and C Robles (CIMMYT, Mexico).

Line	Wheat line	Yield / gm^{-2}	RUE1 / gMJ^{-1}	RUE2 / gMJ^{-1}	RUET / gMJ^{-1}	P_{max} / $\mu mol\ m^{-2}s^{-1}$
1	KUKRI	525	1.156	0.685	0.781	19.8
2	CHEWINK #1	705	1.264	1.459	1.123	25.9
3	SOKOLL//PUB94.15.1.12/WBLL1	603	0.955	1.378	1.055	28.5
4	W15.92/4/PASTOR//HXL7573/2*BAU/3/WBLL1	582	1.473	0.679	0.940	28.3
5	PAVON F 76	504	1.10	0.74	0.82	21.0
6	BACANORA T 88	564	0.92	0.95	0.82	32.2
7	ATTILA	601	1.19	1.17	0.97	21.7
8	BAVIACORA M 92	617	1.27	0.92	0.92	23.9
9	SERI/RAYON	587	1.17	0.98	0.90	28.0
10	BRBT1*2/KIRITATI	597	0.99	0.99	0.91	29.1
11	KRICHAUFF	485	1.12	0.82	0.86	26.1
12	SAUAL/WHEAR//SAUAL	586	1.12	0.82	0.87	24.0
13	SOKOLL/WBLL1	600	1.01	0.98	0.98	26.2
14	MUNAL #1	541	1.51	0.62	0.81	19.4
15	PBW343*2/KUKUNA*2//FRTL/PIFED	601	1.09	0.92	0.85	23.8
16	JANZ	560	1.05	N/A	N/A	26.5
17	EGA BONNIE ROCK	N/A	N/A	N/A	N/A	N/A
18	SOKOLL	N/A	N/A	N/A	N/A	N/A
19	PFAU/WEAVER*2//TRANSFER#12,P88.272.2	569	0.96	0.91	0.84	26.4
20	MEX94.28.2	N/A	N/A	N/A	N/A	N/A

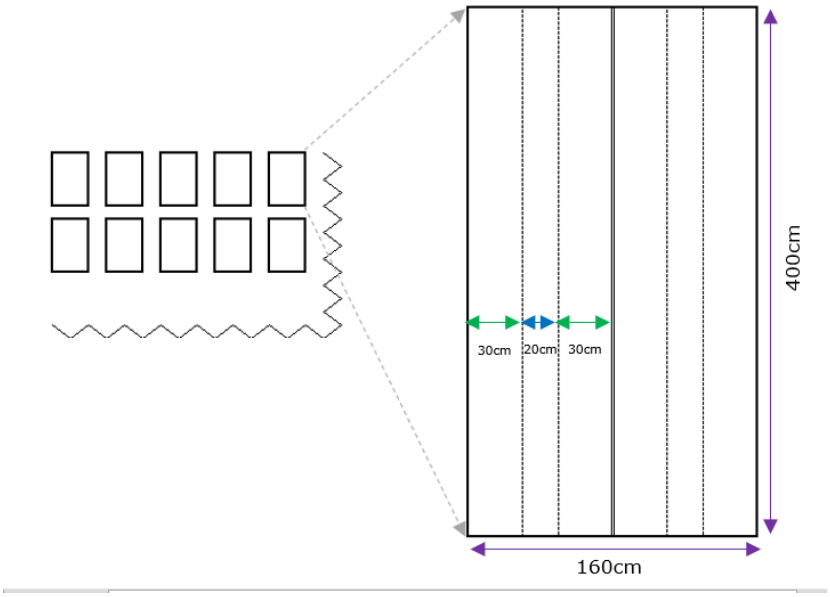


Figure 3-1. Camas sowing system involved two subplots within a plot. Each plot is 400 cm long and 160 cm wide. Within each 80 cm subplot, plants are tightly sown in two rows 20 cm apart from one another leaving a 30 cm gap on the outer sides. Each plot is 100 cm apart from one another from either side.

3.3.2 Physiological measurements

For measurements purposes, the canopies were divided into top and bottom using the midpoint of the canopy height (measured using a metre ruler) as a reference. The part of the canopy above the midpoint was considered the top layer of the canopy and the part below the midpoint was the bottom layer of the canopy (Figure 3-2). Fractional interception for each canopy layer was measured at the top and bottom of each canopy layer using an AccuPAR LP-80 ceptometer (Decagon Devices, Washington, USA) during midday. Five ceptometer measurements were taken diagonally across each plot at the top and bottom positions of each layer (points A and B for top layer and points B and C for bottom layer of the canopy; Figure 3-2). The light incident on the leaf at the point where leaf measurements were made were recorded using

MultiSpeQ (PhotosynQ, Michigan, USA). All chlorophyll fluorescence and gas exchange measurements were made during booting stage (GS 41) between 10:00H and 13:00H of the day. At the top of the canopy, the flag leaf was sampled for measurements whereas at the bottom of the canopy, a green healthy-looking leaf was used in measurements.

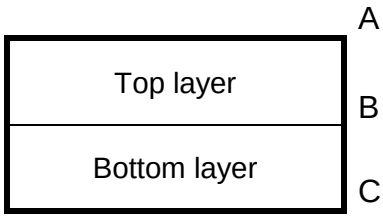


Figure 3-2. A simple two-dimensional illustration of the side view of a canopy. The canopy was divided into two layers based on the midpoint of its height. 'A' is the point at the top of the canopy, 'B' is the mid-point of the canopy while 'C' is the bottom of the canopy which corresponds to ground level.

3.3.2.1 Chlorophyll fluorescence and gas exchange measurements

A LI-6400XT (LI-COR Biosciences, Nebraska, USA) was used for the chlorophyll fluorescence and gas exchange measurements. Measurements were made for Lines 1 to 4 only (Table 3-1). The youngest (or healthiest, in the case of bottom of the canopies) fully expanded leaf was selected for measurements. The width of the leaf was recorded to calculate the leaf area covering the cuvette prior to dark-adaptation with aluminium foil. The leaf section was dark-adapted for a minimum of an hour before carefully attached to the IRGA chamber, making sure that the leaf section was not exposed to ambient light.

An automated programme was used to determine NPQ induction and NPQ relaxation. A two-minute wait time was set at the start of the programme to

allow stabilization of the leaf within the chamber. The sample and reference IRGAs were equilibrated (matched) automatically to prevent drift prior to each measurement. Initially, dark-adapted chlorophyll fluorescence parameters, F_o, F_m, and F_v (=F_m-F_o) were logged. Following this, photosynthesis was induced with PAR supplied at 1800 µmol $m^{-2}s^{-1}$. Gas exchange measurement was logged every ten seconds whereas chlorophyll fluorescence was logged every minute throughout the automated programme. The induction phase consisted of 15 photosynthetic points with the application of a saturating pulse every minute to measure F_s', F_m', F_v' and F_o' which permitted the determination of NPQ, qP, ΦPSII etc. It was then followed by a second phase involving five photosynthetic relaxation points with the application of a saturating pulse every minute as described above but at a lowered PAR of 100 µmol $m^{-2}s^{-1}$. Throughout the whole automated programme, the ambient carbon dioxide concentration in the cuvette was kept at 400ppm, block temperature was maintained at 28°C, flow rate was set at 300mLmin^{-1} and relative humidity set between 55-65%.

3.3.2.2 Rapid $NPQ_{(T)}$ measurements

'Point' measurements of $NPQ_{(T)}$ were made using MultiSpeQ V1.0 (PhotosynQ, Michigan, USA; Kuhlgert *et al.*, 2016) following the protocol outlined in Tietz *et al.* (2017). A standard protocol for plants (Photosynthesis RIDES, Firmware version 1.22) which measures photosynthesis-related parameters (in particular, the new parameter $NPQ_{(T)}$ were of interest; see Supplementary material S3.1 for the list of parameters) were used. MultiSpeQ was clamped onto leaves with the PAR sensor pointing upwards, parallel to the ground. Saturation pulse chlorophyll fluorescence yield parameters were

recorded using one second saturating pulses (10000 µmol photons m^{-2} s^{-1}, λ=650 nm). After saturation pulse, the actinic light was turned off and a far-red light (5 µmol photons m^{-2} s^{-1} from an LED source emitting at 730nm) lasting six seconds was initiated. These allowed for the calculation of light adapted NPQ parameter, $NPQ_{(T)}$, as described in Tietz *et al.* (2017). The ambient light at which samples were exposed to at the point of measurement and chlorophyll. Measurements were made on all the lines listed in Table 3-1 on both adaxial and abaxial sides of selected leaf. At the top of the canopy, flag leaves were used whereas at the bottom of the canopy, healthy leaves below the mid-point height of canopy were used.

3.3.3 Statistical analysis

Analysis of variance (ANOVA) and regression analyses were carried out on the data collected using the statistical package, *Genstat* (19th Edition) for Windows (VSN International Ltd., Hemel Hempstead, UK). They were analysed based on the probability generated by *Genstat* whereby a P value of less than 0.05 ($P<0.05$) shows significant interactions and P value greater than 0.05 ($P>0.05$) shows insignificance. Data were checked to have met the assumption of constant variance and normal distribution of residuals.

3.4 Results

3.4.1 Light environment in the canopy

The light intercepted at each of the three canopy positions (P=0.830; Figure

3-2) within the canopies were not significantly different between each of the lines (Lines 1 to 4, Table 3-1). This can be attributed to “camas” (Figure 3-1) sowing style. However, the light intensity for all the four lines were significantly different at canopy position levels and over the three days of measurements (P=0.015; Figure 3-3). As expected, light intensity at canopy position A was significantly higher than the light at canopy positions B and C (P<0.001). Light at canopy position B was higher than the light at canopy position C (P=0.045). Light intensity was also recorded at leaf level at where the point measurements using MultiSpeQ (PhotosynQ, Michigan, USA) were made. Similarly, there were no differences between each line at each canopy layer (P=0.815) but the top canopy layer had higher light intensity than the bottom of the canopy for all the lines (P<0.001; Figure 3-4).

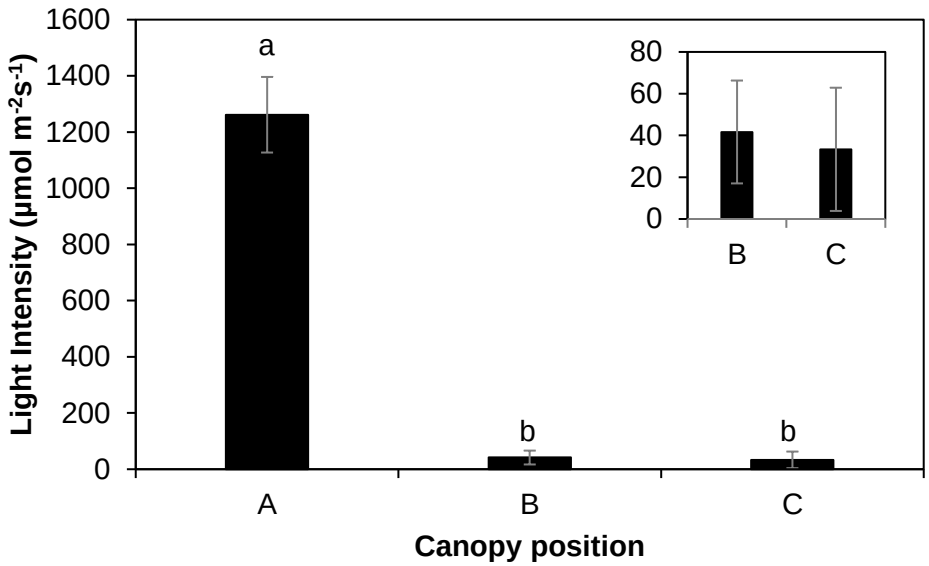


Figure 3-3. The average light intensity measured using a ceptometer (Decagon Devices, Washington, USA) at points A, B and C (Figure 3-2) of the canopy for Lines 1 to 4 (Table 3-1) over three days. The right inset magnified the differences between the light intensity at Point B and Point C of the canopy. The error bars showed standard error of mean amongst the replicates over three days (n=9). Significant differences at 5% are denoted by alphabets a, b etc.

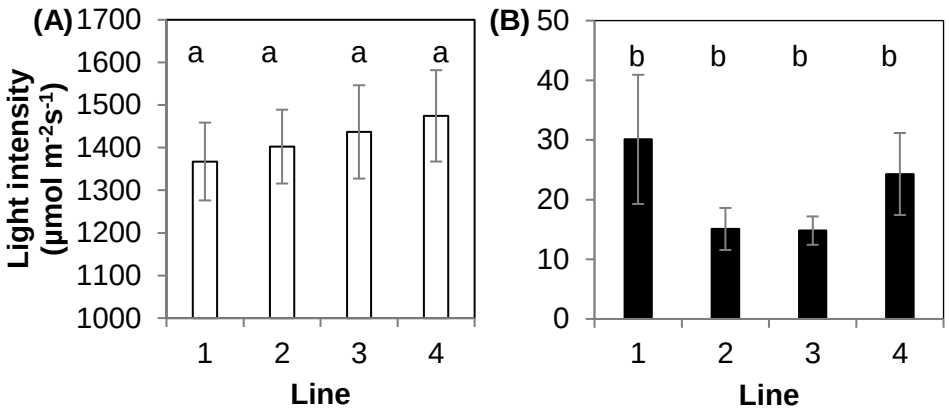


Figure 3-4. A comparison of light intensity measured at the leaf measurement points at the **(A)** top and **(B)** bottom layers of the canopies for Lines 1 to 4 (Table 3-1). The measurements were made using MultiSpeQ (PhotoSynQ, Michigan, USA). The error bars showed standard error of mean amongst the replicates over three days (n=9). Significant differences are denoted by alphabets a, b etc.

Canopy fractional interception was measured on the four lines; there was no statistical significance difference between the four lines regardless of the canopy position (P=0.987; Figure 3-5A). Although the bottom of the canopies showed higher numerical value of fractional interception than the top of the canopies, there was no statistically significant differences between the top and bottom of the canopies (P=0.466). There was a trend indicating that F_v/F_m value at the bottom of the canopy was higher than the top of the canopy at 10% level (P=0.054) indicating photoinhbition at the top of the canopy (F_v/F_m <0.8; Figure 3-5B).

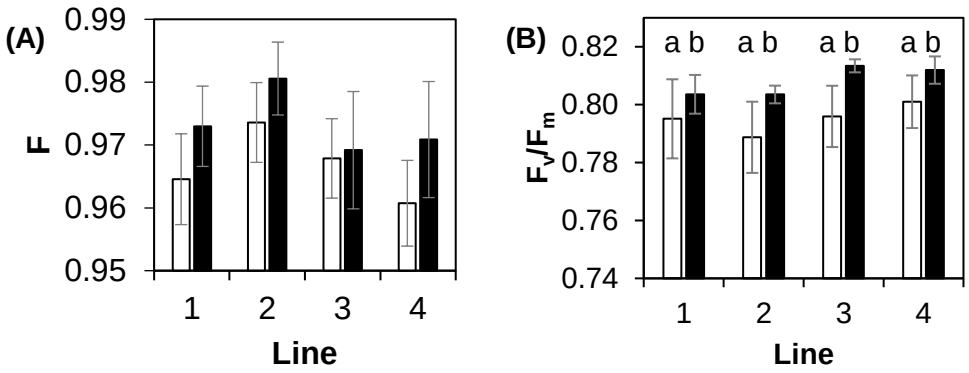


Figure 3-5. A comparison of the **(A)** fractional interception, F and **(B)** maximum quantum efficiency, F_v/F_m values at the top (white) and bottom (black) of the canopies for Lines 1 to 4 (Table 3-1). The error bars showed standard error of mean for measurements over three days (n=9). Significant differences are denoted by alphabets a, b etc.

3.4.2 Chlorophyll fluorescence and gas exchange

Figure 3-6 shows the progress of gas exchange parameters during induction at high light (1800µmol $m^{-2}s^{-1}$) and recovery at low light (100µmol $m^{-2}s^{-1}$) at the top and bottom of the canopy layers using LI-6400XT (LI-COR Biosciences, Nebraska, USA) over time. Carbon assimilation increased at a relatively slower rate and reached a lower capacity at the bottom canopy layer compared to the top layer (Figure 3-6A; $P<0.001$). The bottom of the canopy also showed a slower induction rate of stomatal conductance compared to the top layer (Figure 3-6B; $P=0.001$). However, NPQ at the bottom canopy layer had a slightly lower rate of induction but increased steadily to reach a higher capacity than the top layer which may be due to the generation of slowly relaxation of photoinhibition, qI-type quenching rather than energy-dependant quenching, qE (Figure 3-6C; $P<0.001$). This seems to be confirmed by the retention of high NPQ at low light and the slow accumulation of NPQ in high light during induction in the low light leaves.

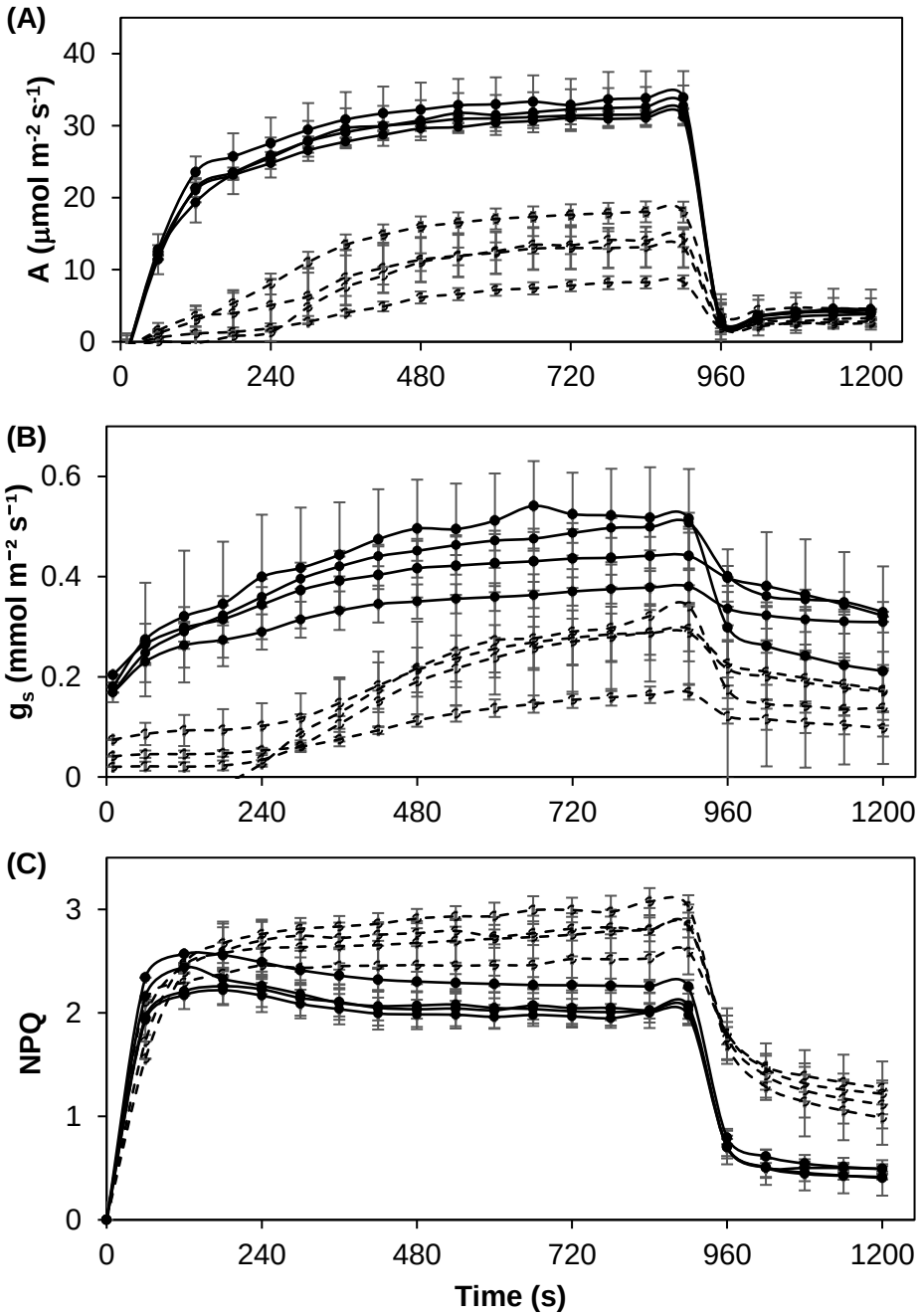


Figure 3-6. Plots of **(A)** carbon dioxide assimilation rate (A), **(B)** stomatal conductance (g_s) and **(C)** non-photochemical quenching (NPQ) of the top and bottom of the canopies for Lines 1 to 4 (Table 3-1) induced at 1800µmol $m^{-2}s^{-1}$ for fifteen minutes followed by 100µmol $m^{-2}s^{-1}$ for five minutes. Measurements for gas exchange were logged every 10 seconds and fluorescence measurements were logged every minute. Solid lines represent the measurements on top of the canopy whereas dashed lines represent the measurements made on the bottom of the canopy. The error bars denote the standard error of mean between the replicates (n=3).

A selection of the steady-state chlorophyll fluorescence and gas exchange parameters of the Lines 1 to 4 (Table 3-1) during each phase was calculated by taking the average of the last three steady state values during each phase. The steady state maximum carbon assimilation rate (A_{max}), quantum efficiency of PSII (ΦPSII) and the parameter denoting the "openness" of the reaction centres, photochemical quenching (qP) between the induction or relaxation phases of Lines 1 to 4 are shown in Figure 3-7. There were no differences in most of the chlorophyll fluorescence and gas exchange parameters at steady state between the four lines except for the carbon dioxide assimilation rate (Figure 3-7A) which was different between the lines after induction at 1800 µmol $m^{-2}s^{-1}$ at 10% significance level (P=0.051). The significant difference in steady-state carbon assimilation between the lines was also observed during relaxation at 100 µmol $m^{-2}s^{-1}$ at a 5% significance level (P=0.040).

Significant differences in ΦPSII, NPQ, qP, maximum carbon assimilation rate, stomatal conductance and transpiration rate were observed between the top and bottom canopy layers indicative of 'classic' indicators of light acclimation and leaf ageing (P<0.001; Table 3-2 and Table 3-3). There were no significant interactions between the wheat lines and canopy layers. It was expected that the younger leaves at the top canopy layer would have relatively higher carbon assimilation and stomatal conductance than the older leaves at the bottom of the canopy during induction phase but not necessarily during the light limited relaxation phase.

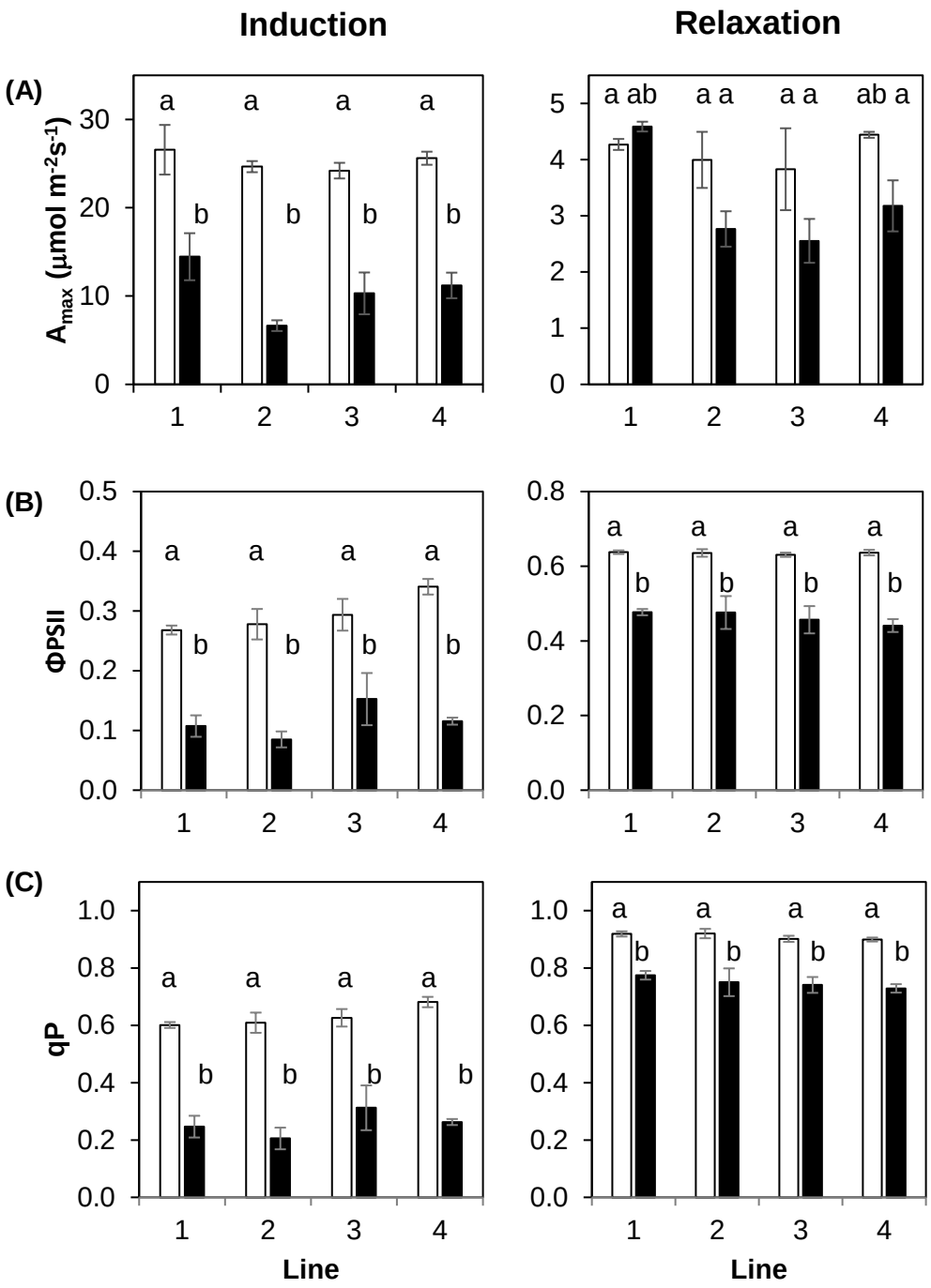


Figure 3-7. The averages of the **(A)** maximum carbon assimilation rate (A_{max}), **(B)** quantum efficiency of PSII (ΦPSII) and **(C)** the parameter denoting the "openness" of the reaction centres, photochemical quenching (qP) between Lines 1 to 4 (Table 3-1) at the top (white) and bottom (black) of the canopies after 15 minutes induction at 1800µmol $m^{-2}s^{-1}$ (left) and 5 minutes relaxation at 100µmol $m^{-2}s^{-1}$ (right). The error bars showed standard error of mean for the replicates (n=3). Significant differences are denoted by alphabets a, b etc.

Table 3-2. The P-values of the ANOVA analysis for the averages of the last three logged values of chlorophyll fluorescence and gas exchange parameters during induction phase of Lines 1 to 4 (Table 3-1; Line) at the two canopy layers (Layer). The interaction between the lines and canopy layers (Line*Layer) was also analysed. Red P-values showed significance at 5% level. Blue P-values showed significance at 10% level.

Parameters	**Line**	**Layer**	**Line*Layer**
Quantum efficiency of PSII, ΦPSII	0.141	<0.001	0.324
Non-photochemical quenching, NPQ	0.326	<0.001	0.519
Photochemical quenching, qP	0.299	<0.001	0.552
Carbon assimilation rate, A (mol $m^{-2}s^{-1}$)	0.051	<0.001	0.342
Stomatal conductance, g_s (mol $m^{-2}s^{-1}$)	0.430	0.001	0.591
Transpiration rate, E (mmol H_2O $m^{-2}s^{-1}$)	0.993	0.006	0.343

Table 3-3. The P-values of the ANOVA analysis for the averages of the last three logged values of chlorophyll fluorescence and gas exchange parameters during relaxation phase of Lines 1 to 4 (Table 3-1; Line) at the two canopy layers (Layer). The interaction between the lines and canopy layers (Line*Layer) was also analysed. Red P-values showed significance at 5% level.

Parameters	**Line**	**Layer**	**Line*Layer**
Quantum efficiency of PSII, ΦPSII	0.806	<0.001	0.843
Non-photochemical quenching, NPQ	0.722	<0.001	0.778
Photochemical quenching, qP	0.575	<0.001	0.782
Carbon assimilation rate, A (mol $m^{-2}s^{-1}$)	0.040	0.004	0.939
Stomatal conductance, g_s (mol $m^{-2}s^{-1}$)	0.614	0.007	0.219
Transpiration rate, E (mmol H_2O $m^{-2}s^{-1}$)	0.742	0.031	0.768

In order to compare the relative rates of induction and relaxation, the carbon assimilation rates, A and NPQ were both normalized to their maximum value at 1800µmol $m^{-2}s^{-1}$ as shown in Figure 3-8. NPQ induction half-times were higher at the top of the canopy than the bottom of the canopy ($P<0.001$; Figure 3-9A). On the contrary, the NPQ relaxation half-times were higher at the bottom of the canopy than the top of the canopy ($P=0.003$; Figure 3-9B).

There was no statistically significant difference found between the four lines in terms of NPQ induction half-times (P=0.893) or NPQ relaxation half-times (P=0.180). However, the NPQ induction half-times were significantly higher at the top of the canopy later than the bottom canopy layer (P<0.001). There was no correlation between the rate of NPQ induction and rate of NPQ relaxation (P=0.888).

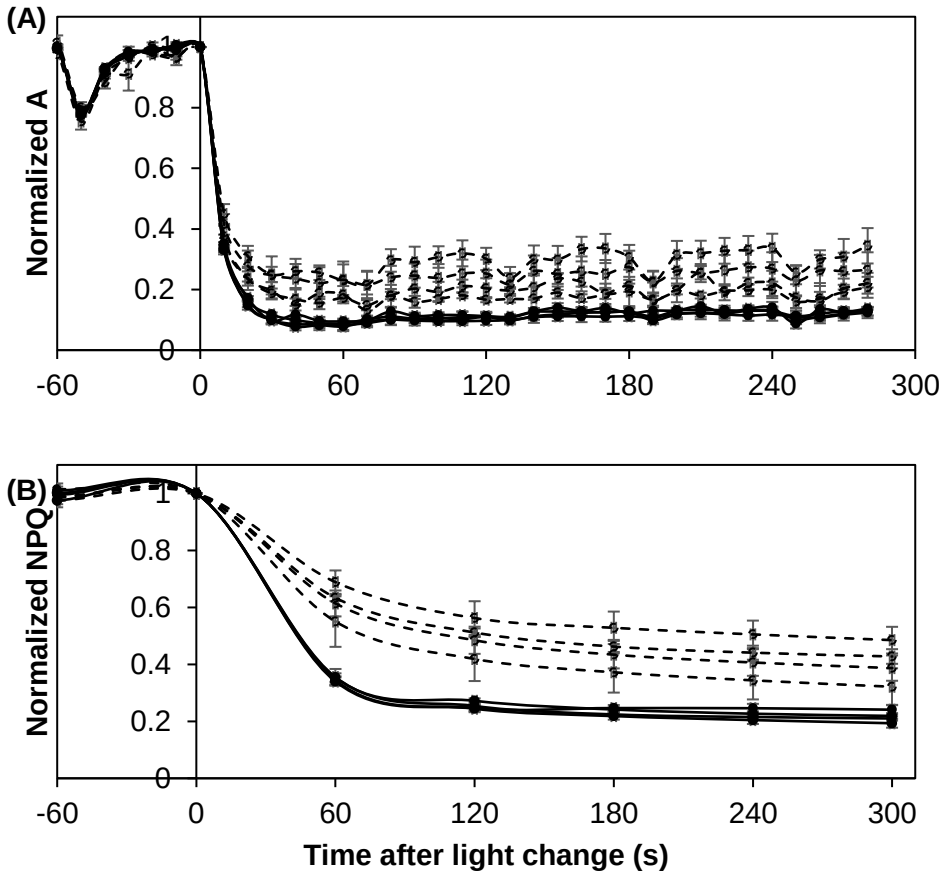


Figure 3-8. The **(A)** carbon assimilation rate (A) recovery and **(B)** non-photochemical quenching (NPQ) recovery of the top and bottom of the canopies for Lines 1 to 4 (Table 3-1) after light intensity was reduced from 1800µmol $m^{-2}s^{-1}$ to 100µmol $m^{-2}s^{-1}$. Values have been normalized against the final value at 1800µmol $m^{-2}s^{-1}$. Measurements for gas exchange was logged every 10 seconds and fluorescence measurements was logged every minute. Solid lines represent the measurements on top of the canopy whereas dashed lines represent the measurements made on the bottom of the canopy. The error bars denote the standard error of mean between the replicates (n=3).

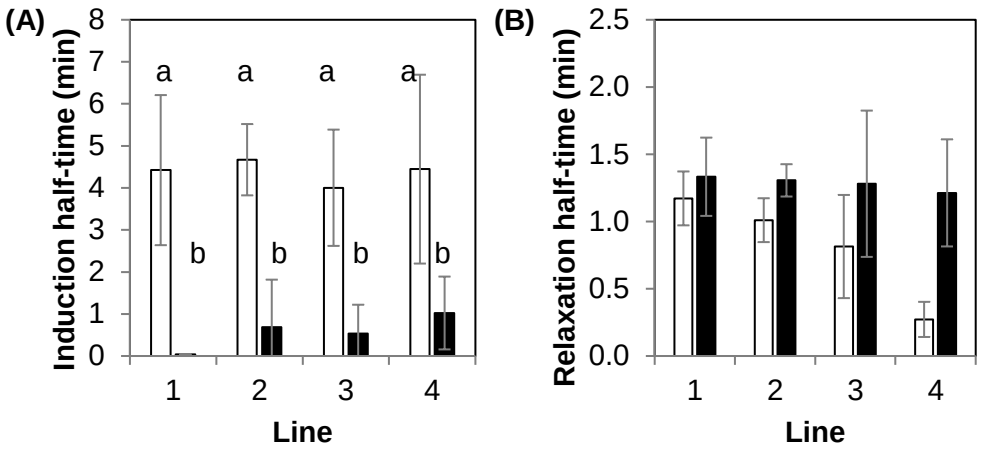


Figure 3-9. The averages of the non-photochemical quenching, NPQ **(A)** induction half-time and **(B)** relaxation half-time for the top (white) and bottom (black) of the canopies for Lines 1 to 4 (Table 3-1). NPQ induction and relaxation data was fitted to an exponential model using MATLAB (Mathworks, version 2019b). The error bars denote the standard error of mean between the replicates (n=3). The significance differences are denoted with the alphabets a, b etc.

3.4.3 Non-photochemical quenching measured under ambient light ($NPQ_{(T)}$) as a screening tool

The MultiSpeQ (PhotosynQ, Michigan, USA) measures $NPQ_{(T)}$ according to the ambient light level by replicating the external photosynthetically active radiation (PAR) using an internal light source in the device. Hence, it makes a crucial comparison with the NPQ measured at saturating light level of 1800µmol $m^{-2}s^{-1}$. Figure 3-10B shows the $NPQ_{(T)}$ values at top and bottom canopy layers. Greater variation (error bars) is observed between the values of $NPQ_{(T)}$ compared to NPQ due to the variation in ambient light. As expected, there were significant differences between the NPQ capacity and $NPQ_{(T)}$ at canopy layers ($P<0.001$). However, they showed opposite trends; the bottom canopy layer showed higher NPQ capacity but had lower NPQ

whereas top canopy later showed lower NPQ capacity but had higher NPQ. These can be explained by the fact that the leaves at the top canopy layer are exposed to high light conditions compared to the bottom canopy layer hence, triggering the increase in NPQ. With respect to NPQ capacity, the bottom canopy layer consisted of mainly older leaves which were reported to show increased photoprotective capacity in Arabidopsis (Carvalho, Ware and Ruban, 2015). There were significant differences in $NPQ_{(T)}$ between the four lines measured but not their NPQ capacity ($NPQ_{(T)}$, P=0.003; NPQ capacity, P=0.337).

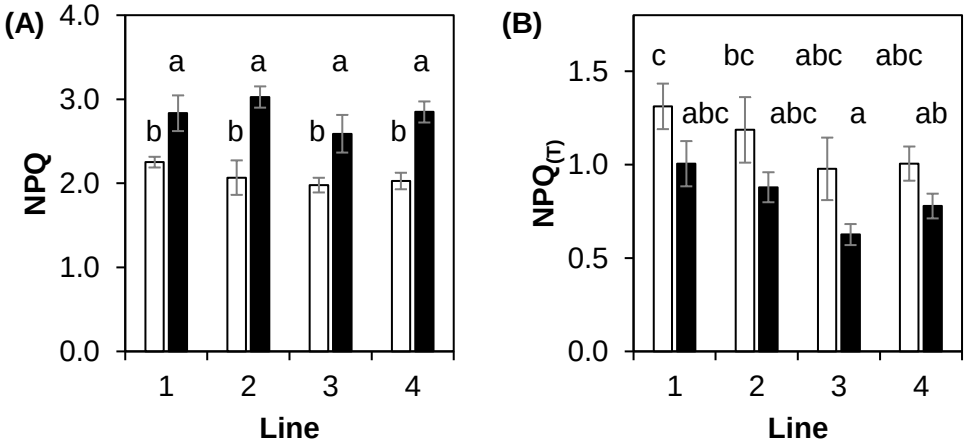


Figure 3-10. The average of the **(A**) non-photochemical quenching, NPQ capacity measured under constant light (1800µm^{-2}s^{-1}) and the **(B)** NPQ measured under ambient light in the field, $NPQ_{(T)}$ at the top (white) and bottom (black) canopy layers of Lines 1 to 4 (Table 3-1). The error bars for NPQ capacity denote the standard error of mean between the replicates (n=3) whereas the error bars for $NPQ_{(T)}$ denote the standard error of mean between the replicates over three days of measurements (n=9). The significance differences are denoted with the alphabets a, b etc.

No correlations were found between the NPQ capacity measured under constant light intensity of 1800µmol m^{-2}s^{-1} and the $NPQ_{(T)}$ measurements made under field midday light conditions for both top (P=0.747) and bottom (P=0.338) of the canopies (Figure 3-11). Figure 3-12 shows the close

relationship between $NPQ_{(T)}$ and the measurement light level. There was a significant negative correlation observed between light intensity and $NPQ_{(T)}$ measurements at the top of the canopy where the light availability was higher ($P<0.001$; Figure 3-12A). At the bottom of the canopies where light levels were under 100 µmol $m^{-2}s^{-1}$, there was no correlation between the light intensity and $NPQ_{(T)}$ measurements observed ($P=0.134$; Figure 3-12B).

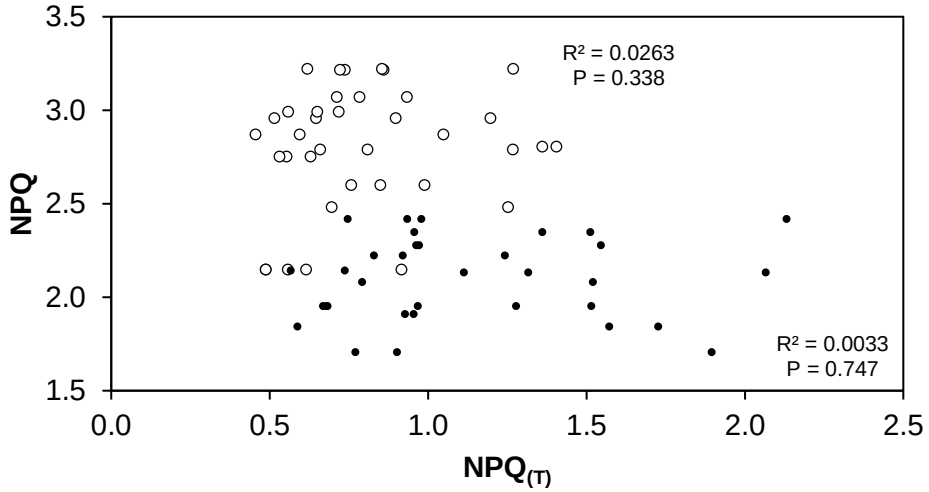


Figure 3-11. A correlation between the NPQ measured under constant light (1800µ$m^{-2}s^{-1}$) and $NPQ_{(T)}$ measured under ambient light in the field at the top (black dots) and the bottom (white dots) canopy layers for all the 20 lines tabulated in Table 3-1. Regression analysis (Genstat, VSN International Ltd., Hemel Hempstead, UK) on the data showed no significant correlation between NPQ and $NPQ_{(T)}$.

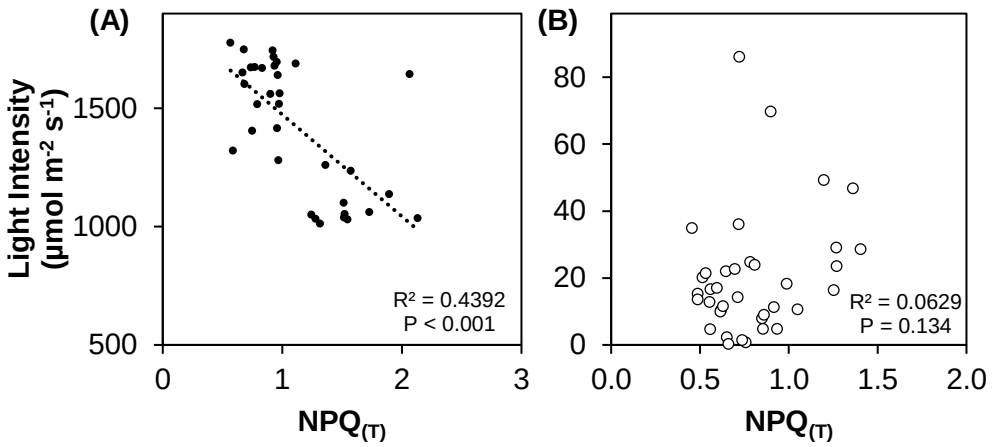


Figure 3-12. A correlation between the light intensity measured and the $NPQ_{(T)}$ measurements made using the MultiSpeQ (PhotosynQ, Michigan, USA) at the **(A)** top canopy layer and **(B)** bottom canopy layer for all the 20 lines tabulated in Table 3-1. Regression analysis (Genstat, VSN International Ltd., Hemel Hempstead, UK) on the data showed a significant correlation of $NPQ_{(T)}$ to light at top canopy layer but not the bottom canopy layer.

A selection of the averages of the chlorophyll fluorescence parameters relevant to photochemical and non-photochemical quenching measured using MultiSpeQ (PhotosynQ, Michigan, USA) are shown in Figure 3-13. The lack of a correlation between light intensity and $NPQ_{(T)}$ in the lower part of the canopy may be due to the retention of quenching as qI due to sunflecks which was not the case in the upper part of the canopy where qE would dominate. The quantum efficiency of PSII (ΦPSII), ratio of incoming light directed to non-photochemical quenching (ΦNPQ), maximum efficiency of PSII photochemistry in light given that all reaction centres were open (F_v'/F_m') and the parameter that gives an indication on the proportion of the open reaction centres, photochemical quenching (qP), were compared between Lines 1 to 4 (Table 3-1) at the top and bottom canopy layer. As expected, there were significant differences between each of these parameters between the canopy layers ($P<0.001$). There were also significant differences detected between the four lines for ΦPSII ($P=0.002$), ΦNPQ ($P<0.001$) and F_v'/F_m'

(P=0.001) but not for qP (P=0.459). As observed, there were less variations between the lines in terms of ΦPSII and qP, compared to ΦNPQ or F_v'/F_m'. The stability of ΦPSII and qP indicate that NPQ is allowing a 'buffering' effect (as reflected in ΦNPQ) between the variation in ambient light and the efficiency of electron transport through PSII (F_v'/F_m').

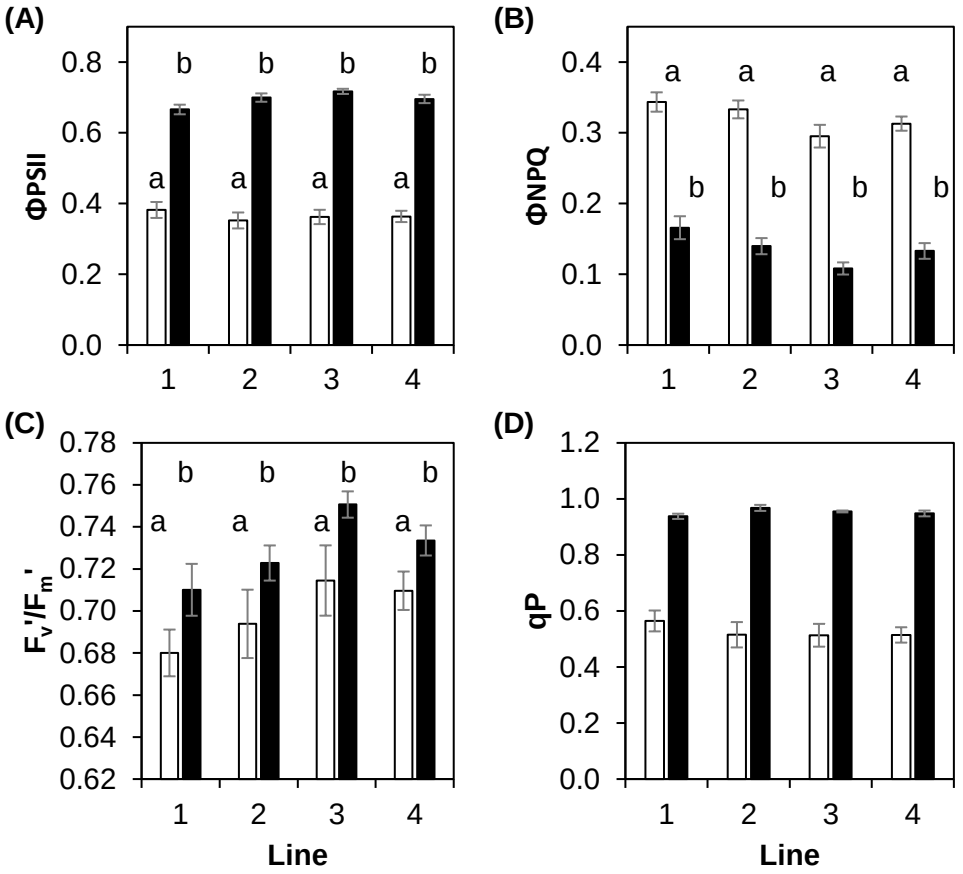


Figure 3-13. A selective presentation of the averages of the chlorophyll fluorescence data measured using MultiSpeQ (PhotosynQ, Michigan, USA); **(A**) quantum efficiency of PSII (ΦPSII), **(B)** ratio of incoming light directed to non-photochemical quenching (ΦNPQ), **(C)** maximum efficiency of PSII photochemistry in light given all reaction centres were open (F_v'/F_m') and **(D)** photochemical quenching (qP) at the top (white) and bottom (black) canopy layers of Lines 1 to 4 (Table 3-1) measured under field ambient midday light conditions. The error bars denote the standard error of mean between the measurements (n=9). The significance differences are denoted with the alphabets a, b etc

There was no correlation between the RUEs recorded from the previous crop cycle (2016/7) and rate of induction of NPQ at the top canopy layer (Figure 3-14); the RUE recorded from initiation of booting to 7-days post anthesis, RUE1 (P=0.297), RUE recorded during grain filling, RUE2 (P=0.874) and the total RUE based on previous crop cycle (2016/7) to $NPQ_{(T)}$ (P=0.982). Similarly, there was also no correlation between the RUEs recorded from the previous crop cycle (2016/7) and rate of relaxation of NPQ at the top canopy layer (Figure 3-14); RUE1 (P=0.404), RUE2 (P=0.700) and RUET (P=0.878).

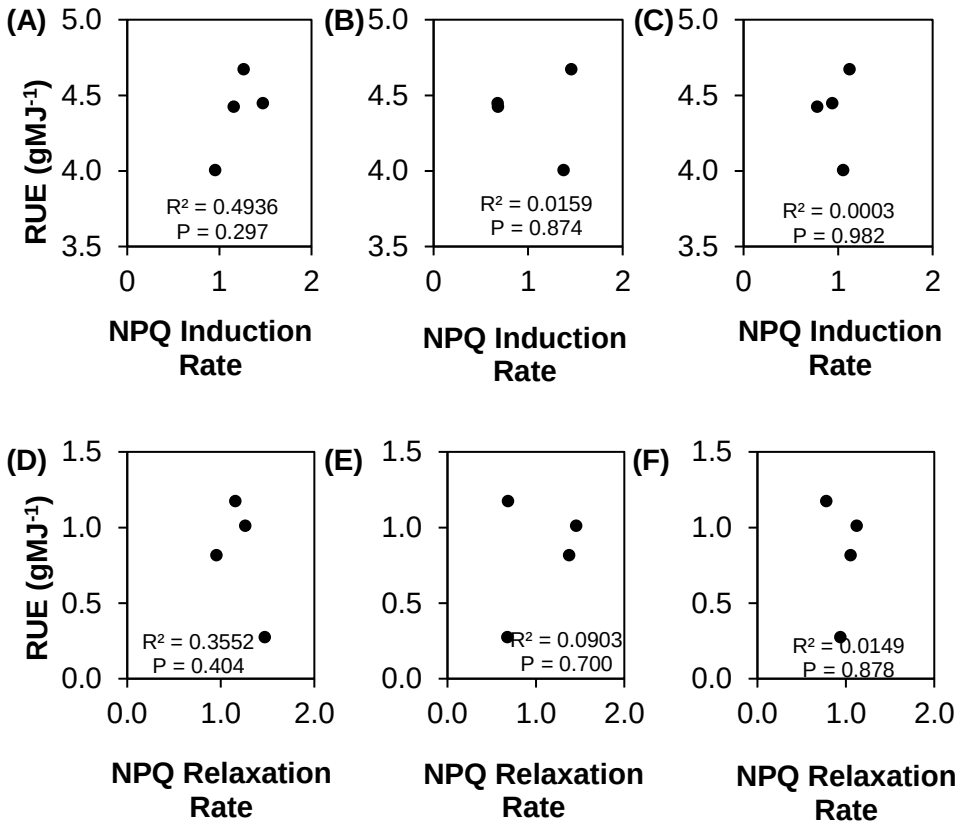


Figure 3-14. A correlation between the radiation use efficiencies (RUE) on 2016/7 crop cycle and rate of induction (**A**, **B** and **C**) and relaxation (**D**, **E** and **F**) of non-photochemical quenching (NPQ) at the top canopy layer; **(A)**, **(D)** RUE recorded from initiation of booting to 7-days post anthesis (RUE1; Table 3-1), **(B)**, **(E)** during grain filling (RUE2; Table 3-1) and **(C)**, **(D)** total RUE recorded during the whole crop cycle (RUET; Table 3-1). Regression analysis (Genstat, VSN International Ltd., Hemel Hempstead, UK) on the data set showed no correlation between rate of NPQ relaxation and RUEs.

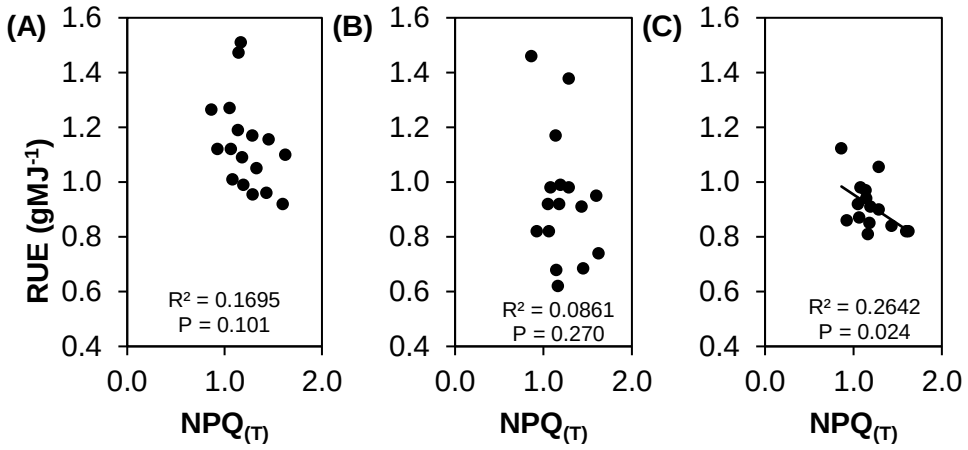


Figure 3-15. A correlation between the radiation use efficiencies (RUE) on 2016/7 crop cycle and non-photochemical quenching measured under ambient light ($NPQ_{(T)}$); **(A)** RUE recorded from initiation of booting to 7-days post anthesis (RUE1; Table 3-1), **(B)** during grain filling (RUE2; Table 3-1) and **(C)** total RUE recorded during the whole crop cycle (RUET; Table 3-1). Regression analysis (Genstat, VSN International Ltd., Hemel Hempstead, UK) showed significance between $NPT_{(T)}$ and RUET only.

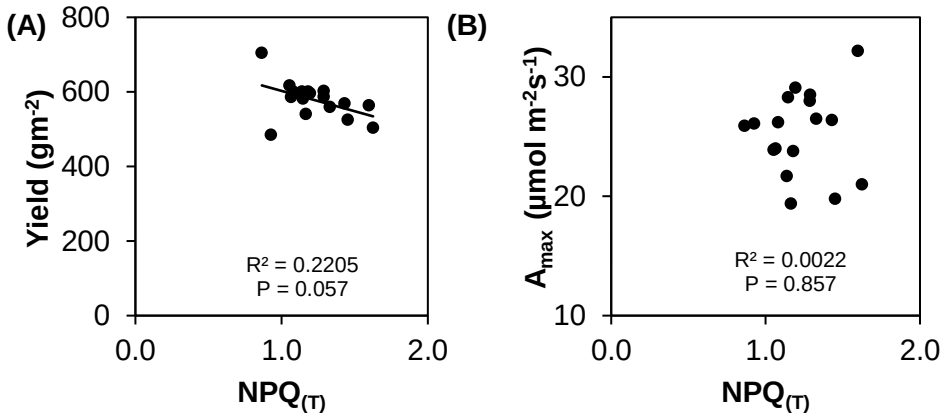


Figure 3-16. A correlation between the non-photochemical quenching measured under ambient light conditions ($NPQ_{(T)}$) and **(A)** Yield of the respective lines from crop cycle 2016/7 (Table 3-1) and **(B)** maximum carbon assimilation (A_{max}) at the top canopy layer. Regression analysis (Genstat, VSN International Ltd., Hemel Hempstead, UK) showed marginal significance between $NPT_{(T)}$ and yield only.

As $NPQ_{(T)}$ could be a quick method to screen for the "photoprotectiveness", a correlation was attempted between the $NPQ_{(T)}$ measured at the top canopy layer of the 20 lines and the RUE data from previous crop cycle 2016/7 (Table

3-1; Figure 3-15). There was significant negative correlation between RUET from previous crop cycle (2016/7) to $NPQ_{(T)}$ (P=0.024) but not for RUE1 (P=0.101) and RUE2 (P=0.270). A marginally significant correlation was found between $NPQ_{(T)}$ and yield data from previous crop cycle 2016/7 (P=0.057; Figure 3-16A) but not between $NPQ_{(T)}$ and maximum carbon assimilation (P=0.857; Figure 3-16B).

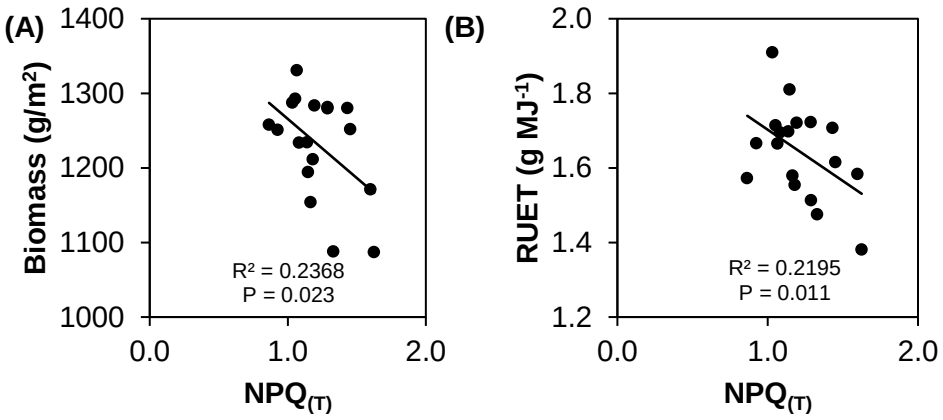


Figure 3-17. A correlation between the non-photochemical quenching measured under ambient light conditions ($NPQ_{(T)}$) and **(A)** Biomass of the respective lines from crop cycle 2017/8 and **(B)** total RUE recorded during the whole crop cycle of 2017/8 (RUET) at the top canopy layer. Regression analysis (Genstat, VSN International Ltd., Hemel Hempstead, UK) showed significant correlations between $NPT_{(T)}$ and biomass and RUET.

A correlation of the $NPQ_{(T)}$ data with the yield and RUE data from the same crop cycle was also made. Similar to the correlation with previous year crop cycle data, there was no significant correlation between $NPQ_{(T)}$ and yield data (R^2=0.0138; P=0.498). As expected there was also no correlation between $NPQ_{(T)}$ and RUE1 (R^2=0.0116; P=0.112) and RUE2 (R^2=0.1551; P=0.941). Similar to the correlation with previous year crop cycle data, there was a significant correlation between $NPQ_{(T)}$ and RUET (P=0.011; Figure 3-17B). Additionally, a significant correlation between $NPQ_{(T)}$ and biomass was observed (P=0.023; Figure 3-17A). Correlations of $NPQ_{(T)}$ data to RUET are

encouraging, whether made based on previous year crop cycle data or the current year crop cycle data.

3.5 Discussion

Stomatal conductance is highly correlated to rates of carbon dioxide assimilation (photosynthesis). From the results, the top of the canopy has higher carbon dioxide assimilation rate (Figure 3-6A) and stomatal conductance (Figure 3-6B) than the bottom of the canopy. Under steady state, diffusion of the gases, carbon dioxide and water vapour, within leaf follows Fick's first law:

$$\text{Equation 3-1: } A = g_{sc}.(C_a - C_i)$$

$$\text{Equation 3-2: } E = g_{sw}.(W_i - W_a)$$

Where A is the carbon dioxide assimilation rate, E is transpiration, g_{sc} and g_{sw} are the stomatal conductance to carbon dioxide and water vapour respectively, C_a and C_i are the atmospheric and intracellular carbon dioxide concentrations respectively and W_a and W_i are the atmospheric and intracellular water concentrations (Gago *et al.*, 2016). Both carbon dioxide assimilation rate and stomatal conductance are interlinked and both indicated rate of photosynthesis. An increase in stomatal conductance meant there was an increase in exchange of carbon dioxide and water, thus correlating it to higher photosynthesis (Kusumi *et al.*, 2012). The differences in carbon dioxide assimilation and stomatal conductance can also be attributed to the age of the leaves measured. The leaves at the bottom of the canopy would be older than those at the top of the canopy. Photosynthetic rates decline with the increase in age of the leaves (Bielczynski *et al.*, 2017). This is also

reflected in the data obtained where the bottom of the canopy has lower rates of photosynthesis than the top.

NPQ dynamics of crop canopies in the nature can be highly complex and hard to decipher (Malnoë, 2018). The light variation within different canopies arising from contrasting plant and canopy architectures can also add complexity into how the canopy responds to light dynamics and thus affecting NPQ. The slow reaction time of plants towards the constantly changing environment results in reduced plant productivity. If the crop plant could react rapidly to close the gap of the time lag in response to the fluctuating light conditions, greater crop productivity could be achieved (Külheim *et al.*, 2002; Ruban, 2017a; Slattery *et al.*, 2018). Using NPQ as a trait for crop breeding, most techniques involved chlorophyll fluorescence measurements at the youngest expanded leaf rather than older leaves. This would only be useful if the plant assumes photosynthetic homogeneity. However, due to many different factors such as age, self-shading of the leaves or canopy gaps, that is impossible (Bielczynski *et al.*, 2017).

As crops grow in complex canopies, more focus should be placed onto different canopy levels for a more realistic estimation and a better study of crop canopy productivity. NPQ dynamics were studied and compared between Lines 1 to 4 (Table 3-1) at the top and bottom of the canopy. In the four lines studied, they were sown at high density in a “camas” planting system. Due to how they were sown and grown, the canopies had already reached full closure (fractional interception>0.9) before GS41. Hence, there were no significant differences in terms of fractional interception between the canopy layers and between the four lines (Figure 3-5A). However, during midday field conditions, the tip of the leaves at the top of the canopy can be exposed to light level that is as high as 1500µmol $m^{-2}s^{-1}$. As expected, the top

of the canopy showed some degree of photoinhibition compared to the bottom of the canopy where there was more self-shading and overlapping leaf layers to protect from the midday high light condition.

Photoacclimation includes a component of long-term photoprotection in plants, whereby constant adjustments are made towards the photosynthetic components in order to accustom themselves to the environmental light conditions (Anderson, Chow and Park, 1995; MacIntyre *et al.*, 2002; Townsend *et al.*, 2018). Referring to Figure 3-6C, when both leaves at the top and bottom of the canopy were subjected to sudden illumination of high light (1800 µmol $m^{-2}s^{-1}$) after an hour of dark adaptation, the rapid induction initially was similar. However, as the induction progressed, the leaf at the top of the canopy developed NPQ at a slower pace and did not reach the NPQ level developed by the leaf at the bottom of the canopy (Induction half-times; Figure 3-9). This photoinhibition (qI) was also reflected in the lower F_v/F_m values at the top of the canopy.

Interestingly, but as expected (see Chapter 4), the NPQ capacity at the bottom of the canopy was higher than the top of the canopy. This agrees with the finding that older leaves of Arabidopsis have higher photoprotection when grown under the same light environment (Carvalho, Ware and Ruban, 2015). In an ideal situation, NPQ would be higher at the top canopy layer than the bottom as the top canopy layer would be exposed to a greater amount of saturating light levels. This would make better sense for the greater productivity part of the canopy to have greater NPQ capacity to accommodate and respond quickly the high light conditions and reduce photoinhibitory effects. However, the top leaves will also have in place photochemical and non-photochemical quenching mechanisms that mean a higher NPQ may not be necessary such as a high photosynthetic rate with higher electron sink

capacity (Mehler reaction, photorespiration). The bottom of the canopies consists of older leaves with a lower photosynthetic capacity and is heavily shaded by leaf layers above it hence will reach saturation at lower irradiances (Pearcy, 1990; Pearcy, Krall and Sassenrath-Cole, 1996; Bielczynski *et al.*, 2017). Hence, it is possible that the higher NPQ, when measured at high light but not low light, was due to photoinhibitory quenching, qI. It could be observed that during relaxation, the four lines appeared to have greater variation in NPQ capacity between themselves at the bottom canopy layer than the top canopy layer. In this experiment, the greater variations observed could be either genotypic or due to the heterogeneity of photosynthesis within the canopy.

In terms of selecting wheat for canopy productivity, higher NPQ capacity throughout the canopy is as important as the ability of the canopy to respond to the environmental changes. Sunflecks are short light burst that could range from a few seconds to more than ten minutes. Sunflecks could present at a light intensity as low as 120 $\mu molm^{-2}s^{-1}$ to as high as 2000 $\mu molm^{-2}s^{-1}$ (Pearcy, 1990; Adams *et al.*, 1999). Most of the leaves at the top of the canopy experiences periods of high light, usually during midday. As we go down the canopy, leaves were mostly shaded and most of the photosynthesis happening are contributed by sunflecks (Pearcy, Krall and Sassenrath-Cole, 1996). A “clever” crop canopy should have both the capacity and also quick response to the sunflecks so as to improve canopy photosynthesis without inducing photoinhibition.

Quick chlorophyll fluorescence yield data were collected using MultiSpeQ (PhotosynQ, Michigan, USA). $NPQ_{(T)}$ is a relatively new parameter that was first defined to be measured using the MultiSpeQ (Tietz *et al.*, 2017). It was hoped that with the use of this new cheap and portable instrument (in

comparison to an LI-6400XT), better screening of field crops could be achieved. This would also present a faster screening (three minutes compared to a minimum of 1.5 hours) as no dark adaptation is required. Dark-adapted NPQ data could divulge many information that $NPQ_{(T)}$ is not able to. However, this does not negate the usefulness of $NPQ_{(T)}$ as a rapid photoprotection parameter for screening and selection of large population sets. In-depth photoprotective studies can be made on selected lines using dark-adapted techniques. They cannot be fully replaced by $NPQ_{(T)}$ as $NPQ_{(T)}$ does not take into consideration the light history of the leaf being sampled and could not measure the maximum NPQ capacity of the leaf. Based on a sample of four lines (Lines 1 to 4, Table 3-1), $NPQ_{(T)}$ does not correlate to either NPQ capacity measured or the rates of induction or relaxation of NPQ at the top of the canopy layer. However, a correlation on all the twenty lines measured (Table 3-1) showed that it was possible to correlate (negatively) $NPQ_{(T)}$ to RUET and biomass and to a certain extent, to grain yield. This is the first time that such correlations have been identified and we suggest that lower NPQ during light transients would benefit yield as suggested by Kromdijk *et al.* (2016) and Hubbart *et al.* (2018). $NPQ_{(T)}$ would present itself as a powerful parameter which can also be used to study NPQ dynamics. As top canopy layer showed higher $NPQ_{(T)}$ than the bottom canopy layer, study of $NPQ_{(T)}$ dynamics under field conditions could be a more useful photoprotection selection tool.

3.6 Summary

Wheat canopies experience photoinhibition under field conditions. No correlation was found between NPQ capacity and NPQ measured at ambient

light conditions in the field ($NPQ_{(T)}$). $NPQ_{(T)}$ was not correlated to rates of induction or relaxation of NPQ. However, a significant negative correlation was found between $NPQ_{(T)}$ and the total RUE of wheat canopy and yield. NPQ capacity and dynamics varied according to canopy depth; bottom canopy layer showed greater capacity for photoprotection than the top. Under midday field conditions, top canopy layer showed higher $NPQ_{(T)}$ than the bottom canopy layer as expected due to the higher light conditions received by the top canopy layer. $NPQ_{(T)}$ dynamics could present itself as a better and quicker tool for selection of “photoprotectiveness”.

Supplementary Material

Supplementary material S3.1

Parameters measured on “Photosynthesis RIDES” protocol

Measures the same photosynthesis-related parameters in <15 seconds as 'Leaf Photosynthesis MutlispeQ v1.0' plus additional PS1 and P700 measurements.

- Chlorophll Fluorescence: Phi2, PhiNPQ, PhiNO, NPQt, qL, LEF
- Relative Chlorophyll
- ATP synthase conductivity, proton motive force parameters through DIRK(ECS): ECSt mAU, vH+, gH+
- Saturation pulse estimation of PSI parameters: PS1 active centers, PS1 open, PS1 oxidized and PS1 over reduced
- Absorbance at: 450, 535, 605, 650, 730, 850, 880, and 940nm.
- The rate of turnover of the cytochrome b6f complex through DIRKP(700)
- Leaf Thickness (in mm), angle, and cardinal direction
- Leaf Temperature and differential from ambient temperature
- Environmental conditions: PAR and ambient temperature/pressure/humidity

Chapter 4 Canopy architecture and protective energy dissipation in rice canopy with altered levels of *PsbS*

C.C. Foo[1], A. J. Burgess[1], R. Retkute, A. Ruban[2] and E.H. Murchie[1]

[1] Plant and Crop Science Division, School of Bioscience, University of Nottingham, Sutton Bonington LE12 5RD UK

[2] School of Biological and Chemical Sciences, Queen Mary University of London, London E1 4NS UK

Author contribution:

Experiment conceived by EH Murchie, A Ruban and CC Foo

Project supervision performed by EH Murchie

Experimental work (experimental design, planning and set up, physiological measurements including weekly measurements, chlorophyll fluorescence and gas exchange and harvest data) by CC Foo

Three-dimensional reconstruction and modelling by AJ Burgess and R Retkute

Written by CC Foo, AJ Burgess and EH Murchie

4.1 Abstract

High sunlight can stimulate plant growth rates but can potentially cause cellular damage. The likelihood of deleterious effects is lowered by a sophisticated set of photoprotective mechanisms, one of the most important being the controlled dissipation of energy from chlorophyll within photosystem II (PSII) measured as non-photochemical quenching (NPQ). Although ubiquitous, the role of NPQ in plant productivity remains uncertain because it momentarily reduces the quantum efficiency of photosynthesis. Here we use plants overexpressing and deficient in the gene encoding a central regulator of NPQ, the protein *PSBS*, within rice to assess the effect of protective effectiveness of NPQ at the whole canopy scale. Using a combination of modelling and gas exchange measurements, we determine the influence of altered NPQ capacity on whole canopy performance in terms of light interception and overall protective capacity using high resolution canopy representations. We show that in comparison to wild-type plants, *PsbS* overexpressors have a reduced risk of photoinactivation, demonstrating that photoprotective mechanisms could be altered as a means to improve rice crop productivity.

4.2 Introduction

Photosynthetic efficiency is a limitation to achieving the increases in crop yields needed to meet the demands of an expanding population. However, we lack an understanding of how canopy structure and internal biochemistry determine the absorption and utilisation of light, particularly within the field setting. The within canopy light environment is highly dynamic, with up to 50-fold difference in light intensity between the top and bottom layers (Niinemets and Keenan, 2012). This is further confounded by changes in canopy architecture, such as leaf angle or area, and shading effects brought about by overlapping foliage, solar movement, cloud cover and displacement of leaf material (Burgess *et al.*, 2016, 2017; Townsend *et al.*, 2018). The fluctuating light environment poses a problem for photosynthetic machinery; with the need to maximise the efficient harvesting and utilisation of light energy whilst minimising any deleterious effects associated with exposure to high light.

A number of mechanisms are employed by plants in order to limit damage to photosynthetic machinery, however, through their action they momentarily reduce the quantum use efficiency of photosynthesis, thus limiting the productivity of the plant. Here, we use the term photoinactivation to describe the light-induced inactivation and therefore functional closure of reaction centres (RCs), including damage, which leads to a decrease in the yield of PSII (ΦPSII; Sonoike, 1996; Horton, 2000; Takahashi and Badger, 2011; Matloobi, 2012; Murata, Allakhverdiev and Nishiyama, 2012). The susceptibility of a leaf to photoinactivation depends upon multiple factors including life history (e.g. growing conditions), genetic adaption, and physiological status (Aro, Virgin and Andersson, 1993; Murchie and Niyogi, 2011; Demmig-Adams *et al.*, 2012). A number of strategies exist in order to

prevent or minimise photoinactivation including dissipative pathways that prevent energy accumulation (Ruban, 2012, 2016). The fastest process employed by plants to relieve excitation pressure on the photosynthetic membrane is nonphotochemical quenching (NPQ) of chlorophyll fluorescence, where excess energy is dissipated harmlessly as heat (Horton and Ruban, 1992; Jahns and Holzwarth, 2012). The fastest component of NPQ is qE, or energy-dependent quenching, and is triggered by the generation of a pH gradient across the thylakoid membrane (Krause, 1974; Horton, Wentworth and Ruban, 2005; Zulfugarov *et al.*, 2007). qE is also known to be modulated by the carotenoid zeaxanthin and the protein PSII subunit S (*PsbS*), which act as allosteric regulators to alter the structure of the membrane and antenna conformation in order to enhance the affinity for protons, thus facilitating qE formation and relaxation (Demmig *et al.*, 1987; Külheim *et al.*, 2002; Niyogi *et al.*, 2005; Johnson and Ruban, 2010, 2011; Kereiche *et al.*, 2010; Murchie and Niyogi, 2011; Goral *et al.*, 2012; Ruban, 2012; Zaks *et al.*, 2012; Harbinson, 2012; Roach and Krieger-Liszkay, 2012; Sacharz *et al.*, 2017).

In recent years, there has been increasing interest in the role of NPQ in determining plant productivity and it's manipulation in order to increase crop yield (Murchie and Niyogi, 2011; Hubbart *et al.*, 2012, 2018; Kromdijk *et al.*, 2016; Głowacka *et al.*, 2018). Studies by Hubbart et al. (2012, 2018) indicated that overexpression of *PsbS* can enhance qE and biomass production in rice through increased canopy radiation use efficiency during fluctuating light. Hence, we hypothesize that an increase in overexpression of *PsbS* will improve photoprotective responses and reduce photoinactivation throughout the canopy structure leading to improved whole canopy photosynthesis, biomass and yield.

The existence of multiple NPQ and repair pathway components acting over different time periods necessitated the development of an approach to test the *in vivo* photoprotective function. Ruban and Murchie (2012) developed a protocol for the measurement of NPQ that can provide information of the protective effectiveness of processes occurring in the photosynthetic membrane (termed protective NPQ; pNPQ) in a relatively rapid, non-destructive way. The protocol entails a gradually increasing actinic light (AL) routine to track the relationship between ΦPSII, NPQ, and qP (the quantum coefficient of photochemical quenching) measured in the dark following light exposure (termed qP_d). This parameter can be used to define pNPQ - the NPQ and corresponding AL intensity treatment after which all RCs remain active (i.e. open). This method provides a number of advantages over previous methods and allows a quantitative approach to define the relationship between photoinactivation and NPQ and their contribution to the decline in the ΦPSII. qP_d provides a prompt marker of both initial and long-term photoinactivation as it reflects the true state of RCs enabling the tracking of the early signs of their loss of activity. In this context, the closure of the RCs as a result of light is termed “photoinactivation” as photoinhibition could occur not only due to light but also other factors such as temperatures, carbon dioxide, etc.

It is not known how much of NPQ can be considered to be protective. Over-protection will lead to a reduction in quantum yield but under-protection might jeopardise photosynthetic efficiency further as repair is often very costly (Raven, 1989). Hence, studying pNPQ at the canopy level is important for crop canopy productivity. Another difficulty is that many crops are usually cultivated in a complex, monocropped canopy, and so variation in canopy architectural traits poses difficulties in scaling cellular levels processes up to

infer information on canopy productivity. Recent advances in using realistic three dimensional (3D) reconstructions and modelling approaches have proved useful in accounting for canopy traits when scaling up processes (Burgess *et al.*, 2015, 2017; Pound *et al.*, 2017). When this is coupled with the aforementioned pNPQ technique, light tolerance level at different canopy levels could be assessed simultaneously. This work would divulge information on the "cost" of photoprotection in terms of the productivity of rice canopies.

Previously, the pNPQ protocol has been used within *Arabidopsis thaliana* to study the contribution of photoprotection versus photoinhibition (Townsend, Ware and Ruban, 2018); the contribution of photosystem I (PSI) fluorescence to NPQ (Giovagnetti and Ruban, 2015) and the role of carotenoids and components of NPQ in light tolerance (Ware, Belgio and Ruban, 2015a, 2015b; Ware, Dall'Osto and Ruban, 2016). Here, we have applied these methods within rice in combination with 3-dimensional (3D) modelling and ray tracing with the aim to (a) evaluate the distribution of pNPQ according to canopy structure and the in-canopy light environment; (b) evaluate the role of *PsbS* expression on pNPQ capacity and (c) quantitatively evaluate the effect of altered *PsbS* expression on canopy structure. This paper will focus on the effects of *PsbS* on the regulation of NPQ under fluctuating light conditions in rice canopies using a novel non-destructive method as described in Ruban and Murchie (2012). Fluorescence data will be used in combination with high-resolution 3-dimensional (3D) reconstruction and light modelling in order to determine the distribution of photoprotection throughout the rice canopies.

Materials and methods

4.2.1 Plant material, experimental design and plant maintenance

Oryza sativa L. 'Kaybonnet' rice overexpressing *PsbS* (OE99) and *PsbS* RNAi lines (RNAi134; *PsbS* genomic sequence: Os01g64960) provided by Syngenta (Research Triangle Park, NC, USA) were used in this study. Plants were sown in the FutureCrop Glasshouse facilities, University of Nottingham, Sutton Bonington Campus (52°49'59" N, 1°14'50" W), UK. The same facility was used in Hubbart *et al.* (2018). It is a south-facing glasshouse constructed to contain two 5m by 5m by 1.25m tanks at ground level (CambridgeHOK, Brough, UK). The tank was filled with sandy loam soil which was extracted from local fields and sieved through a fine mesh. Seeds of WT (Kaybonnet), OE (OE99) and RNAi (RNAi134) were sown into modular trays in a compost mix consisting 50% John Innes Number 1 and 50% Levington M3 on the 27th April 2017. On 10th May 2017, the seedlings were transplanted into prepared soil bed in randomized block design with four replicates. Each plot consisted of 8 by 7 plants, spaced 12 cm apart. A photoperiod of 12H (0700H to 1900H) was maintained using blackout blinds. Additional lighting was supplied using Sodium (Son T-Agro, Philips) lamps whenever the photosynthetically active radiation (PAR) fell below 300 µmol $m^{-2}s^{-1}$. An automatic drip irrigation was applied for 30 minutes, twice daily at 0600H and 1800H. A temperature of 30±3°C and relative humidity (RH) of 50-60% was maintained throughout.

4.2.2 Physiological Measurements

4.2.2.1 Plant physiological data

Plant height and tiller number were recorded weekly. Fractional interception data were collected weekly to track canopy development. Leaf area index (LAI) was not measured manually during the experiment due to restrictions of transferring GM plants into non-GM laboratory workspace. Experimental measurements were carried out on a single leaf basis at the top and bottom of the canopies at three different stages of canopy formation which are determined by fractional interception (f) of the canopy. Fractional interception was measured using AccuPAR LP-80 ceptometer (Decagon Devices, Washington, USA). Measurements were taken during midday after manually switching off the supplementary lighting in the glasshouse. Five measurements were taken diagonally across each plot at each layer. Three plants per plot were harvested after the end of the second (5th July 2017) and third round (24th July 2017) of measurements for dry weight records. Samples were bagged and oven-dried at 70°C for 48 hours until a stable weight was observed.

4.2.2.2 Chlorophyll fluorescence measurements

For chlorophyll fluorescence measurements, the rice canopies were studied as a two-layer canopy. Using the middle point of the canopy height as a reference, the canopy layer above that was considered the top of the canopy whereas the canopy layer below that was the bottom of the canopy. Chlorophyll fluorescence and gas exchange measurements were collected based on the development of the canopies and made at three stages based

on fractional interception (Chapter 4.2.2.1) hereby known as growth stage (GS) 1, 2 and 3; corresponded to 35, 50 and 75 days after transplanting (DAT), respectively. A Mini PAM fluorometer (Heinz Walz GmbH, Effeltrich, Germany) was used to measure dark adapted F_v/F_m at around midday, during each round of pNPQ measurements. Five leaves per layer of each plot were dark adapted using clips for 25 minutes.

Leaf chlorophyll fluorescence and gas exchange measurements were carried out using a LI-COR 6400XT infra-red gas exchange analyser (LI-COR Biosciences, Nebraska, USA). The healthiest youngest leaf within the canopy layers were chosen and dark-adapted with an aluminium foil for an hour prior to measurements. The width of the leaves sampled were recorded to calculate the leaf area in the cuvette. An hour-long automated NPQ induction protocol consisting of an initial log of dark-adapted chlorophyll fluorescence parameters, followed by 15 minutes of induction phase at 1500µmol $m^{-2}s^{-1}$ (logged every minute) and ended with five minutes of relaxation phase (logged every minute) by reducing light to 200µmol $m^{-2}s^{-1}$ was carried out. Immediately after the induction protocol, a light response curve from 0 to 2000 µmol m^{-2} s^{-1} (Light steps: 0, 50, 100, 150, 200, 250, 300, 500, 1000, 1500 and 2000 µmol m^{-2} s^{-1}) was carried out. Prior to each measurement, the sample and reference IRGAs were equilibrated (matched) automatically to prevent drift. The block temperature was kept at 30°C and carbon dioxide concentration was maintained at 400 ppm at a flow rate of 500 mL min^{-1}. All the light was provided by a built-in light at a mix of red and 10% blue light emitting diodes.

pNPQ measurements were made using Junior-PAM chlorophyll fluorometer (Heinz Walz GmbH, Effeltrich, Germany) attached to laptop or tablet with WinControl-3 software (version 3.25; Heinz Walz GmbH, Effeltrich, Germany)

installed. A 100cm fiber-optic connecting the Junior-PAM and a magnetic leaf clip were used for the measurements following Ruban and Murchie (2012) at three different maximum light levels (2000, 2500 and 3000 μmol m^{-2} s^{-1}) at top and bottom of the canopies. The light level emitted from the fiber optic was calibrated using a mini quantum sensor (MQS-B/A; Heinz Walz GmbH, Effeltrich, Germany) attached to the universal light meter (ULM-500; Heinz Walz GmbH, Effeltrich, Germany) every morning of the measurements. The setting of a maximum light level would automatically scale the light parameter to nine levels (Refer to Table 4-1 for the corresponding light levels).

Table 4-1. The individual light levels for each maximum light level setting on the Junior PAM.

	Maximum light level setting (μmol$m^{-2}s^{-1}$)		
Light level	**2000**	**2500**	**3000**
1	0	0	0
2	120	150	180
3	253	317	380
4	380	475	570
5	560	700	840
6	833	1042	1250
7	1127	1408	1690
8	1533	1917	2300
9	2000	2500	3000

The leaves were dark adapted using aluminium foil for an hour prior to running of the pNPQ measurements. The pNPQ procedure was run as a pre-programmed batch file where the scheme was (SP)-(AL on)-(120s)-(SP)-(180s)-(SP)-(AL off/FR on)-(7s)-(SP)-(5s)-(AL on/FR off)-repeat; where AL is the actinic light, SP is the saturating pulse and FR is far-red light (Figure 4-1). Due to the mechanics of Junior-PAM, each protocol run according to the light settings was run based on a scale with a set maximum light intensity. Ten measurements per maximum light intensity per layer were carried out at leach

growth stage. There were three maximum light intensities used to build the light tolerance curve to increase the reliability of the data points and to collect sufficient data points throughout the whole light curve. The maximum light levels used in this experiment were also increased substantially to make sure the light output was saturating at the higher levels.

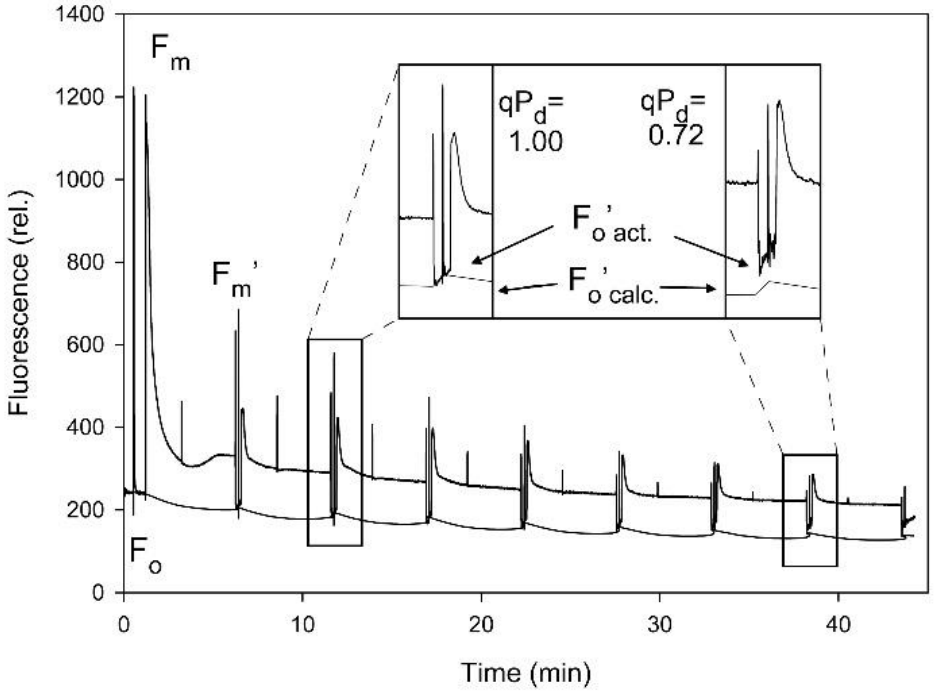


Figure 4-1. Example scheme of induction of chlorophyll fluorescence programme with an eight-step actinic light (AL) routine made on a Junior-PAM (Heinz Walz GmbH, Effeltrich, Germany). For a detailed explanation of the routine development, see Ruban and Belgio (2014). **Inset**: The gradually increasing AL routine induces photoinactivation which can be readily observed as a divergence between $F_o'_{act.}$ and $F_o'_{calc.}$ and be seen as a decrease in the qP_d parameter.

The Junior-PAM uses blue and white actinic lights for measurement. However, red light is preferable for measurement of NPQ. Blue light promotes the movement of chloroplasts within the cells which could result in false positive quenching recorded (Cazzaniga *et al.*, 2013; Dall'Osto *et al.*, 2014; Malnoë, 2018). Moreover, there would be effects during the lower light

measurements where the state transition component of NPQ (qT) was not taken into account. However, the use of the same method throughout this experiment made the results comparable.

4.2.2.2.1 Theory behind pNPQ protocol

The yield of photosystem II (ΦPSII) is reduced by two processes: non-photochemical quenching of chlorophyll a fluorescence (NPQ) and the photoinhibition of reaction centre of Photosystem II (RCII).

Equation 4-1: $\phi PSII = \frac{qPd.\frac{Fv}{Fm}}{[1+\left(1-\frac{Fv}{Fm}\right).NPQ]}$

F_v/F_m is the maximum photochemical quantum yield of PSII, which is calculated as $(F_m-F_o)/F_m$, with F_m and F_o being the maximum and minimum yields of fluorescence, respectively. NPQ is calculated as (F_m/F_m')-1. qP_d, the coefficient of photochemistry in the dark is calculated as:

Equation 4-2: $qPd = \frac{(Fm'-Fo'act.)}{(Fm'-Fo'calc.)}$

Where F_o'act. and F_o'calc. are the actual and calculated minimum levels of fluorescence in the dark after prior actinic light (AL) illumination. F_o'calc. is quantified according to the formula of Oxborough and Baker (1997):

Equation 4-3: $Fo'calc. = \frac{1}{\frac{1}{Fo}-\frac{1}{Fm}+\frac{1}{Fm'}}$

Under low light intensities, the F_o'calc. matches F_o'act., however under high light intensities, the two F_o' values diverge. This is due to the rise in minimum fluorescence caused by the photoinduced permanent closure of RCII. This causes F_o'calc. < F_o'act. and qP_d < 1.00, and at this point, the leaf is

considered to be photoinactivated. When $qP_d > 0.98$, NPQ is considered to be protective and is thus called pNPQ. For a detailed description of the principles of the method, see Ruban and Murchie (2012).

4.2.3 Canopy imaging, reconstruction and ray tracing

3D analysis of plants was made according to the protocol of Pound *et al.* (2014) and further details are given in Burgess *et al.* (2015). One rice plant per plot (i.e. four per line) was selected at each of the growth stages and carefully removed for imaging. Water was supplied to the roots to prevent wilting. At least 40 images per plant were taken and reconstructions made as described in Burgess *et al.* (2015). Reconstructed canopies were formed by duplicating and randomly rotating the three best reconstructed plants in a 3 by 3 grid, with 12 cm between plants, within and between rows in accordance with the planting pattern.

Total light per unit leaf area was predicted using a forward ray-tracing algorithm implemented in fastTracer (fastTracer version 3; PICB, Shanghai, China; Song, Zhang and Zhu (2013). Latitude was set at 53 (for Sutton Bonington, UK), atmospheric transmittance 0.5, light reflectance 7.5%, light transmittance 7.5%, days 164, 180 and 205 (13th June, 29th June and 24th July). FastTracer3 calculates light as direct, diffused and transmitted components separately; these were combined together to give a single irradiance level for all canopy positions. The diurnal course of light intensities over a whole canopy was recorded in one-minute intervals. The ray tracing boundaries were positioned within the outside plants so as to reduce boundary effects.

4.2.4 Modelling

All modelling was carried out in Mathematica (Wolfram Research Inc., Illinois, USA). We assumed that a relationship between the percentage of photoinactivated leaves (*p*) and light intensity (L) is given by a sigmoidal Hill function with five parameters:

$$\text{Equation 4-4: } f(L) = a - \frac{a-b}{\left(1+exp\left(c(L-d)\right)\right)^{e}}$$

Five parameters were chosen to accommodate asymmetry and allowed greater flexibility when fitting to data. Parameters were fitted to experimental data using a least squared method with *Mathematica* function *FindFit*. After the model has been fitted to data, an estimate for light intensity which gives a percentage of photoinactivated leaves, can be obtained using the inverse of Equation 4-4):

$$\text{Equation 4-5: } L(p) = \frac{c\,d - \log\left(\frac{1}{\left(\frac{a-b}{a-p}\right)^{1/e}-1}\right)}{c}$$

An example for a fitted *f(L)* and *L(p)* for a data derived from measurements for WT rice is shown in Supplementary Figure S 4-1. Profiles of photoinactivated surface area can be constructed by dividing the percentage into bins $\{\boldsymbol{p_i}, \boldsymbol{p_{i+1}}\},\ \boldsymbol{p_i} = \boldsymbol{10i}, \boldsymbol{i} = \boldsymbol{0}..\boldsymbol{9}$. Then using Equation 4-5, the corresponding limits of light intensity $\boldsymbol{L_i} = \boldsymbol{L}(\boldsymbol{p_i})$ can be found. Based on the light intensities computed from the ray-tracer, the fraction of a surface having light intensity within $\{\boldsymbol{L_i}, \boldsymbol{L_{i+1}}\}$ at time, *t*, can be calculated.

4.2.5 Statistical analysis

Analysis of variance (ANOVA) was carried out on the data collected using the statistical package, *Genstat* (19th Edition) for Windows (VSN International Ltd., Hemel Hempstead, UK). They were analysed based on the probability generated by *Genstat* whereby a P value of less than 0.05 ($P<0.05$) shows significant interactions and P value greater than 0.05 ($P>0.05$) shows insignificance. Data were checked to have met the assumption of constant variance and normal distribution of residuals.

4.3 Results

4.3.1 Canopy architecture

Three different growth stages of the rice canopies were selected to study the effects of NPQ throughout rice canopy development. First growth stage (GS1) was prior to canopy closure ($f \geq 0.6$), followed by second growth stage (GS2) during the canopy closure stage ($f \geq 0.8$) and last growth stage (GS3) when the canopy was fully closed and dense ($f \geq 0.9$). The fractional interception between OE, RNAi and WT at top and bottom canopy layers measured at the aforementioned three growth stages are shown in Figure 4-2. At GS1, the canopy was small and thus fractional interception was taken as a complete canopy instead of dividing it into two-layered canopy. There were no differences in fractional interception between OE, RNAi and WT at GS1 ($P=0.311$). As expected, at GS2 and GS3, light intercepted at the top layer was significantly lower than the bottom of the canopy ($P<0.001$). However, there were no differences in fractional interception either at the top or bottom

of the canopy layer between OE, RNAi and WT at both GS2 (P=0.302) and GS3 (P=0.382).

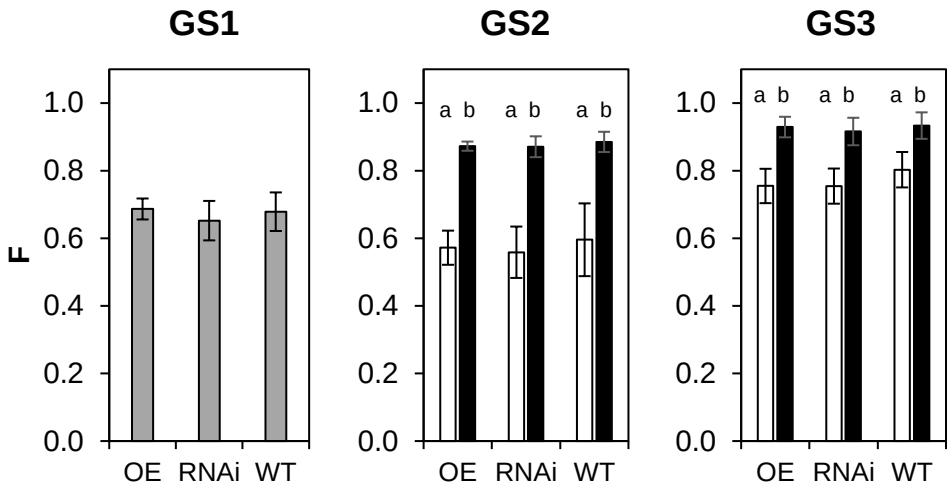


Figure 4-2. Fractional interception, F was measured within the plots of rice overexpressing *PsbS* (OE), rice with downregulated *PsbS* (RNAi) and wildtype (WT) at the three growth stages (GS) at GS1, GS2 and GS3. At GS1, F was measured for the whole canopy as one (grey). At GS2 and GS3, F was measured at the top layer (white) and bottom layer (black) of the canopies. Error bars denote the standard error between the plots (n=4). Significant differences are denoted by alphabets a, b etc.

Tiller number and plant height were measured at the three growth stages (Figure 4-3). There were no differences in tiller number at all three growth stages between OE, RNAi and WT at 5% significance level (GS1, P=0.78; GS2, P=0.09; GS3, P=0.117). Tiller number did not vary between the growth stages between OE, RNAi and WT (P=0.818) as measurements started when the plants were tillering. RNAi had the lowest plant height compared to OE and WT, throughout the three growth stages (GS1, 0.002; GS2, P=0.060; GS3, P=0.015). However, the differences in plant height did not result in any significant differences between the dry weights of OE, RNAi and WT (P=0.708). As expected, the dry weight of all the plants was significantly greater at GS3 compared to GS2 (P<0.001; Figure 4-4).

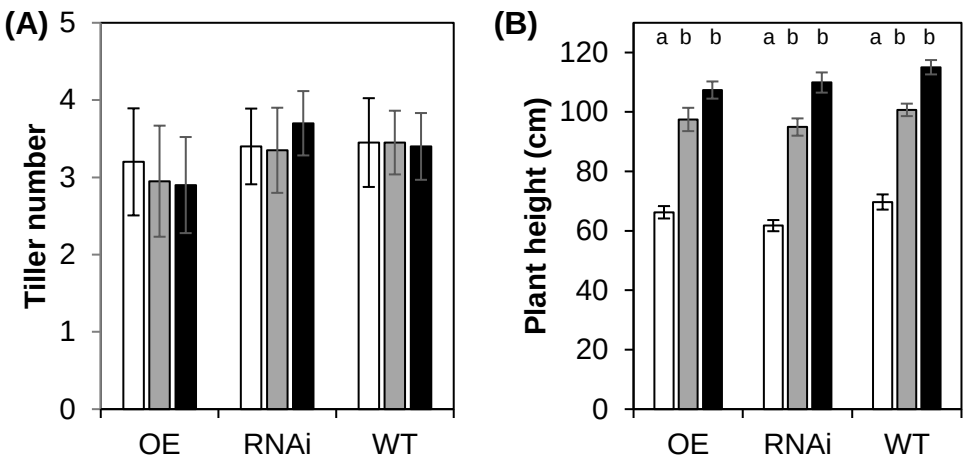


Figure 4-3. The **(A)** tiller number and **(B)** plant height in cm recorded for rice overexpressing *PsbS* (OE), rice with downregulated *PsbS* (RNAi) and wildtype (WT) at the three growth stages (GS) at GS1 (white), GS2 (grey) and GS3 (black). Five plants per plot were sampled. Error bars denote the standard error between the plots (n=4). Significant differences are denoted by alphabets a, b etc.

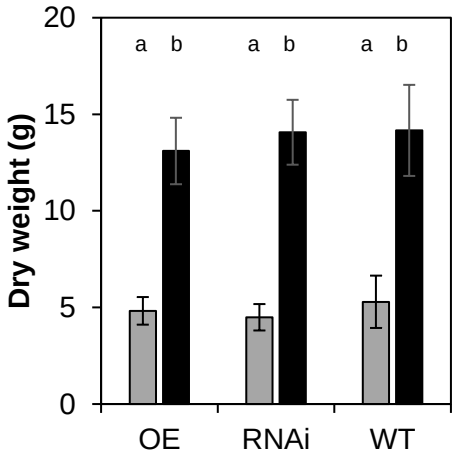


Figure 4-4. Dry weights of three plants per plot were measured for for rice overexpressing *PsbS* (OE), rice with downregulated *PsbS* (RNAi) and wildtype (WT) at GS2 (grey) and GS3 (black). Error bars denote the standard error between the plots (n=4). Significant differences are denoted by alphabets a, b etc.

The cumulative leaf area index (cLAI) from the top of the canopy to the bottom of the canopy was modelled for each of the rice canopies using the data from the 3D reconstructed rice canopies (Figure 4-5A) and light distribution data from ray tracing (Figure 4-10B).

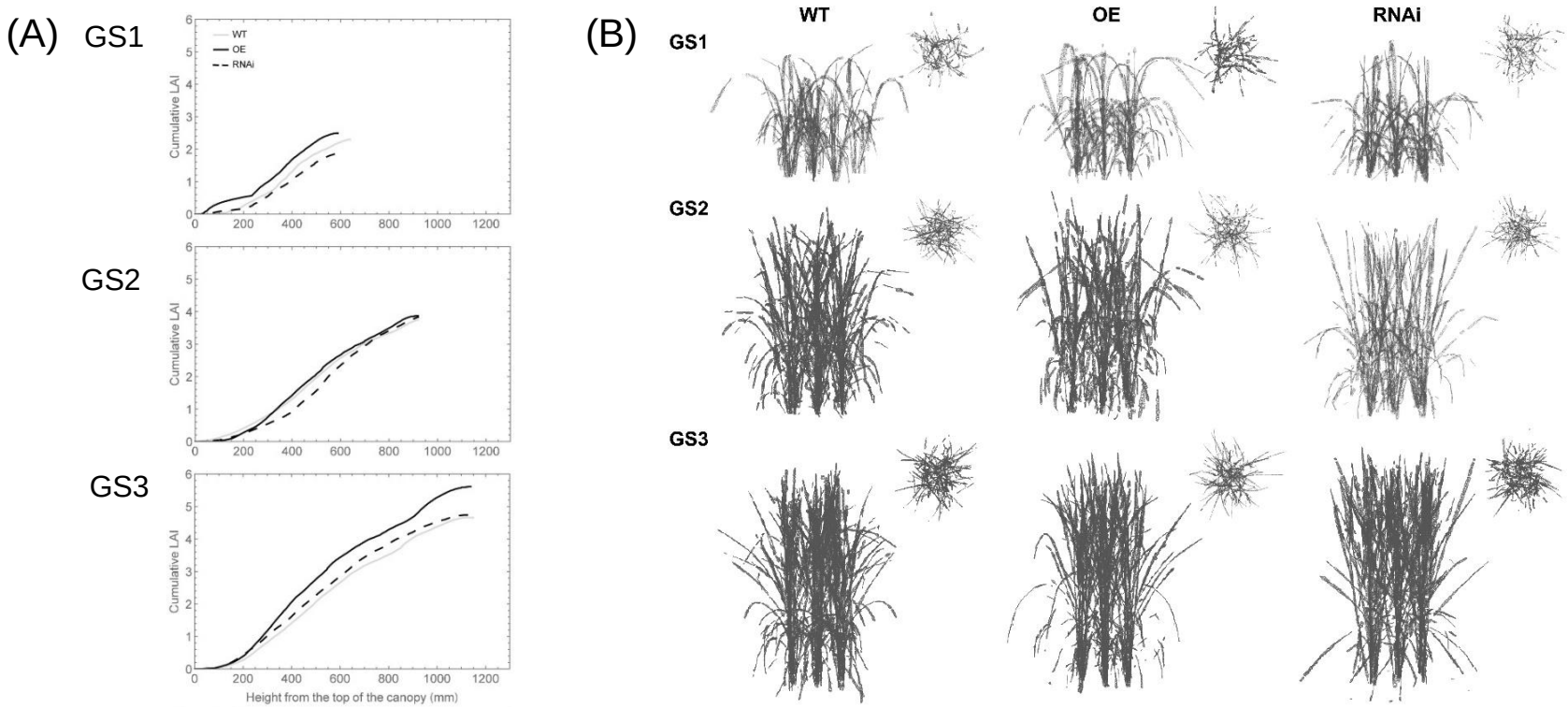


Figure 4-5. **(A)** The modelled cumulative leaf area index (cLAI); the area of leaf material (or mesh area) per unit ground as a function of the height from the top of the canopy between rice overexpressing *PsbS* (OE; black solid line), rice with downregulated *PsbS* (RNAi; black dashed line) and wildtype (WT; grey solid line) at GS1, GS2 and GS3. The steepness of the curve indicates how much leaf material is present at each layer. **(B)** The reconstructed 3D canopies of WT, OE and RNAi rice lines at GS1, GS2 and GS3 following the imaging methodology described. Main figure shows the side-on view whilst the inset shows the top-down view.

It was shown previously that modelled cLAI correlates well to manual LAI measurements (Burgess *et al.*, 2015). Although there was no significant difference between tiller number and dry weight, the plant height and the modelled cLAI of OE, RNAi and WT showed that OE canopies accumulated greater leaf area at GS1 for light interception. The 3D reconstructed rice canopies (Figure 4-5B) also showed the variations in their vertical profiles that were not parameterised through tiller number and dry weights. The canopies have differences which matched up with the modelled cLAI and 3D reconstruction. During GS1, the RNAi canopy had a “sparser” top canopy whilst OE and WT canopies had the least “sparse” top canopy. OE and RNAi plants also had more upright leaves at the top of the canopy than the WT plants. However, there were relatively more horizontal leaves in OE canopy, when viewed from the side and top of the canopy, compared to the RNAi canopy. At GS2, RNAi canopies were visibly smaller and thinner than the WT or OE canopies. At GS3, all canopies were fully closed.

Overexpression of *PsbS* or downregulation of *PsbS* resulted in NPQ differences but did not affect photosynthesis and stomatal conductance (Figure 4-6). There were no significant differences in terms of maximum carbon assimilation (at 2000 µmol $m^{-2}s^{-2}$ light intensity) between OE, RNAi and WT at all three growth stages (GS1, P=0.305; GS2, P=0.864; GS3, P=0.136). However, the top canopy layer had higher maximum carbon assimilation (at 2000 µmol $m^{-2}s^{-1}$ light intensity) than the lower canopy layer at all three growth stages with the exception of RNAi line at GS1 (GS1, P=0.099; GS2, P<0.001; GS3, P<0.001). There was no significance difference in stomatal conductance at both canopy layers between OE, RNAi and WT (GS1, P=0.360; GS2, P=0.304; GS3, P=0.355). The NPQ was higher in OE compared to WT and RNAi at GS1 (P=<0.001) and GS3 (P<0.001) but

not GS2 (P=0.189).

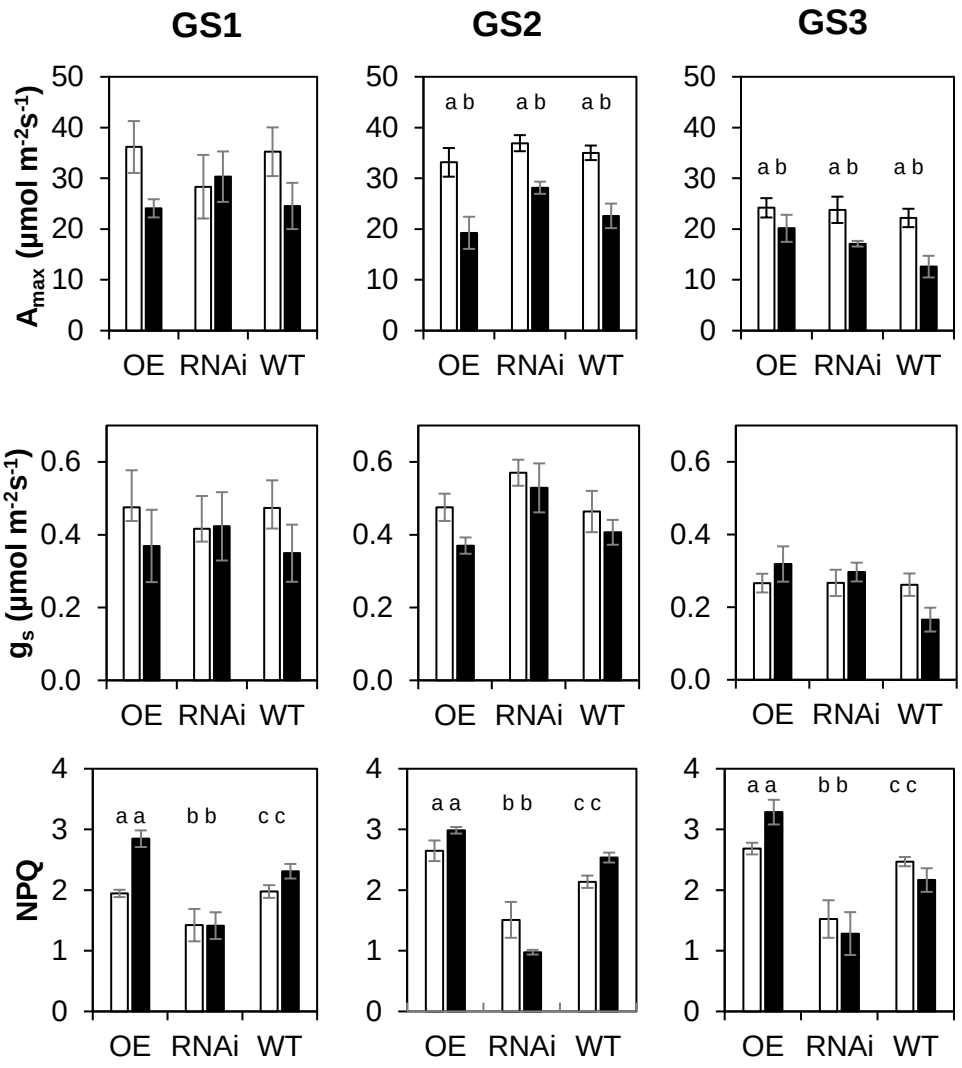


Figure 4-6. A selective comparison of maximum carbon assimilation (Amax), stomatal conductance (gs) and non-photochemical quenching (NPQ) measured at 2000 µmol $m^{-2}s^{-1}$ at the top (white) and bottom (black) of the canopies of rice overexpressing *PsbS* (OE), rice with downregulated *PsbS* (RNAi) and wildtype (WT). Data from the three growth stages (GS), GS1, GS2 and GS3 are shown. Error bars denote the standard error between the plots (n=4). Significant differences at 5% based on ANOVA are denoted by alphabets a, b, c etc.

At GS1, the top layer of the canopies was photoinactivated with F_v/F_m values lower than 0.83; 0.767±0.021, 0.699±0.033 and 0.742±0.010 for WT, OE and RNAi respectively. The F_v/F_m at the bottom layer of the canopy was

significantly higher than the top layer of the canopy at GS1 (P<0.001) and GS2 (P=0.001). However, at GS3, the bottom layer of the canopy had lower F_v/F_m than the top layer of the canopy (P<0.001). There were no differences in terms of F_v/F_m between the rice lines at GS1 (P=0.139). However, at both GS2 and GS3, OE had highest F_v/F_m values while RNAi lines had the lowest F_v/F_m (GS2, P=0.044; GS3, P<0.001; Figure 4-7).

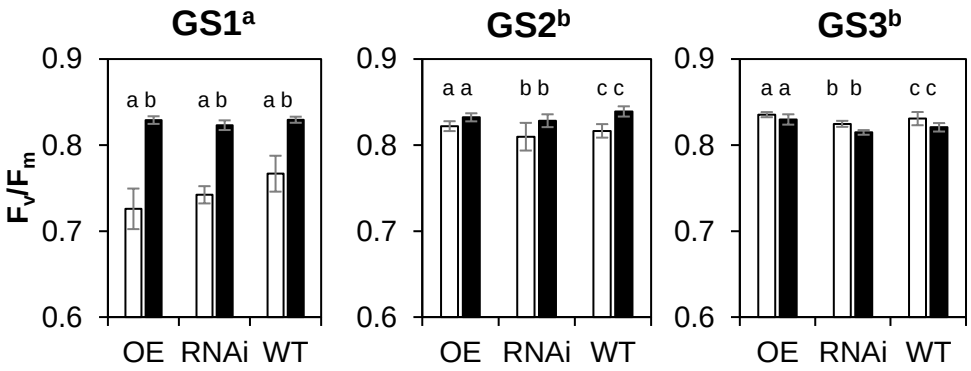


Figure 4-7. F_v/F_m values were measured at the top (white) and bottom (black) of the canopies of rice overexpressing *PsbS* (OE), rice with downregulated *PsbS* (RNAi) and wildtype (WT) at the three growth stages (GS), GS1, GS2 and GS3. Five plants per plot per canopy layer were sampled. Error bars denote the standard error between the plots (n=4). Significant differences at 5% based on ANOVA are denoted by alphabets a, b, c etc.

Plants were considered photoinactivated when qPd<0.98. Ten repeats of the pNPQ protocol were performed at each light intensity scales, resulting in 30 pNPQ protocol measurements to build each light tolerance curve. Figure 4-8 indicates the light intensity that caused photoinactivation in 50% of the leaves within the canopy layer ($I_{50\%}$), which was derived from the light tolerance curves. Here there were inconsistent patterns. No statistical comparison could be made based on the $I_{50\%}$ obtained from the light tolerance curves. The complete analysis for OE, RNAi and WT at each canopy later at each growth stage can be found in Supplementary material S2.1 (GS1), Supplementary material S2.2 (GS2) and Supplementary material S2.3 (GS3). It can be

observed that at GS1, the top of the canopy had greater $I_{50\%}$ than the bottom of the canopy but this was not the case for the other growth stages. At GS2, OE had higher $I_{50\%}$ (as expected) for both layers but this was not the case for GS3 where $I_{50\%}$ was higher in the lower parts of the canopy.

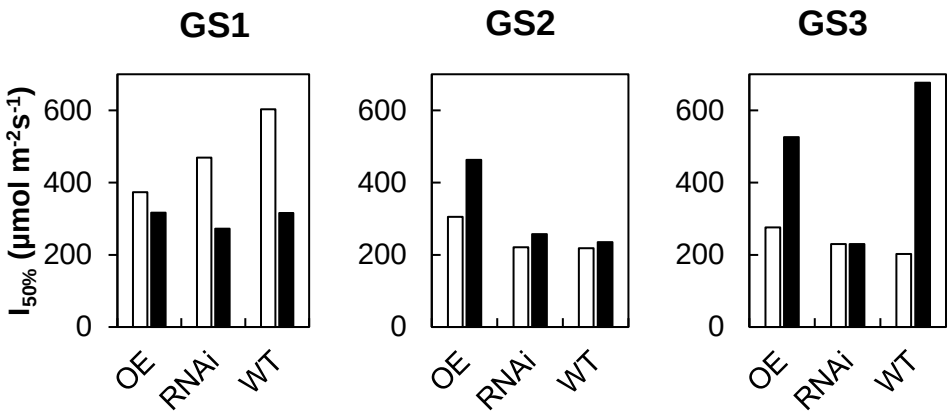


Figure 4-8. A comparison of the light intensities at which 50% of the leaves within the canopy layer are photoinactivated ($I_{50\%}$) at the top (white) and bottom (black) layers of the canopy of rice overexpressing *PsbS* (OE), rice with downregulated *PsbS* (RNAi) and wildtype (WT) at the three growth stages (GS), GS1, GS2 and GS3. No statistical analysis was possible.

The photosynthetic photon flux density (PPFD) varies due to solar movement. This fluctuating light environment led to different profiles of light intensity within the canopy that can be quantified using the ray tracing algorithm. To account for this PPFD profiles were generated to show the differences between OE, RNAi and WT canopies at midday (example shown in Figure 4-9). Coupled with the canopy architecture and position within the canopy, a large combination of light profiles could arise. Figure 4-10b illustrated a possible light “mosaic” within WT rice canopy at GS3 during midday. Each light tolerance curve was colour-coded to “10% photoinactivation” bins (Figure 4-10a). The area under each bin would correspond to the surface area of leaves that were photoinactivated. The light intensity ranges (right hand panel, Figure 4-10b) would also correspond to the colour codes used to

colour the “10% photoinactivation” bins. Applying the ray-tracing techniques, the light course of a point within the rice canopies could be predicted (Figure 4-10c). It can show how PPFD varies at different position within the canopy. During midday, the top of the canopy was exposed to prolonged periods of higher light intensity but often with a diurnal pattern relating to solar movement. Low light intensities interspersed with high light peaks or sunflecks, can be observed at the bottom of the canopy.

These data altogether were useful for the creation of the profiles of photoinactivation across the surface area of a plant canopy, which has not been demonstrated before (Figure 4-11). These profiles give a visual representation of the percentage of leaves (leaf area) within the canopies that were photoinactivated throughout the day from sunrise to sunset. At GS1, when the canopy was just starting to develop, most of the leaves were experiencing some sort of photoinactivation. There would be higher photoinactivation during midday as expected. The proportion of leaves experiencing higher amount of photoinactivation was also found to be higher. From the modelling, RNAi canopies experienced higher levels of photoinactivation at 70-80%, compared to WT and OE which experienced about 20% photoinactivation. When the canopy starts to close and mature (GS2 and GS3), it can be observed that a large proportion of the leaves would remain unaffected by photoinactivation. In WT and RNAi canopies, there were higher levels of photoinactivation of leaf surface areas compared to OE where most leaves in the upper portion of the canopy experience relatively lower levels of photoinactivation.

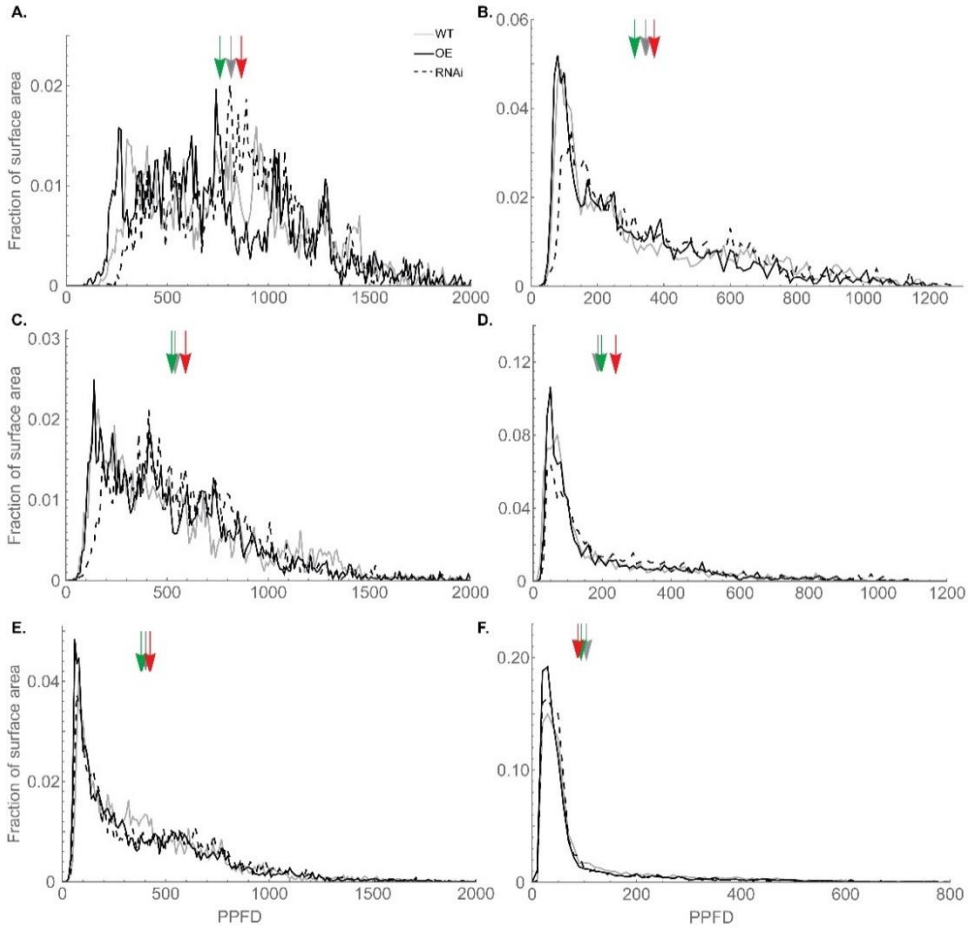


Figure 4-9. Frequency of PPFD values according to the fraction of surface received at 1200H in the **A**, **C** and **E**. top of the canopy and **B**, **D** and **F.** bottom of the canopy where **A**, **B**. GS1, **C**, **D**. GS2 and **E**, **F**. GS3 and the grey, green and red arrows indicate the average PPFD value for wildtype (WT) rice, rice overexpressing *PsbS* (OE) and rice with downregulated *PsbS* (RNAi) respectively.

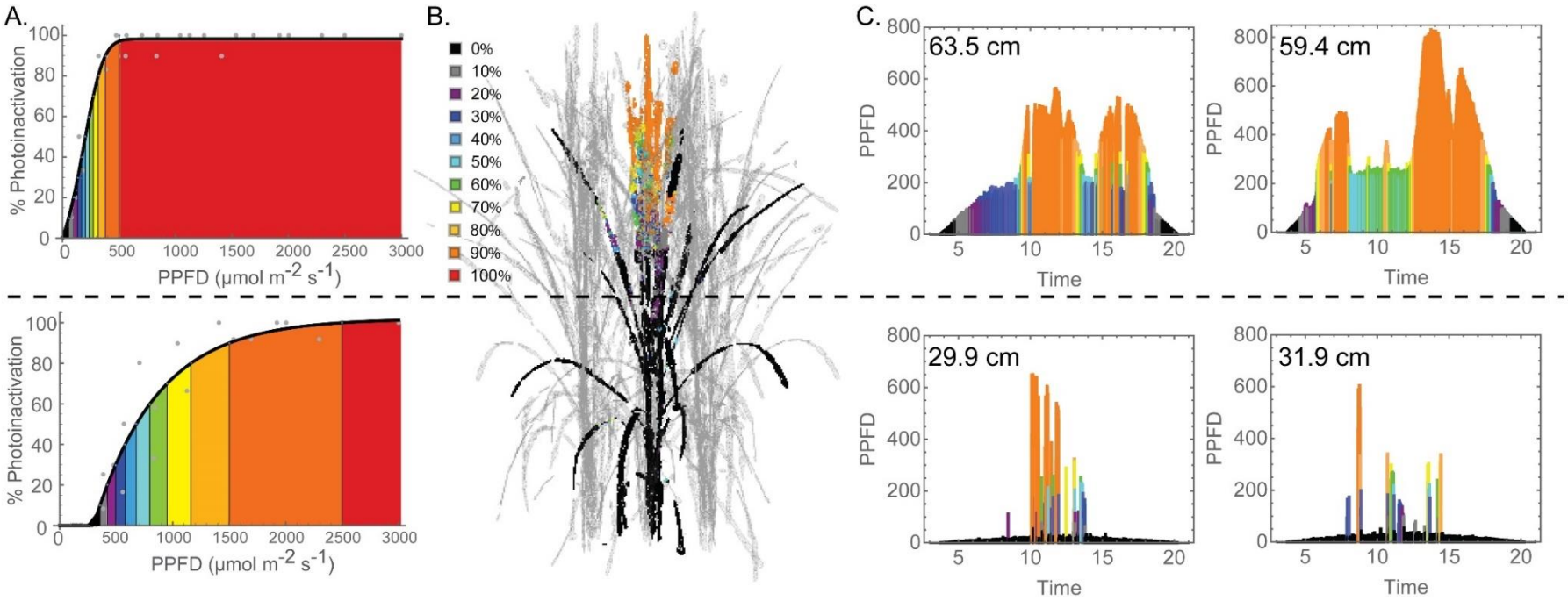


Figure 4-10. Light tolerance curves combined with canopy light profiles enable the visualisation of photoinactivation according to canopy position **A**. Wildtype (WT) rice population tolerance curve calculated using the fluorescence routine on the Junior-PAM (Heinz Walz GmbH, Effeltrich, Germany). The photosynthetic photon flux density (PPFD) ranges that correspond to a set photoinactivation per canopy top or bottom are colour coded. **B**. A representative reconstructed WT rice canopy at GS3 with a single plant in bold. Right panel showed the colour-coded photoinactivation range. **C**. The PPFD during the course of a day at four representative canopy positions, with the height of each canopy location from the ground given the top left corner of each graph, calculated using ray-tracing technique.

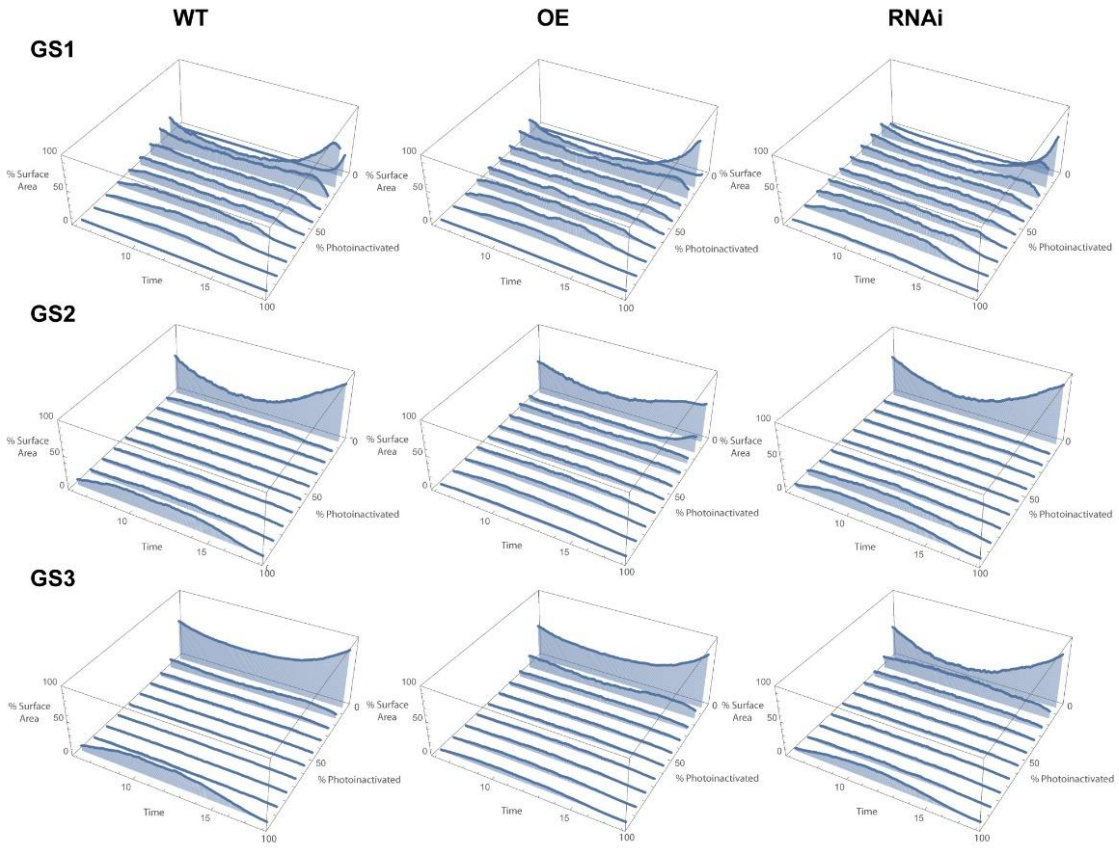


Figure 4-11. Profiles of photoinactivation (expressed in terms of percentage of leaves photoinactivated) according to the total surface area of leaves (expressed in percentage) and the time of the day (between 0600H and 1800H) for rice overexpressing *PsbS* (OE), rice with downregulated *PsbS* (RNAi) and wildtype (WT) at the three growth stages (GS), GS1, GS2 and GS3.

4.4 Discussion

NPQ has positive and negative effects within canopies; whilst photoprotection is required to prevent damage, over-protection may also reduce photosynthesis efficiency. The pNPQ protocol allowed the assessment of the protective capacity of NPQ and, when measured at different canopy positions, enabled whole canopy pNPQ to be assessed (Ruban, 2017b). It does not only allow the building of light tolerance curves which can indicate the early detection of onset of photoinactivation but also allowed the possibility of estimating the light tolerance level simultaneously in leaves (within a canopy) at different states of light saturation. Reconstruction of the canopies made it possible to model the light movement within the canopies using ray-tracing techniques. This technique has been applied to study different crop canopy physiology (see Burgess *et al.*, 2015, 2016, 2017; Retkute *et al.*, 2015; Townsend, Ware and Ruban, 2018) but not on pNPQ. Aligned with the increased interest in canopy level NPQ (Kromdijk *et al.*, 2016; Głowacka *et al.*, 2018; Hubbart *et al.*, 2018), these techniques come together to allow an accurate assessment of the trade-offs between photoprotection and productivity through 3D reconstruction as shown in Figure 4-10.

In this study, pNPQ was studied at leaf level in rice plants with either upregulated or downregulated *PsbS* rice lines to develop light tolerance curves and was in turn was modelled into canopy level. This is the first time that a cellular level process quantified using chlorophyll fluorescence has been scaled up to a whole canopy level using 3D reconstruction of plant canopies. The plant material used in this study was previously studied (Hubbart *et al.*, 2012, 2018). The rice *PsbS* overexpressor (OE) lines have consistently showed to have improved grain yield and to be not

photosynthetically impaired. Likewise, the *PsbS* RNAi (RNAi) lines were also smaller (as also observed in this experiment) with lower grain yield (Hubbart *et al.*, 2012). High-resolution reconstruction enables quantification of canopy architectural traits and indicates key differences between the lines. For example, this method has shown differences in the accumulation of leaf material according to canopy height (Figure 4-5a), such as the sparsity the top of the rice RNAi canopies, particularly at GS2 (Figure 4-5b). However, the tiller number, plant height and above-ground dry weight did not reflect this. This is justifiable as the RNAi rice plants, although they did not have much actual height difference compared to OE or WT, they had smaller cLAI at GS1 and GS2 and only caught up with the OE during GS3. This is important as plant architecture at GS1 is critical in determining photosynthesis characteristics (Burgess *et al.*, 2017). In this study, it is shown that OE had greater early advantage based on the greater cLAI and relatively denser canopy structure than WT. The greater cLAI could be due to the faster growth rate and RUE seen in these lines (Hubbart et al 2018). Hence, increasing *PsbS* does not only confer early growth advantage but also increases canopy growth with reduced light intensity within the canopy. These are consistent with previous results (Hubbart *et al.*, 2018).

The bottom of the rice canopies showed higher light tolerance than the top of the canopies, the first time this has been observed. It was previously reported that older Arabidopsis leaves can tolerate higher levels of light (Carvalho, Ware and Ruban, 2015). We would expect the same for the rice plants too except that in rice plants, leaves grow from the base and extend up. The same leaf can sit within the top half and bottom half of the canopy. Hence, careful random selection of leaves during measurements took this into consideration. The light tolerance data obtained for GS1 were not exactly as

expected. At GS1, the canopies were young and not fully formed. Hence, there was more space between the plants, exposing them to higher light levels. In general, rice *PsbS* OE canopies had higher $I_{50\%}$ than WT and RNAi as expected. The light history of each point measurements should be taken into consideration. However, the dark adaptation of the leaves prior to measurements allowed the assumption that the leaves were given a similar "light history".

Unlike during GS1, GS2 and GS3 had fuller canopies which allowed better studying of the canopy at in two different layers. Most of the flag leaves at the top were mainly upright and the other leaves were also relatively erect and fell at an angle. Another factor to consider is the solar angle. The sun moves throughout the day adding another layer of complexity. At the top of the canopies, WT and OE would have higher proportions of self-shading resulting in a reduced light within the layer and this would be multiplied down to the bottom canopy (dilution effect). In the RNAi, there were more spaces in between the leaves and plants, allowing greater light penetration. In comparison, the OE and RNAi leaves fell in such a way that they were more horizontal than the WT at the bottom of the canopy. So, less leaves were sticking out of an assumed "canopy grid" in a WT rice canopy.

Canopies are heterogeneous (Bielczynski *et al.*, 2017) and most studies do not account for this. High resolution 3D reconstructions used in this study can account for the variations between the rice lines and within the canopies (Burgess *et al.*, 2015, 2016, 2017; Townsend, Ware and Ruban, 2018). This allows the analysis of the changes in structural traits arising from the altered expression of *PsbS*. Although difficult to interpret, the profiling of the photoinactivated leaves throughout a day (Figure 4-11) allowed a better comparison of the effect of *PsbS* in rice at whole canopy level over time of the

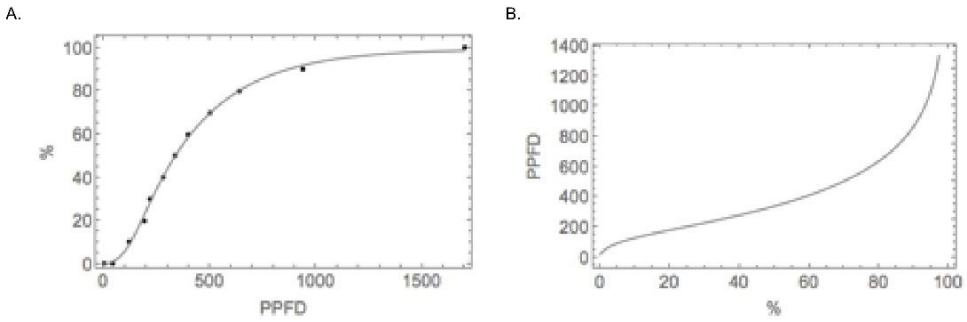
day, the first time this kind of distribution has been shown. This new kind of approach is required to demonstrates the relative distribution of inactivation in a plant canopy. It is useful in comparison with the expected degree of light saturation of photosynthesis at different canopy positions, for example where inactivation at the upper part of the canopy is less likely to lead to a loss of productivity than inactivation lower in the canopy where it is more likely to influence quantum yield. Future studies would benefit from the further application of these techniques as plant architecture as it has such a big influence on the canopy light environment. A combination of altered architecture and improved biochemistry modelled under a range of different environments can be used to fine tune and maximise productivity.

4.5 Summary

PsbS over expression was associated with faster cLAI accumulation which resulted in differences in light environment within the canopies. The use of high-resolution 3D reconstructions can for the first-time account for the variations in photoprotection across leaf surfaces within the canopy that arise from interactions between light dynamics and changes in biochemistry. We observe enhanced light tolerance at lower levels in the canopy, contrary to expectation. Furthermore, cellular level processes could be magnified to observe the canopy level effects.

Supplementary Material

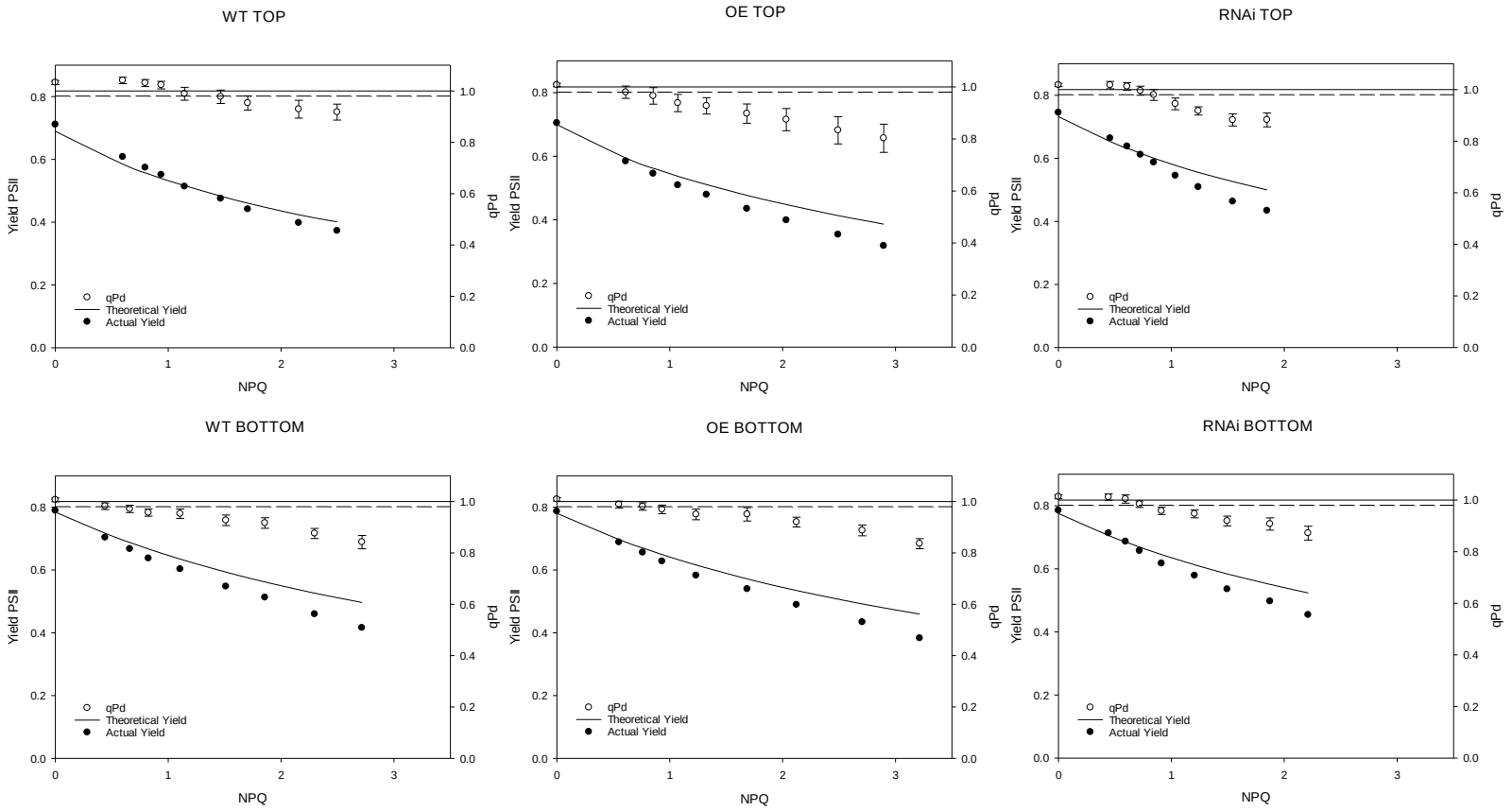
Supplementary Figure S4-1



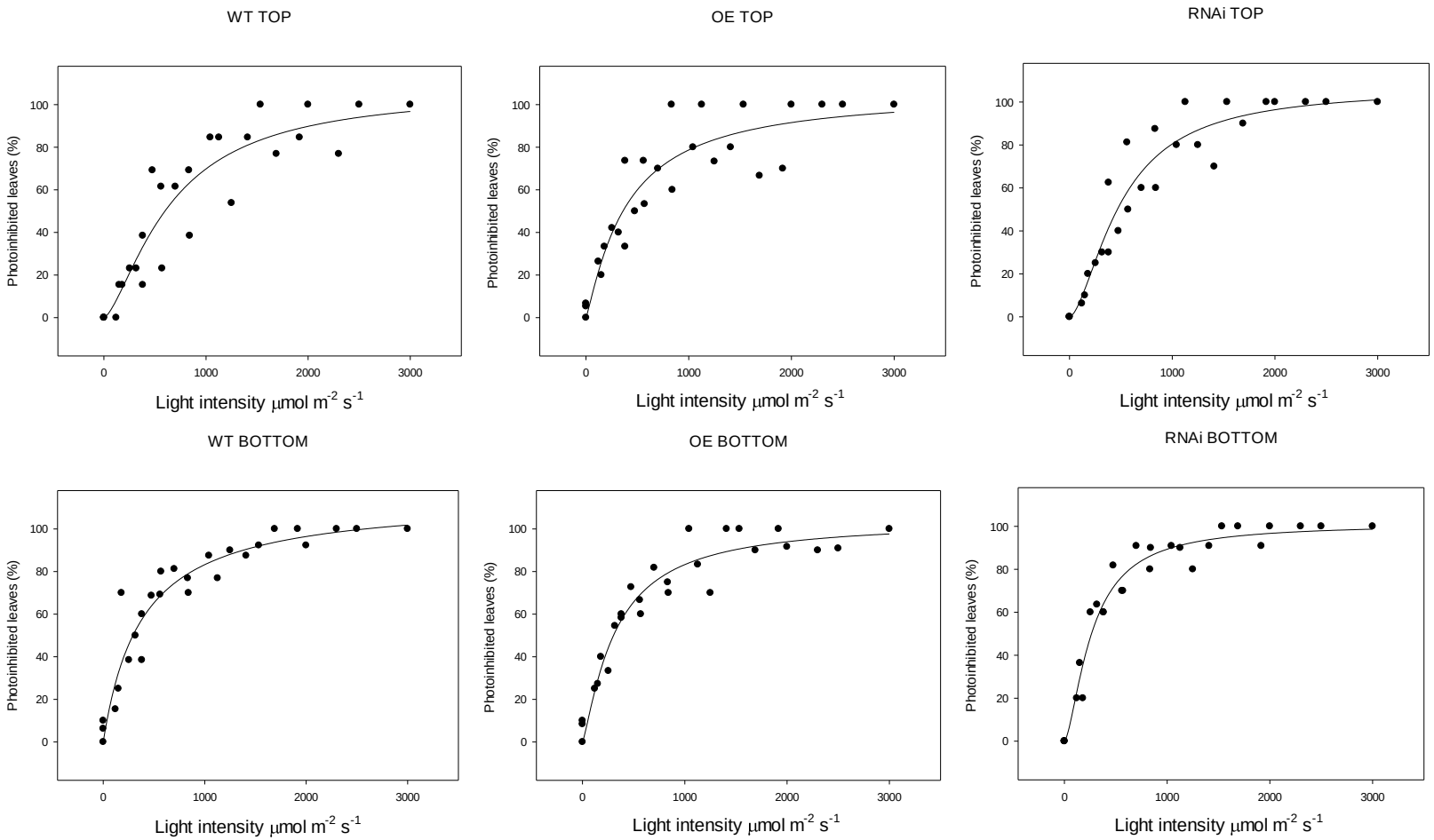
Supplementary Figure S 4-1. pNPQ data from the top layer of WT plants with associated fitted curves. **A**. Relationship between the percentage of photoinactivated leaves and light. **B**. Relationship between light intensity and the percentage of photoinactivated leaves. Here a=41.7, b=99.4, c=1.2, d=0.06 and e=0.12

Supplementary Material S4-2

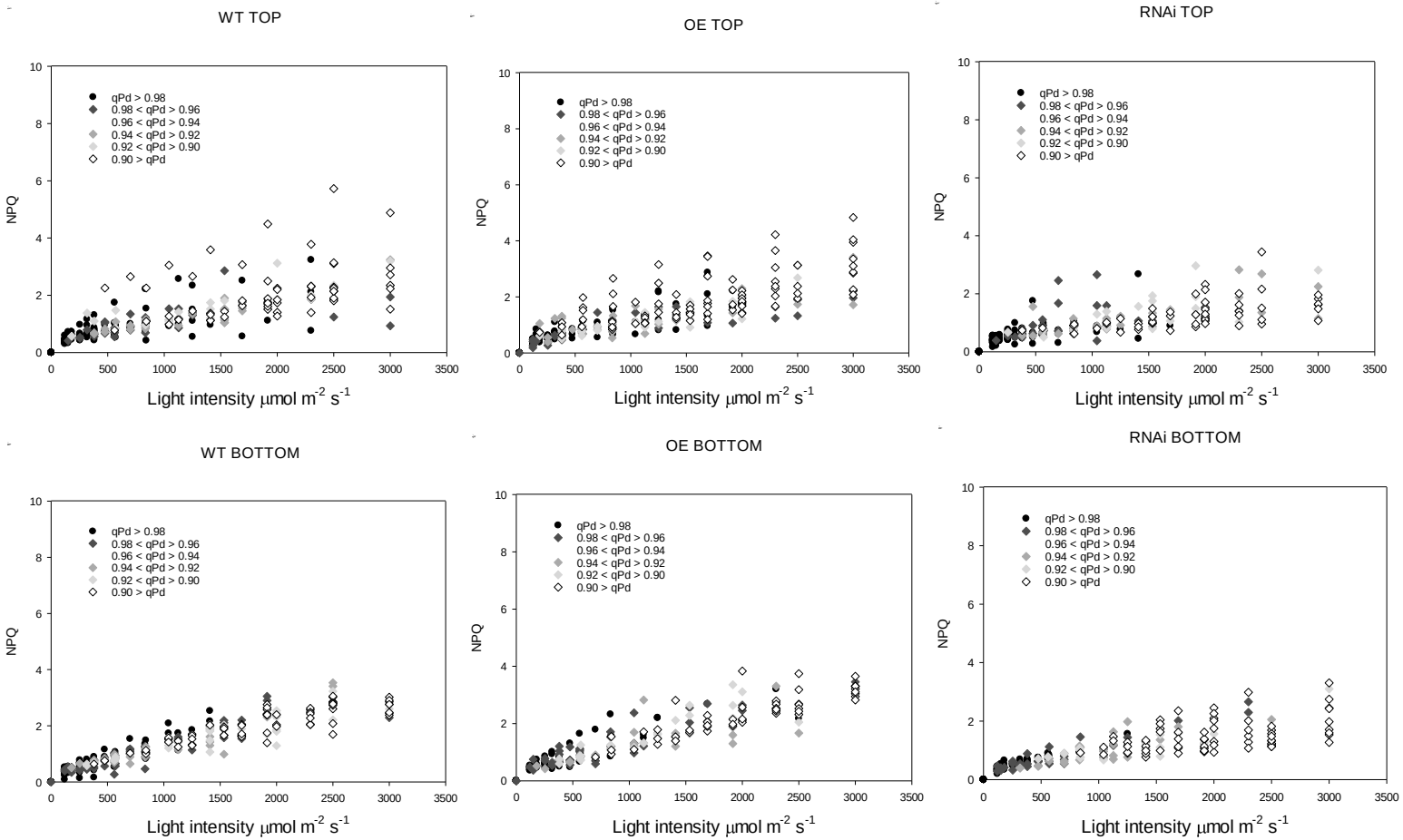
Relationship between ΦPSII, qPd and NPQ for WT, OE and RNAi at top and bottom of the canopy layers at GS1.



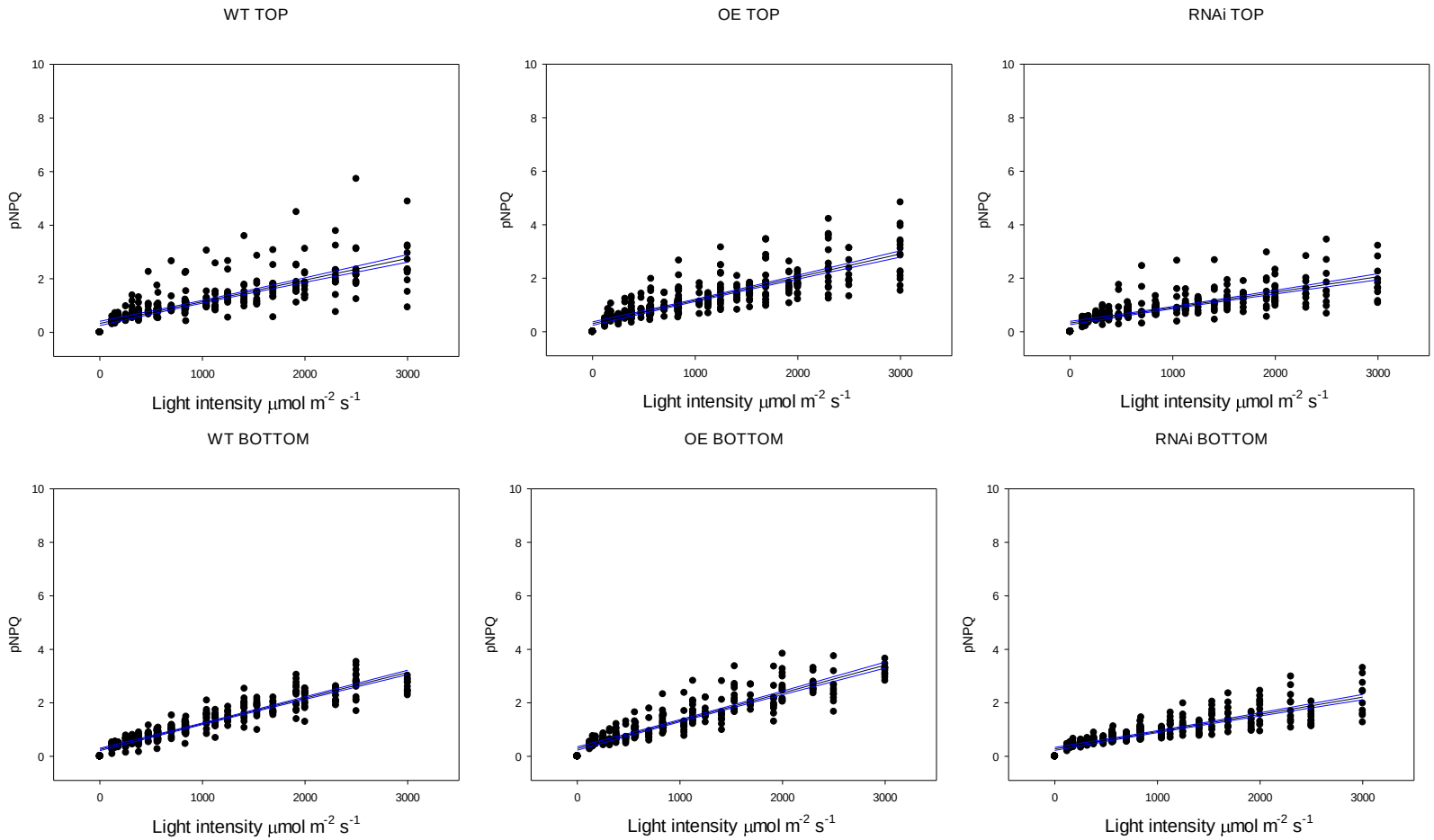
Light tolerance curves for WT, OE and RNAi at top and bottom of the canopy layers at GS1.



A 3D representation of the openness of reaction centres (qP_d), with the corresponding pNPQ and AL intensity for WT, OE and RNAi at top and bottom of the canopy layers at GS1.

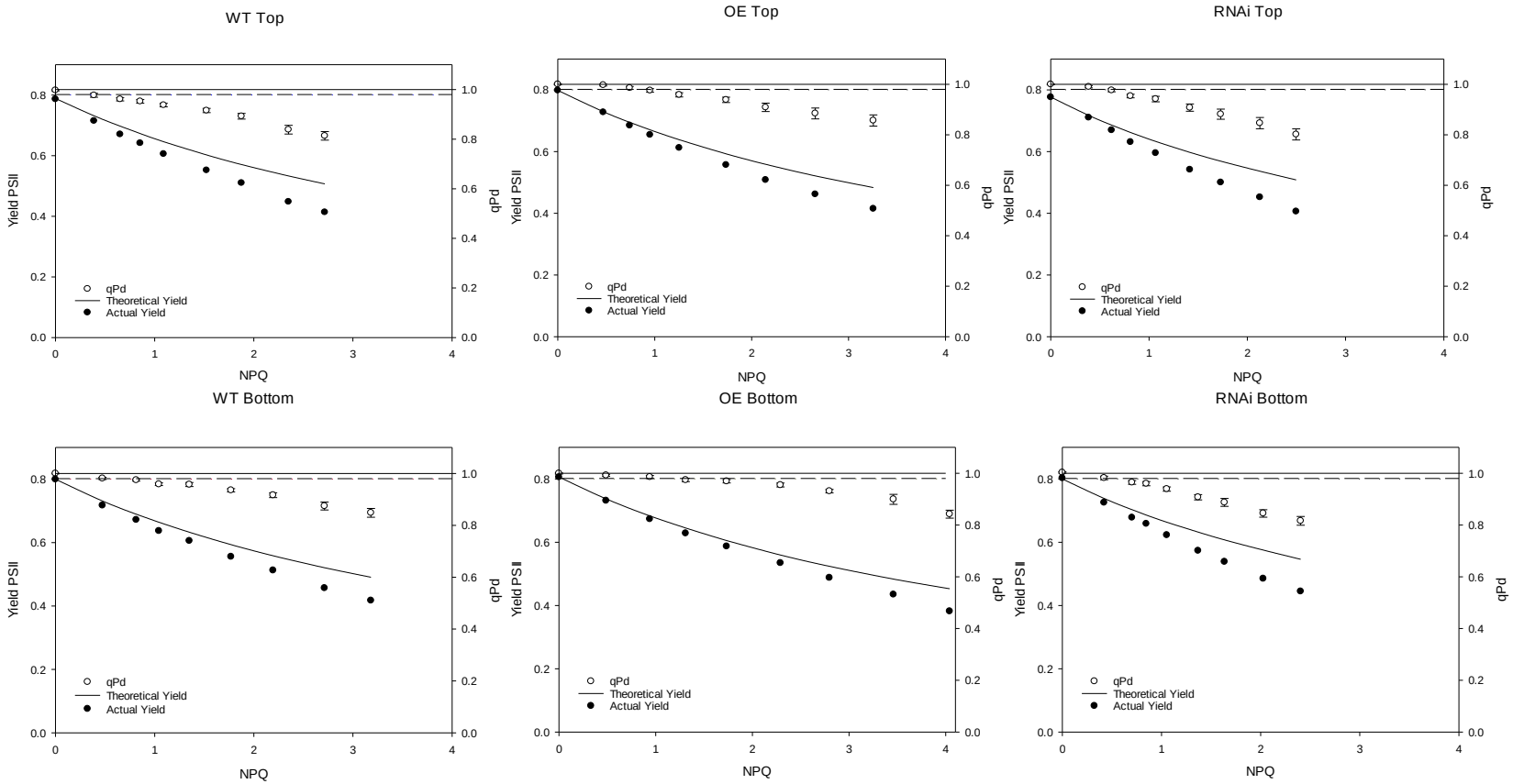


The plots between pNPQ and AL intensity for WT, OE and RNAi at top and bottom of the canopy layers at GS1.

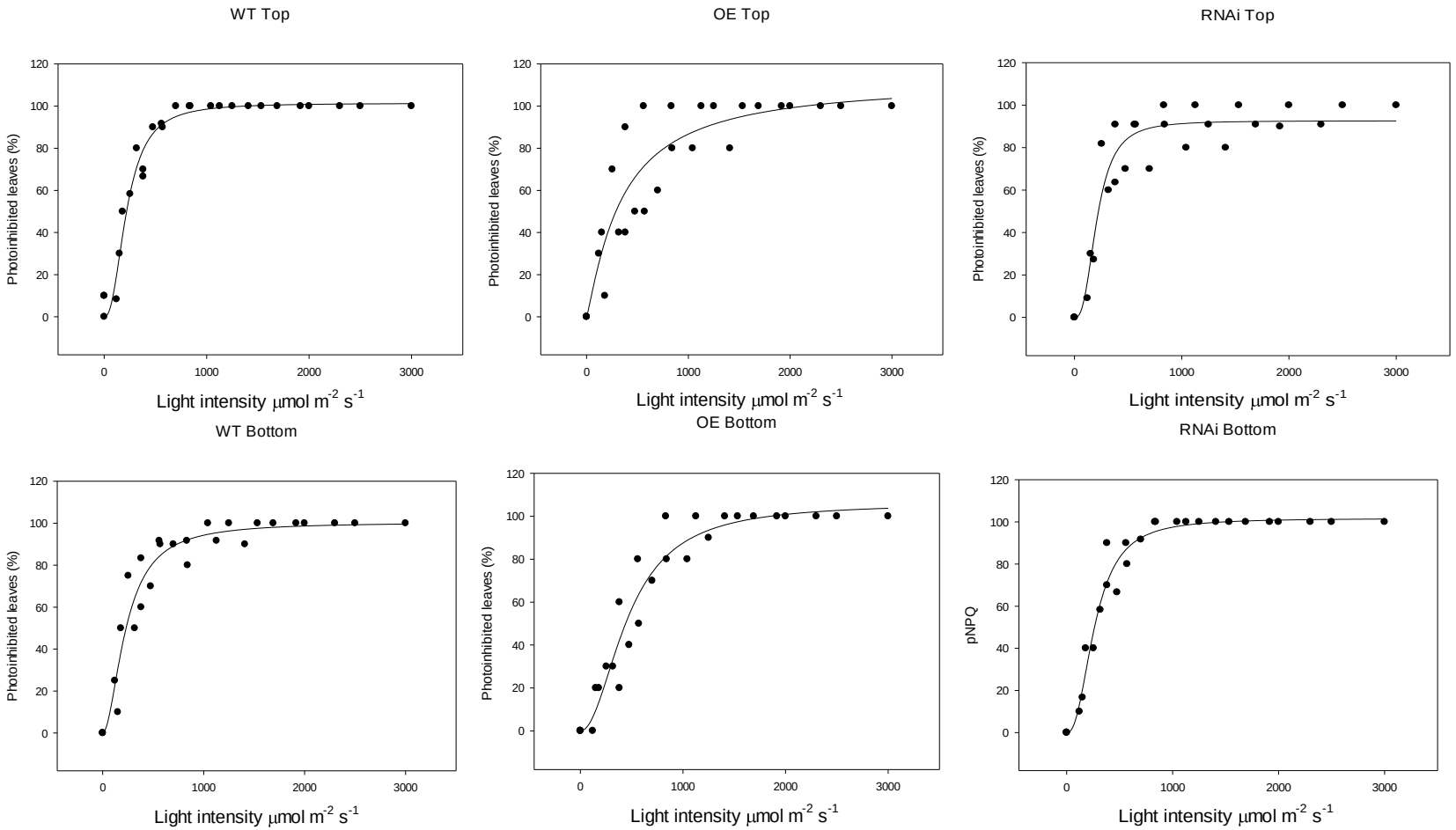


Supplementary Material S4-3

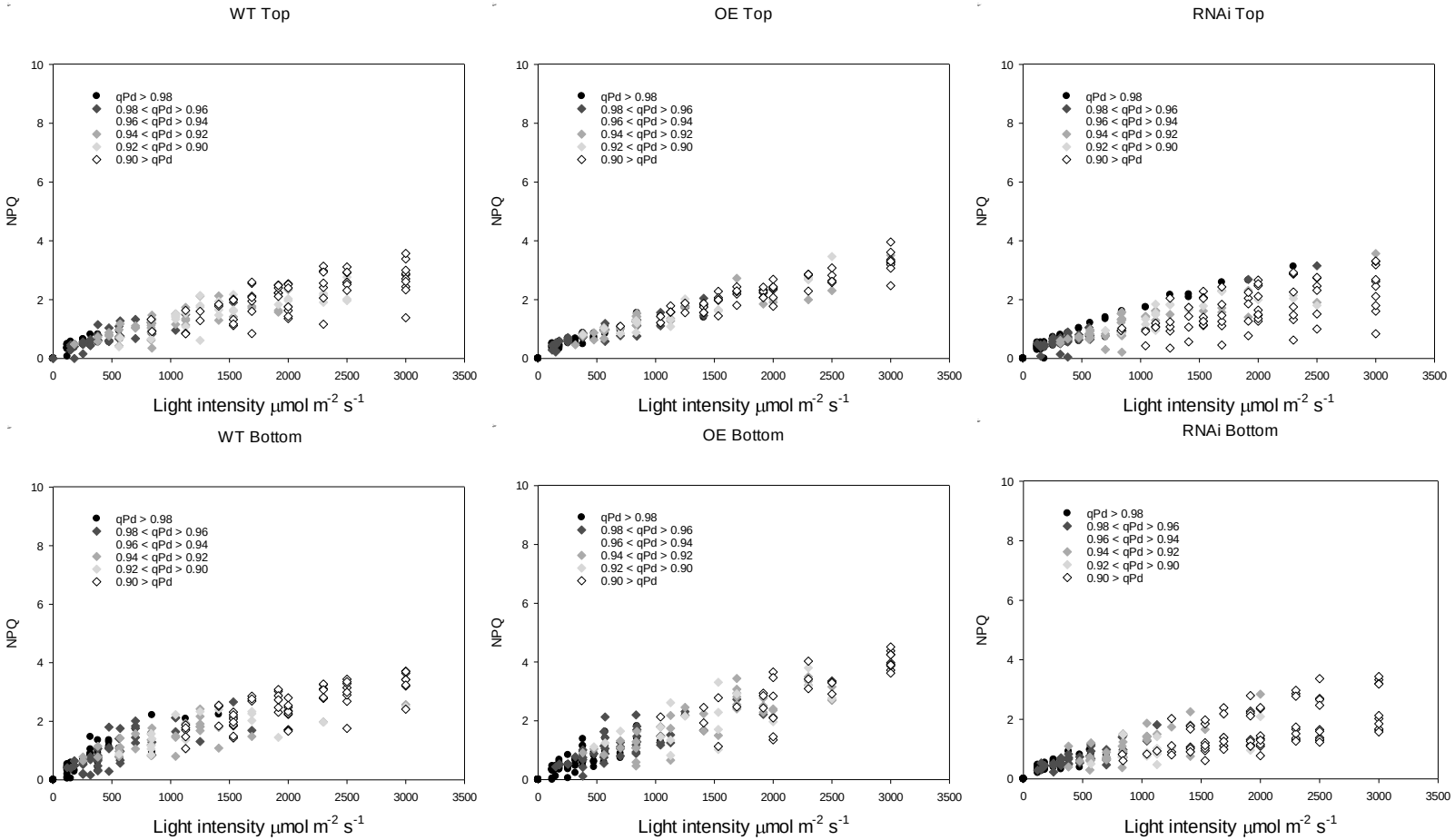
Relationship between ΦPSII, qPd and NPQ for WT, OE and RNAi at top and bottom of the canopy layers at GS2.



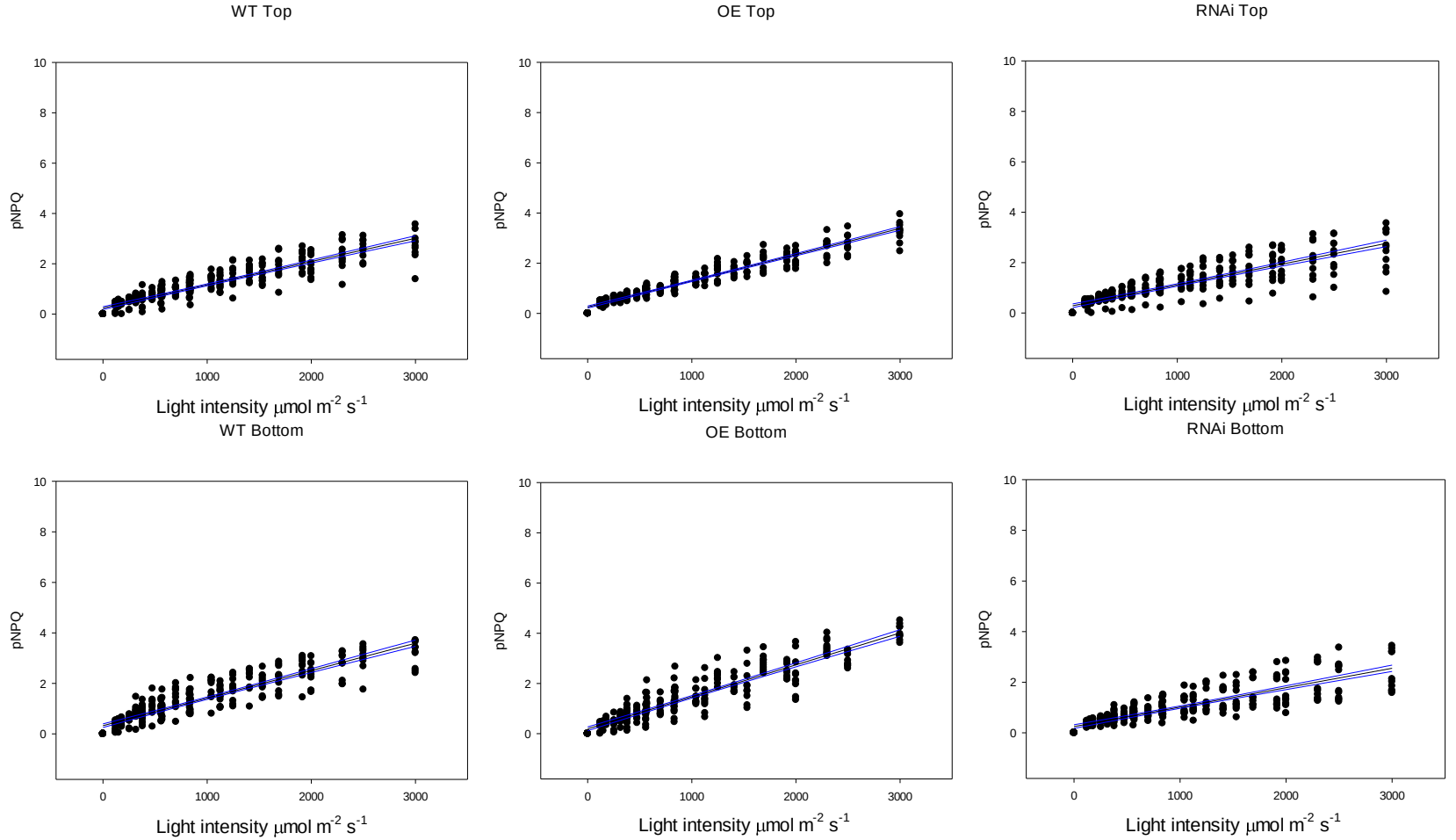
Light tolerance curves for WT, OE and RNAi at top and bottom of the canopy layers at GS2.



A 3D representation of the openness of reaction centres (qP_d), with the corresponding pNPQ and AL intensity for WT, OE and RNAi at top and bottom of the canopy layers at GS2.

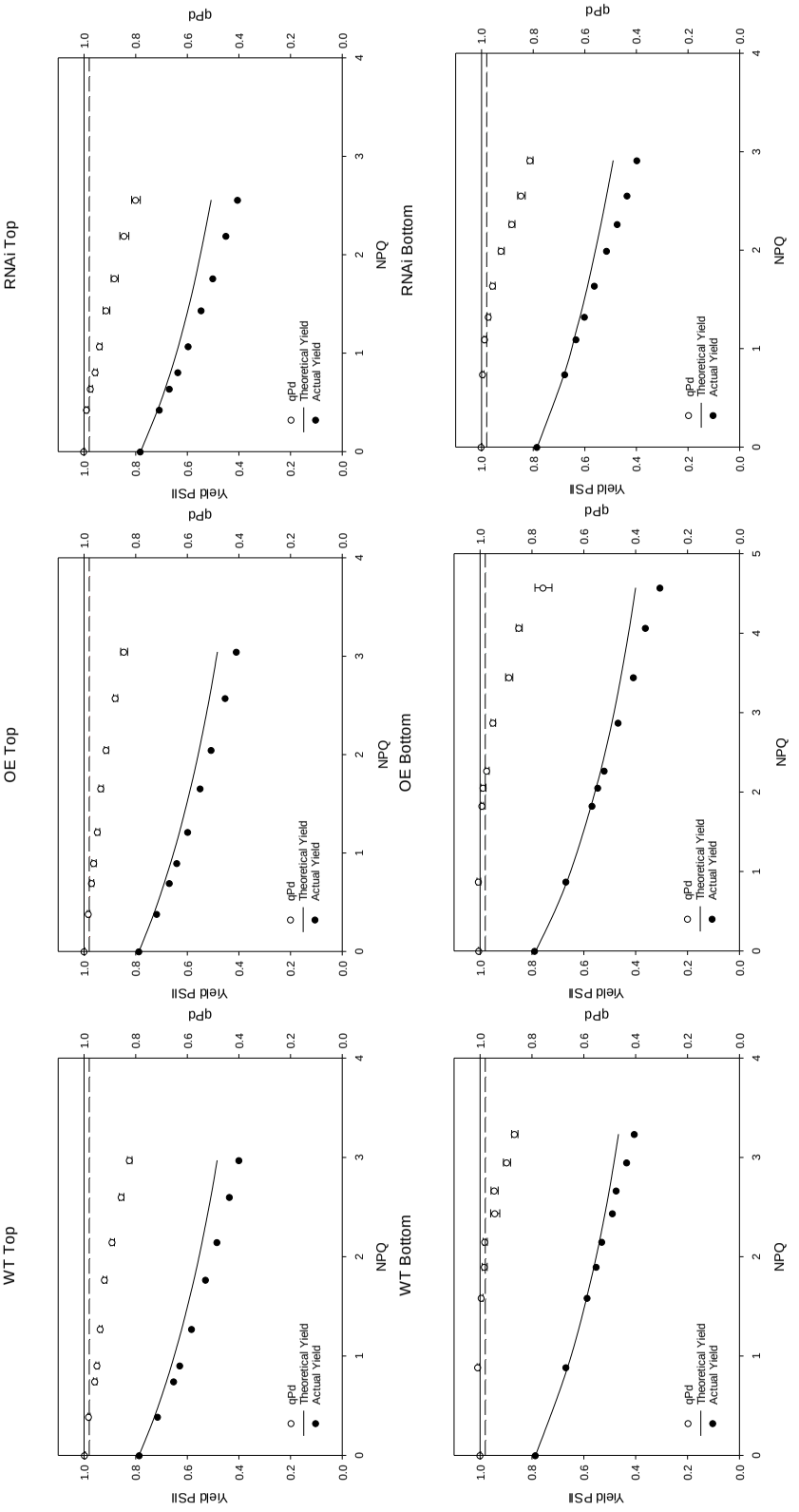


The plots between pNPQ and AL intensity for WT, OE and RNAi at top and bottom of the canopy layers at GS2.

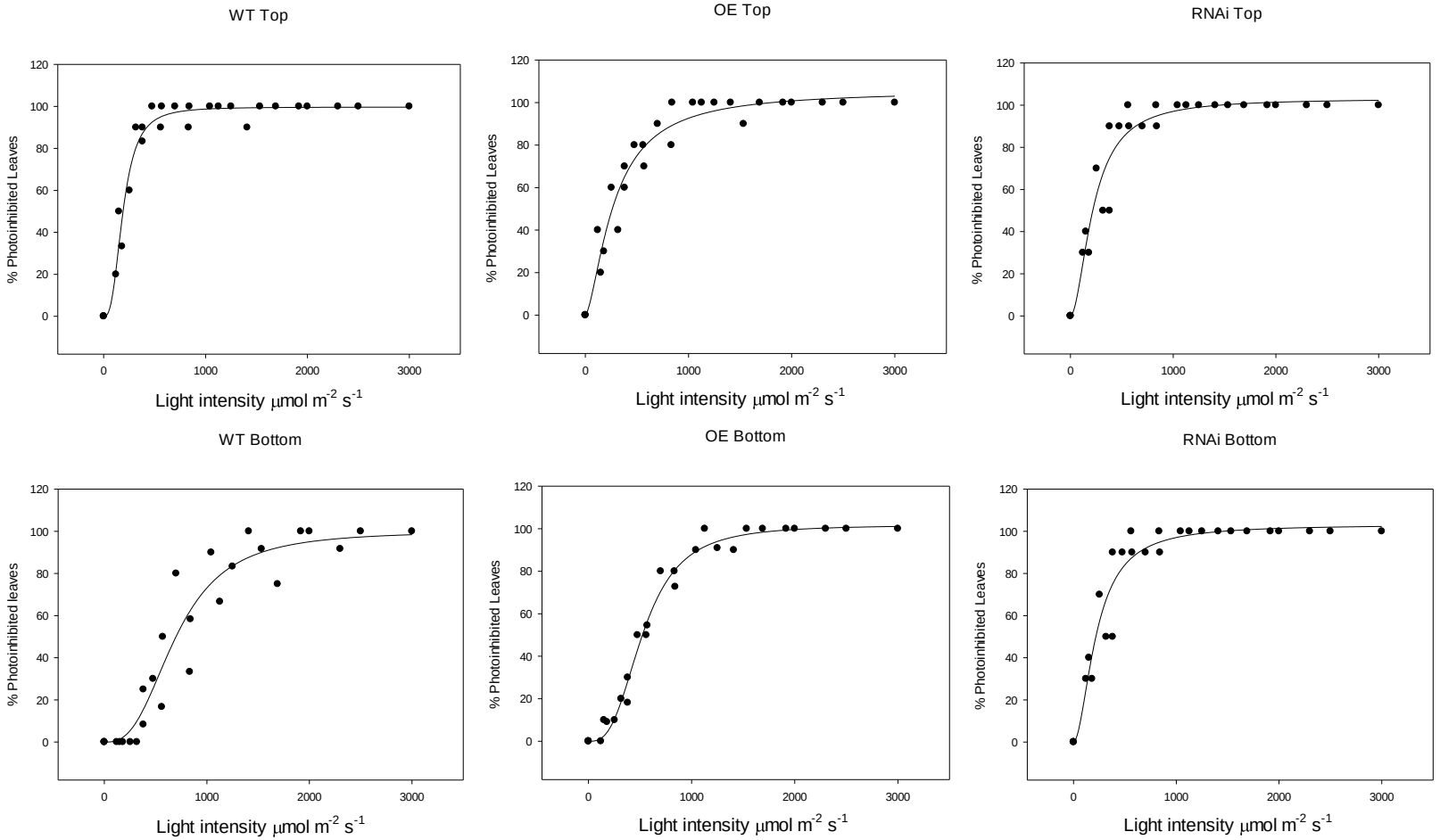


Supplementary Material S4-4

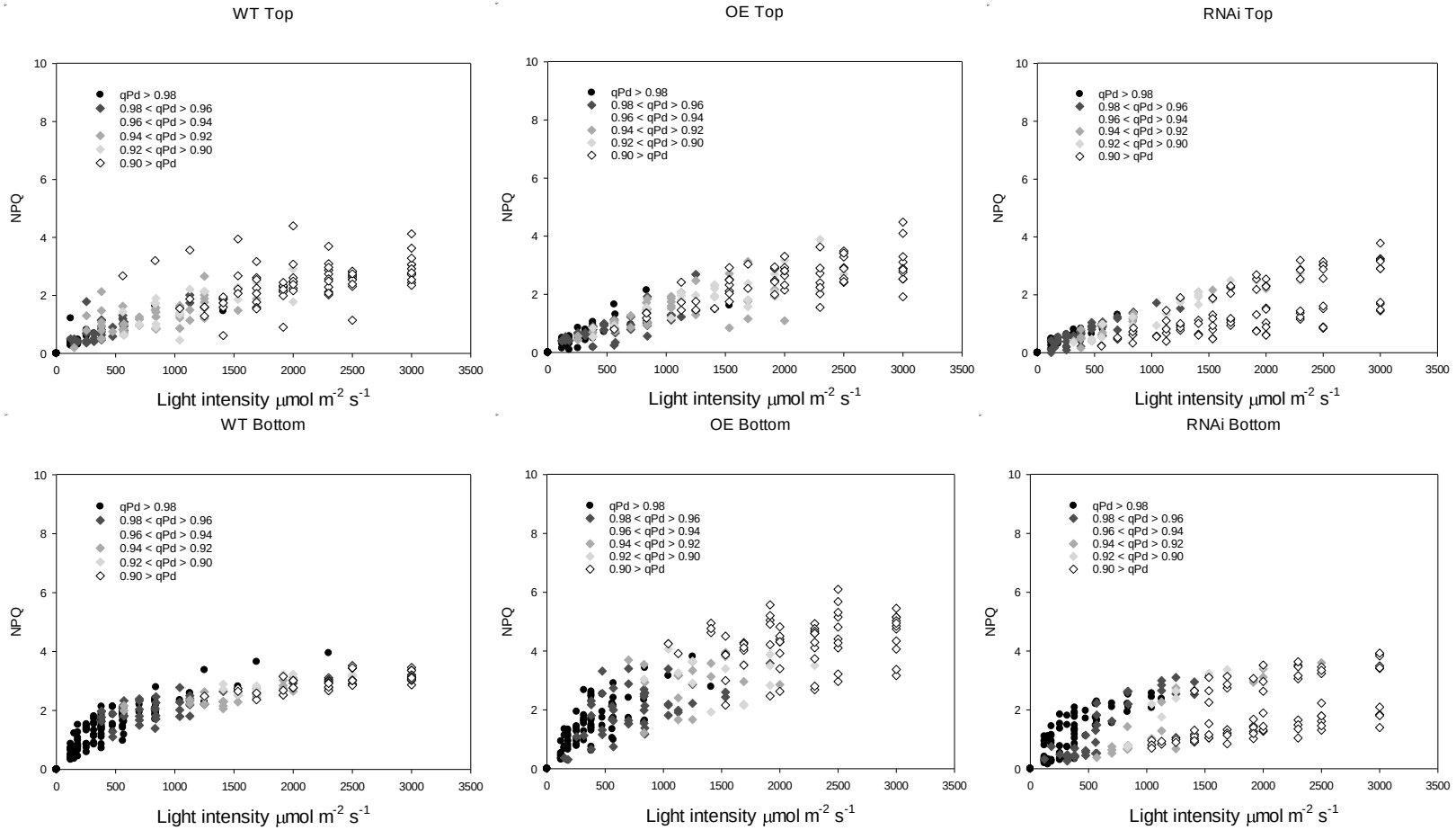
Relationship between ΦPSII, qPd and NPQ for WT, OE and RNAi at top and bottom of the canopy layers at GS3.



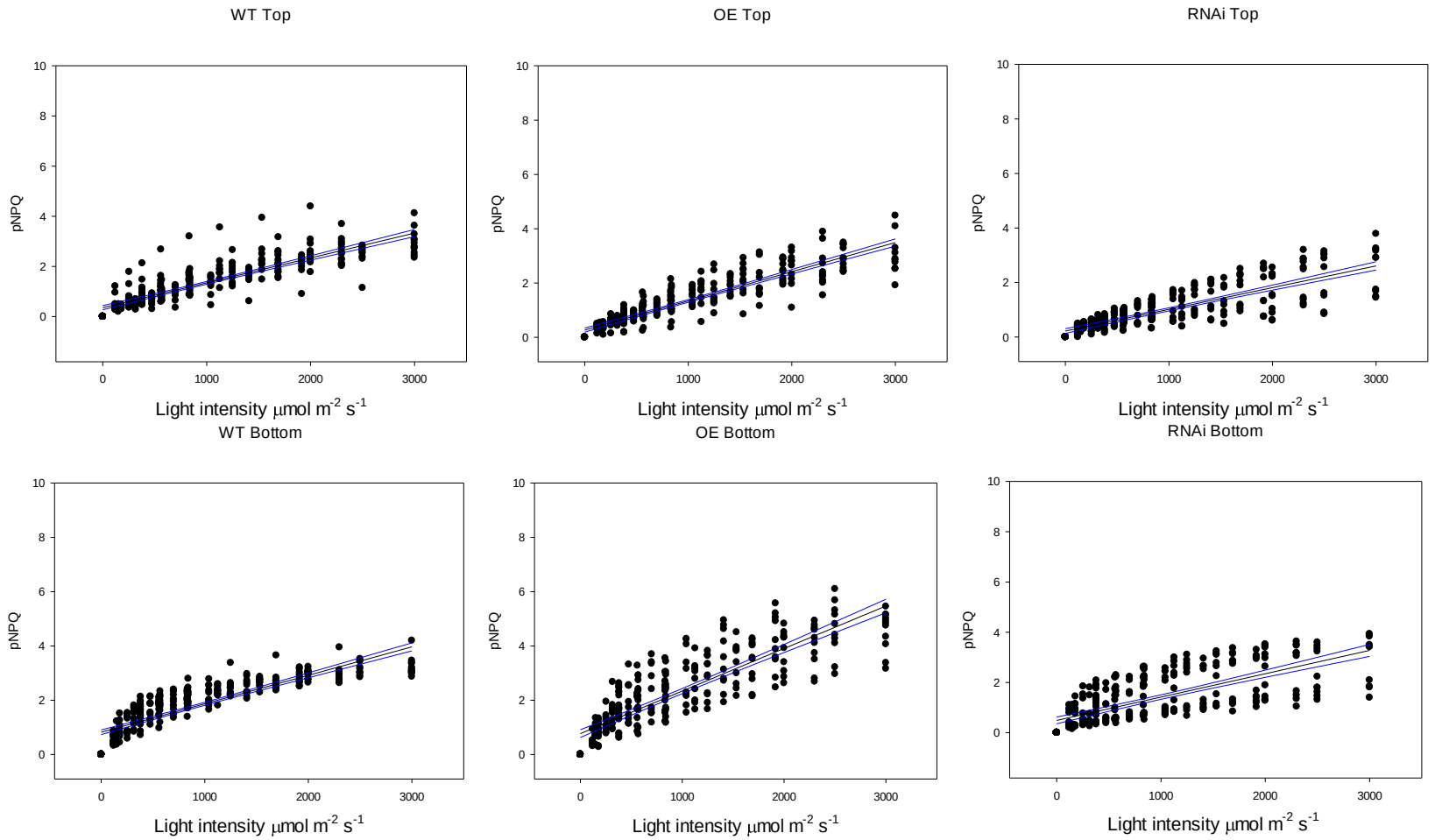
Light tolerance curves for WT, OE and RNAi at top and bottom of the canopy layers at GS3.



A 3D representation of the openness of reaction centres (qP_d), with the corresponding pNPQ and AL intensity for WT, OE and RNAi at top and bottom of the canopy layers at GS3.



The plots between pNPQ and AL intensity for WT, OE and RNAi at top and bottom of the canopy layers at GS3.



Chapter 5 Overexpression of *PsbS* could Improve Water Use Efficiency (WUE) in Rice

C.C. Foo and E. H. Murchie

Plant and Crop Science Division, School of Biosciences, University of Nottingham, Sutton Bonington LE12 5RD UK

Author contribution:

Experiment conceived by EH Murchie and CC Foo

Project supervision performed by EH Murchie

All experimental work by CC Foo

Written by CC Foo

5.1 Abstract

Głowacka *et al.* (2018) observed a higher water use efficiency in field-grown tobacco plants overexpressing *PsbS* and suggested stomata could be controlled by a light dependent signal related to NPQ and the function of *PsbS* in the thylakoid membrane whereby *PsbS* acts to alter the speed of stomatal opening and closing. To test this in rice, plants overexpressing *PsbS* were grown under controlled growth room conditions and leaves subjected to a light transition from low to high and back to low. No light-dependent control of stomata was observed. A mild water deficit was subsequently imposed on the rice plants overexpressing *PsbS* to partially reduce stomatal conductance. Under mild water deficit the *PsbS* overexpressor rice plants showed higher intrinsic water use efficiency than the wildtype rice plants. Under no water deficit, no differences in intrinsic water use efficiency was observed between the *PsbS* overexpressor rice plants and wildtype rice plants. Hence, we suggest that the light dependent signal observed in tobacco by Głowacka *et al.* (2018) is not present in rice but that a similar signal may be linked to water status of the plants.

5.2 Introduction

Water availability and water use efficiency in crops are important targets for crop productivity. Agriculture and food productivity are highly dependent on the availability of freshwater. It is more important than ever to work towards developing water use efficient crops for sustainable agriculture due to the impending lack of available freshwater and climate change (Araus *et al.*, 2002; Chaves *et al.*, 2002; Morison *et al.*, 2008; Urban *et al.*, 2017; Caine *et al.*, 2019; Hatfield and Dold, 2019b). Water use efficiency (WUE) links water use in plant to its productivity through the quantifying of the biomass produced for every unit of water used by the plant.

There are two main ways to quantify WUE at the leaf level using gas exchange equipment; 1. Instantaneous WUE which is the ratio of net carbon assimilation rate to transpiration rate and 2. Intrinsic WUE which is the ratio of net carbon assimilation rate to stomatal conductance (Lavoie-Lamoureux *et al.*, 2017; Hatfield and Dold, 2019b). For this chapter, instantaneous WUE will be referred to WUE and intrinsic WUE will be referred to as WUE_i. Water use can be studied from leaf level to whole canopy level. For example growth rate and dry weight can be normalised to water application and usage but the most apparent interactions should start at leaf level as they are not affected by the additional complexity of 3D plant architecture and canopies; in this case WUE_i (Hatfield and Dold, 2019b).

In the quantification of WUE_i, stomata play a key role whether in terms of its conductance or its role in transpiration. Stomata, described as “microvalves” on leaves, play the most important role in atmospheric gas exchange and account for most of the foliar water loss (Lawson, 2009; Lawson *et al.*, 2014; Henry *et al.*, 2019). As small as they are, their impact can vary from plant

level to global scale affecting water and carbon cycles and energy fluxes. Regulation of the opening and closing of the stomata is important for plant productivity and survival involving processes like photosynthesis, water use and protection from excessive water loss (Franks *et al.*, 2017; Martin-StPaul, Delzon and Cochard, 2017; Urban *et al.*, 2017). It is generally recognised that four environmental factors regulate the opening of the stomatal pore; light, humidity, carbon dioxide concentration and temperature (Table 5-1).

Table 5-1. Environmental factors that affect the opening and closing of the stomatal pore.

Environmental factors	**Stomatal pore state**	
	Open	**Close**
Light intensity	high	low
Humidity	high	low
Carbon dioxide concentration	low	high
Temperature	low	high

Within the context of this study, stomatal response to light and to soil water are of interest. The two main components recognised with a role in stomatal responses to irradiance are either dependent (red-light) or independent (blue-light) responses towards photosynthesis. The red-light response is usually photosynthetically-driven by a reduction of intercellular carbon dioxide concentration of leaves (C_i) by mesophyll cells. It is found to respond to the red-light region and possibly, blue-light region of the photosynthetically active radiation. On the other hand, the blue light response which is highly correlated to the content of zeaxanthin regulates the opening and closing of the stomatal pore (Sharkey and Raschke, 1981; Mott, 1988; Roelfsema *et al.*, 2002, 2006; Zeiger *et al.*, 2002; Lawson, 2009).

A recent study by Głowacka *et al.* (2018) showed improved intrinsic water use efficiency in tobacco overexpressing *PsbS*, under both controlled conditions

and field conditions. This was surprising because *PsbS* is recognised to play a key role in thylakoid photoprotection (Li *et al.*, 2000; Xiao Ping Li *et al.*, 2002) but not generally observed to affect water use efficiency in plants. In the study by Głowacka *et al.* (2018), field-grown tobacco plants overexpressing *PsbS* would partially close their stomata as a response to lower light availability while still maintaining photosynthesis, hence resulting in a 25% improvement in leaf level intrinsic water use efficiency in comparison to control plants. This was observed under fluctuating light and not during steady state as it seemed to involve the modulation of the primary plastoquinone electron acceptor, Q_A redox state. They hypothesized that when *PsbS* is overexpressed, there is a greater oxidation of Q_A which brings about a decrease in stomatal conductance without affecting photosynthesis (Figure 5-1).

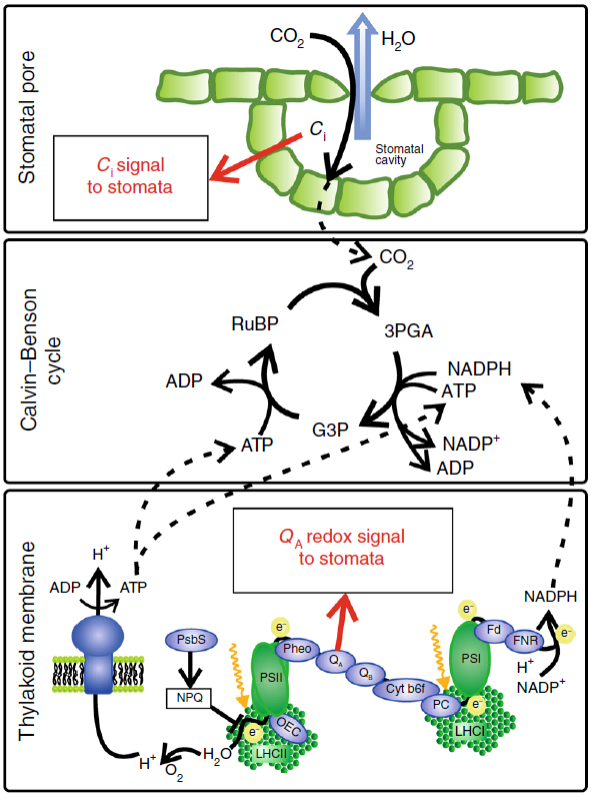


Figure 5-1. A hypothetical schematic of a proposed Q_A redox signal initiated from plastoquinone derived signalling resulting in control of stomata when there *PsbS* expression is modified (Głowacka *et al.*, 2018).

The study by Głowacka *et al.* (2018) assumed the same *PsbS* regulation of stomata and response during light fluctuations without any alteration to the photosynthetic mechanism for all higher plants. In their hypothesis, the change in stomatal conductance as a result of change in plastoquinone redox state (Q_A redox state) is not dependent on the intercellular carbon dioxide concentration. However, previous studies established that stomatal responses towards light are linked to leaf photosynthesis albeit the mechanism is not fully understood (Messinger, Buckley and Mott, 2006). Furthermore, Kulasek *et al.* (2016) showed that stomata affect carbon assimilation through the regulation of water content in the leaves. This in turn is related to the leaf surface temperature and increased photosynthetic activity. However, there is no correlation between NPQ and leaf surface temperature, which could be inferred as no evidence showing correlation between *PsbS* and stomata activity, which contradicted the study by Głowacka *et al.* (2018). Previous studies (Hubbart *et al.*, 2012, 2018) and experimental observations involving rice overexpression of *PsbS* in rice under fluctuating lights did not show any correlations between stomatal conductance light and WUE.

The current study aims to specifically investigate whether water use efficiency would be improved in rice overexpressing *PsbS*. Transgenic rice plants overexpressing *PsbS* were grown under restricted water conditions in controlled environment conditions. Gas exchange and fluorescence measurements were made to track their response during the suboptimal water stress period with the aim of establishing whether a chloroplast derived signal could influence stomatal conductance and leaf water use efficiency. Based on previous observations, we hypothesized that *PsbS* is not related to stomata regulation.

5.3 Materials and methods

5.3.1 Plant material

Transgenic rice (*Oryza sativa* L. 'Kaybonnet') lines overexpressing *PsbS* (OE74 and OE99; *PsbS* genomic sequence: Os01g64960) provided by Syngenta (Research Triangle Park, NC, USA) were used in this experiment. Rice plants were transformed by Syngenta using an Agrobacterium tumafaciens-mediated technique (see Chapter 4.2.1). The *PsbS* transgene was driven by the Cestrum yellow leaf curling virus promoter which contains the promoter region including the TATA box and enhancer factors. These rice lines were screened and selected for *PsbS* and NPQ. These two lines used in this experiment are part of the selected stable homozygous lines with confirmed higher *PsbS* protein and NPQ expression as described in Hubbart *et al.* (2012). Wildtype untransformed Kaybonnet rice (WT) was used as a control.

5.3.2 Growth conditions

Rice seeds were germinated in 50% John Innes 3 and 50% Levington M3 composts on a modular tray for about ten days before transplanting into individual 2L deep pots with the same compost mix. Rice plants were grown in individual 2L-deep pots placed on a tray. A randomized block experimental design was used with eight replicates in each experiment. Two experiments were carried out between July 2018 and September 2018 in a growth room suitable for tropical plants. The photoperiod was set at 12 hours with a 28/26°C day/night temperature. The growth room relative humidity was

maintained at 50-60%. The growth room set up included a combination of 400 W metal halide and incandescent lamps (Siemens, UK; bulbs Osram, Germany) giving a light intensity of 450 µmol $m^{-2}s^{-1}$ at the middle of the room.

5.3.3 Water restriction regime

The rice plants were allowed to establish in individual pots and grow to five-leaf stage on trays under well-watered condition. After that, the water in the trays were allowed to gradually dry (usually about three days) and after this, each pot was then carefully watered with a fixed amount of water every afternoon, depending on soil wetness. The goal was to impose a mild water deficit treatment that would result in a partial stomata closure, not a severe drought stress.

Soil moisture was determined every morning throughout using a calibrated thetaprobe ML3x (Delta-T Devices Limited, Cambridge, UK). The thetaprobe has a working range between 0.000 and 0.460 m^3m^{-3}. Fresh unwatered compost mix would have a reading of 0.0741 ± 0.003 m^3m^{-3} (n=4). A fully wet pot of soil (i.e. addition of 600mL of water) would have a thetaprobe reading of 0.450 ± 0.003 m^3m^{-3} (n=4). For water restriction regime, the soil in the pots were left to dry unwatered (usually about three days). The top surface of the soil would feel slightly moist and would be maintained with 80mL per pot every evening thereafter. They had thetaprobe reading of about 0.193 ± 0.003 m^3m^{-3} (n=38) indicating a mild water deficit. Thetaprobe measurements were taken throughout the measurement period.

5.3.4 Chlorophyll fluorescence and gas exchange

Chlorophyll fluorescence and gas exchange measurements were started when the rice plants were at leaf five stage and well-watered. All measurements were made within the growth room. After sufficient data for well-watered stage were collected, water restriction regime was initiated. The second round of measurements would follow about a week after the initiation of water restriction for collection of water-restricted stage data. Youngest fully expanded leaf was selected for the measurements.

Gas exchange and fluorescence measurements were made using LI-6400XT or LI-6800 (Li-COR Biosciences, Nebraska). For each of the measurements, the width of the leaf to be measured was recorded to calculate the leaf area covering the cuvette. The leaf sections were dark-adapted for an hour using aluminium foil. Following dark adaptation, the dark-adapted leaf was placed in IRGA chamber for two minutes to allow the chamber to reach stable conditions before the measurement of an initial dark-adapted chlorophyll fluorescence parameters F_o, F_m and F_v ($=F_m-F_o$). For all of the measurements, the ambient carbon dioxide concentration in the cuvette was kept at 400 ppm and the relative humidity of samples were maintained between 55% and 65%. Block temperature was maintained at 30°C. Flow rate was set at 500 $mLmin^{-1}$ and pressure was set at 101 kPa. Prior to each measuring pulse, the sample and reference IRGAs were equilibrated (matched) automatically to prevent drift. The stability wait time for each measurement was set between a minimum of 120 seconds and a maximum of 180 seconds.

An induction light response curve was made at a series of light steps; 200, 500, 1000 and 1500 µmol $m^{-2}s^{-1}$ to observe the physiological difference between rice line overexpressing *PsbS* (OE99) and wildtype (WT) rice. During

each light step, a saturating flash was applied at 180 seconds to measure F_s', F_m', F_v' and F_o' which permitted the determination NPQ and photochemical quenching (qP). Gas exchange data (carbon assimilation and stomatal conductance in particular) were recorded every 10 seconds throughout the protocol.

A second auto-programme consisting of three phases was set up to study the NPQ induction and relaxation in the rice overexpressing *PsbS* (OE74 and OE99) and wildtype (WT) rice. The first phase consisted of 15 photosynthetic inductions with the application of a saturating pulse every minute to measure F_s', F_m', F_v' and F_o' which permitted the determination of NPQ, qP etc at 1500 µmol $m^{-2}s^{-1}$. The second phase involved similar measurements but at 200 µmol $m^{-2}s^{-1}$ lasting six minutes. During both phases, gas exchange data were recorded every 30 seconds. The auto-programme ended with a light response curve with these light steps: 50, 100, 150, 200, 250, 300, 500, 1000, 1500 and 2000 µmol$m^{-2}s^{-1}$.

5.3.5 Relative water content (RWC)

Three leaf discs from the middle part of the youngest fully expanded leaf were collected from each rice plant using a core borer (#5, 8mm in diameter). Leaf discs were placed into falcon tubes and their fresh weights (FW) were noted down immediately. The tubes were filled with deionised water to the brim. The leaf discs were kept soaking in deionised water for a minimum of 12 hours in a cold room. Leaf discs were pat dried with tissue and weighed again to obtain their turgid weights (TW). Leaf discs were returned into the falcon tubes with fresh deionised water as previously and returned to the cold room

for a minimum of 12 hours to make sure a stable TW was obtained. Leaf discs were subsequently oven dried at 80°C for 48 hours to obtain the dry weights (DW). The relative water content was calculated as per Equation 5-1 (Barrs and Weatherley, 1962; Smart and Bingham, 1974).

Equation 5-1: RWC (%) = [(FW – DW)/(TW – DW)] X 100%

5.3.6 Statistical analysis

Analysis of variance (ANOVA) was carried out on the data collected using the statistical package, *Genstat* (19th Edition) for Windows (VSN International Ltd., Hemel Hempstead, UK). They were analysed based on the probability generated by *Genstat* whereby a P value of less than 0.05 (P<0.05) shows significant interactions and P value greater than 0.05 (P>0.05) shows insignificance. Data were checked to have met the assumption of constant variance and normal distribution of residuals.

5.4 Results

5.4.1 Comparison between rice overexpressing *PsbS* (OE99) and wildtype (WT) rice

There were no differences in the NPQ capacity between rice line overexpressing *PsbS* (OE99) and the wildtype (WT) rice (P=0.504; Figure 5-2 Induction A). As expected, there were no differences between OE99 and WT in terms of carbon assimilation (P=0.215; Figure 5-2 Induction B), stomatal conductance (P=0.486; Figure 5-2 Induction C). Not only was there no

differences between OE99 and WT in NPQ, carbon assimilation and stomatal conductance during transition from high light to low light, but there was also no differences between them during transition from low light to incremental high light levels (NPQ, P=0.722; carbon assimilation, P=0.906; stomatal conductance, P=0.942; Figure 5-2 Light response).

Photochemical quenching, qP is a parameter used to estimate the “openness” of the reaction centres, assuming the antennas are independent photosynthetic units (‘puddle’ model) whereas qL is a parallel parameter with the ‘lake’ model assumption that the antennas are shared photosynthetic units (Kramer *et al.*, 2004). Q_A redox state is estimated as 1-qL. At steady state, qP for OE99 was higher than WT at steady state (P=0.022; Figure 5-3A) but there was no difference in their Q_A redox state (P=0.384; Figure 5-3B). OE99 had greater WUE_i than WT (P=0.025; Figure 5-4). These significant differences observed between OE99 and WT can be attributed to *PsbS* overexpression. However, there is no evidence that showed *PsbS* regulates stomatal conductance. There were no differences in the leaf RWC between WT, OE74 and OE99 (P=0.776: Figure 5-4B) indicating there was no differences in leaf hydration, leaf water deficit and physiological water status between them.

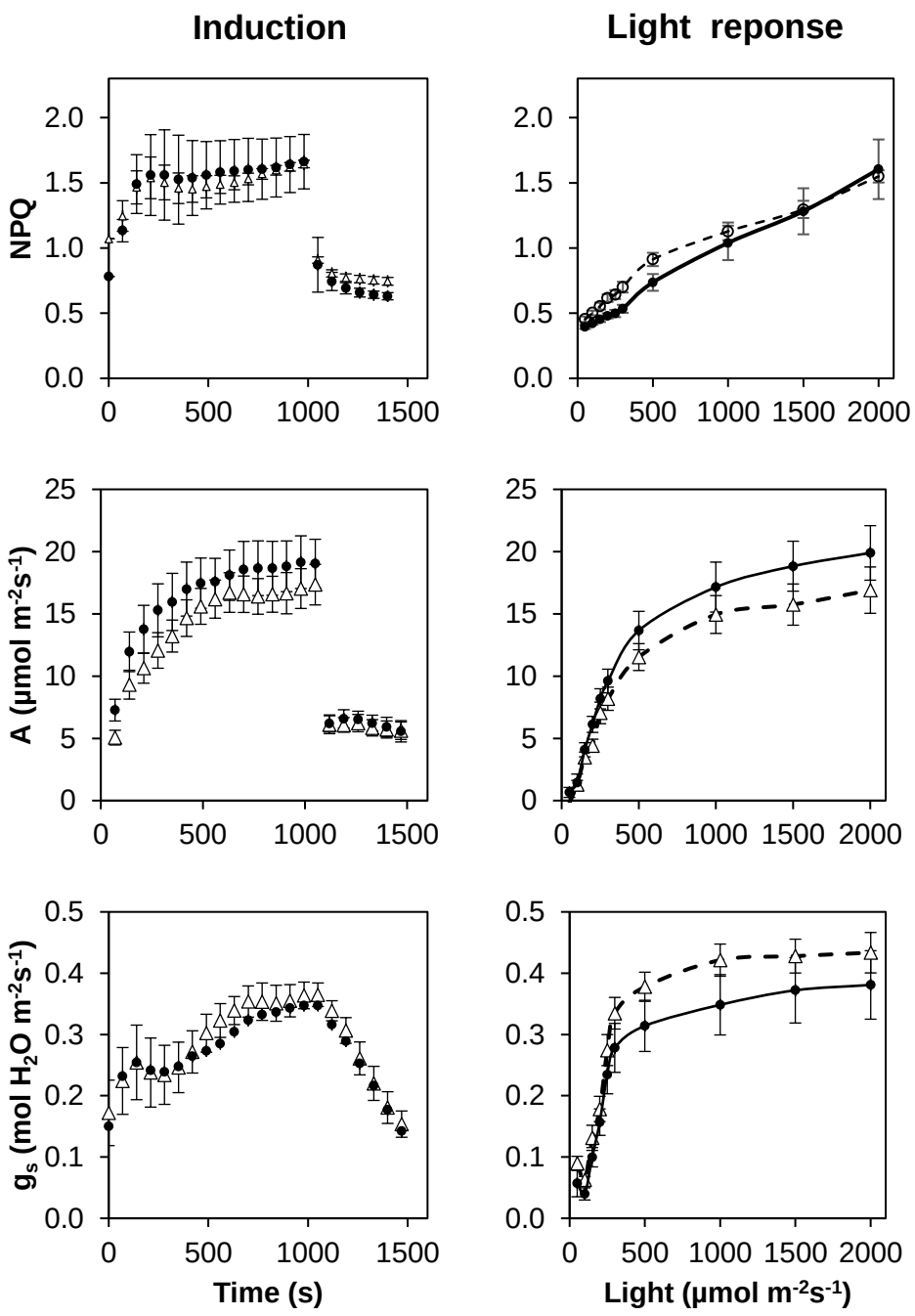


Figure 5-2. A comparison of the induction (left) and light response (right) curves for **(A)** non-photochemical quenching (NPQ), **(B)** carbon assimilation rate (A) and **(C)** stomatal conductance (g_s) between rice line overexpressing *PsbS* (OE99; black ●) and the wildtype rice (WT; white Δ) at 1500 µmol $m^{-2}s^{-1}$ for fifteen minutes followed by 200 µmol $m^{-2}s^{-1}$ for six minutes. Gas exchange measurements were logged every 30 seconds but data at every minute is shown. Error bars denote the standard error of mean between replicates (n=4). No significant differences in NPQ, carbon assimilation rate and stomatal conductance were observed between OE99 and WT.

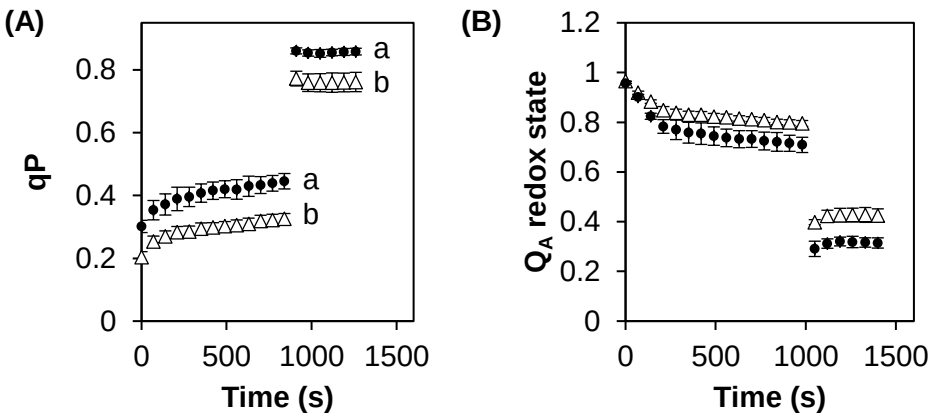


Figure 5-3. A comparison of the **(A)** photochemical quenching (qP) and **(B)** Q_A redox state (1-qL) between rice line overexpressing *PsbS* (OE99; black ●) and the wildtype rice (WT; white Δ) at 1500 µmol $m^{-2}s^{-1}$ for fifteen minutes followed by 200 µmol $m^{-2}s^{-1}$ for six minutes. Error bars denote the standard error of mean between replicates (n=8). Statistical significance is denoted with alphabets a, b etc.

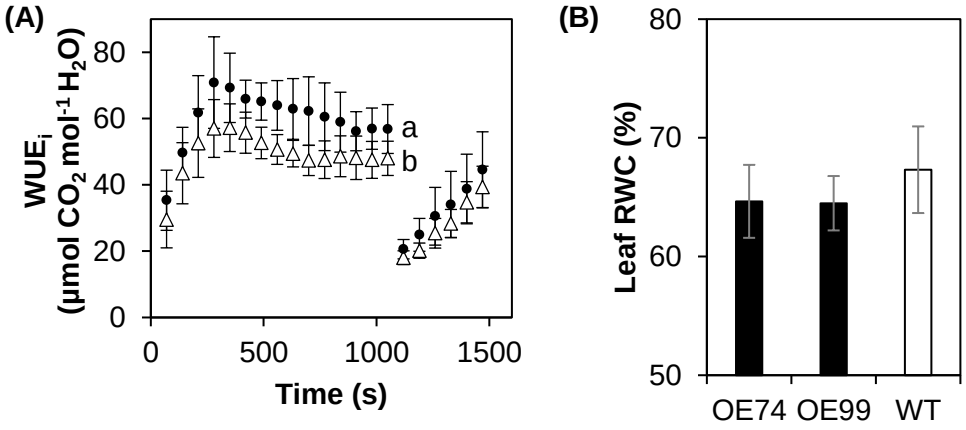


Figure 5-4. **(A)** A comparison of the intrinsic water use efficiency (WUE_i) between rice line overexpressing *PsbS* (OE99; black ●) and the wildtype rice (WT; white Δ) at 1500 µmol $m^{-2}s^{-1}$ for fifteen minutes followed by 200 µmol $m^{-2}s^{-1}$ for six minutes. Error bars denote the standard error of mean between replicates (n=8). **(B)** A comparison of the leaf relative water content (RWC) between *PsbS* overexpressor lines, OE74 and OE99 (black bars) and wildtype (WT) rice. Error bar denotes standard error of mean (three leaf discs per plant, n=6). Statistical significance is denoted with alphabets a, b etc.

5.4.2 Comparison between rice overexpressing *PsbS* (OE74 and OE99) and wildtype (WT) rice under water deficit

In this study, the rice plants were given a water restriction treatment. There was no intention to put the rice plants under any form of severe drought stress but rather impose a gradual and controlled stomatal closure. Hence, after the water in the trays dried out, careful watering into each pot was carried out and plants were monitored for no wilting signs. This section will focus on the results from the experiment which started in July 2018. The results from the second experiment which started in September 2018 are placed under Supplementary material S5.1 as water restriction was not implemented sufficiently to result in a drastic lowering of the stomatal conductance.

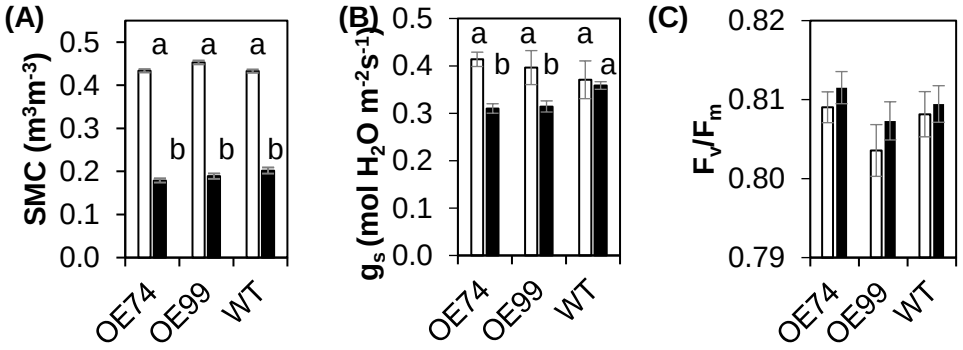


Figure 5-5. A comparison between **(A)** soil moisture content (SMC) measured using thetaprobe, **(B)** stomatal conductance (g_s) and **(C)** the dark-adapted quantum efficiency of Photosystem II (F_v/F_m) of the rice plants before (white bars) and after (black) stable water restriction for a minimum of three days for the first experiment. OE74 and OE99 are rice plants overexpressing *PsbS* and WT refers to wildtype Kaybonnet rice. Error bars denotes the standard error of mean (n=8). Statistical significance is denoted by alphabets a, b etc.

Water restriction was successfully imposed in the first experiment which resulted in a lowered soil moisture content (SMC; $P<0.001$; Figure 5-5A) and

stomatal conductance (P=0.004; Figure 5-5B) in the rice plants. There were no differences between the dark-adapted quantum efficiency of Photosystem II (F_v/F_m) before and after water restriction (P=0.651; Figure 5-5C). The plants were not stressed from the water restriction regime with 'healthy' F_v/F_m values greater than 0.80.

A selection of key chlorophyll fluorescence and gas exchange parameters for the two *PsbS* overexpressor rice lines OE74 and OE99 (OE) and wildtype (WT) rice for the first experiment are shown in Figure 5-6. There were no differences in the maximum carbon assimilation between OE and WT (P=0.114; Figure 5-6A). As expected, NPQ was significantly higher in OE compared to WT rice (P<0.001; Figure 5-6B). There were no significant differences in quantum yield of Photosystem II (ΦPSII; P=0.506, Figure 5-6C), photochemical quenching (qP; P=0.346, Figure 5-6E) and plastoquinone redox state (Q_A redox state (=1-qL); P=0.377, Figure 5-6F) between the OE and WT rice before and after the water restriction regime. However, significant differences in WUE_i were observed between OE and WT (P=0.026). In terms of WUE_i, there were no differences between the *PsbS* overexpressor lines, OE74 and OE99 (P=0.475) but there were differences between OE74 and WT at 10% significant level (P=0.091) and between OE99 and WT at 5% significance level (P=0.012). Higher WUE_i observed in OE compared to WT could be attributed to *PsbS* OE and water deficit imposed on the rice plants. This is also further supported by the second experiment (See Supplementary material) where the water deficit did not result in a significantly lowered stomatal conductance in one of the *PsbS* lines (OE99), there was no differences in WUE_i between OE and WT (P=0.556).

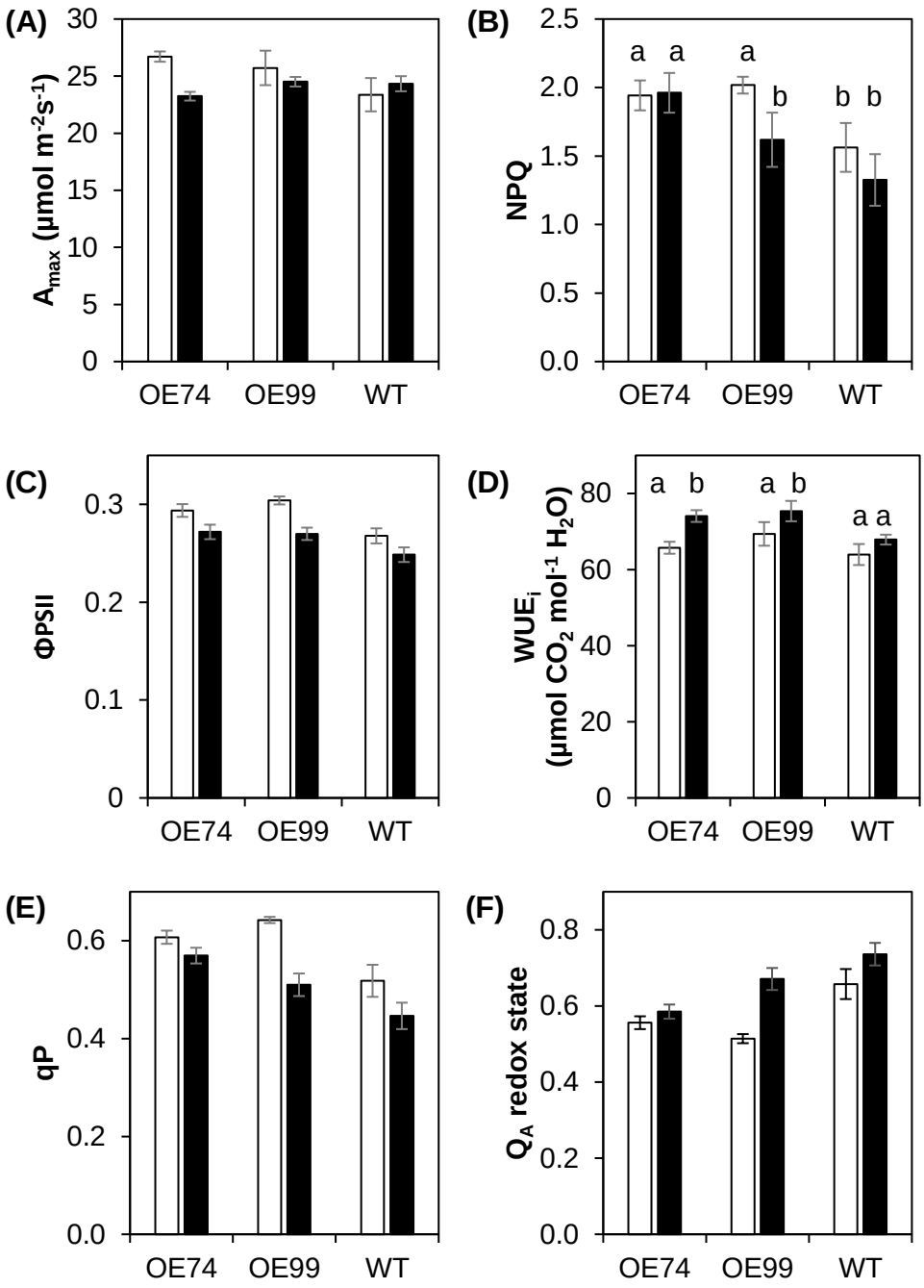


Figure 5-6. A comparison between **(A)** maximum carbon assimilation (A_{max}), **(B)** non-photochemical quenching (NPQ), **(C)** quantum yield of Photosystem II (ΦPSII), **(D)** intrinsic water use efficiency (WUE_i), **(E)** photochemical quenching (qP) and **(F)** plastoquinone redox state (Q_A redox state, =1-qL) of the rice plants before (white bars) and after (black) stable water restriction for a minimum of three days. OE74 and OE99 are rice plants overexpressing *PsbS* and WT refers to wildtype Kaybonnet rice. Error bars denotes the standard error of mean (n=8). Statistical significance is denoted by alphabets a, b etc.

5.5 Discussion

This experiment was carried out to follow up the findings of Głowacka *et al.*, (2018) in which a higher WUE_i was observed in field-grown tobacco plants overexpressing *PsbS*. However, working with rice plants overexpressing *PsbS* in glasshouses and growth rooms, this has never been observed. Głowacka *et al.* (2018) carried out their experiment under field conditions where plants can show greater variations amongst themselves when grown under natural conditions (Frenkel *et al.*, 2009). This experiment was carried out in growth room for a more stable and controlled environment to properly examine the effect of stomatal conductance on *PsbS* expression in wildtype rice (WT) and rice lines overexpressing *PsbS* (OE74 and OE99).

Głowacka *et al.* (2018) hypothesized that during light transition, there was an unknown chlorophyll fluorescence mediated signal controlling the stomata resulting in a change in stomatal conductance in tobacco plants. However, an induction experiment carried out here on one of the *PsbS* overexpressor rice lines, OE99 and wildtype (WT) rice confirmed that there were no differences in the stomatal conductance in between light transitions from low light to high light, and back to low light. Hence, this experiment showed no evidence that the light dependent signal observed by Głowacka *et al.* (2018) was present in rice.

As no differences were observed during light shifts, the growth room experiment progressed with the use of two *PsbS* overexpressor rice lines under a water restriction regime to investigate the changes in stomatal conductance and water use efficiency in *PsbS* overexpressor rice lines. A successful mild water deficit resulted in a partially closed stomata in the rice plants which in turn resulted in an improved intrinsic water use efficiency in

the *PsbS* overexpressor rice lines than the wildtype rice plants. Another water deficit regime where the water deficit was not so strictly imposed showed no differences in water use efficiency between the OE and WT rice plants. Tourneux and Peltier (1995) found that the F_v/F_m of potato leaves is not affected by water deficit of more than 50%. This indicated that potato plants could perform normally under high water deficit. This could be the same for rice plants.

The advantage of *PsbS* regulation over stomatal function would seem to be that it provides a direct link between light use and light energy processing (which is the central function of NPQ) with the availability of CO_2 as a substrate and the loss of water. For example, if light levels decrease, there is less need for CO_2 and so stomata should close rapidly. *PsbS* active state via protonation provides the leaf with a direct signal of the proton motive force and hence electron transport rate (via Q_A redox state). The rationale for such signals was laid out in Głowacka *et al.* (2018) and previously such levels of photosynthetic control have been discussed in reviews such as Murchie *et al.* (2018). It was also and further validated in Kromdijk, Głowacka and Long (2019).

This raises the crucial question of why rice should behave differently to tobacco in terms of the *PsbS* light-dependent signal. Components of the signal transduction pathway may be missing in rice but present in tobacco, they are evolutionarily distant plant groups (monocotyledonous vs dicotyledonous) after all. Perhaps part of the answer lies in relative morphology and behaviour of cereal and broad-leaved stomata. Cereals possess smaller more frequent stomata which generally are faster at opening and closing in response to environmental stimuli than the larger broadleaved stomata (Hetherington and Woodward, 2003; Lawson and Vialet-Chabrand,

2019). This is thought to be linked to drier environments in which grasses originally evolved and fast stomatal responses coupled with rapid photosynthetic rates would be of benefit. If rice stomata are already adapted to speedy responses then there may not be a need for an additional *PsbS* and light- dependent signal to speed up responses. It is also possible that *PsbS* is of less importance in signalling during fluctuating light in rice plants. Evolution may rather have had greater pressure to link *PsbS* with stomatal closure during water stress when conservation of moisture would have been of greater importance.

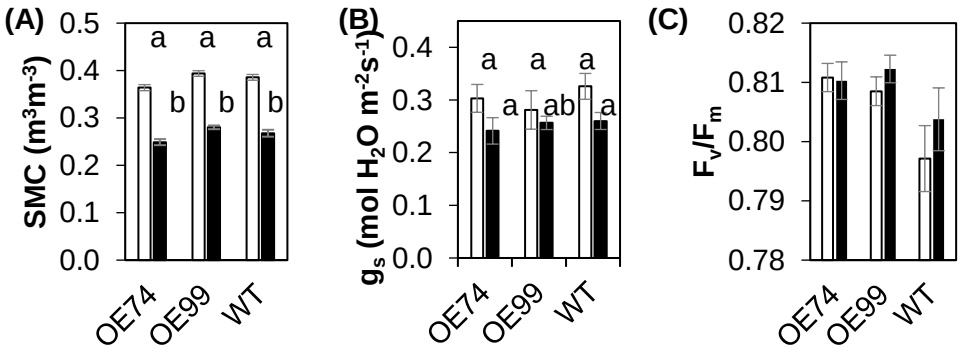
5.6 Summary

The study showed that *PsbS* does not affect stomatal conductance in rice plants grown under controlled well-watered growth room conditions. There is no light-dependent control of stomata. However, when a mild water deficit was imposed on the plants, the *PsbS* overexpressor rice plants showed higher intrinsic water use efficiency than the wildtype rice plants. Under insufficient water stress, no differences in intrinsic water use efficiency was observed between the *PsbS* overexpressor rice plants and wildtype rice plants.

Supplementary material

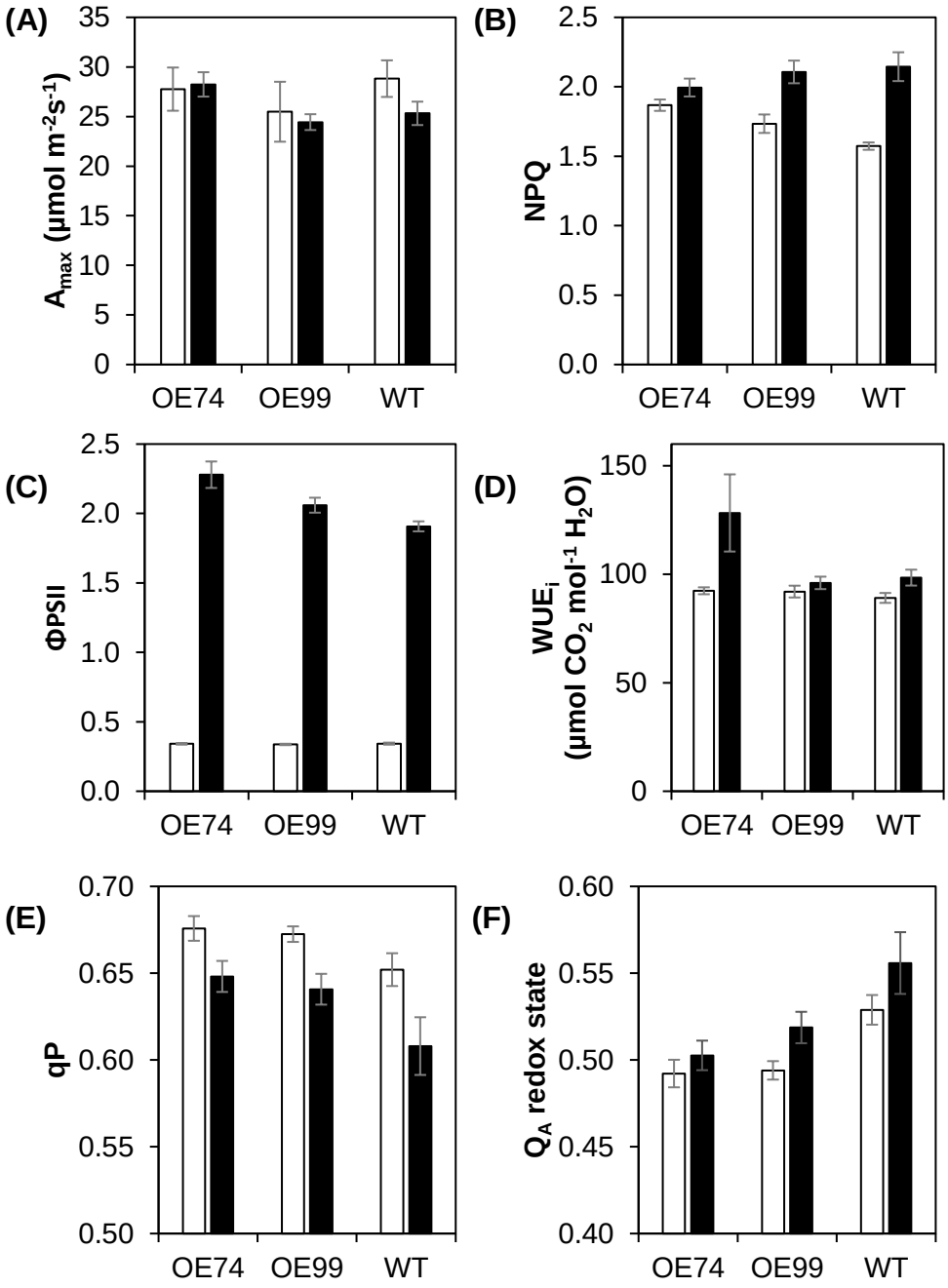
Supplementary material S5.1

Water restriction was successfully imposed in the second experiment which resulted in a lowered soil moisture content (SMC; P<0.001, Supplementary Figure S 5-1A) and stomatal conductance (P=0.02, Supplementary Figure S 5-1B) in the rice plants. However, the stomatal conductance after water restriction was not sufficiently low for OE99. There were no differences between the dark-adapted quantum efficiency of Photosystem II (F_v/F_m) before and after water restriction (P=0.889; Supplementary Figure S 5-1C). The plants were not stressed from the water restriction regime with 'healthy' F_v/F_m values around 0.80. There were no differences in the maximum carbon assimilation (P=0.250) and NPQ (P=0.509) between the two *PsbS* overexpressor rice lines OE74 and OE99 (OE) and wildtype (WT) rice (P=0.114).



Supplementary Figure S 5-1. A comparison between **(A)** soil moisture content (SMC) measured using thetaprobe, **(B)** stomatal conductance (g_s) and **(C)** the dark-adapted quantum efficiency of Photosystem II (F_v/F_m) of the rice plants before (white bars) and after (black) water restriction for a minimum of three days in the second experiment. OE74 and OE99 are rice plants overexpressing *PsbS* and WT refers to wildtype Kaybonnet rice. Error bars denotes the standard error of mean (n=8). Statistical significance is denoted by alphabets a, b etc.

A selection of key chlorophyll fluorescence and gas exchange parameters for the two *PsbS* overexpressor rice lines OE74 and OE99 (OE) and wildtype (WT) rice for the second experiment are shown in Supplementary Figure S 5-2. There were no differences in maximum carbon assimilation between OE and WT (P=0.250) but unexpectedly, NPQ was also not significantly different between OE and WT (P=0.509). Similar to the first experiment, there were no significant differences in photochemical quenching (qP; P=0.689, Supplementary Figure S 5-2E) and plastoquinone redox state (Q_A redox state (=1-qL); P=0.681, Supplementary Figure S 5-2F) between the OE and WT rice before and after the water restriction regime. The quantum yield of Photosystem II (ΦPSII; P=0<0.001, Supplementary Figure S 5-2C) and WUE_i (P=0.098, Supplementary Figure S 5-2D) were significantly higher in OE than WT under the water restriction treatment. However, there were no differences between each of the OE lines and WT (OE74 and WT, P=1.000; OE99 and WT, P=0.630; OE74 and OE99, P=0.366).



Supplementary Figure S 5-2. A comparison between **(A)** maximum carbon assimilation (A_{max}), **(B)** non-photochemical quenching (NPQ), **(C)** quantum yield of Photosystem II (ΦPSII), **(D)** intrinsic water use efficiency (WUE_i), **(E)** photochemical quenching (qP) and **(F)** plastoquinone redox state (Q_A redox state, =1-qL) of the rice plants before (white bars) and after (black) water restriction for a minimum of three days in the second experiment. OE74 and OE99 are rice plants overexpressing *PsbS* and WT refers to wildtype Kaybonnet rice. Error bars denotes the standard error of mean (n=8). Statistical significance is denoted by alphabets a, b etc.

Chapter 6 Improving Photosynthesis in Rice Using Nitrogen-Fixing Bacteria

C.C. Foo[1], Y.K. Poon[1], E. Smail[2], C. Owen[2], E.H. Murchie[1] and P. Carvalho[2]

[1] Plant and Crop Science Division, School of Biosciences, University of Nottingham, Sutton Bonington LE12 5RD UK

[2] Azotic Technologies Ltd, Bio City, Pennyfoot Street, Nottingham NG1 1G UK

Author contribution:

Experiment conceived by CC Foo, EH Murchie and P Carvalho

Project supervision performed by EH Murchie and P Carvalho

Experimental work (experimental design, planning and setup, seed inoculation and measurements at key growth stages) by CC Foo

Weekly collection of growth data and final biomass measurements by YK Poon and CC Foo

Statistical analysis on whole data set by CC Foo

Gd colonization analysis by E Smail and C Owen

Written by CC Foo

6.1 Abstract

This experiment aimed to study the association of Gd bacteria in Spanish rice (Valencia sp.) under controlled conditions, in parallel with efforts made in the fields. Other than that, the effects of nitrogen supplementation on Gd inoculation of rice were also investigated. Rice seeds (*Oryza sativa* var. 'Valencia') were inoculated with a liquid microbial inoculant containing *Gluconacetobacter diazotrophicus* bacteria (with 1% sucrose and 0.3% tween 80, pH 6.5). Seeds were sown directly into tubs creating "mini-canopies". Nitrogen fertilization at three treatment levels (0%, 50% and 100% based on maximum field recommendation of 150kg N per hectare) was applied at tillering stage. A 100% colonization of rice seedlings with Gd was observed. However, the successful Gd colonization did not translate to enhanced growth. At no nitrogen supplementation, there was marginal improvement in photosynthesis which could be of magnified consequences in the field.

6.2 Introduction

6.2.1 Importance of nitrogen

The element Nitrogen (N) is abundant and makes up about 79% of the atmosphere. However, it is not readily metabolized by most microorganisms due to the stable dinitrogen gaseous state, N_2. Yet, N is essential for all living things as it provides building blocks of nucleic acids amino acids and other molecules which are the basis of growth. The biological availability of nitrogen is often a limiting factor in plant growth and productivity (Eskin, Vessey and Tian, 2014; Krapp, 2015; Mus *et al.*, 2016).

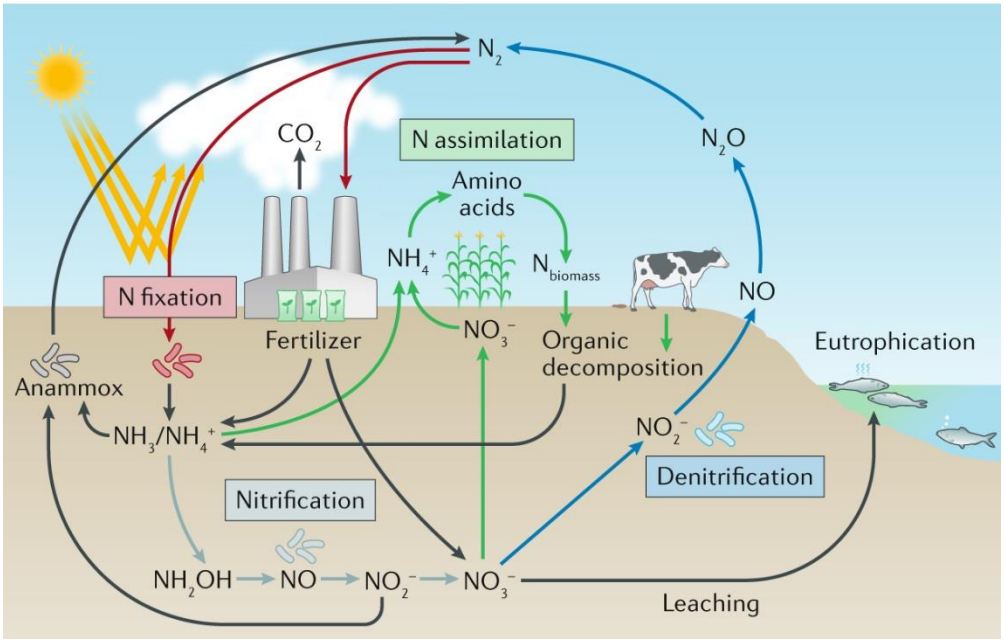


Figure 6-1. A simple depiction of the nitrogen cycle (Vitousek *et al.*, 1997).

The nitrogen cycle (Figure 6-1) starts with nitrogen fixation of atmospheric nitrogen into the soil. Although nitrogen is abundant in the atmosphere, most of the nitrogen fixation occurs within the soil environment, via nitrogen fixing bacteria containing the enzyme nitrogenase. The atmospheric nitrogen is converted to ammonia or other nitrogen-based compounds (ammonium, nitrites and nitrates), which can be taken up and metabolized by

microorganisms and plants. These microorganisms would then excrete or eventually, die and decompose to release nitrogen back into the soil as urea or ammonia. These nitrogenous compounds are then converted back to the gaseous form and released into the atmosphere or taken up directly by plants and used for metabolism and growth. This cycle is crucial for maintaining growth of plants. However, it does not generally provide sufficient available nitrogen to achieve the high yields and quality required for global food production: more often than not, cropping systems require additional nitrogen in the form of synthetic fertilizers (Haas, Wetterich and Köpke, 2001; Doltra, Lægdsmand and Olesen, 2011; Chiew *et al.*, 2015; Reese *et al.*, 2016).

Atmospheric N_2 can be used to generate ammonia in an industrial process known as Haber-Bosch. This process does not only require large quantities of energy but also the input of non-renewable natural gas (Ladha and Reddy, 1995; Kandemir *et al.*, 2013; Cherkasov, Ibhadon and Fitzpatrick, 2015). These 'artificial' fertilizers are often applied in agricultural systems to ensure high yields. However, plants are very inefficient in the uptake of those applied fertilizers resulting in agricultural runoff (Santi, Bogusz and Franche, 2013) which often leach into water systems resulting in eutrophication, polluting nearby water bodies. Not only will there be socioeconomic problems from the loss of productivity of the water bodies, but the remediation of these polluted water bodies can be very costly (Dodds *et al.*, 2009). There are constant issues of greenhouse gases emission from agriculture sector, which is worsened with nitrogen fertilization of the farmlands (Jeuffroy *et al.*, 2013; Dent and Cocking, 2017). Denitrification of nitrates (NO_3^-) results in the release of greenhouse gas, nitrous oxide (N_2O), which has been identified as the greatest ozone-depleting substance (Ravishankara, Daniel and Portmann, 2009). Hence, there is a need to reduce the dependence on fertilizers and

move towards a more sustainable and safer way of providing plants with suitable forms of available nitrogen (Ravishankara, Daniel and Portmann, 2009; Jensen *et al.*, 2012; Hawkesford, 2014; Mus *et al.*, 2016; Dent and Cocking, 2017).

6.2.2 Nitrogen-fixing bacteria

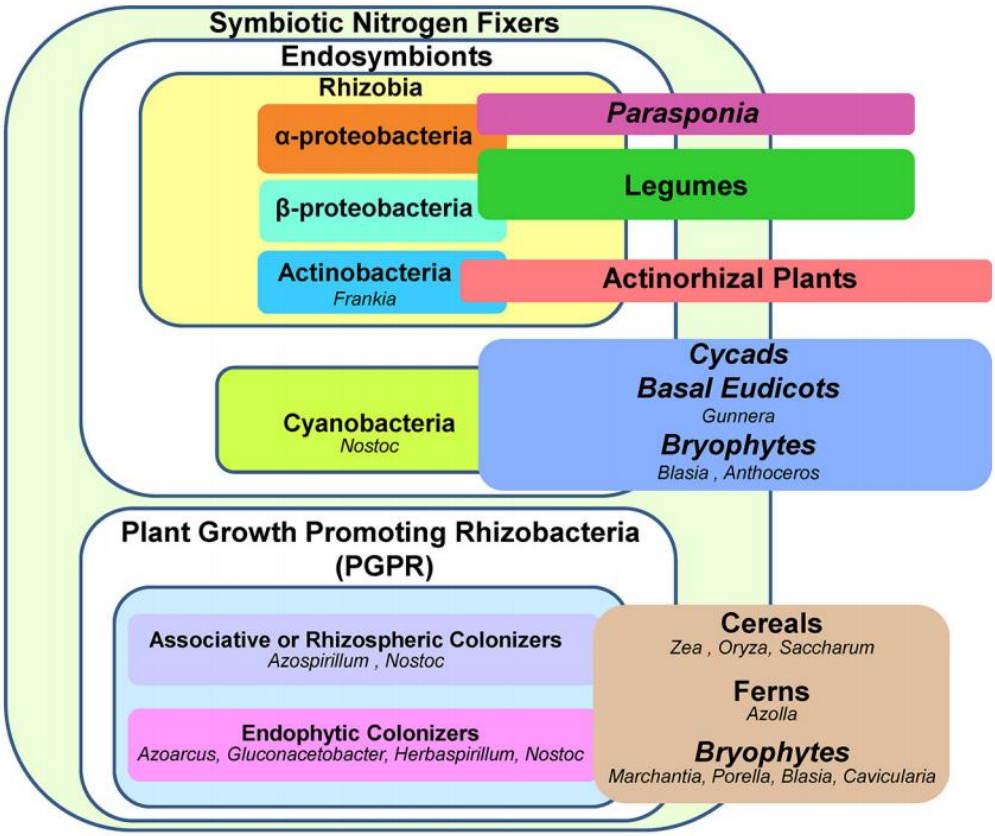


Figure 6-2. A schematic diagram of the diazotrophs and their associations with host plants (Mus *et al.*, 2016).

Diazotrophs are microorganisms that are capable of assimilating and fixing atmospheric nitrogen. These nitrogen fixers can form symbiotic relationships with host plants. Figure 6-2 shows a schematic diagram of the different symbiotic nitrogen fixing bacteria and the respective host plants they could possibly colonize. Endosymbionts usually form close associations with the

host plants via colonization of the plant tissue. They continue to proliferate within the host plants without killing the host plants. Plant growth promoting Rhizobacteria (PGPR) can either be endophytic or they can colonize the rhizosphere (surrounding roots) and form a nitrogen-fixing symbiosis with the host plants (Santi, Bogusz and Franche, 2013; Mus *et al.*, 2016).

As aforementioned, there exist soil dwelling nitrogen fixing bacteria which are beneficial and could be explored to meet the nitrogen gap required by crops in an agricultural system. Some plants such as legumes, have the ability to form an endo-symbiotic relationship with some bacteria such as species within the genus of Rhizobium. These legumes provide Rhizobium a shelter in structures known as root nodules and carbon from photosynthate. In return, these bacteria fix atmospheric nitrogen for assimilation by the plant. When the plants die and decompose, the nitrogen in bioavailable forms would then be recycled into the soil, benefitting the subsequent crop cycles. Consequently, crop rotation cycles often include legumes. Additionally, it can help mitigate greenhouse gases emissions (Jensen *et al.*, 2012; Jeuffroy *et al.*, 2013; Dequiedt and Moran, 2015; Dent and Cocking, 2017; Lötjönen and Ollikainen, 2017).

The endo-symbiotic relationship between leguminous plants and Rhizobia provides great benefit not only to cropping system but also the environment. Unfortunately, Rhizobia failed to present qualities for successful colonization in non-leguminous plants. Parallel forms of such relationship have thus been explored and extended to non-leguminous plants through other nitrogen-fixing bacteria. This is crucial as most crops that feed the world are non-legumes (Mus *et al.*, 2016; Dent and Cocking, 2017).

6.2.3 *Gluconacetobacter diaztrophicus* (Gd) in crops

Cereals are actually capable of establishing non-endosymbiotic relationships with some associative or endophytic nitrogen-fixing bacteria (Santi, Bogusz and Franche, 2013; Mus *et al.*, 2016). It was of great interest when *Gluconacetobacter diaztrophicus* (Gd) was found to be responsible for nitrogen fixation in sugarcane fields (Cavalcante and Dobereiner, 1988). Although it feeds on sucrose after colonization of the plant, it does not have high plant specificity and can be found to form associations with sugar-rich and sugar-poor plants (Muthukumarasamy *et al.*, 2005; Eskin, Vessey and Tian, 2014). This was probably because of its ability to synthesize hydrolytic enzymes such as endoxylogluconase, endopolymethylgalacturonase and endoglucanase through assimilation of sucrose (Adriano-Anaya *et al.*, 2005). These enzymes are required to break down plant cell wall and facilitate Gd entry into plant cells. Gd was found occurring naturally in a wide range of crops such as coffee (Jimenez-Salgado *et al.*, 1997; Madhaiyan *et al.*, 2004), pineapple (Tapia-Hernández *et al.*, 2000), carrot, radish and beetroot (Madhaiyan *et al.*, 2004) and wetland rice (Muthukumarasamy *et al.*, 2005) to name a few.

Gd is also an endophytic “hardy” bacteria that can survive harsh conditions and capable of colonizing non-legumes without the formation of nodules, providing the host plant with a significant amount of nitrogen relative to that of symbiotic rhizobia (Madhaiyan *et al.*, 2004; Eskin, Vessey and Tian, 2014). In comparison to associative diazotrophs, endophytic diazotrophs could better allow plants to retain and use the nitrogen fixed (Ladha and Reddy, 1995). Other than that, it is not inhibited by nitrate and only partially affected by ammonium. Hence, supplementation of nitrate and ammonium fertilizers or

nitrogen rich soil would not threaten its proliferation (Cojho *et al.*, 1993; Dent and Cocking, 2017). Gd was also reported to promote plant growth via fixing of phosphorus in strawberry plants (Delaporte-Quintana *et al.*, 2017). A study in *Arabidopsis thaliana* also showed that Gd could improve water use efficiency and photosynthesis (Rangel de Souza *et al.*, 2016). If this is also true in crop plants, it would also intrinsically improve the productivity of the crop plant and improve yield. As no additional nutrients are applied to the plant, the productivity per unit applied nutrients may improve while the photosynthetic nitrogen use efficiency may not be altered (photosynthesis per unit leaf nutrient).

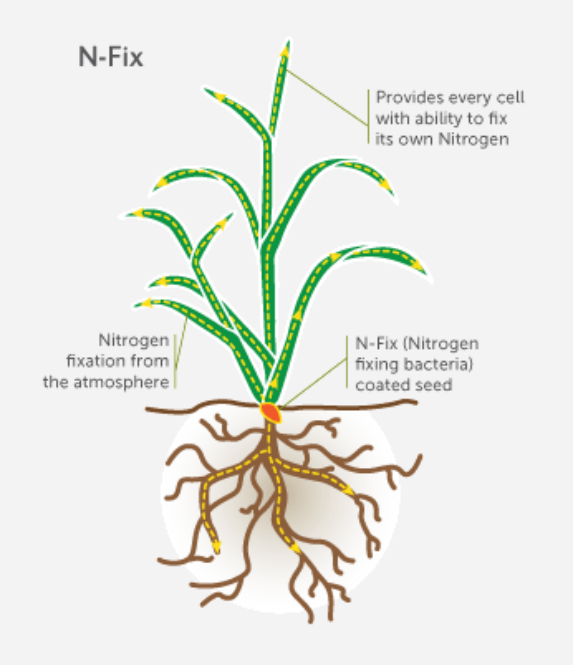


Figure 6-3. The principle of Gd inoculation that could be applied to all crops. This inoculant is proposed to allow the induction of Gd into host plant in an intracellular manner, replacing half of the plant's nitrogen demand (Azotic Technologies Ltd, 2018).

Since Gd discovery in sugarcane, studies were made to stably inoculate Gd to other non-leguminous crops which require sorting out the requirements for successful inoculation of seeds as most crops are cultivated from seeds (Luna *et al.*, 2010). The successful association of Gd to cereal crops could

reduce the need for nitrogen supplementation in the field to the benefit of both farmers and environment in the long run (Ladha, De Bruijn and Malik, 1997). Increased fruit yield was observed in tomatoes when tomato seedlings were inoculated with Gd (Luna *et al.*, 2012). Another example of Gd inoculation is provided by N-Fix®, which is a novel seed inoculum technology commercialised by Azotic Technologies (Nottingham, UK). It aimed to allow all inoculated crops to fix atmospheric nitrogen within their own tissues, making agriculture a sustainable and earth friendly industry (Figure 6-3). Azotic Technologies have shown that using Gd could improve maize, soybean and wheat yields (Dent and Cocking, 2017). This seems to be a great milestone as more than half of the nitrogen fertilizers manufactured are applied on cereal crops (Santi, Bogusz and Franche, 2013).

Similar efforts are being made in rice, a staple food that feeds half the world and makes up about 20% of the world calorie intake (Ladha, De Bruijn and Malik, 1997; Gyaneshwar *et al.*, 2001). Wetland rice growth environment presents a wide range of nitrogen-fixing organisms and cyanobacteria has long been used to supplement soil nitrogen (Venkataraman, 1981; Ladha, De Bruijn and Malik, 1997). However, these are insufficient to support the nitrogen demand of wetland rice cultivation (Buresh, Casselman and Patrick, 1980; Rao, Jena and Adhya, 1987). More often than not, nitrogen fertilizers are unavailable or unaffordable to farmers. Hence, provision of nitrogen via other high efficiency nitrogen fixing microorganisms such as Gd could be a long term solution (Ladha, De Bruijn and Malik, 1997). With respect to nitrogen-fixing bacteria, several studies have identified and isolated nitrogen fixing bacteria from rice (Gillis *et al.*, 1995; Ueda *et al.*, 1995; Yanni *et al.*, 1997; Engelhard, Hurek and Reinhold-Hurek, 2000; Gyaneshwar *et al.*, 2001; Santi, Bogusz and Franche, 2013). These bacteria, especially endophytes,

served as better provider of nitrogen in terms of efficiency and interaction with host (Gyaneshwar *et al.*, 2001). Although realising the great potential of these endophytic nitrogen fixing bacteria in rice cultivation, no such efforts have been reported in the literature (Muthukumarasamy *et al.*, 2005). Azotic Technologies (Nottingham, UK) recently reported successful trials using a solution termed N-Fix® (a method for inoculating plants with Gd) on rice fields achieving significant yield increase (Dent and Cocking, 2017; Azotic Technologies, 2018), although the mechanism by which this was achieved has not been confirmed. This project aimed to study the association of Gd bacteria (inoculated using N-Fix® in Spanish rice (Valencia sp.) under controlled conditions, in parallel with efforts made in the fields. The hypothesis presented is that successful colonisation of rice plants by the Gd bacteria will result in enhanced N uptake from N-deprived soil and this will stimulate growth via mechanisms that include enhanced photosynthetic rate.

6.3 Materials and methods

6.3.1 Plant material

Rice seeds (*Oryza sativa* var. 'Valencia') were provided by Azotic Technologies (Nottingham, UK). Rice seeds were treated with fresh N-Fix® solution (Azotic Technologies, Nottingham, UK) before sowing. N-Fix® solution is a liquid microbial inoculant based on *Gluconacetobacter diazotrophicus* bacteria (with 1% sucrose and 0.3% tween 80, pH 6.5). Refer to Chapter 6.3.3 for further details on seed inoculation. Controls were set up following similar method but treated in deionised water instead. Controls were handled prior to moving on to seeds treated with N-Fix® solution to prevent

cross-contamination of controls with Gd.

6.3.2 Plant growth conditions

Experiments were carried out in a tropical glasshouse, A1, on University of Nottingham, Sutton Bonington campus during summer months of April to July in 2017. A photoperiod of 12 hours was controlled by blinds which were set to open at 7:00H and close at 19:00H. The temperatures and relative humidity were tracked regularly using a Tinytag Ultra 2 Model: TGU-4500 (Gemini Data Loggers Limited, UK). The glasshouse was maintained at 32±3.8°C and at relative humidity of 43±12.8% during daytime and at 24±1.3°C and at relative humidity of 63±9.3% during night time, automatically controlled by vents. However, this GM facility has fine mesh covering the vents resulting in temperatures exceeding 40°C at times during the warmest summer weeks. The vents were closed when it was windy.

6.3.3 Seed inoculation with Gd

N-Fix® solution was removed from fridge and left to return to room temperature for a minimum of 1 hour prior to seed inoculation. Rice seeds were soaked and fully submerged in N-Fix® solution. Seeds were stirred slowly to ensure that the liquid wets the seeds completely. After the seeds were soaked for 24 hours at 26°C, they were drained and spread into a thin layer in plastic containers. They were then incubated for 38 hours at 32°C. Seeds were sown directly in the glasshouse immediately after this. The same procedure is followed for controls, replacing N-Fix® solution with deionised

water. The seeds were inoculated on the 13th April 2017 and sown on the 16th April 2017. For the ease of reference, the Gd treatment with this version of N-Fix® solution and deionised water following this protocol will be referred to as GdN and GdW respectively.

6.3.4 Nitrogen treatment

The soil used for this experiment was a standard rice compost mix consisting of 50% Klassman lowest nutrient compost mix and 50% John Innes No. 1. Three different nitrogen treatments, 0%, 50% and 100% based on field recommendation of a maximum of 150kg/Ha (which corresponded to 0kg/Ha, 75kg/Ha and 150kg/Ha respectively) were made. This treatment took into account the residual N content of the soil used. The final compost mix was sampled and sent to NRM Laboratories (Bracknell, UK) for total nitrogen content analysis to account for the subsequent supplementation required with nitrogen pellets. Nitrogen pellets were applied to each tub during tillering stage with the amount varying depending on nitrogen treatment (6th May 2017). Each tub was flooded with water to at least one cm above the soil surface. Once the rice plants started to tiller, they were supplemented with a customized mix of zero nitrogen feed (0:30:30 NPK) with trace elements (Hortifeeds, Lincoln, UK).

6.3.5 Experimental design

Eight plants were grown in a 20L tub (Figure 6-4) of dimensions 42 cm by 30 cm and 23 cm deep to mimic small field-like canopies. Three seeds were

sown in each of the eight position to ensure there will be surviving plants to form the small canopies. Thinning took place when the seedlings were large enough and the extra seedlings were also sampled for bacteria colonization analysis. Any other excess would be trimmed after ensuring proper establishment of a plant in each position (red circles). A complete randomized block design was implemented. Destructive measurements with five replicates were planned for three key stages of the plant growth: stem elongation, anthesis and at full maturity. All the 90 tubs sat on the cemented floor insulated by a layer of Styrofoam to prevent the heating up of the tubs. Watering was maintained by a dedicated glasshouse team daily.



Figure 6-4. Each 20L tub was filled with up to the brim with standard rice compost, mixed by SB glasshouse team. Each tub was flooded with tap water and allowed to settle before sowing of treated seeds (left). Red circles showed the positioning of eight seeds in each tub (right).

6.3.6 *Gluconacetobacter diazotrophicus* (Gd) colonization analysis

After seeds were sown, they were monitored for emergence. Once any green shoots appeared, Azotic Technologies were informed for seedling sample

collection. Seedlings samples were collected five days after emergence on the 25th April 2017. Samples for control plants were collected before moving onto the treatment tubs to avoid cross-contamination. Gd colonization analysis was carried out by Azotic Technologies (Nottingham, UK) following a semi-solidified culture media protocol adapted from Baldani *et al.* (2014). The method involved the separation of each seedling into five sections; leaf tip, stem, seed, mid-root and root tip. These separated parts were placed on nitrogen-free, sterile semi-solidified LGI-P (refer to Baldani *et al.* (2014) for explanation of what LGI-P stands for) with a reduced agar content (0.1% w/v). These plates were incubated for three days at 28°C. Growth of Gd could be observed as an orange colouration around the cut sides of the samples within the culture media. The presence of the specific strain of Gd bacteria in N-Fix® solution was detected molecularly using strain-specific PCR primers.

6.3.7 Experimental measurements

6.3.7.1 Physiological measurements

Plant morphological and physiological measurements were measured weekly starting from four weeks post-sowing. The morphological changes in terms of leaf number, tiller number and plant height were recorded. Canopy temperature was also recorded using handheld non-contact digital laser infrared thermometer (Etekcity, California, USA). The soil-plant analysis development (SPAD) value and quantum yield of open Photosystem II reaction centres were measured using SPAD 502 meter (Konica-Minolta, Osaka, Japan) and FluorPen FP-100 (Photon Systems Instruments, Brno, Czech Republic) respectively. Measurements were made on the youngest

fully expanded leaf of the plant. Leaf area index (LAI) was also measured using a GreenSeeker® handheld crop sensor (Trimble®, California, USA).

6.3.7.2 Chlorophyll fluorescence and gas exchange measurements

Chlorophyll fluorescence and gas exchange measurements were carried out during stem elongation (27th May 2017), booting (5th June 2017) and anthesis (9th June 2017). Spot measurements for maximum photosynthesis (A_{max}) and associated gas exchange parameters were measured using LI-6400XT (Li-COR Biosciences, Nebraska, USA) with the 6400-40 leaf chamber fluorometer attachment. Measurements were made on the youngest fully expanded leaf of the plant. The width of the leaves sampled was recorded to calculate the leaf area in the cuvette. Measurements were carried out with flow set at 500 mL min^{-1}, block temperature maintained at 30°C, carbon dioxide maintained at 400ppm and relative humidity of maintained between 55 and 65%. Light at 1500 µmol $m^{-2}s^{-1}$ was provided by a combination of built-in red (640nm) and blue (470nm) light-emitting diodes (LEDs). A consistent stability wait time between 120 to 180 seconds was maintained for each spot measurement. Immediately following a saturating pulse and dark pulse was applied to obtain fluorescence parameters.

6.3.7.3 Dry weights

The experiment was set up in a way that two plants per tub could be harvested at three key stages as aforementioned. All samples were collected in paper bags and dried in ovens at 70°C for 48 hours for dry weights measurements. Seeds were counted using a seed counter to derive the

thousand grain weights. The grains and straws samples were subsequently sent to NRM Laboratories (Bracknell, UK) for total nitrogen analysis.

6.3.8 Statistical analysis

Analysis of variance (ANOVA) was carried out on the data collected using the statistical package, *Genstat* (19th Edition) for Windows (VSN International Ltd., Hemel Hempstead, UK). They were analysed based on the probability generated by *Genstat* whereby a P value of less than 0.05 ($P<0.05$) shows significant interactions and P value greater than 0.05 ($P>0.05$) shows insignificance. Data were checked to have met the assumption of constant variance and normal distribution of residuals.

6.4 Results

6.4.1 Successful colonization of Gd in GdN rice seedlings

The inoculation of the rice seeds with N-Fix® solution was successful and there was 100% Gd colonization in all five parts of the GdN seedlings (n=10) tested (Figure 6-5). There was no cross-contamination between the tubs as GdW seedlings (n=5) showed 0% Gd colonization. This was the first time that a 100% colonization of the Gd bacteria throughout the rice seedlings was observed under controlled environments (Charles Owen, Azotic Technologies, pers. comm.). Unlike the GdW rice seeds, most of the GdN rice seeds did not germinate right after seed inoculation. After nine days of sowing, the GdW seeds were observed to germinate better at 76% than the

GdN seeds at 51%.

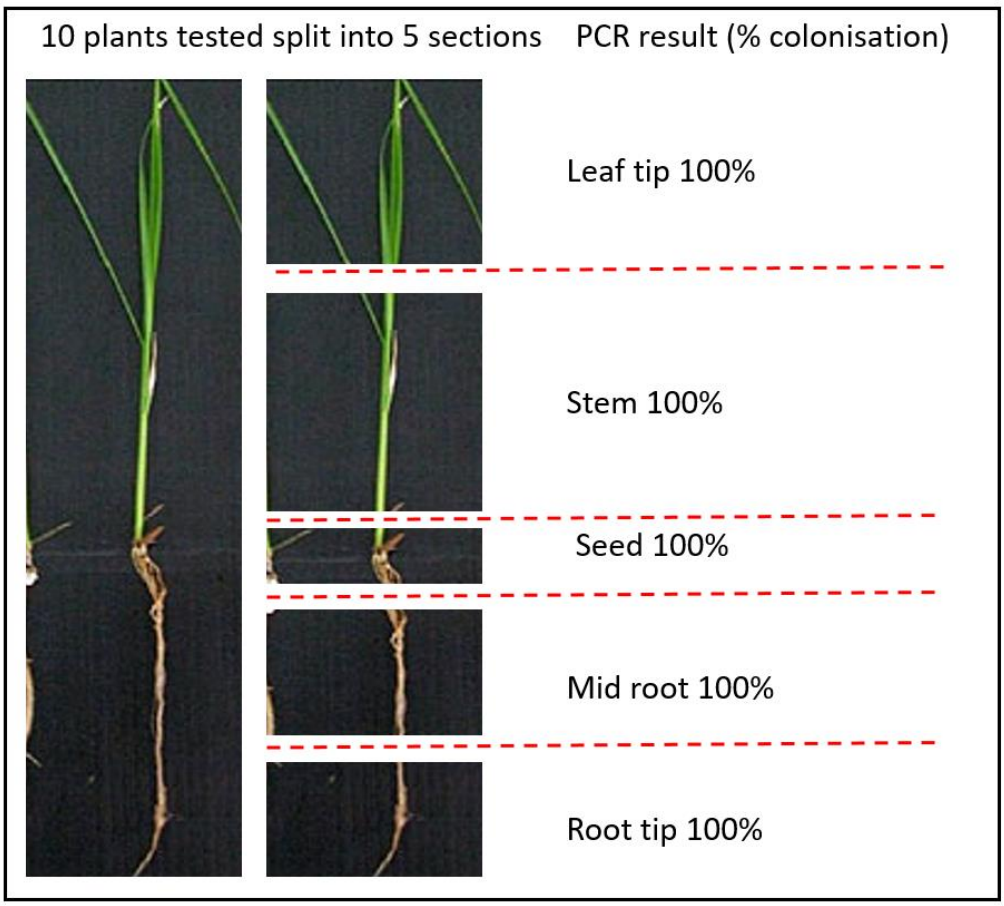


Figure 6-5. GdN rice seedling was separated into five sections for Gd detection and analysis. Colonization of Gd was highly successful with 100% colonization of Gd bacteria in all five parts of the seedling tested.

6.4.2 The effect of GdN and GdW at different nitrogen treatment levels

The morphological and physiological parameters (Refer to Table 6-1 for the complete list of parameters) measured between GdN and GdW rice plants were compared during three key growth stages, i.e. stem elongation, booting and anthesis. As expected, the differences of each parameter between growth stages were significant ($P<0.05$). The final biomass was additionally

compared between GdN and GdW rice plants at full maturity. The ear weight, seed weight and counts were also made at full maturity. In general, it was found that the results were inconsistent between the GdN and GdW rice plants across the different nitrogen treatment levels. Most of these parameters showed no significant differences between the Gd treatment. The nitrogen treatment alone was expected to have large effect on growth and photosynthesis parameters. This was indeed observed with many key indicators of a nitrogen effect. Statistical differences between GdN and GdW and their interactioncs with nitrogen treatments were analysed for different parameters and their P-values are tabulated in Table 6-1.

Table 6-1. Summary of the P-values of the ANOVA analysis for morphological and yield parameters between Gd treated (GdN) rice plants and non-Gd treated (GdW) rice plants at both the Gd treatment (Gd) and the three nitrogen treatments at 0%, 50% and 100% of the field recommended 150kg N per hectare (nitrogen) levels at the different key growth stages (stem elongation, booting, anthesis and at full maturity). The interaction between the treatments were also analysed (Gd*Nitrogen). In cases where no measurement was made are shaded in grey. At instances where P-values (at 5% or 10%) showed significance, the significance was inconsistent between GdN and GdW throughout the growth stages. The comparison of differences of each parameter between growth stages were significant (P<0.05).

Parameters	**Treatment**	**Growth stage**			
		Stem Elongation	**Booting**	**Anthesis**	**Full maturity**
Chlorophyll content (SPAD)	Gd	0.056	0.624	0.137	
	Nitrogen	<0.001	<0.001	0.019	
	Gd*Nitrogen	0.423	0.124	0.635	
Canopy temperature	Gd	0.360	0.431	0.024	
	Nitrogen	0.038	0.066	0.045	
	Gd*Nitrogen	0.818	0.402	0.486	
Leaf area index, LAI	Gd	0.320	0.752	0.533	
	Nitrogen	<0.001	<0.001	<0.001	
	Gd*Nitrogen	0.593	0.839	0.077	
Leaf number	Gd	0.869	0.576	0.868	
	Nitrogen	0.095	<0.001	0.563	
	Gd*Nitrogen	0.920	0.719	0.433	
Tiller number	Gd	0.930	0.902	0.748	
	Nitrogen	<0.001	<0.001	<0.001	
	Gd*Nitrogen	0.715	0.380	0.783	

*Continued next page

Parameters	Treatment	Growth stage			
		Stem Elongation	Booting	Anthesis	Full maturity
Height	Gd	0.575	0.608	0.451	
	Nitrogen	0.016	<0.001	<0.001	
	Gd*Nitrogen	0.435	0.653	0.309	
Total dry weight	Gd	0.086		0.818	0.594
	Nitrogen	0.221		<0.001	<0.001
	Gd*Nitrogen	0.243		0.232	0.346
Fertile shoot	Gd				0.236
	Nitrogen				<.001
	Gd*Nitrogen				0.264
Seed count	Gd				0.661
	Nitrogen				<0.001
	Gd*Nitrogen				0.217
Seed weight	Gd				0.692
	Nitrogen				<0.001
	Gd*Nitrogen				0.231
Thousand grain weight, TGW	Gd				0.875
	Nitrogen				0.073
	Gd*Nitrogen				0.459
Ear weight	Gd				0.666
	Nitrogen				<0.001
	Gd*Nitrogen				0.222

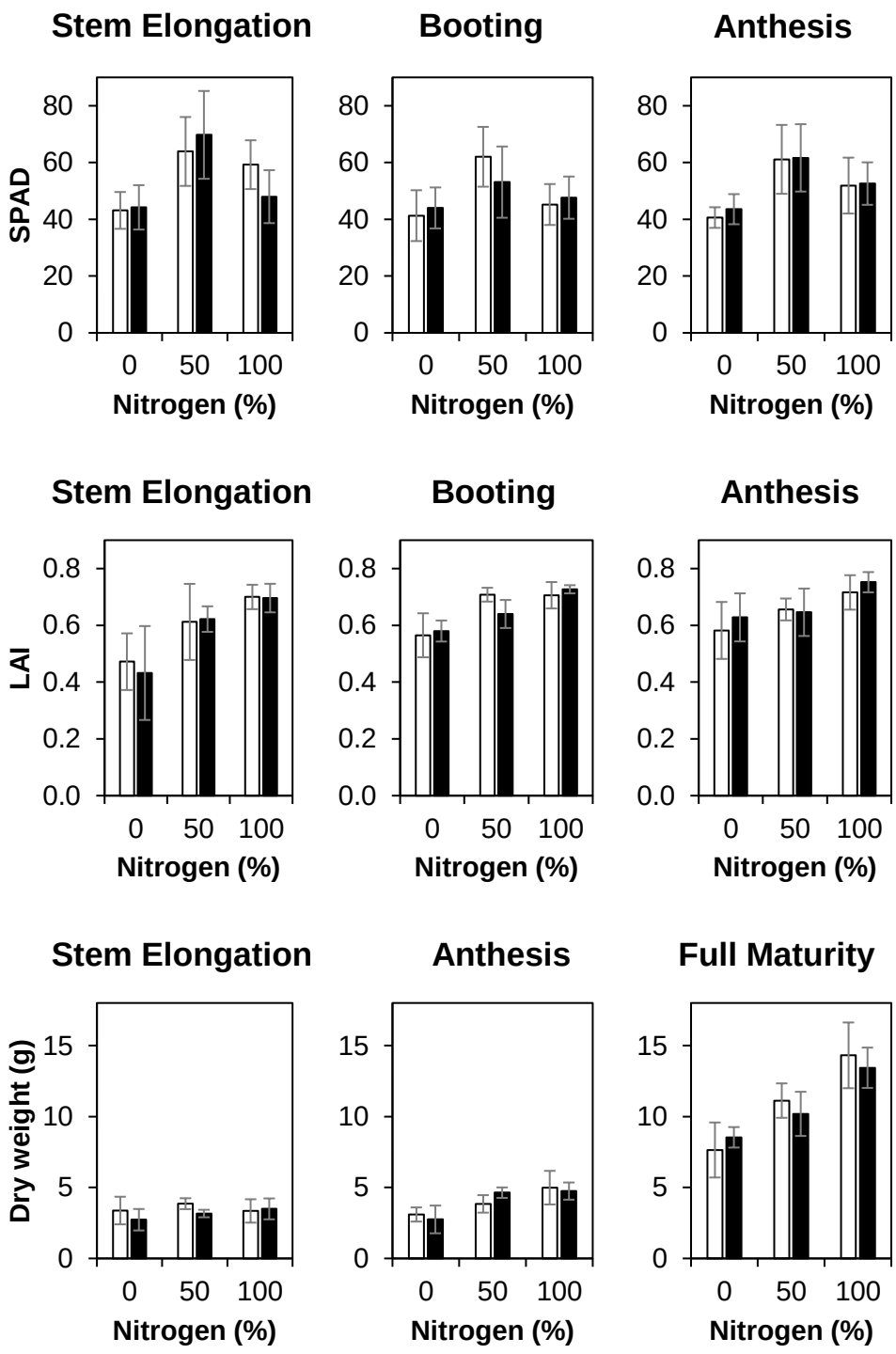


Figure 6-6. A selected comparison of the SPAD (proxy for chlorophyll content), leaf area index and dry weight per plant between GdW (white) and GdN (black) at 0%, 50% and 100% nitrogen treatments at stem elongation (week 6), booting (week 7), anthesis (week 8) and full maturity. Growth stages are noted at the top of each graph. The error bars denote the standard error between the replicates (n=5). No statistical differences were observed between treatments.

Nitrogen related parameters such as LAI, SPAD values and dry weights were selected for comparison across the different growth stages and nitrogen treatment levels (Figure 6-6). Of the three nitrogen related parameters, SPAD values showed a significance at 10% level during stem elongation. However, it was inconsistent between the treatments; the GdN rice plants were showing higher SPAD for 0% and 50% nitrogen supplementation but lower at 100% nitrogen supplementation (P=0.056). The dry weight results (Figure 6-6) are shown in some detail due to the importance of this parameter. There were no significant differences at P<0.05 between the total dry weights at the different growth stages. The lower dry weights of the GdN rice plants could be due to the slow germination of the GdN rice plants as aforementioned. Despite the slow germination, the GdN plants caught up with the growth of GdW towards the end (no significance difference).

Results of gas exchange and fluorescence analysis are shown in Table 6-2. It was again expected that the nitrogen treatment would have large effects on photosynthesis parameters. At booting stage, the parameter that indicates how ‘open’ or ‘closed’ the reaction centres are, photochemical quenching (qP) was significantly different between GdN and GdW rice plants (P=0.04) at 5% significance level. There were also some photosynthetic parameters (maximum photosynthetic rate, P=0.078 rate; quantum yield of PSII, P=0.065 and electron transport rate, P=0.066) that were significantly different between GdN and GdW rice plants at 10% significance level (Table 6-2). This observation is consistent with the observed higher chlorophyll content at stem elongation (P<0.1). However, these significant differences are not consistent between the GdN and GdW rice plants at different nitrogen treatments and growth stages. A selected comparison of these four physiological parameters which showed statistical significance can be found in Figure 6-7.

Table 6-2. Summary of the P-values of the ANOVA analysis for chlorophyll fluorescence and gas exchange parameters between Gd treated (GdN) rice plants and non-Gd treated (GdW) rice plants at both the Gd treatment (Gd) and the three nitrogen treatments at 0%, 50% and 100% of the field recommended 150 kg N per hectare (nitrogen) levels at the different key growth stages (stem elongation, booting, anthesis and at full maturity). The interaction between the treatments were also analysed (Gd*Nitrogen). At instances where P-values (at 5% or 10%) showed significance, the significance was inconsistent between GdN and GdW throughout the growth stages. The comparison of differences of each parameter between growth stages was significant ($P<0.05$).

Parameters	**Treatment**	**Growth stage**		
		Stem Elongation	**Booting**	**Anthesis**
Maximum photosynthetic rate, A_{max}	Gd	0.684	0.078	0.417
	Nitrogen	0.001	<0.001	<0.001
	Gd*Nitrogen	0.042	0.028	0.804
Photochemical quenching, qP	Gd	0.964	0.040	0.525
	Nitrogen	0.015	0.015	0.022
	Gd*Nitrogen	0.256	0.743	0.005
Rate of transpiration, E	Gd	0.728	0.169	0.823
	Nitrogen	0.005	<0.001	<0.001
	Gd*Nitrogen	0.314	0.057	0.024
Stomatal conductance, g_s	Gd	0.844	0.130	0.202
	Nitrogen	0.003	<0.001	<0.001
	Gd*Nitrogen	0.022	0.078	0.645
Quantum yield of PSII, ΦPSII	Gd	0.894	0.065	0.827
	Nitrogen	0.003	<0.001	<0.001
	Gd*Nitrogen	0.092	0.181	0.023
Electron transport rate, ETR	Gd	0.895	0.066	0.823
	Nitrogen	0.003	<0.001	<0.001
	Gd*Nitrogen	0.090	0.174	0.024
Fv'/Fm'	Gd	0.877	0.782	0.326
	Nitrogen	0.211	0.003	0.018
	Gd*Nitrogen	0.248	0.266	0.166
Quantum yield of PSII (Fluopen)	Gd	0.106	0.269	0.158
	Nitrogen	0.673	0.258	0.495
	Gd*Nitrogen	0.272	0.815	0.340

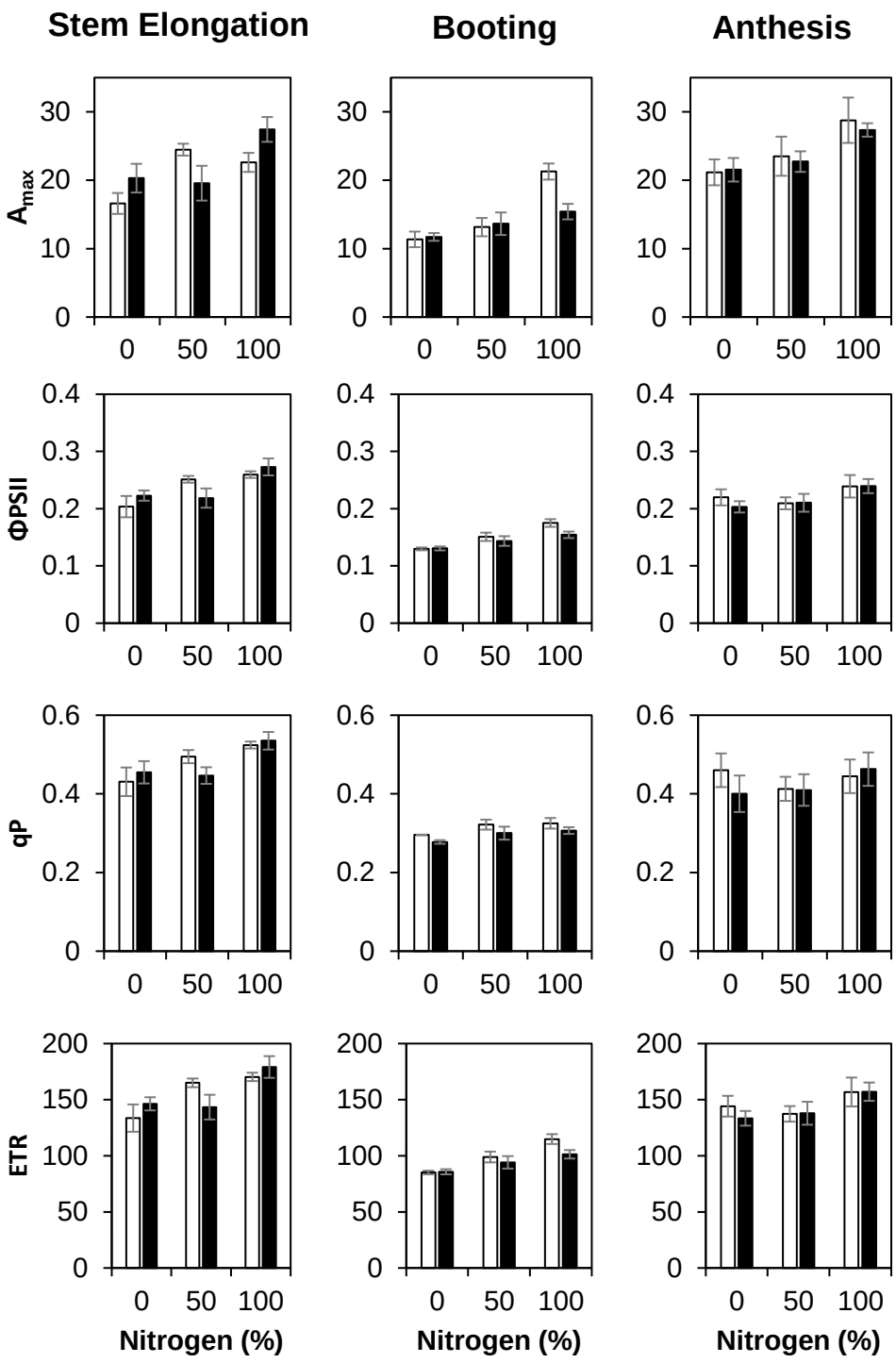


Figure 6-7. A selected comparison of the maximum photosynthetic rate (A_{max}), quantum yield of PSII (ΦPSII), photochemical quenching (qP) and electron transport rate (ETR) between GdW (white) and GdN (black) at 0%, 50% and 100% nitrogen treatments at stem elongation (week 6), booting (week 7) and anthesis (week 8). Growth stages are noted at the very top. The error bars denote the standard error between the replicates (n=5). No statistical differences were observed between treatments.

6.4.3 Nitrogen content of seeds

The seeds were sent to NRM Laboratories (Bracknell, UK) for nitrogen content analysis. As each nitrogen analysis of the seeds required a minimum of 100 g, the seeds for each treatment was pooled to form one sample. Hence, no statistical analysis could be performed on the results. Protein content was estimated based on the specific (Jones) factor provided by Food and Agriculture Organization. The specific (Jones) factor for conversion of nitrogen content to protein content for rice is 5.95 (FAO, 2003). At zero nitrogen supplementation, seeds of GdN rice plants had 4.3% more protein content than the seeds of GdW rice plants. However, the opposite trend was observed for 100% nitrogen.

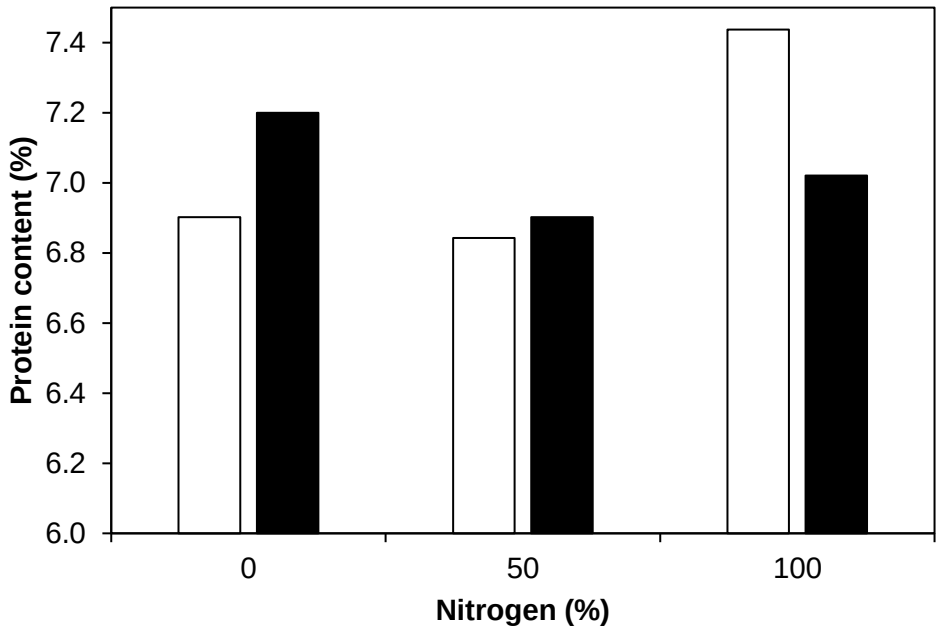


Figure 6-8. A comparison of the protein content (w/w%) between GdW (white) and GdN (black) at different nitrogen treatment levels. Protein content was converted from nitrogen content analysis based on specific (Jones) factor provided by Food and Agriculture Organization. No statistical analysis was carried out on the data.

6.4.4 GdN treatment at no nitrogen supplementation

The previous section data indicated that while differences between GdW and GdN were observed, there were inconsistent trends complicated by the use of higher N treatments. It is fully expected that the effects of colonization will have the greatest benefits at low soil nitrogen content. Hence, here we look in more detail at the no nitrogen supplementation treatment on a time-dependant basis, focussing on the key traits of biomass and yield formation and photosynthesis. Week 6, 7 and 8 correspond to the growth stages stem elongation, booting and anthesis respectively.

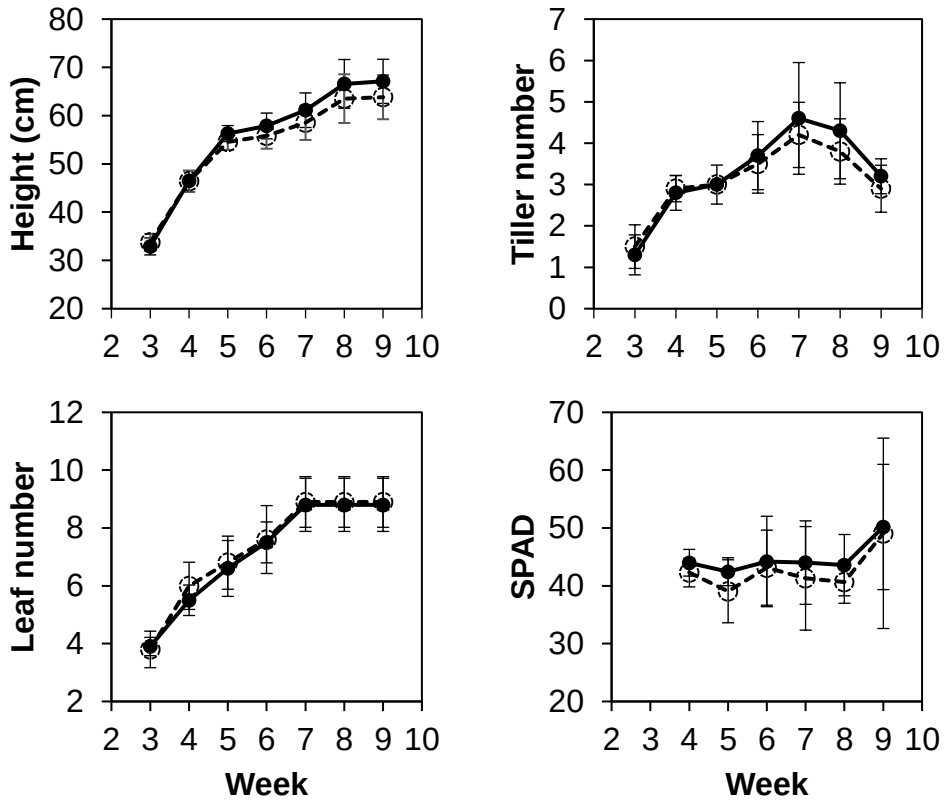


Figure 6-9. A comparison of the general growth trends between GdW (white circles) and GdN (black circles) rice plants during from the Week 3 to Week 8, in terms of average leaf number, tiller number and plant height per plant and the average SPAD value (proxy for chlorophyll content). Week 6, 7 and 8 correspond to the growth stages stem elongation, booting and anthesis respectively. Error bars show standard deviation (n=5). No statistical differences were observed between treatments.

Figure 6-9 shows consistently higher height, tiller number and SPAD across a sustained number of weeks in GdN rice plants compared to GdW rice plants under zero nitrogen supplementation, even if the data at each time point was not significant. This was also despite the initial slow germination and growth rate (Figure 6-6) of the GdN rice plants which was likely to be an artefact of the colonization process. After Week 5, GdN rice plants achieved the values of GdW rice plants in terms of the leaf number, tiller number and plant height. GdN plants also had greater SPAD values, showing greater chlorophyll content, than GdW plants (not statistically significant).

Under zero nitrogen supplementation, GdN rice plants had higher yield per plant than GdW rice plants, although the results are not significantly significant (Figure 6-10). The GdN plants had more fertile shoots, heavier ears and greater seed number and weight than the GdW rice plants (not statistically significant). Despite greater seed counts and seed weights per plant, GdN had a lower thousand grain weight (TGW) than GdW numerically. Similarly, in terms of gas exchange and chlorophyll fluorescence measurements, GdN treated rice plants also performed better than the GdW rice plants under zero nitrogen supplementation (Figure 6-7), but none of these differences were significant. These results are consistent with the increased protein content in GdN rice seeds compared to GdW rice seeds under no nitrogen supplementation (Figure 6-8). These results stacked together consistently at no nitrogen supplementation.

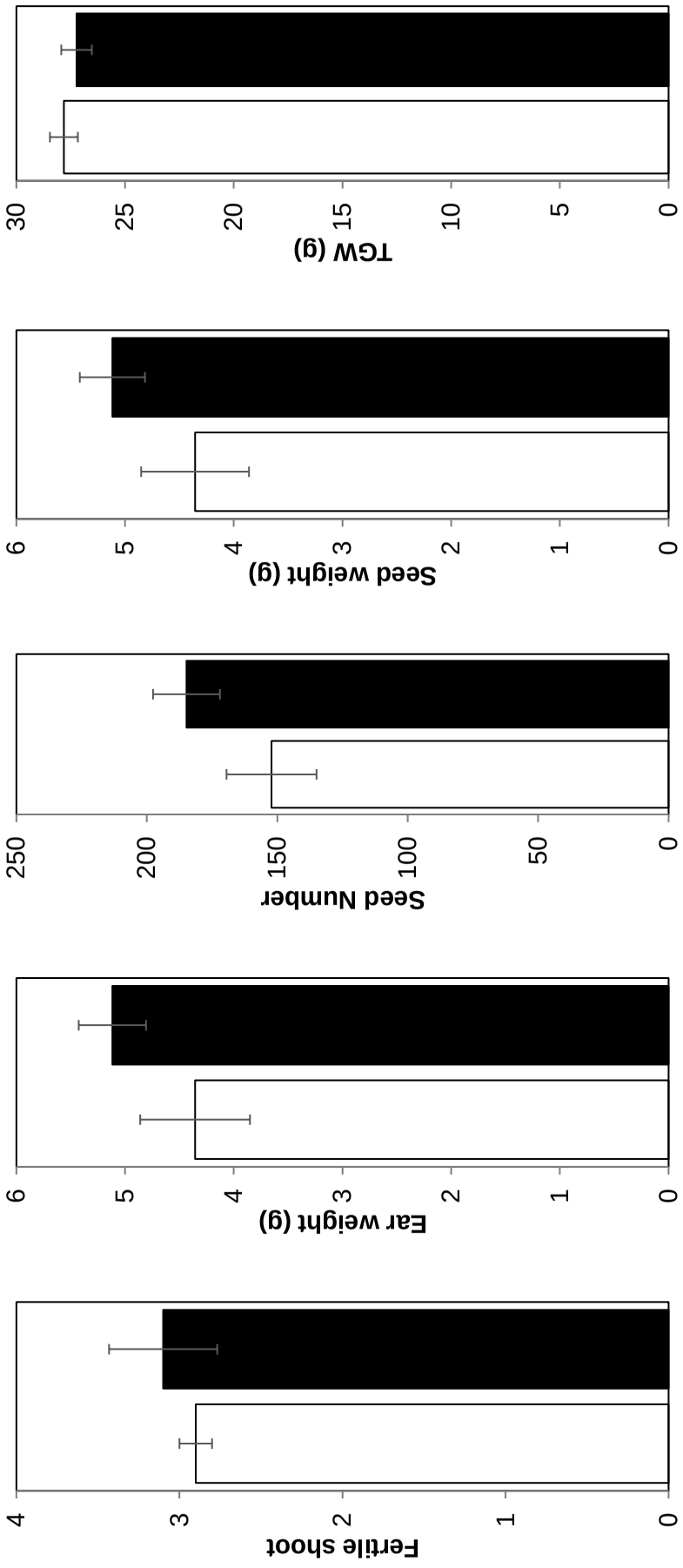


Figure 6-10. A comparison of the average fertile shoot per plant, ear weight per plant, seed number per plant, seed weight per plant and thousand grain weight (TGW) between GdW (white) and GdN (black) rice plants, under zero nitrogen supplementation at full maturity. Error bars showed standard error between the replicates (n=5). No statistical differences were observed between treatments.

6.5 Discussion

6.5.1 Successful Gd colonization does not translate to yield

Gd association with plants has been found widely in their natural conditions to improve yield of their host plants without depleting soil nitrogen. A successful dual inoculation using Gd and arbuscular mycorrhizal fungi showed about 6% increase in nitrogen content of 35 days old sorghum under laboratory conditions (Meenakshisundaram and Santhaguru, 2011). Suman *et al.* (2005) also reported improved growth in sugarcane using Gd, especially under 100% nitrogen supplementation (based on the maximum field recommendation of 150kg N per hectare). However, there were also reports of Gd ineffective in improving nitrogen deficiency in maize fields or under controlled conditions (Riggs *et al.*, 2001). In our experiment, we saw some possible enhancements at no nitrogen supplementation using low nitrogen compost under glasshouse conditions. When nitrogen was supplemented at either 50% or 100% based on the maximum field recommendations of 150kg N per hectare, the results were inconsistent between Gd treatments. The nitrogenase in Gd is not inhibited by nitrites and also not completely inhibited by ammonium (Stephan *et al.*, 1991; Fisher and Newton, 2005). Hence, Gd is capable of fixing nitrogen in the presence of some ammonia-based fertilizers. At high N supplementation, this could have inhibited the nitrogen fixing capability of Gd as observed in this experiment.

Better germination rates were observed for GdW than GdN rice seeds. It was also observed that GdN seeds germinated one week slower than GdW seeds. Although GdN rice plants started out slower than GdW rice plants, GdN caught up with GdW to give (not statistically significant) higher seed count,

seed weight and total biomass. The N-Fix® inoculant used contained 1% sucrose and this possibly reduced the rate of imbibition of the GdN seeds and resulted in a lower germination rate than the GdW seeds. The presence of a readily accessible food source is an advantage for the establishment and maintenance of the microbial community (Hirota *et al.*, 1978). As Gd metabolizes sucrose (via secreting the enzyme levansucrase) to produce cell-wall penetrating enzymes, the addition of sucrose is important for the success of colonization of the Gd bacteria (Cavalcante and Dobereiner, 1988; Gillis *et al.*, 1989; Cojho *et al.*, 1993; Eskin, Vessey and Tian, 2014; Dent and Cocking, 2017). Although sucrose concentration in N-Fix® inoculant solution was added at 10-fold lower concentration than the optimal sucrose concentration reported in literature (compared to 10% w/v), complete Gd colonization of the plant was possible. The use of 1% sucrose could possibly be further reduced to 0.8% (reflecting the sucrose concentration in sugarcane juice; Cojho *et al.*, 1993) to improve germination rate yet ensuring 100% Gd colonization. The successful Gd colonization of the plants was crucial for the success of the experiment.

Despite successful colonization of the Gd bacteria, no significant differences were found between the GdN and GdW rice plants, except at different nitrogen treatments. Gd might have been lacking a sufficiently concentrated sucrose environment to proliferate well after colonizing the plant, limiting its nitrogen-fixing capability. Rao, Jena and Adhya (1987) pointed out that the initial inoculation of the bacteria can be highly successful. However, its population is prone to diminish. This effect could be more apparent in these tub experiments compared to the field given the soil volume. As no samples were collected for Gd colonization analysis, it remains unknown whether the non-significant result observed was due to diminished Gd population or due to

the nitrogen treatment effect. Furthermore, the efficiency of Gd and nitrogen-fixing capability could vary drastically depending on the Gd strain, plant genotype and plant growth stages. However, the environment could present a greater variability (Hirota *et al.*, 1978; Rao, Jena and Adhya, 1987; Santi, Bogusz and Franche, 2013). There could be other conditions resulting in the inhibition of nitrogen fixation or conditions unmet during the experiment, when compared to the conditions in the field, such as the rhizosphere and soil pH as aforementioned. In this experiment, the standard rice mix used would present a different microflora and microfauna to that of the field soil (Hirota *et al.*, 1978). The soil environment of flooded rice fields have a wide diversity of nitrogen-fixing microorganisms in which Gd can interact with (Ladha, De Bruijn and Malik, 1997).

6.5.2 Photosynthesis and nitrogen fixing bacteria

Rangel de Souza *et al.* (2016) supported that Gd can potentially improve photosynthesis. This is highly relevant as plants would require the additional nitrogen fixed for biosynthesis of photosynthetic pigments, enzymes and other structural components (Verhoeven, Demmig-Adams and Adams, 1997; Lawlor, 2002). At the same time, the successful colonization of Gd in crop plants requires huge energy maintenance (14 molecules of ATP is required to produce one molecule of ammonia) which is usually met through the provision of substrates from photosynthesis (Kirizii, Vorobei and Kots', 2007; Dent and Cocking, 2017). This forms the basis of symbiotic relationship between plants and nitrogen fixing bacteria. It was found that the nitrogen fixation rate and photosynthesis are closely related. Photosynthesis is limited by availability of nitrogen and more often that not, photosynthesis and

nitrogen fixing by microorganisms are positively correlated (Evans, 1989).

Photosynthesis is enhanced with an increase in nitrogen fixation, especially when there is some degree of nitrogen limitation (Kirizii, Vorobei and Kots', 2007; Bassi, Menossi and Mattiello, 2018). It was also observed than an increased nitrogen availability for plant also resulted in better photosynthesis recovery under drought conditions (Zhong *et al.*, 2019) and better water use efficiency (Dent and Cocking, 2017). All this can result in increased photosynthetic areas for greater light interception and productivity (Lawlor, 2002). The increase in nitrogen fixation rate can result in increased photosynthesis-related nitrogen-based components such as chlorophyll and Rubisco (Maekawa and Kokubun, 2005). However, the gap between Rubisco and Rubisco activase activities also showed that there is an optimal nitrogen fixation rate for photosynthesis to be useful (Kirizii, Vorobei and Kots', 2007).

It was also reported that it is difficult to assess the exact benefit of inoculated bacteria in agriculture and quite often, the rate of nitrogen fixation and metabolism of nitrogen are not always reflected in aboveground biomass and yield (Rao, Jena and Adhya, 1987; Lawlor, 2002; Kirizii, Vorobei and Kots', 2007). From this experiment, the maximum carbon dioxide assimilation rate, electron transport rate, photochemical quenching and quantum efficiency of Photosystem II of the GdN rice plants was greater than the GdW rice plants at booting stage at no nitrogen supplementation ($P<0.01$). However, this did not reflect in the yield of the plants. As suggested by Makino (2003), the observed increase at leaf level might not translate to higher biomass. These observed improved photosynthetic parameters could have greater significance in a rice field where the effect can be magnified. It was observed that canopy photosynthesis were greater in field Arabidopsis (Rangel de Souza *et al.*, 2016).

There is a consistent albeit not statistically significant trend whereby GdN rice plants grow better than the GdW rice plants where there is no nitrogen supplementation in glasshouse experiments; the GdN rice plants were taller, had a greater number of tillers, more leaves and were greener (reflected in higher SPAD values) than the GdW rice plants. These matched with the better photosynthetic parameters observed in GdN rice plants, compared to GdW rice plants. This is supported by the finding that GdN treated plants showed improved photosynthesis (Dent and Cocking, 2017). Azotic Technologies Ltd also reported of successful wheat experiments and rice field trials (Azotic Technologies, 2017). They reported an increase in 22% yield in direct sowing of rice when trials were run at full fertilizer recommendation. When the nitrogen fertilization was reduced by more than half, a higher yield increase of 33% was recorded. Using the transplanting method, only 10% increase in yield was recorded at full fertilizer application. However, when the fertilizer application was reduced by a 25%, a higher yield increase of 14% was observed (Azotic Technologies, 2017; Dent and Cocking, 2017).

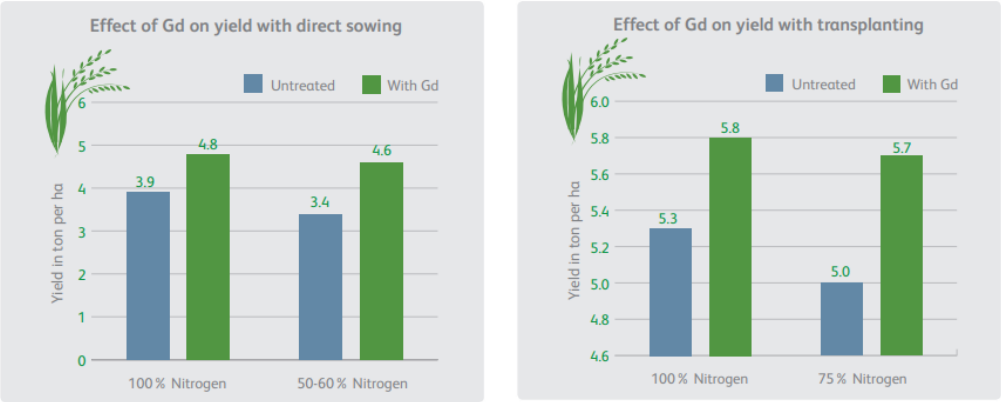


Figure 6-11. Yield increase were observed with Gd treatment and nitrogen supplementation in Vietnamese rice fields, either through direct sowing or transplanting of rice seedlings (Azotic Technologies, 2017).

At no nitrogen supplementation level, GdN rice plants showed a non-statistically significant trend of higher seed count and seed weight than GdW

rice plants at harvest. However, this trend is not reflected in the TGW; GdN rice plants had greater number of seeds that were smaller in size than GdW rice plants. Although TGW has a high heritability, it is not always positively correlated to yield (Simmonds *et al.*, 2014). This is not only attributed to genetic factors but also more importantly, the environment and its interaction with the genetic factors (Zanke *et al.*, 2015). The genetic factors determining TGW themselves could be quite complex, ranging from the position of the grain on the ear to duration of grain filling or the rate of grain filling (Baillot *et al.*, 2018). As pointed out in Chapter 6.4.4, the GdN inoculant could have resulted in relatively slower germination of the seeds. Final grain weight is usually determined at a later growth stage, from anthesis onwards (Baillot *et al.*, 2018). Hence, the final grain weight should not be affected by the slower initial development. It could be that there were more resources for the GdN rice plants to create more seeds but insufficient time for the grain to fully develop. The rice variety used is in the experiment are of quick maturity nature, taking about three months to reach full maturity. The relatively short grain filling period could explain the greater number of seeds of lower grain weight.

6.5.3 The prospect of using Gd in Spanish rice

Azotic Technologies Ltd had rice field experiments using this Spanish rice and this largely determined the use of this rice variety in this experiment. In general, there was no consistent and statistically significant differences between all the parameters measured. However, this cannot be directly compared to the results found in the field due to the differences between the rhizosphere of the rice plants between this experiment and the commercial

field as discussed previously. There is no statistically significant interaction between nitrogen treatment and GdN treatment. Studies had shown that there is positive interaction between addition of nitrogen-based fertilizer and use of Gd (Rao, Jena and Adhya, 1987). This was also reported in the field trials by Azotic Technologies Ltd. (Nottingham, UK). However, this is not observed in the glasshouse experiment.

The use of naturally occurring nitrogen fixing bacteria cannot replace the use of synthetic fertilizer to maintain or increase yield of cereals. It was found that nitrogen-fixing bacteria could only contribute to up to half the amount of nitrogen required by cereal crops (Ormeño-Orrillo, Hungria and Martinez-Romero, 2013; Rosenblueth *et al.*, 2018). Hence, diazotrophs mutants have been investigated and found to be great plant growth promoter (Rosenblueth *et al.*, 2018). The N-Fix® inoculant containing an endophytic Gd (strain not disclosed) provided by Azotic Technologies Ltd. could have used a mutant variant of the Gd to give greater advantage of their technology for application in a wide range of crops. However, there are reports that plants have a greater effect in determining the success of the colonization and the nitrogen-fixing activities of the nitrogen fixing bacteria (Hirota *et al.*, 1978; Rosenblueth *et al.*, 2018).

Additionally, rice is generally classed as low protein food (Iida, Amano and Nishio, 1993; Shih, 2003). Improvement of grain protein without genetic manipulation or selection of high protein varieties is very interesting and would prove useful in creating more nutritious food. In the fight for higher agriculture productivity in a sustainable context to secure food security, we should not neglect the need for more nutritious food too (McKenzie and Williams, 2015). Hence, the production of seeds with a 4.3% more protein content in GdN rice plants than GdW rice plants at no nitrogen fertilizer

supplementation (no statistical comparison was made) showed great potential in increasing rice protein content.

6.6 Summary

A 100% colonization of Gd was observed in rice seedlings. However, there was no statistically significant improvement to rice growth, physiologically or in terms of yield. There were some indications that under no nitrogen supplementation, Gd could improve photosynthesis and hence, yield. The use of Gd to achieve greater photosynthesis and yield in crops under field conditions could potentially make a great contribution to agriculture industry, not only in terms of increasing yield but also provision of more nutritious crops with higher protein content.

Chapter 7 General Discussion

7.1 Physiological studies should be made at canopy level

Photoprotection is gaining traction in research context as more people realise its importance in enhancing photoprotection under dynamic conditions (Murchie and Niyogi, 2011; Hubbart *et al.*, 2012, 2018; Kromdijk *et al.*, 2016). The latter point is important: it is now considered insufficient to solely study gene or plant traits at cell or leaf level. This does not negate the importance of crop physiology studies under controlled environment. Crops do not grow as a lone standing plant but in a complex canopy environment which can be affected not only by environmental factors such as sun and cloud movement, but also by other different factors such as canopy architecture, self-shading or shading by leaf layers above (Burgess *et al.*, 2016, 2017; Townsend *et al.*, 2018) and resource availability (Głowacka *et al.*, 2018). Hence, studies of crop plants should be magnified to canopy level, encompassing a combination of on-field physiology studies, remote sensing to generate a larger “view” of the crop canopies and realistic modelling of the crop canopy (Murchie *et al.*, 2018). This PhD thesis aimed to study such diverse aspects of photoprotection in both rice and wheat at canopy level, using new techniques involving protective non-photochemical quenching (pNPQ; Ruban and Murchie, 2012) and finding efficient and rapid ways of screening crop populations for “photoprotectiveness” using new the new parameter $NPQ_{(T)}$ (Tietz *et al.*, 2017).

7.2 Photoprotection is a key trait in crop breeding

The introgression of rice *PsbS* into wheat was successful (Chapter 2) but selection for homozygosity was laborious and time consuming (Bhalla, 2006). It was unexpectedly difficult to work with rice *PsbS* gene in wheat, not only in terms of genotyping but also to maintain the fidelity of the transgene. Although rice and wheat are closely related, perhaps it would be better to work with known wheat gene rather than introducing a transgene for better success rates (Hospital, 2005). 'Pyramiding' of several genes related to the mechanism being studied could also result in a more robust and wider spectrum of gene-related response as seen with the successful study by Kromdijk *et al.* (2016). Agrobacterium-mediated transformation comes with different issues such as inconsistent expression of transgenes which more often than not, do not correlate well to the transgene copy number (Mlynarova *et al.*, 1995). Positional effect is another well-known issue with this transformation technique where the transgene could randomly be integrated into transcriptionally active or silent regions (Campisi *et al.*, 1999; Gelvin, 2003). Moreover, there are reports that transgenes introduced into cereals did not necessarily segregate according to Mendel's laws (McElroy and Brettell, 1994; Cheng *et al.*, 1997; Demeke *et al.*, 1999; Jones, 2005). In the case of the introgression of rice *PsbS* into wheat, the transgene was not retained well into the next generation for further investigations.

With all these issues, it could have been easier and more efficient to select for photoprotection in the natural genetic variation readily present in a large wheat population. In Chapter 3, marked differences in photoprotection capacity were identified within a small subset of a genetically diverse wheat population under field conditions as expected. The study of NPQ at canopy

level also showed the importance of identifying the genotypes that do not only have greater capacity but are also more responsive to fluctuating conditions throughout the canopy. Improving of photoprotection capacity and response in crop plants could possibly present a greater advantage to plants in terms of energy cost. Photoinhibition is costly, inevitable and occurs on a long-term basis resulting in lowered plant productivity (Jansen, Mattoo and Edelman, 1999; Chow *et al.*, 2005; Raven, 2011). However, if the plant possesses the capacity and is photoresponse-ready, then its plant productivity could outweigh the cost spent in maintaining the photoprotectiveness. This was successfully shown in field grown tobacco plants where an improved NPQ recovery resulted in 20% increase in yield (Kromdijk *et al.*, 2016). In contrast to photoinhibition, plants would have a time lag in responding to environmental light cues which result in not only diminished productivity but also require investment of more resources for the constant repair of D_1.

7.3 Improving non-photochemical quenching (NPQ) response outweighs cost of photoinhibition

Studying NPQ at canopy level (Chapter 3 and Chapter 4) showed that the bottom of the canopy had greater NPQ capacity and variations than the top of the canopy. This presented a question as to why the bottom of the canopy requires high NPQ capacity. This could be due to older leaves incapable of photosynthesis as efficiently as younger leaves at the top of the canopy or the allocation of photoprotective ability of the canopy towards the bottom of the canopy where there are higher occurrences of sunflecks or sudden high fluctuating light. Leaves would continue to age and it would perhaps be more

rational to continue investing resources in countering and protecting the canopy from the fluctuating light environment. This should be essential as these rapid fluctuating lights account for up to 90% of the light received at the bottom of the canopy for photosynthesis (Pearcy, 1990). Moreover, the improvement of NPQ capacity and response in plants would likely to also confer advantages to the top of the canopy. The top of the canopy is photoacclimated to high light but an increased capacity would allow more room for "buffering" towards the high light conditions. This is important as the top layer of the canopy accounts for up to three quarter of the canopy carbon gain (Long *et al.*, 2006). Quantification of the phototolerance at canopy level showed that in canopies where *PSbS* was overexpressed, the top of the canopy also showed improved phototolerance.

7.4 Dynamic stomatal response to light at canopy level

Plants adjust their stomatal conductance in response to a range of environmental cues such as humidity, CO_2 and light environment (Pieruschka, Huber and Berry, 2010) and it was shown that the leaves within an Arabidopsis canopy were capable of working together to optimize stomatal response under dynamic conditions (Devireddy *et al.*, 2018). Stomatal response is translated to water use efficiency and crop productivity. When stomata are not responding well to the environmental cues, this results in lowered water use efficiency and lost productivity (Lawson and Blatt, 2014; McAusland *et al.*, 2016). Studies of stomata within a canopy usually assume it behaves as a 'big leaf' and under steady-state but this is inaccurate because

stomata respond to light in a non-linear way (Ding *et al.*, 2014). There are more incidences of stomatal closure further down the canopy where light is limited which should be accounted for when modelling stomatal conductance (Song, Jiang and Gao, 2016). Furthermore, the heterogeneity of light within a canopy (shown in Chapter 4) also increase the complications in estimating stomatal conductance not accounted for during modelling (Bonan *et al.*, 2011; Wehr *et al.*, 2017). Other than that, the photosynthesis and stomatal conductance at the bottom of the canopy are limited by the age of the leaves. It was also shown that overexpression of PsbS could improve intrinsic water use efficiency in tobacco (Głowacka *et al.*, 2018) and rice (Chapter 5), albeit through different rationales. As aforementioned, light travels exponentially down the canopy and coupled with increased phototolerance at the bottom of the canopy, PsbS could be implicated in more than just providing crop canopies with greater protection from light but also more efficient water use within the canopy. This showed the complexity of photosynthesis and light-related controls in plant productivity.

7.5 Improvement of photoprotection via biological methods

It is possible to enhance photosynthesis and improve crop yield through microorganisms (Chapter 6). Most studies attributed the bacteria related improvements to increased accessibility to resources (nitrogen, phosphorus, water, minerals, etc.) contributed by the bacteria which in turn resulted in better growth (Alam *et al.*, 2001; Bashan, Holguin and De-Bashan, 2004). Reports of improvement in photosynthesis in crops inoculated with plant-

growth promoting bacteria were usually related to larger, healthier and greener (increase in chlorophyll content) in plants (Sharma *et al.*, 2003; Bashan, Holguin and De-Bashan, 2004; Bashan *et al.*, 2006). However, Bashan *et al.* (2006) took a step further to investigate the chlorophyll changes. Bashan *et al.* (2006) extracted and quantified the photoprotective pigments in wheat plants successfully inoculated with plant growth promoting bacteria, *Azospirillum brasilense* Cd and found that increased photoprotective pigments were produced although the wheat plants were not subjected to any stress. They attributed the enhanced growth to a combination of advantage brought about by the inoculation of plant growth promoting bacteria, including the increase in photoprotection.

7.6 Future work

It is important to develop more resilient crops that do not compromise yield and productivity to secure global food security, especially in face of climate change. In terms of breeding crops for improved photoprotection, employing of new tools and parameters such as $NPQ_{(T)}$ would be the way forward. $NPQ_{(T)}$ allows for relatively quick measurements of photoprotection and more work is required to study and establish this parameter as a robust photoprotective trait “indicator” to allow for more efficient screening tool. This could be done in different crops with increased sample size to correlate with other yield data such as biomass, grain yield and total RUE. Most importantly, this will also allow improved measurements made under fluctuating conditions in the field at a larger scale than possible at the moment.

Breeding for crops with improved photoprotective traits should also include

sustainability and optimization of agricultural practices. In specific relation to photoprotection, different seeding density should be investigated in different crops. Planting density could create a huge variation in the light environment within the canopy itself (Stewart *et al.*, 2003). Sunflecks account for most of the bottom crop canopy productivity. An optimal seed rate should take into consideration of the light interception down the canopy to allow for optimal carbon assimilation induced by sunflecks. From another aspect, improvement could also be made to crops by employing biological nitrogen fixations. There were indications that increased nitrogen could result in improved photosynthesis and photoprotection. In continuation to the study where rice was inoculated with Gd, confirmatory work should be made to double check that the Gd population continued to flourish within the rice plants instead of only at the initial seedling stage. This could provide more conclusive results as to whether Gd inoculation helped improved photosynthesis and photoprotection in rice plants.

There were also indications that *PsbS* is implicated in improved WUE in tobacco and rice. More detailed work should be carried out to divulge the proper mechanisms and tease apart the differences in signalling pathway in tobacco and rice. They are essentially very different kind of crops; tobacco is a biomass dicotyledonous plant and rice is a grain monocotyledonous plant. Hence, unsurprising to observe possibly different signalling pathways between these two crops. The overexpression of *PsbS* resulting in improved WUE should also be studied in other crops to investigate whether similar signal is present in other plants – either under a light shift or drought regime.

7.7 Concluding remarks

There is a need to continuously put in effort to improve plant productivity in a sustainable way and improving photosynthesis in plants would be a great option. Photosynthetic regulation is still not fully understood but many are still looking at it as enhancing photosynthesis in plants will be a major breakthrough for plant productivity. There are many possibilities to improve photosynthesis and photoprotection; through genetic engineering to overexpress photoprotective genes, selection for improved photoprotective ability within wheat populations or through the use of harmless bacteria. New technologies such as high-resolution reconstruction of canopies, improved modelling techniques coupled with validated models and new tools or parameters can help with better selection and breeding of more resilient and productive crop plants to feed the future population.

References

Adams, W. W. *et al.* (1999) ‘Rapid changes in xanthophyll cycle-dependent energy dissipation and photosystem II efficiency in two vines, Stephania japonica and Smilax australis, growing in the understory of an open Eucalyptus forest’, *Plant, Cell and Environment*, 22(2), pp. 125–136. doi: 10.1046/j.1365-3040.1999.00369.x.

Adriano-Anaya, M. *et al.* (2005) ‘Plant cell-wall degrading hydrolytic enzymes of Gluconacetobacter diazotrophicus’, *Symbiosis*, 40(3), pp. 151–156.

Ahn, T. K. *et al.* (2008) ‘Architecture of a Charge-Transfer State Regulating Light Harvesting in a Plant Antenna Protein’, *Science*, 320(5877), pp. 794–797. doi: 10.1126/science.1154800.

Aisawi, K. A. B. *et al.* (2015) ‘The physiological basis of the genetic progress in yield potential of CIMMYT spring wheat cultivars from 1966 to 2009’, *Crop Science*, 55(4), pp. 1749–1764. doi: 10.2135/cropsci2014.09.0601.

Alam, S. M. *et al.* (2001) ‘Grain yield and related physiological characteristics of rice plants (Oryza sativa L.) Inoculated with free-living rhizobacteria’, *Plant Production Science*, 4(2), pp. 126–130. doi: 10.1626/pps.4.126.

Anderson, J. M. (1986) ‘Photoregulation of the Composition, Function, and Structure of Thylakoid Membranes’, *Annual Review of Plant Physiology*, 37(1), pp. 93–136. doi: 10.1146/annurev.pp.37.060186.000521.

Anderson, J. M., Chow, W. S. and Park, Y. Il (1995) ‘The grand design of photosynthesis: Acclimation of the photosynthetic apparatus to environmental cues’, *Photosynthesis Research*, pp. 129–139. doi: 10.1007/BF00020423.

Anderson, L. E. (1971) ‘Chloroplast and cytoplasmic enzymes II. Pea leaf triose phosphate isomerases’, *BBA - Enzymology*, 235(1), pp. 237–244. doi: 10.1016/0005-2744(71)90051-9.

Araus, J. L. *et al.* (2002) ‘Plant breeding and drought in C3 cereals: What should we breed for?’, *Annals of Botany*, 89, pp. 925–940. doi: 10.1093/aob/mcf049.

Araus, J. L., Serret, M. D. and Lopes, M. S. (2019) ‘Transgenic solutions to

increase yield and stability in wheat: Shining hope or flash in the pan?', *Journal of Experimental Botany*, 70(5), pp. 1419–1424. doi: 10.1093/jxb/erz077.

Arkebauer, T. J. *et al.* (1994) 'In defense of radiation use efficiency: a response to Demetriades-Shah et al. (1992)', *Agricultural and Forest Meteorology*, 68(3–4), pp. 221–227. doi: 10.1016/0168-1923(94)90038-8.

Aro, E. M., Virgin, I. and Andersson, B. (1993) 'Photoinhibition of Photosystem II. Inactivation, protein damage and turnover', *BBA - Bioenergetics*, pp. 113–134. doi: 10.1016/0005-2728(93)90134-2.

Awika, J. M. (2011) 'Major cereal grains production and use around the world', in *ACS Symposium Series*, pp. 1–13. doi: 10.1021/bk-2011-1089.ch001.

Azotic Technologies, L. (2017) *Azotic Technologies and Koppert Biological Systems*. Available at: https://www.azotictechnologies.com/assets/Uploads/Azotic-Koppert-Rice-Information.pdf? (Accessed: 30 August 2019).

Azotic Technologies, L. (2018) *Azotic's natural nitrogen fixing technology is now commercially available in the USA » Natural nitrogen to boost agriculture*. Available at: https://www.azotictechnologies.com/news-and-insight/latest-news/heading-5/ (Accessed: 30 August 2019).

Badger, M. R. (1985) 'Photosynthetic Oxygen Exchange', *Annual Review of Plant Physiology*, 36(1), pp. 27–53. doi: 10.1146/annurev.pp.36.060185.000331.

Badger, M. R. *et al.* (2000) 'Electron flow to oxygen in higher plants and algae: Rates and control of direct photoreduction (Mehler reaction) and rubisco oxygenase', in *Philosophical Transactions of the Royal Society B: Biological Sciences*, pp. 1433–1446. doi: 10.1098/rstb.2000.0704.

Bagley, J. *et al.* (2015) 'The influence of photosynthetic acclimation to rising CO2 and warmer temperatures on leaf and canopy photosynthesis models', *Global Biogeochemical Cycles*, 29(2), pp. 194–206. doi: 10.1002/2014GB004848.

Baillot, N. *et al.* (2018) 'Different grain-filling rates explain grain-weight differences along the wheat ear', *PLoS ONE*. Edited by A. Zhang. Public Library of Science, 13(12), p. e0209597. doi: 10.1371/journal.pone.0209597.

Baker, N. R. (2008) 'Chlorophyll Fluorescence: A Probe of Photosynthesis In Vivo', *Annual Review of Plant Biology*, 59(1), pp. 89–113. doi: 10.1146/annurev.arplant.59.032607.092759.

Baldani, J. I. *et al.* (2014) 'The art of isolating nitrogen-fixing bacteria from non-leguminous plants using N-free semi-solid media: a practical guide for microbiologists', *Plant and Soil*, 384(1–2), pp. 413–431. doi: 10.1007/s11104-014-2186-6.

Barber, J. and Andersson, B. (1992) 'Too much of a good thing: light can be bad for photosynthesis', *Trends in Biochemical Sciences*, (February), pp. 61–66. doi: 10.1016/0968-0004(92)90503-2.

Barros, T. and Kühlbrandt, W. (2009) 'Crystallisation, structure and function of plant light-harvesting Complex II', *Biochimica et Biophysica Acta - Bioenergetics*, pp. 753–772. doi: 10.1016/j.bbabio.2009.03.012.

Barrs, H. and Weatherley, P. (1962) 'A Re-Examination of the Relative Turgidity Technique for Estimating Water Deficits in Leaves', *Australian Journal of Biological Sciences*, 15(3), p. 413. doi: 10.1071/bi9620413.

Bashan, Y. *et al.* (2006) 'Increase in auxiliary photoprotective photosynthetic pigments in wheat seedlings induced by Azospirillum brasilense', *Biology and Fertility of Soils*, 42(4), pp. 279–285. doi: 10.1007/s00374-005-0025-x.

Bashan, Y., Holguin, G. and De-Bashan, L. E. (2004) 'Azospirillum-plant relationships: Physiological, molecular, agricultural, and environmental advances (1997-2003)', *Canadian Journal of Microbiology*, pp. 521–577. doi: 10.1139/w04-035.

Bassi, D., Menossi, M. and Mattiello, L. (2018) 'Nitrogen supply influences photosynthesis establishment along the sugarcane leaf', *Scientific Reports*. Nature Publishing Group, 8(1). doi: 10.1038/s41598-018-20653-1.

Battisti, D. S. D. and Naylor, R. L. (2009) 'Historical Warnings of Future Food Insecurity with Unprecedented Seasonal Heat', *Science*, 323, pp. 240–244.

doi: 10.1126/science.1164363.

Bauwe, H., Hagemann, M. and Fernie, A. R. (2010) 'Photorespiration: players, partners and origin', *Trends in Plant Science*, pp. 330–336. doi: 10.1016/j.tplants.2010.03.006.

Beddington, J. R. *et al.* (2012) 'Agriculture: What next for agriculture after Durban?', *Science*. American Association for the Advancement of Science, pp. 289–290. doi: 10.1126/science.1217941.

Bergantino, E. *et al.* (2003) *Light- and pH-dependent structural changes in the PsbS subunit of photosystem II*, *Proceedings of the National Academy of Sciences of the United States of America*. doi: 10.1073/pnas.2533072100.

Berners-Lee, M. *et al.* (2018) 'Current global food production is sufficient to meet human nutritional needs in 2050 provided there is radical societal adaptation', *Elem Sci Anth*. University of California Press, 6(1), p. 52. doi: 10.1525/elementa.310.

Betti, M. *et al.* (2016) 'Manipulating photorespiration to increase plant productivity: Recent advances and perspectives for crop improvement', *Journal of Experimental Botany*, pp. 2977–2988. doi: 10.1093/jxb/erw076.

Bhalla, P. L. (2006) 'Genetic engineering of wheat - current challenges and opportunities', *Trends in Biotechnology*, pp. 305–311. doi: 10.1016/j.tibtech.2006.04.008.

Bielczynski, L. W. *et al.* (2017) 'Leaf and plant age affects photosynthetic performance and photoprotective capacity', *Plant Physiology*, 175(4), pp. 1634–1648. doi: 10.1104/pp.17.00904.

Björkman, O. and Demmig, B. (1987) 'Photon yield of O2 evolution and chlorophyll fluorescence characteristics at 77 K among vascular plants of diverse origins', *Planta*, 170(4), pp. 489–504. doi: 10.1007/BF00402983.

Bonan, G. B. *et al.* (2011) 'Improving canopy processes in the Community Land Model version 4 (CLM4) using global flux fields empirically inferred from FLUXNET data', *Journal of Geophysical Research*, 116(G2). doi: 10.1029/2010jg001593.

Bonente, G. *et al.* (2008) ‘Interactions between the photosystem II subunit PsbS and xanthophylls studied in vivo and in vitro’, *Journal of Biological Chemistry*, 283(13), pp. 8434–8445. doi: 10.1074/jbc.M708291200.

Bravdo, B.-A. and Canvin, D. (1979) ‘Effect of Carbon Dioxide on Photorespiration’, *Plant Physiology*, 63(2), pp. 399–401. doi: 10.1104/pp.63.2.399.

Brestic, M. *et al.* (1995) ‘Does photorespiration protect the photosynthetic apparatus in french bean leaves from photoinhibition during drought stress?’, *Planta*. Springer-Verlag, 196(3), pp. 450–457. doi: 10.1007/BF00203643.

Brisson, N. *et al.* (2010) ‘Why are wheat yields stagnating in Europe? A comprehensive data analysis for France’, *Field Crops Research*, 119(1), pp. 201–212. doi: 10.1016/j.fcr.2010.07.012.

Brooks, M. D. *et al.* (2013) ‘A thioredoxin-like/β-propeller protein maintains the efficiency of light harvesting in Arabidopsis.’, *Proceedings of the National Academy of Sciences of the United States of America*, 110(29), pp. E2733-40. doi: 10.1073/pnas.1305443110.

Buresh, R. J., Casselman, M. E. and Patrick, W. H. (1980) ‘Nitrogen fixation in flooded soil systems, a review’, *Advances in Agronomy*, 33(C), pp. 149–192. doi: 10.1016/S0065-2113(08)60166-2.

Burgess, A. J. *et al.* (2015) ‘High-resolution three-dimensional structural data quantify the impact of photoinhibition on long-term carbon gain in wheat canopies in the field’, *Plant Physiology*, 169(2), pp. 1192–1204. doi: 10.1104/pp.15.00722.

Burgess, A. J. *et al.* (2016) ‘The 4-dimensional plant: Effects of wind-induced canopy movement on light fluctuations and photosynthesis’, *Frontiers in Plant Science*, 7, p. 1392. doi: 10.3389/fpls.2016.01392.

Burgess, A. J. *et al.* (2017) ‘Image-based 3D canopy reconstruction to determine potential productivity in complex multi-species crop systems’, *Annals of botany*, 119(4), pp. 517–532. doi: 10.1093/aob/mcw242.

von Caemmerer, S. and Evans, J. R. (2010) ‘Enhancing C3 Photosynthesis’, *Plant Physiology*, 154(2), pp. 589–592. doi: 10.1104/pp.110.160952.

Von Caemmerer, S., Quick, W. P. and Furbank, R. T. (2012) 'The development of C4 rice: Current progress and future challenges', *Science*, pp. 1671–1672. doi: 10.1126/science.1220177.

Caine, R. S. *et al.* (2019) 'Rice with reduced stomatal density conserves water and has improved drought tolerance under future climate conditions', *New Phytologist*, 221(1), pp. 371–384. doi: 10.1111/nph.15344.

Calderini, D. F. and Slafer, G. A. (1998) 'Changes in yield and yield stability in wheat during the 20th century', *Field Crops Research*, 57(3), pp. 335–347. doi: 10.1016/S0378-4290(98)00080-X.

Callis, J., Fromm, M. and Walbot, V. (1987) 'Introns increase gene expression in cultured maize cells.', *Genes & development*, 1(10), pp. 1183–1200. doi: 10.1101/gad.1.10.1183.

Campisi, L. *et al.* (1999) 'Generation of enhancer trap lines in Arabidopsis and characterization of expression patterns in the inflorescence', *Plant Journal*, 17(6), pp. 699–707. doi: 10.1046/j.1365-313X.1999.00409.x.

Carvalho, F. E. L., Ware, M. A. and Ruban, A. V. (2015) 'Quantifying the dynamics of light tolerance in Arabidopsis plants during ontogenesis', *Plant, Cell and Environment*, 38(12), pp. 2603–2617. doi: 10.1111/pce.12574.

Castiglioni, P. *et al.* (2008) 'Bacterial RNA Chaperones Confer Abiotic Stress Tolerance in Plants and Improved Grain Yield in Maize under Water-Limited Conditions', *Plant Physiology*, 147(2), pp. 446–455. doi: 10.1104/pp.108.118828.

Cavalcante, V. A. and Dobereiner, J. (1988) 'A new acid-tolerant nitrogen-fixing bacterium associated with sugarcane', *Plant and Soil*, 108(1), pp. 23–31. doi: 10.1007/BF02370096.

Cazzaniga, S. *et al.* (2013) 'Interaction between avoidance of photon absorption, excess energy dissipation and zeaxanthin synthesis against photooxidative stress in Arabidopsis', *Plant Journal*, 76(4), pp. 568–579. doi: 10.1111/tpj.12314.

Challinor, A. J. *et al.* (2014) 'A meta-analysis of crop yield under climate change and adaptation', *Nature Climate Change*. Nature Publishing Group,

4(4), pp. 287–291. doi: 10.1038/nclimate2153.

Chaves, M. M. *et al.* (2002) ‘How plants cope with water stress in the field. Photosynthesis and growth’, *Annals of Botany*, 89, pp. 907–916. doi: 10.1093/aob/mcf105.

Cheng, M. *et al.* (1997) ‘Genetic transformation of wheat mediated by Agrobacterium tumefaciens’, *Plant Physiology*, 124(6), pp. 575–580. doi: https://doi.org/10.1104/pp.115.3.971.

Cheng, Y.-C. and Fleming, G. R. (2009) ‘Dynamics of Light Harvesting in Photosynthesis’, *Annual Review of Physical Chemistry*, 60(1), pp. 241–262. doi: 10.1146/annurev.physchem.040808.090259.

Cherkasov, N., Ibhadon, A. O. and Fitzpatrick, P. (2015) ‘A review of the existing and alternative methods for greener nitrogen fixation’, *Chemical Engineering and Processing: Process Intensification*, pp. 24–33. doi: 10.1016/j.cep.2015.02.004.

Chiew, Y. L. *et al.* (2015) ‘Environmental impact of recycling digested food waste as a fertilizer in agriculture - A case study’, *Resources, Conservation and Recycling*. Elsevier, 95, pp. 1–14. doi: 10.1016/j.resconrec.2014.11.015.

Chmeliov, J. *et al.* (2016) ‘Excitation migration in fluctuating light-harvesting antenna systems’, *Photosynthesis Research*, 127(1), pp. 49–60. doi: 10.1007/s11120-015-0083-3.

Choudhury, N. K. and Behera, R. K. (2001) ‘Photoinhibition of Photosynthesis: Role of Carotenoids in Photoprotection of Chloroplast Constituents’, *Photosynthetica*, 39(4), pp. 481–488. doi: 10.1023/A:1015647708360.

Chow, W. S. *et al.* (2005) ‘Photoinactivation of photosystem II in leaves’, *Photosynthesis Research*, 84, pp. 35–41.

Cojho, E. H. *et al.* (1993) ‘Interactions of Acetobacter diazotrophicus with an amylolytic yeast in nitrogen-free batch culture’, *FEMS Microbiology Letters*, 106(3), pp. 341–346. doi: 10.1111/j.1574-6968.1993.tb05986.x.

Dall’Osto, L. *et al.* (2014) ‘On the origin of a slowly reversible fluorescence

decay component in the Arabidopsis npq4 mutant', *Philosophical Transactions of the Royal Society B: Biological Sciences*, 369(1640), p. 20130221. doi: 10.1098/rstb.2013.0221.

Delaporte-Quintana, P. *et al.* (2017) 'Contribution of Gluconacetobacter diazotrophicus to phosphorus nutrition in strawberry plants', *Plant and Soil*, 419(1–2), pp. 335–347. doi: 10.1007/s11104-017-3349-z.

Demeke, T. *et al.* (1999) 'Transgene inheritance and silencing in hexaploid spring wheat', *Theoretical and Applied Genetics*, 99(6), pp. 947–953. doi: 10.1007/s001220051401.

Demmig-Adams, B. *et al.* (2012) 'Modulation of photosynthetic energy conversion efficiency in nature: From seconds to seasons', in *Photosynthesis Research*, pp. 75–88. doi: 10.1007/s11120-012-9761-6.

Demmig-Adams, B. and Adams, W. (1996) 'The role of xanthophyll cycle carotenoids in the protection of photosynthesis', *Trends in Plant Science*, 1(1), pp. 21–26. doi: 10.1016/S1360-1385(96)80019-7.

Demmig-Adams, B. and Adams, W. W. I. (1992) 'Photoprotection and Other Responses of Plants to High Light Stress', *Annual Review of Plant Physiology and Plant Molecular Biology*, 43(1), pp. 599–626. doi: 10.1146/annurev.arplant.43.1.599.

Demmig-Adams, B., Gilmore, A. M. and Adams, W. W. (1996) 'Carotenoids 3: in vivo function of carotenoids in higher plants.', *FASEB journal : official publication of the Federation of American Societies for Experimental Biology*, 10(4), pp. 403–12.

Demmig, B. *et al.* (1987) 'Photoinhibition and Zeaxanthin Formation in Intact Leaves: A Possible Role of the Xanthophyll Cycle in the Dissipation of Excess Light Energy', *Plant Physiology*, 84(2), pp. 218–224. doi: 10.1104/pp.84.2.218.

Denison, R. F. (2011) 'Past evolutionary tradeoffs represent opportunities for crop genetic improvement and increased human lifespan', *Evolutionary Applications*, 4(2), pp. 216–224. doi: 10.1111/j.1752-4571.2010.00158.x.

Dent, D. and Cocking, E. (2017) 'Establishing symbiotic nitrogen fixation in

cereals and other non-legume crops: The Greener Nitrogen Revolution', *Agriculture and Food Security*, p. 7. doi: 10.1186/s40066-016-0084-2.

Dequiedt, B. and Moran, D. (2015) 'The cost of emission mitigation by legume crops in French agriculture', *Ecological Economics*, 110, pp. 51–60. doi: 10.1016/j.ecolecon.2014.12.006.

Devireddy, A. R. *et al.* (2018) 'Coordinating the overall stomatal response of plants: Rapid leaf-to-leaf communication during light stress', *Science Signaling*, 11(518). doi: 10.1126/scisignal.aam9514.

Ding, R. *et al.* (2014) 'Scaling up stomatal conductance from leaf to canopy using a dual-leaf model for estimating crop evapotranspiration', *PLoS ONE*. Edited by B. Bond-Lamberty, 9(4), p. e95584. doi: 10.1371/journal.pone.0095584.

Dodds, W. K. *et al.* (2009) 'Eutrophication of U. S. freshwaters: Analysis of potential economic damages', *Environmental Science and Technology*. American Chemical Society, 43(1), pp. 12–19. doi: 10.1021/es801217q.

Doltra, J., Lægdsmand, M. and Olesen, J. E. (2011) 'Cereal yield and quality as affected by nitrogen availability in organic and conventional arable crop rotations: A combined modeling and experimental approach', *European Journal of Agronomy*, 34(2), pp. 83–95. doi: 10.1016/j.eja.2010.11.002.

Dominici, P. *et al.* (2002) 'Biochemical properties of the PsbS subunit of photosystem II either purified from chloroplast or recombinant', *Journal of Biological Chemistry*, 277(25), pp. 22750–22758. doi: 10.1074/jbc.M200604200.

Dreccer, M. F. *et al.* (2000) 'Radiation and nitrogen use at the leaf and canopy level by wheat and oilseed rape during the critical period for grain number definition', *Australian Journal of Plant Physiology*, 27(10), pp. 899–910. doi: 10.1071/pp00019.

Durchan, M., Vácha, F. and Krieger-Liszkay, A. (2001) 'Effects of severe CO2 starvation on the photosynthetic electron transport chain in tobacco plants', *Photosynthesis Research*, 68(3), pp. 203–213. doi: 10.1023/A:1012917428003.

Eckerstorfer, M. F. *et al.* (2019) ‘Plants developed by new genetic modification techniques-Comparison of existing regulatory frameworks in the EU and Non-EU countries’, *Frontiers in Bioengineering and Biotechnology*. doi: 10.3389/fbioe.2019.00026.

Edgerton, M. D. (2009) ‘Increasing crop productivity to meet global needs for feed, food, and fuel’, *Plant Physiology*, pp. 7–13. doi: 10.1104/pp.108.130195.

Ehleringer, J. R. and Cerling, T. E. (2002) ‘C3 and C4 photosynthesis’, *Encyclopedia of Global Environmental Change.The earth system: biological and ecological dimensions of global environmental change*, 2, pp. 186–190.

Ellis, E. C. *et al.* (2010) ‘Anthropogenic transformation of the biomes, 1700 to 2000’, *Global Ecology and Biogeography*, 19(5), pp. 589–606. doi: 10.1111/j.1466-8238.2010.00540.x.

Engelhard, M., Hurek, T. and Reinhold-Hurek, B. (2000) ‘Preferential occurrence of diazotrophic endophytes, Azoarcus spp., in wild rice species and land races of Oryza sativa in comparison with modern races’, *Environmental Microbiology*, 2(2), pp. 131–141. doi: 10.1046/j.1462-2920.2000.00078.x.

Ericksen, P. J., Ingram, J. S. I. and Liverman, D. M. (2009) ‘Food security and global environmental change: emerging challenges’, *Environmental Science and Policy*, pp. 373–377. doi: 10.1016/j.envsci.2009.04.007.

Eskin, N., Vessey, K. and Tian, L. (2014) ‘Research progress and perspectives of nitrogen fixing bacterium, gluconacetobacter diazotrophicus, in monocot plants’, *International Journal of Agronomy*, pp. 1–13. doi: 10.1155/2014/208383.

Evans, J. R. (1989) ‘Photosynthesis and nitrogen relationships in leaves of C3 plants’, *Oecologia*, 78(1), pp. 9–19. doi: 10.1007/BF00377192.

Ewert, F. *et al.* (2005) ‘Future scenarios of European agricultural land use: I. Estimating changes in crop productivity’, *Agriculture, Ecosystems and Environment*. Elsevier, 107(2–3), pp. 101–116. doi: 10.1016/j.agee.2004.12.003.

FAO (2003) ‘Food energy - methods of analysis and conversion factors’, in

Food energy – methods of analysis and conversion factors. Rome: FAO, pp. 1–7. Available at: http://www.fao.org/3/Y5022E/y5022e03.htm (Accessed: 29 November 2019).

FAO (2019) *FAO Cereal Supply and Demand Brief*. Available at: http://www.fao.org/worldfoodsituation/csdb/en/ (Accessed: 22 February 2019).

Feng, L. *et al.* (2007) 'Overexpression of SBPase enhances photosynthesis against high temperature stress in transgenic rice plants', *Plant Cell Reports*, 26(9), pp. 1635–1646. doi: 10.1007/s00299-006-0299-y.

Finger, R. (2010) 'Evidence of slowing yield growth - The example of Swiss cereal yields', *Food Policy*, 35(2), pp. 175–182. doi: 10.1016/j.foodpol.2009.11.004.

Firek, S. *et al.* (1993) 'A wound-induced promoter driving npt-II expression limited to dedifferentiated cells at wound sites is sufficient to allow selection of transgenic shoots', *Plant Molecular Biology*, 22(1), pp. 129–142. doi: 10.1007/BF00039001.

Fischer, R. A. (1985) 'Number of kernels in wheat crops and the influence of solar radiation and temperature', *The Journal of Agricultural Science*, 105(2), pp. 447–461. doi: 10.1017/S0021859600056495.

Fisher, K. and Newton, W. E. (2005) 'Nitrogenase proteins from Gluconacetobacter diazotrophicus, a sugarcane-colonizing bacterium', *Biochimica et Biophysica Acta - Proteins and Proteomics*, 1750(2), pp. 154–165. doi: 10.1016/j.bbapap.2005.04.010.

Flavell, R. B. *et al.* (1974) 'Genome size and the proportion of repeated nucleotide sequence DNA in plants', *Biochemical Genetics*, 12(4), pp. 257–269. doi: 10.1007/BF00485947.

Foo, C. C. (2014) *Characterization of Spring Wheat (Triticum aestivum) Transformed with Rice PsbS Gene*. University of Nottingham.

Franks, P. J. *et al.* (2017) 'Stomatal function across temporal and spatial scales: Deep-time trends, land-atmosphere coupling and global models', *Plant Physiology*, 174(2), pp. 583–602. doi: 10.1104/pp.17.00287.

Frenkel, M. *et al.* (2009) 'Improper excess light energy dissipation in Arabidopsis results in a metabolic reprogramming', *BMC Plant Biology*, 9(1), p. 12. doi: 10.1186/1471-2229-9-12.

Funk, C. *et al.* (1994) 'The intrinsic 22 kDa protein is a chlorophyll-binding subunit of photosystem II', *FEBS Letters*, 342(3), pp. 261–266. doi: 10.1016/0014-5793(94)80513-X.

Furbank, R. T., Quick, W. P. and Sirault, X. R. R. (2015) 'Improving photosynthesis and yield potential in cereal crops by targeted genetic manipulation: Prospects, progress and challenges', *Field Crops Research*, 182, pp. 19–29. doi: 10.1016/j.fcr.2015.04.009.

Gago, J. *et al.* (2016) 'Relationships of leaf net photosynthesis, stomatal conductance, and mesophyll conductance to primary metabolism: A multispecies meta-analysis approach', *Plant Physiology*, 171(1), pp. 265–279. doi: 10.1104/pp.15.01660.

Gelvin, S. B. (2003) 'Agrobacterium-Mediated Plant Transformation: the Biology behind the "Gene-Jockeying" Tool', *Microbiology and Molecular Biology Reviews*, 67(1), pp. 16–37. doi: 10.1128/mmbr.67.1.16-37.2003.

Genty, B., Briantais, J. M. and Baker, N. R. (1989) 'The relationship between the quantum yield of photosynthetic electron transport and quenching of chlorophyll fluorescence', *Biochimica et Biophysica Acta - General Subjects*, 990(1), pp. 87–92. doi: 10.1016/S0304-4165(89)80016-9.

Gerbaud, A. and André, M. (1980) 'Effect of CO2 , O2 , and Light on Photosynthesis and Photorespiration in Wheat', *Plant Physiology*, 66(6), pp. 1032–1036. doi: 10.1104/pp.66.6.1032.

Gerland, P. *et al.* (2014) 'World population stabilization unlikely this century', *Science*, 346(6206), pp. 234–237. doi: 10.1126/science.1257469.

Gillis, M. *et al.* (1989) 'Acetobacter diazotrophicus sp. nov., a nitrogen-fixing acetic acid bacterium associated with sugarcane', *International Journal of Systematic Bacteriology*, 39(3), pp. 361–364. doi: 10.1099/00207713-39-3-361.

Gillis, M. *et al.* (1995) 'Polyphasic taxonomy in the genus Burkholderia

leading to an emended description of the genus and proposition of Burkholderia vietnamiensis sp. nov. for N2-fixing isolates from rice in Vietnam', *International Journal of Systematic Bacteriology*, 45(2), pp. 274–289. doi: 10.1099/00207713-45-2-274.

Giovagnetti, V. and Ruban, A. (2015) 'Discerning the effects of photoinhibition and photoprotection on the rate of oxygen evolution in Arabidopsis leaves', *Journal of Photochemistry and Photobiology B: Biology*, 152, pp. 272–278. doi: 10.1016/j.jphotobiol.2015.09.010.

Głowacka, K. *et al.* (2018) 'Photosystem II Subunit S overexpression increases the efficiency of water use in a field-grown crop', *Nature Communications*, 9(1). doi: 10.1038/s41467-018-03231-x.

Goral, T. *et al.* (2012) 'Light-harvesting antenna composition controls the macrostructure and dynamics of thylakoid membranes in Arabidopsis', *Plant Journal*, 69(2), pp. 289–301. doi: 10.1111/j.1365-313X.2011.04790.x.

Guan, X. Q. *et al.* (2004) 'Photoprotective function of photorespiration in several grapevine cultivars under drought stress', *Photosynthetica*, 42(1), pp. 31–36. doi: 10.1023/B:PHOT.0000040566.55149.52.

Gyaneshwar, P. *et al.* (2001) 'Endophytic colonization of rice by a diazotrophic strain of Serratia marcescens', *Journal of Bacteriology*, 183(8), pp. 2634–2645. doi: 10.1128/JB.183.8.2634-2645.2001.

Haake, V. *et al.* (1999) 'Changes in aldolase activity in wild-type potato plants are important for acclimation to growth irradiance and carbon dioxide concentration, because plastid aldolase exerts control over the ambient rate of photosynthesis across a range of growth condition', *Plant Journal*, 17(5), pp. 479–489. doi: 10.1046/j.1365-313X.1999.00391.x.

Haas, G., Wetterich, F. and Köpke, U. (2001) 'Comparing intensive, extensified and organic grassland farming in southern Germany by process life cycle assessment', *Agriculture, Ecosystems and Environment*, 83(1–2), pp. 43–53. doi: 10.1016/S0167-8809(00)00160-2.

Hammer, G. L. and Wright, G. C. (1994) 'A theoretical analysis of nitrogen and radiation effects on radiation use efficiency in peanut', *Australian Journal of Agricultural Research*, 45(3), pp. 575–589. doi: 10.1071/AR9940575.

Harbinson, J. (2012) ‘Modeling the protection of photosynthesis’, *Proceedings of the National Academy of Sciences of the United States of America*, 109(39), p. 15533. doi: 10.1073/pnas.1213195109.

Hatfield, J. L. and Dold, C. (2019a) ‘Photosynthesis in the solar corridor system’, in *The Solar Corridor Crop System*, pp. 1–33. doi: 10.1016/b978-0-12-814792-4.00001-2.

Hatfield, J. L. and Dold, C. (2019b) ‘Water-use efficiency: Advances and challenges in a changing climate’, *Frontiers in Plant Science*. doi: 10.3389/fpls.2019.00103.

Haupt-Herting, S. and Fock, H. P. (2000) ‘Exchange of oxygen and its role in energy dissipation during drought stress in tomato plants’, *Physiologia Plantarum*, 110(4), pp. 489–495. doi: 10.1111/j.1399-3054.2000.1100410.x.

Hawkesford, M. J. (2014) ‘Reducing the reliance on nitrogen fertilizer for wheat production’, *Journal of Cereal Science*, pp. 276–283. doi: 10.1016/j.jcs.2013.12.001.

Hay, R. K. M. (1995) ‘Harvest index: a review of its use in plant breeding and crop physiology’, *Annals of Applied Biology*, 126(1), pp. 197–216. doi: 10.1111/j.1744-7348.1995.tb05015.x.

Henkes, S. *et al.* (2001) ‘A small decrease of plastid transketolase activity in antisense tobacco transformants has dramatic effects on photosynthesis and phenylpropanoid metabolism’, *Plant Cell*, 13(3), pp. 535–551. doi: 10.1105/tpc.13.3.535.

Henry, C. *et al.* (2019) ‘A stomatal safety-efficiency trade-off constrains responses to leaf dehydration’, *Nature Communications*, 10(1). doi: 10.1038/s41467-019-11006-1.

Hetherington, A. M. and Woodward, F. I. (2003) ‘The role of stomata in sensing and driving environmental change’, *Nature*, pp. 901–908. doi: 10.1038/nature01843.

Hibberd, J. M., Sheehy, J. E. and Langdale, J. A. (2008) ‘Using C4 photosynthesis to increase the yield of rice-rationale and feasibility’, *Current Opinion in Plant Biology*, pp. 228–231. doi: 10.1016/j.pbi.2007.11.002.

Hieber, A. D., Bugos, R. C. and Yamamoto, H. Y. (2000) 'Plant lipocalins: Violaxanthin de-epoxidase and zeaxanthin epoxidase', *Biochimica et Biophysica Acta - Protein Structure and Molecular Enzymology*, 1482(1–2), pp. 84–91. doi: 10.1016/S0167-4838(00)00141-2.

Hirota, Y. *et al.* (1978) 'Nitrogen fixation in the rhizosphere of rice', *Nature*, pp. 416–417. doi: 10.1038/276416a0.

Holt-Giménez, E. *et al.* (2012) 'We Already Grow Enough Food for 10 Billion People... and Still Can't End Hunger', *Journal of Sustainable Agriculture*, 36(6), pp. 595–598. doi: 10.1080/10440046.2012.695331.

Holt, R. R. (2014) 'Population growth: limits of food supply.', *Science (New York, N.Y.)*, p. 561. doi: 10.1126/science.346.6209.561-b.

Horton, P. (2000) 'Prospects for crop improvement through the genetic manipulation of photosynthesis: morphological and biochemical aspects of light capture.', *Journal of experimental botany*, 51(February), pp. 475–485. doi: 10.1093/jexbot/51.suppl_1.475.

Horton, P. and Ruban, A. (1992) 'Regulation of Photosystem II', *Photosynthesis Research*, 35, pp. 375–385. doi: 10.1007/BF00029812.

Horton, P., Wentworth, M. and Ruban, A. (2005) 'Control of the light harvesting function of chloroplast membranes: The LHCII-aggregation model for non-photochemical quenching', *FEBS Letters*, 579(20), pp. 4201–4206. doi: 10.1016/j.febslet.2005.07.003.

Hospital, F. (2005) 'Selection in backcross programmes', *Philosophical Transactions of the Royal Society B: Biological Sciences*, pp. 1503–1511. doi: 10.1098/rstb.2005.1670.

Hubbart, S. *et al.* (2012) 'The photoprotective protein PsbS exerts control over CO2 assimilation rate in fluctuating light in rice', *Plant Journal*, 71(3), pp. 402–412. doi: 10.1111/j.1365-313X.2012.04995.x.

Hubbart, S. *et al.* (2018) 'Enhanced thylakoid photoprotection can increase yield and canopy radiation use efficiency in rice', *Communications Biology*, 1(1), p. 22. doi: 10.1038/s42003-018-0026-6.

Iida, S., Amano, E. and Nishio, T. (1993) ‘A rice (Oryza sativa L.) mutant having a low content of glutelin and a high content of prolamine’, *Theoretical and Applied Genetics: International Journal of Plant Breeding Research*, 87(3), pp. 374–378. doi: 10.1007/BF01184926.

Ishida, S. *et al.* (2011) ‘Allocation of absorbed light energy in PSII to thermal dissipations in the presence or absence of PsbS subunits of rice’, *Plant and Cell Physiology*, 52(10), pp. 1822–1831. doi: 10.1093/pcp/pcr119.

Ishida, Y. *et al.* (2015) ‘Wheat (Triticum aestivum L.) Transformation Using Immature Embryos’, in Wang, K. (ed.) *Methods in Molecular Biology, Agrobacterium Protocols*. 3rd edn. New York: Humana Press, pp. 189–198.

Jahns, P. and Holzwarth, A. R. (2012) ‘The role of the xanthophyll cycle and of lutein in photoprotection of photosystem II’, *Biochimica et Biophysica Acta - Bioenergetics*, pp. 182–193. doi: 10.1016/j.bbabio.2011.04.012.

Jansen, M. A. K., Mattoo, A. K. and Edelman, M. (1999) ‘D1-D2 protein degradation in the chloroplast: Complex light saturation kinetics’, *European Journal of Biochemistry*, 260(2), pp. 527–532. doi: 10.1046/j.1432-1327.1999.00196.x.

du Jardin, P. (2015) ‘Plant biostimulants: Definition, concept, main categories and regulation’, *Scientia Horticulturae*, pp. 3–14. doi: 10.1016/j.scienta.2015.09.021.

Jensen, E. S. *et al.* (2012) ‘Legumes for mitigation of climate change and the provision of feedstock for biofuels and biorefineries. A review’, *Agronomy for Sustainable Development*. Springer-Verlag, pp. 329–364. doi: 10.1007/s13593-011-0056-7.

Jensen, P. E. and Leister, D. (2014) ‘Chloroplast evolution, structure and functions’, *F1000Prime Reports*. Faculty of 1000 Ltd, 6, p. 40. doi: 10.12703/p6-40.

Jeuffroy, M. H. *et al.* (2013) ‘Nitrous oxide emissions from crop rotations including wheat, oilseed rape and dry peas’, *Biogeosciences*, 10(3), pp. 1787–1797. doi: 10.5194/bg-10-1787-2013.

Jimenez-Salgado, T. *et al.* (1997) ‘Coffea arabica L., a new host plant for

Acetobacter diazotrophicus, and isolation of other nitrogen-fixing acetobacteria', *Applied and Environmental Microbiology*, 63(9), pp. 3676–3683.

Johnson, G. N. *et al.* (1993) 'The dissipation of excess excitation energy in British plant species', *Plant, Cell & Environment*, 16(6), pp. 673–679. doi: 10.1111/j.1365-3040.1993.tb00485.x.

Johnson, M. P. and Ruban, A. V. (2010) 'Arabidopsis plants lacking PsbS protein possess photoprotective energy dissipation', *Plant Journal*, 61(2), pp. 283–289. doi: 10.1111/j.1365-313X.2009.04051.x.

Johnson, M. and Ruban, A. (2011) 'Restoration of rapidly reversible photoprotective energy dissipation in the absence of PsbS protein by enhanced ΔpH', *Journal of Biological Chemistry*, 286(22), pp. 19973–19981. doi: 10.1074/jbc.M111.237255.

Jones, H. D. (2005) 'Wheat transformation: Current technology and applications to grain development and composition', *Journal of Cereal Science*, 41(2), pp. 137–147. doi: 10.1016/j.jcs.2004.08.009.

Jung, H. and Niyogi, K. K. (2009) 'Quantitative genetic analysis of thermal dissipation in Arabidopsis.', *Plant Physiology*, 150(2), pp. 977–86. doi: 10.1104/pp.109.137828.

Kandemir, T. *et al.* (2013) 'The Haber-Bosch process revisited: On the real structure and stability of "ammonia iron" under working conditions', *Angewandte Chemie - International Edition*, 52(48), pp. 12723–12726. doi: 10.1002/anie.201305812.

Karki, S., Rizal, G. and Quick, W. P. (2013) 'Improvement of photosynthesis in rice (Oryza sativa L.) by inserting the C4 pathway', *Rice*, pp. 1–8. doi: 10.1186/1939-8433-6-28.

Kasajima, I. *et al.* (2011) 'Molecular distinction in genetic regulation of nonphotochemical quenching in rice.', *Proceedings of the National Academy of Sciences of the United States of America*, 108(33), pp. 13835–40. doi: 10.1073/pnas.1104809108.

Kawaguchi, H. *et al.* (1992) 'Dynamical behavior of psb gene transcripts in

greening wheat seedlings. I. Time course of accumulation of the psbA through psbN gene transcripts during light-induced greening', *Plant Molecular Biology*, 20(4), pp. 695–704. doi: 10.1007/BF00046454.

Kereiche, S. *et al.* (2010) 'The PsbS protein controls the macro-organisation of photosystem II complexes in the grana membranes of higher plant chloroplasts', *FEBS Letters*, 584(4), pp. 759–764. doi: 10.1016/j.febslet.2009.12.031.

Keren, N. *et al.* (1997) 'Mechanism of photosystem II photoinactivation and D1 protein degradation at low light: The role of back electron flow', *Plant Biology*, 94(February), pp. 1579–1584.

Kim, S. *et al.* (1992) 'Characterization of a spinach psbS cDNA encoding the 22 kDa protein of photosystem II', *FEBS Letters*, 314(1), pp. 67–71. doi: 10.1016/0014-5793(92)81463-V.

Kirizii, D. A., Vorobei, N. A. and Kots', S. Y. (2007) 'Relationships between nitrogen fixation and photosynthesis as the main components of the productivity in alfalfa', *Russian Journal of Plant Physiology*, 54(5), pp. 589–594. doi: 10.1134/S1021443707050032.

Klimyuk, V. I. *et al.* (1993) 'Alkali treatment for rapid preparation of plant material for reliable PCR analysis', *The Plant Journal*, 3(3), pp. 493–494. doi: 10.1111/j.1365-313X.1993.tb00169.x.

Kozaki, A. and Takeba, G. (1996) 'Photorespiration protects C3 plants from photooxidation', *Nature*, 384(6609), pp. 557–560. doi: 10.1038/384557a0.

Kramer, D. M. *et al.* (2004) 'New fluorescence parameters for the determination of QA redox state and excitation energy fluxes', *Photosynthesis Research*, 79, pp. 209–218.

Krapp, A. (2015) 'Plant nitrogen assimilation and its regulation: A complex puzzle with missing pieces', *Current Opinion in Plant Biology*, pp. 115–122. doi: 10.1016/j.pbi.2015.05.010.

Krause, G. (1974) 'Changes in chlorophyll fluorescence in relation to light-dependent cation transfer across thylakoid membranes', *Biochimica et Biophysica Acta - Bioenergetics*, 333(2), pp. 301–313. doi: 10.1016/0005-

2728(74)90013-9.

Kromdijk, J. *et al.* (2016) ‘Improving photosynthesis and crop productivity by accelerating recovery from photoprotection’, *Science*, 354(6314), pp. 857–861.

Kromdijk, J., Głowacka, K. and Long, S. P. (2019) ‘Predicting light-induced stomatal movements based on the redox state of plastoquinone: theory and validation’, *Photosynthesis Research*, 141(1), pp. 83–97. doi: 10.1007/s11120-019-00632-x.

Kromdijk, J. and Long, S. P. (2016) ‘One crop breeding cycle from starvation? How engineering crop photosynthesis for rising CO2 and temperature could be one important route to alleviation.’, *Proceedings. Biological sciences / The Royal Society*, 283(1826), pp. 20152578-. doi: 10.1098/rspb.2015.2578.

Kuhlgert, S. *et al.* (2016) ‘MultispeQ Beta: A tool for large-scale plant phenotyping connected to the open photosynQ network’, *Royal Society Open Science*, 3(10). doi: 10.1098/rsos.160592.

Kulasek, M. *et al.* (2016) ‘Contribution of PsbS function and stomatal conductance to foliar temperature in higher plants’, *Plant and Cell Physiology*, 57(7), pp. 1495–1509. doi: 10.1093/pcp/pcw083.

Külheim, C. *et al.* (2002) ‘Rapid regulation of light harvesting and plant fitness in the field.’, *Science (New York, N.Y.)*, 297(5578), pp. 91–3. doi: 10.1126/science.1072359.

Kusumi, K. *et al.* (2012) ‘Increased leaf photosynthesis caused by elevated stomatal conductance in a rice mutant deficient in SLAC1, a guard cell anion channel protein’, *Journal of Experimental Botany*, 63(15), pp. 5635–5644. doi: 10.1093/jxb/ers216.

Ladha, J. K. *et al.* (2003) ‘How extensive are yield declines in long-term rice-wheat experiments in Asia?’, *Field Crops Research*, 81(2–3), pp. 159–180. doi: 10.1016/S0378-4290(02)00219-8.

Ladha, J. K., De Bruijn, F. J. and Malik, K. A. (1997) ‘Introduction: Assessing opportunities for nitrogen fixation in rice - A frontier project’, in *Plant and Soil*, pp. 1–10.

Ladha, J. K. and Reddy, P. M. (1995) ‘Extension of nitrogen fixation to rice - Necessity and possibilities’, *GeoJournal*, 35(3), pp. 363–372. doi: 10.1007/BF00989144.

Lavoie-Lamoureux, A. *et al.* (2017) ‘Factors influencing stomatal conductance in response to water availability in grapevine: a meta-analysis’, *Physiologia Plantarum*, 159(4), pp. 468–482. doi: 10.1111/ppl.12530.

Lawlor, D. W. (2002) ‘Carbon and nitrogen assimilation in relation to yield: mechanisms are the key to understanding production systems’, *Journal of Experimental Botany*, 53(370), pp. 773–787. doi: 10.1093/jexbot/53.370.773.

Lawson, T. (2009) ‘Guard cell photosynthesis and stomatal function’, *New Phytologist*, pp. 13–34. doi: 10.1111/j.1469-8137.2008.02685.x.

Lawson, T. *et al.* (2014) ‘Mesophyll photosynthesis and guard cell metabolism impacts on stomatal behaviour’, *New Phytologist*, pp. 1064–1081. doi: 10.1111/nph.12945.

Lawson, T. and Blatt, M. R. (2014) ‘Stomatal size, speed, and responsiveness impact on photosynthesis and water use efficiency’, *Plant Physiology*, 164(4), pp. 1556–1570. doi: 10.1104/pp.114.237107.

Lawson, T. and Vialet-Chabrand, S. (2019) ‘Speedy stomata, photosynthesis and plant water use efficiency’, *New Phytologist*, pp. 93–98. doi: 10.1111/nph.15330.

Lazár, D. (1999) ‘Chlorophyll a fluorescence induction’, *Biochimica et Biophysica Acta - Bioenergetics*, pp. 1–28. doi: 10.1016/S0005-2728(99)00047-X.

Lefebvre, S. *et al.* (2005) ‘Increased sedoheptulose-1,7-bisphosphatase activity in transgenic tobacco plants stimulates photosynthesis and growth from an early stage in development’, *Plant Physiology*, 138(1), pp. 451–460. doi: 10.1104/pp.104.055046.

Li, X. P. *et al.* (2000) ‘A pigment-binding protein essential for regulation of photosynthetic light harvesting’, *Nature*, 403(6768), pp. 391–395. doi: 10.1038/35000131.

Li, X.P. *et al.* (2002) *PsbS-dependent enhancement of feedback de-excitation protects photosystem II from photoinhibition*, *Proceedings of the National Academy of Sciences*. doi: 10.1073/pnas.232447699.

Li, Xiao Ping *et al.* (2002) 'Structure-function analysis of photosystem II subunit S (PsbS) in vivo', in *Functional Plant Biology*, pp. 1131–1139. doi: 10.1071/FP02065.

Ljungberg, U., Åkerlund, H. -E and Andersson, B. (1986) 'Isolation and characterization of the 10-kDa and 22-kDa polypeptides of higher plant photosystem 2', *European Journal of Biochemistry*. John Wiley & Sons, Ltd (10.1111), 158(3), pp. 477–482. doi: 10.1111/j.1432-1033.1986.tb09779.x.

Lloyd, J. and Farquhar, G. D. (1994) '13C discrimination during CO2 assimilation by the terrestrial biosphere', *Oecologia*, pp. 201–215. doi: 10.1007/BF00627732.

Lobell, D. B. *et al.* (2005) 'Analysis of wheat yield and climatic trends in Mexico', *Field Crops Research*, 94(2–3), pp. 250–256. doi: 10.1016/j.fcr.2005.01.007.

Long, S. P. *et al.* (2006) 'Can improvement in photosynthesis increase crop yields?', *Plant, Cell and Environment*, pp. 315–330. doi: 10.1111/j.1365-3040.2005.01493.x.

Long, S. P., Marshall-Colon, A. and Zhu, X. G. (2015) 'Meeting the global food demand of the future by engineering crop photosynthesis and yield potential', *Cell*, pp. 56–66. doi: 10.1016/j.cell.2015.03.019.

Lopes, M. S. *et al.* (2012) 'Genetic yield gains and changes in associated traits of CIMMYT spring bread wheat in a "Historic" set representing 30 years of breeding', *Crop Science*, 52(3), pp. 1123–1131. doi: 10.2135/cropsci2011.09.0467.

Lötjönen, S. and Ollikainen, M. (2017) 'Does crop rotation with legumes provide an efficient means to reduce nutrient loads and GHG emissions?', *Review of Agricultural, Food and Environmental Studies*. Springer Paris, 98(4), pp. 283–312. doi: 10.1007/s41130-018-0063-z.

Lu, Q. *et al.* (2003) 'Photoinhibition and photoprotection in senescent leaves

of field-grown wheat plants', *Plant Physiology and Biochemistry*, 41(8), pp. 749–754. doi: 10.1016/S0981-9428(03)00098-6.

Luna, M. F. *et al.* (2010) 'Colonization of sorghum and wheat by seed inoculation with Gluconacetobacter diazotrophicus', *Biotechnology Letters*, 32(8), pp. 1071–1076. doi: 10.1007/s10529-010-0256-2.

Luna, M. F. *et al.* (2012) 'Colonization and yield promotion of tomato by Gluconacetobacter diazotrophicus', *Applied Soil Ecology*, 61, pp. 225–229. doi: 10.1016/j.apsoil.2011.09.002.

Lutz, W. *et al.* (2014) 'Population growth: peak probability.', *Science (New York, N.Y.)*, p. 561. doi: 10.1126/science.346.6209.561-a.

Lutz, W., Sanderson, W. and Scherbov, S. (1997) 'Doubling of world population unlikely', *Nature*, 387(6635), pp. 803–805. doi: 10.1038/42935.

Lutz, W., Sanderson, W. and Scherbov, S. (2001) 'The end of world population growth', *Nature*, 412(6846), pp. 543–545. doi: 10.1038/35087589.

MacIntyre, H. L. *et al.* (2002) 'Photoacclimation of photosynthesis irradiance response curves and photosynthetic pigments in microalgae and cyanobacteria', *Journal of Phycology*, pp. 17–38. doi: 10.1046/j.1529-8817.2002.00094.x.

Madhaiyan, M. *et al.* (2004) 'Occurrence of Gluconacetobacter diazotrophicus in tropical and subtropical plants of Western Ghats, India', *Microbiological Research*, 159(3), pp. 233–243. doi: 10.1016/j.micres.2004.04.001.

Maekawa, T. and Kokubun, M. (2005) 'Correlation of leaf nitrogen, chlorophyll and rubisco contents with photosynthesis in a supernodulating soybean genotype Sakukei 4', *Plant Production Science*, 8(4), pp. 419–426. doi: 10.1626/pps.8.419.

Makino, A. (2003) 'Rubisco and nitrogen relationships in rice: Leaf photosynthesis and plant growth', *Soil Science and Plant Nutrition*, pp. 319–327. doi: 10.1080/00380768.2003.10410016.

Makino, A. (2011) 'Photosynthesis, grain yield, and nitrogen utilization in rice and wheat', *Plant Physiology*, 155(1), pp. 125–129. doi:

10.1104/pp.110.165076.

Malnoë, A. (2018) ‘Photoinhibition or photoprotection of photosynthesis? Update on the (newly termed) sustained quenching component qH’, *Environmental and Experimental Botany*, pp. 123–133. doi: 10.1016/j.envexpbot.2018.05.005.

Manès, Y. *et al.* (2012) ‘Genetic yield gains of the CIMMYT International semi-arid wheat yield trials from 1994 to 2010’, *Crop Science*, 52(4), pp. 1543–1552. doi: 10.2135/cropsci2011.10.0574.

Mann, C. C. (1999) ‘Genetic Engineers Aim to Soup Up Crop Photosynthesis’, *Science*, 283(5400), pp. 314–316. doi: 10.1126/science.283.5400.314.

Martin-StPaul, N., Delzon, S. and Cochard, H. (2017) ‘Plant resistance to drought depends on timely stomatal closure’, *Ecology Letters*, pp. 1437–1447. doi: 10.1111/ele.12851.

Mason, N. M., Jayne, T. S. and Shiferaw, B. (2015) ‘Africa’s Rising Demand for Wheat: Trends, Drivers, and Policy Implications’, *Development Policy Review*, 33(5), pp. 581–613. doi: 10.1111/dpr.12129.

Matloobi, M. (2012) ‘Light harvesting and photosynthesis by the canopy’, *Advances in Photosynthesis - Fundamental Aspects*, c, pp. 235–256.

Maxwell, K. and Johnson, G. N. (2000) ‘Chlorophyll fluorescence--a practical guide.’, *Journal of experimental botany*, 51(345), pp. 659–668. doi: 10.1093/jexbot/51.345.659.

McAusland, L. *et al.* (2016) ‘Effects of kinetics of light-induced stomatal responses on photosynthesis and water-use efficiency’, *The New phytologist*, 211(4), pp. 1209–1220. doi: 10.1111/nph.14000.

McElroy, D. *et al.* (1990) ‘Isolation of an efficient actin promoter for use in rice transformation’, *Plant Cell*, 2(2), pp. 163–171. doi: 10.2307/3868928.

McElroy, D. and Brettell, R. I. S. (1994) ‘Foreign gene expression in transgenic cereals’, *Trends in Biotechnology*, pp. 62–68. doi: 10.1016/0167-7799(94)90102-3.

McKenzie, F. C. and Williams, J. (2015) ‘Sustainable food production: constraints, challenges and choices by 2050’, *Food Security*, 7(2), pp. 221–233. doi: 10.1007/s12571-015-0441-1.

Meenakshisundaram, M. and Santhaguru, K. (2011) ‘Studies on association of arbuscular mycorrhizal fungi with Gluconacetobacter diazotrophicus and its effect on improvement of Sorghum bicolor (L .)’, *Internation Journal of Current Scientific Research*, 1(2), pp. 23–30.

Mellis, A. (1999) ‘Photosystem-II damage and repair cycle in chloroplasts: What modulates the rate of photodamage in vivo?’, *Trends in Plant Science*, pp. 130–135. doi: 10.1016/S1360-1385(99)01387-4.

Messinger, S. M., Buckley, T. N. and Mott, K. A. (2006) ‘Evidence for involvement of photosynthetic processes in the stomatal response to CO2’, *Plant Physiology*, 140(2), pp. 771–778. doi: 10.1104/pp.105.073676.

Mlynarova, L. *et al.* (1995) ‘The MAR-mediated reduction in position effect can be uncoupled from copy number-dependent expression in transgenic plants’, *Plant Cell*, 7(5), pp. 599–609. doi: 10.1105/tpc.7.5.599.

Molero, G. *et al.* (2019) ‘Elucidating the genetic basis of biomass accumulation and radiation use efficiency in spring wheat and its role in yield potential’, *Plant Biotechnology Journal*, 17(7), pp. 1276–1288. doi: 10.1111/pbi.13052.

Morales-Ruiz, A. *et al.* (2016) ‘Efficiency on the Use of radiation and corn yield under three densities of sowing’, *International Journal of Agronomy*, 2016. doi: 10.1155/2016/6959708.

Morison, J. I. L. *et al.* (2008) ‘Improving water use in crop production’, *Philosophical Transactions of the Royal Society B: Biological Sciences*. Royal Society, pp. 639–658. doi: 10.1098/rstb.2007.2175.

Morita, K. ichi *et al.* (2013) ‘The electron transport in psbS-silenced rice’, in *Advanced Topics in Science and Technology in China*, pp. 481–484. doi: 10.1007/978-3-642-32034-7_101.

Mott, K. A. (1988) ‘Do Stomata Respond to CO2 Concentrations Other than Intercellular?’, *Plant Physiology*, 86(1), pp. 200–203. doi:

10.1104/pp.86.1.200.

Müller, P., Li, X. P. and Niyogi, K. K. (2001) ‘Non-photochemical quenching. A response to excess light energy’, *Plant Physiology*, 125(4), pp. 1558–1566. doi: 10.1104/pp.125.4.1558.

Murata, N., Allakhverdiev, S. I. and Nishiyama, Y. (2012) ‘The mechanism of photoinhibition in vivo: Re-evaluation of the roles of catalase, α-tocopherol, non-photochemical quenching, and electron transport’, in *Biochimica et Biophysica Acta - Bioenergetics*, pp. 1127–1133. doi: 10.1016/j.bbabio.2012.02.020.

Murchie, E. H. *et al.* (2002) ‘Acclimation of Rice Photosynthesis to Irradiance under Field Conditions’, *Plant Physiology*, 130(4), pp. 1999–2010. doi: 10.1104/pp.011098.

Murchie, E. H. (2017) ‘Safety conscious or living dangerously: what is the “right” level of plant photoprotection for fitness and productivity?’, *Plant Cell and Environment*, pp. 1239–1242. doi: 10.1111/pce.12965.

Murchie, E. H. *et al.* (2018) ‘Measuring the dynamic photosynthome’, *Annals of Botany*, pp. 207–220. doi: 10.1093/aob/mcy087.

Murchie, E. H., Ali, A. and Herman, T. (2015) ‘Photoprotection as a Trait for Rice Yield Improvement: Status and Prospects’, *Rice*, 8(1), p. 31. doi: 10.1186/s12284-015-0065-2.

Murchie, E. H. and Lawson, T. (2013) ‘Chlorophyll fluorescence analysis: A guide to good practice and understanding some new applications’, *Journal of Experimental Botany*, 64(13), pp. 3983–3998. doi: 10.1093/jxb/ert208.

Murchie, E. H. and Niyogi, K. K. (2011) ‘Manipulation of photoprotection to improve plant photosynthesis.’, *Plant physiology*, 155(1), pp. 86–92. doi: 10.1104/pp.110.168831.

Murchie, E. H., Pinto, M. and Horton, P. (2009) ‘Agriculture and the new challenges for photosynthesis research’, *New Phytologist*, pp. 532–552. doi: 10.1111/j.1469-8137.2008.02705.x.

Mus, F. *et al.* (2016) ‘Symbiotic nitrogen fixation and the challenges to its

extension to nonlegumes', *Applied and Environmental Microbiology*. American Society for Microbiology, pp. 3698–3710. doi: 10.1128/AEM.01055-16.

Muthukumarasamy, R. *et al.* (2005) 'Natural association of Gluconacetobacter diazotrophicus and diazotrophic Acetobacter peroxydans with wetland rice', *Systematic and Applied Microbiology*, 28(3), pp. 277–286. doi: 10.1016/j.syapm.2005.01.006.

Nature (2010) *Concept: Plant Cells, Chloroplasts, and Cell Walls*. Available at: https://www.nature.com/scitable/topicpage/plant-cells-chloroplasts-and-cell-walls-14053956/ (Accessed: 14 November 2019).

Nauš, J., Šmecko, S. and Špundová, M. (2016) 'Chloroplast avoidance movement as a sensitive indicator of relative water content during leaf desiccation in the dark', *Photosynthesis Research*, 129(2), pp. 217–225. doi: 10.1007/s11120-016-0291-5.

Nelson, N. and Yocum, C. F. (2006) 'Structure and Function of Photosystems I and II', *Annual Review of Plant Biology*, 57(1), pp. 521–565. doi: 10.1146/annurev.arplant.57.032905.105350.

Niinemets, Ü. and Keenan, T. F. (2012) 'Measures of light in studies on light-driven plant plasticity in artificial environments', *Frontiers in Plant Science*, 3(JUL). doi: 10.3389/fpls.2012.00156.

Nilkens, M. *et al.* (2010) 'Identification of a slowly inducible zeaxanthin-dependent component of non-photochemical quenching of chlorophyll fluorescence generated under steady-state conditions in Arabidopsis', *Biochimica et Biophysica Acta - Bioenergetics*, 1797(4), pp. 466–475. doi: 10.1016/j.bbabio.2010.01.001.

Niyogi, K. K. (1999) 'Photoprotection Revisited: Genetic and Molecular Approaches', *Annual Review of Plant Physiology and Plant Molecular Biology*, 50(1), pp. 333–359. doi: 10.1146/annurev.arplant.50.1.333.

Niyogi, K. K. *et al.* (2001) 'Photoprotection in a zeaxanthin- and lutein-deficient double mutant of Arabidopsis.', *Photosynthesis research*, 67(1–2), pp. 139–45. doi: 10.1023/A:1010661102365.

Niyogi, K. K. *et al.* (2005) ‘Is PsbS the site of non-photochemical quenching in photosynthesis?’, *Journal of Experimental Botany*, 56(411), pp. 375–382. doi: 10.1093/jxb/eri056.

Nogués, S. and Alegre, L. (2002) ‘An increase in water deficit has no impact on the photosynthetic capacity of field-grown Mediterranean plants’, *Functional Plant Biology*, 29(5), pp. 621–630. doi: 10.1071/PP01117.

Oerke, E. C. and Dehne, H. W. (2004) ‘Safeguarding production - Losses in major crops and the role of crop protection’, *Crop Protection*, 23(4), pp. 275–285. doi: 10.1016/j.cropro.2003.10.001.

Okuley, J. *et al.* (1994) ‘Arabidopsis FAD2 gene encodes the enzyme that is essential for polyunsaturated lipid synthesis’, *Plant Cell*, 6(1), pp. 147–158. doi: 10.2307/3869682.

Van Oosten, M. J. *et al.* (2017) ‘The role of biostimulants and bioeffectors as alleviators of abiotic stress in crop plants’, *Chemical and Biological Technologies in Agriculture*. doi: 10.1186/s40538-017-0089-5.

Ormeño-Orrillo, E., Hungria, M. and Martinez-Romero, E. (2013) ‘Dinitrogen-fixing prokaryotes’, in *The Prokaryotes: Prokaryotic Physiology and Biochemistry*, pp. 427–451. doi: 10.1007/978-3-642-30141-4_72.

Ourworldindata (2019a) *Future Population Growth by Max Roser*. Available at: https://ourworldindata.org/future-population-growth (Accessed: 14 November 2019).

Ourworldindata (2019b) *Half of the world’s habitable land is used for agriculture by Hannah Ritchie*. Available at: https://ourworldindata.org/global-land-for-agriculture (Accessed: 14 November 2019).

Oxborough, K. and Baker, N. R. (1997) ‘Resolving chlorophyll a fluorescence images of photosynthetic efficiency into photochemical and non-photochemical components - Calculation of qP and Fv’/Fm’ without measuring Fo’’, *Photosynthesis Research*, 54(2), pp. 135–142. doi: 10.1023/A:1005936823310.

Papageorgiou, G. C. and Govindjee (2014) ‘The Non-Photochemical Quenching of the Electronically Excited State of Chlorophyll a in Plants:

Definitions, Timelines, Viewpoints, Open Questions', in Demmig-Adams, B. et al. (eds) *Non-Photochemical Quenching and Energy Dissipation in Plants, Algae and Cyanobacteria. Advances in Photosynthesis and Respiration (Including Bioenergy and Related Processes)*. Springer, Dordrecht, pp. 1–44. doi: 10.1007/978-94-017-9032-1_1.

Parry, M. A. J. *et al.* (1999) 'Rubisco: attempts to reform a promiscuous enzyme', in *Regulation of Primary Metabolic Pathways in Plants*. Dordrecht: Springer Netherlands, pp. 1–16. doi: 10.1007/978-94-011-4818-4_1.

Parry, M. A. J. *et al.* (2008) 'Rubisco regulation: A role for inhibitors', in *Journal of Experimental Botany*. Narnia, pp. 1569–1580. doi: 10.1093/jxb/ern084.

Parry, M. A. J. *et al.* (2011) 'Raising yield potential of wheat. II. Increasing photosynthetic capacity and efficiency', *Journal of Experimental Botany*, 62(2), pp. 453–467. doi: 10.1093/jxb/erq304.

Pearcy, R. W. (1990) 'Sunflecks and photosynthesis in plant canopies', *Annual Review of Plant Physiology and Plant Molecular Biology*, 41(1), pp. 421–453. doi: 10.1146/annurev.pp.41.060190.002225.

Pearcy, R. W., Krall, J. P. and Sassenrath-Cole, G. F. (1996) 'Photosynthesis in Fluctuating Light Environments', in Baker, N. R. (ed.) *Photosynthesis and the Environment*. The Netherlands: Kl, pp. 321–346. doi: 10.1007/0-306-48135-9_13.

Peltonen-Sainio, P., Jauhiainen, L. and Laurila, I. P. (2009) 'Cereal yield trends in northern European conditions: Changes in yield potential and its realisation', *Field Crops Research*, 110(1), pp. 85–90. doi: 10.1016/j.fcr.2008.07.007.

Peterhansel, C. and Maurino, V. G. (2011) 'Photorespiration Redesigned', *Plant physiology*. American Society of Plant Biologists, 155(1), pp. 49–55. doi: 10.1104/pp.110.165019.

Peterhansel, C., Niessen, M. and Kebeish, R. M. (2008) 'Metabolic engineering towards the enhancement of photosynthesis', in *Photochemistry and Photobiology*, pp. 1317–1323. doi: 10.1111/j.1751-1097.2008.00427.x.

Pierre, C. Saint *et al.* (2012) ‘Phenotyping transgenic wheat for drought resistance’, *Journal of Experimental Botany*, 63(5), pp. 1799–1808. doi: 10.1093/jxb/err385.

Pieruschka, R., Huber, G. and Berry, J. A. (2010) ‘Control of transpiration by radiation’, *Proceedings of the National Academy of Sciences of the United States of America*. National Academy of Sciences, 107(30), pp. 13372–13377. doi: 10.1073/pnas.0913177107.

Pingali, P. L. (2012) ‘Green revolution: Impacts, limits, andthe path ahead’, *Proceedings of the National Academy of Sciences of the United States of America*, pp. 12302–12308. doi: 10.1073/pnas.0912953109.

Pingali, P. L. and Heisey, P. W. (1999) ‘Cereal crop productivity in developing countries: Past trends and future prospects (CIMMYT Economics Paper 99-03)’, *Agricultural Economics*.

Pinnola, A. and Bassi, R. (2018) ‘Molecular mechanisms involved in plant photoprotection’, *Biochemical Society Transactions*, pp. 467–482. doi: 10.1042/BST20170307.

Poorter, H. *et al.* (2009) ‘Causes and consequences of variation in leaf mass per area (LMA): A meta-analysis’, *New Phytologist*, pp. 565–588. doi: 10.1111/j.1469-8137.2009.02830.x.

Portis, A. R. and Parry, M. A. J. (2007) ‘Discoveries in Rubisco (Ribulose 1,5-bisphosphate carboxylase/oxygenase): A historical perspective’, *Photosynthesis Research*, pp. 121–143. doi: 10.1007/s11120-007-9225-6.

Pound, M. *et al.* (2017) ‘Deep Machine Learning provides state-of-the-art performance in image-based plant phenotyping’, *GigaScience*, pp. 1–10. doi: 10.1101/053033.

Pound, M. P. *et al.* (2014) ‘Automated recovery of three-dimensional models of plant shoots from multiple color images’, *Plant Physiology*, 166(4), pp. 1688–1698. doi: 10.1104/pp.114.248971.

Raines, C. A. *et al.* (2000) ‘Investigating the role of the thiol-regulated enzyme sedoheptulose-1,7-bisphosphatase in the control of photosynthesis’, *Physiologia Plantarum*, 110(3), pp. 303–308. doi: 10.1034/j.1399-

3054.2000.1100303.x.

Raines, C. A. (2006) ‘Transgenic approaches to manipulate the environmental responses of the C3 carbon fixation cycle’, *Plant, Cell and Environment*, pp. 331–339. doi: 10.1111/j.1365-3040.2005.01488.x.

Rangel de Souza, A. L. S. *et al.* (2016) ‘Endophytic colonization of Arabidopsis thaliana by Gluconacetobacter diazotrophicus and its effect on plant growth promotion, plant physiology, and activation of plant defense’, *Plant and Soil*, 399(1–2), pp. 257–270. doi: 10.1007/s11104-015-2672-5.

Ranson, S. L. and Thomas, M. (1960) *Crassulacean acid metabolism*, *Annual Review of Plant Physiology*.

Rao, V. R., Jena, P. K. and Adhya, T. K. (1987) ‘Inoculation of rice with nitrogen-fixing bacteria -problems and perspectives’, *Biology and Fertility of Soils*, 4(1–2), pp. 21–26. doi: 10.1007/BF00280346.

Raven, J. A. (1989) ‘Fight or flight: The economics of repair and avoidance of photoinhibition of photosynthesis’, *Functional Ecology*. British Ecological Society, 3(1), pp. 5–19. doi: 10.2307/2389670.

Raven, J. A. (2011) ‘The cost of photoinhibition’, *Physiologia Plantarum*. Blackwell Publishing Ltd, 142(1), pp. 87–104. doi: 10.1111/j.1399-3054.2011.01465.x.

Ravishankara, A. R., Daniel, J. S. and Portmann, R. W. (2009) ‘Nitrous oxide (N2O): The dominant ozone-depleting substance emitted in the 21st century’, *Science*, 326(5949), pp. 123–125. doi: 10.1126/science.1176985.

Rawsthorne, S. (1992) ‘C3–C4 intermediate photosynthesis: linking physiology to gene expression’, *The Plant Journal*, pp. 267–274. doi: 10.1111/j.1365-313X.1992.00267.x.

Ray, D. K. *et al.* (2012) ‘Recent patterns of crop yield growth and stagnation’, *Nature communications*, 3, p. 1293. doi: 10.1038/ncomms2296.

Ray, D. K. *et al.* (2015) ‘Climate variation explains a third of global crop yield variability’, *Nature Communications*, 6(1), p. 5989. doi: 10.1038/ncomms6989.

Ray, D. K. *et al.* (2019) ‘Climate change has likely already affected global food production’, *PLoS ONE*. Edited by Y. H. Jung. Public Library of Science, 14(5), p. e0217148. doi: 10.1371/journal.pone.0217148.

Reese, M. *et al.* (2016) ‘Performance of a Small-Scale Haber Process’, *Industrial and Engineering Chemistry Research*, 55(13), pp. 3742–3750. doi: 10.1021/acs.iecr.5b04909.

Retkute, R. *et al.* (2015) ‘Exploiting heterogeneous environments: does photosynthetic acclimation optimize carbon gain in fluctuating light?’, *Journal of Experimental Botany*, 66(9), pp. 2437–2447. doi: 10.1093/jxb/erv055.

Riggs, P. J. *et al.* (2001) ‘Enhanced maize productivity by inoculation with diazotrophic bacteria’, in *Australian Journal of Plant Physiology*, pp. 829–836. doi: 10.1071/PP01045.

Risacher, T. *et al.* (2009) ‘Highly efficient Agrobacterium-mediated transformation of wheat via in planta inoculation’, *Methods in Molecular Biology*, 478, pp. 115–124. doi: 10.1007/978-1-59745-379-0_7.

Roach, T. and Krieger-Liszkay, A. (2012) ‘The role of the PsbS protein in the protection of photosystems i and II against high light in Arabidopsis thaliana’, *Biochimica et Biophysica Acta - Bioenergetics*, 1817(12), pp. 2158–2165. doi: 10.1016/j.bbabio.2012.09.011.

Roelfsema, M. R. G. *et al.* (2002) ‘CO2 provides an intermediate link in the red light response of guard cells’, *Plant Journal*, 32(1), pp. 65–75. doi: 10.1046/j.1365-313X.2002.01403.x.

Roelfsema, M. R. G. *et al.* (2006) ‘Guard cells in albino leaf patches do not respond to photosynthetically active radiation, but are sensitive to blue light, CO2 and abscisic acid’, *Plant, Cell and Environment*, 29(8), pp. 1595–1605. doi: 10.1111/j.1365-3040.2006.01536.x.

Roháček, K. (2002) ‘Chlorophyll fluorescence parameters: The definitions, photosynthetic meaning, and mutual relationships’, *Photosynthetica*, pp. 13–29. doi: 10.1023/A:1020125719386.

Rosegrant, M. W. and Cline, S. A. (2003) ‘Global food security: Challenges and policies’, *Science*, 302, pp. 1917–1919.

Rosenblueth, M. *et al.* (2018) ‘Nitrogen fixation in cereals’, *Frontiers in Microbiology*. doi: 10.3389/fmicb.2018.01794.

Rosenzweig, C. *et al.* (2014) ‘Assessing agricultural risks of climate change in the 21st century in a global gridded crop model intercomparison.’, *Proceedings of the National Academy of Sciences of the United States of America*, 111(9), pp. 3268–73. doi: 10.1073/pnas.1222463110.

Rötter, R. P. (2014) ‘Agricultural Impacts: Robust uncertainty’, *Nature Climate Change*, pp. 251–252. doi: 10.1038/nclimate2181.

Rötter, R. P. *et al.* (2015) ‘Use of crop simulation modelling to aid ideotype design of future cereal cultivars’, *Journal of Experimental Botany*, pp. 3463–3476. doi: 10.1093/jxb/erv098.

Ruban, A. (2012) *The photosynthetic membrane: molecular mechanisms and biophysics of light harvesting*, *The Photosynthetic Membrane: Molecular Mechanisms and Biophysics of Light Harvesting*. doi: 10.1002/9781118447628.

Ruban, A. (2016) ‘Nonphotochemical chlorophyll fluorescence quenching: mechanism and effectiveness in protecting plants from photodamage’, *Plant Physiology*, 170(4), pp. 1903–1916. doi: 10.1104/pp.15.01935.

Ruban, A. V. (2017a) ‘Plant science: Crops on the fast track for light’, *Nature*, pp. 36–37. doi: 10.1038/541036a.

Ruban, A. V. (2017b) ‘Quantifying the efficiency of photoprotection’, *Philosophical Transactions of the Royal Society B: Biological Sciences*. doi: 10.1098/rstb.2016.0393.

Ruban, A. V., Johnson, M. P. and Duffy, C. D. P. (2012) ‘The photoprotective molecular switch in the photosystem II antenna’, *Biochimica et Biophysica Acta - Bioenergetics*, 1817(1), pp. 167–181. doi: 10.1016/j.bbabio.2011.04.007.

Ruban, A. V. and Murchie, E. H. (2012) ‘Assessing the photoprotective effectiveness of non-photochemical chlorophyll fluorescence quenching: A new approach’, *Biochimica et Biophysica Acta - Bioenergetics*, 1817(7), pp. 977–982. doi: 10.1016/j.bbabio.2012.03.026.

Ruban, A. V (2009) ‘Plants in light.’, *Communicative & integrative biology*, 2(1), pp. 50–5.

Ruban, A. V and Belgio, E. (2014) ‘The relationship between maximum tolerated light intensity and photoprotective energy dissipation in the photosynthetic antenna: chloroplast gains and losses.’, *Philosophical transactions of the Royal Society of London. Series B, Biological sciences*, 369(1640), p. 20130222. doi: 10.1098/rstb.2013.0222.

Sacharz, J. *et al.* (2017) ‘The xanthophyll cycle affects reversible interactions between PsbS and light-harvesting complex II to control non-photochemical quenching’, *Nature Plants*, 3, p. 16225. doi: 10.1038/nplants.2016.225.

Sage, R. F. (2004) ‘The evolution of C4 photosynthesis’, *New Phytologist*, pp. 341–370. doi: 10.1111/j.1469-8137.2004.00974.x.

Sage, R. F., Sage, T. L. and Kocacinar, F. (2012) ‘Photorespiration and the Evolution of C 4 Photosynthesis’, *Annual Review of Plant Biology*, 63(1), pp. 19–47. doi: 10.1146/annurev-arplant-042811-105511.

Sage, R. F. and Stata, M. (2015) ‘Photosynthetic diversity meets biodiversity: The C4 plant example’, *Journal of Plant Physiology*, pp. 104–119. doi: 10.1016/j.jplph.2014.07.024.

Santi, C., Bogusz, D. and Franche, C. (2013) ‘Biological nitrogen fixation in non-legume plants’, *Annals of Botany*, pp. 743–767. doi: 10.1093/aob/mct048.

Schünmann, P. H. D. *et al.* (2003) ‘A suite of novel promoters and terminators for plant biotechnology’, *Functional Plant Biology*, 30(4), pp. 443–452. doi: 10.1071/FP02166.

Sharkey, T. D. (1985) ‘Photosynthesis in intact leaves of C3 plants: Physics, physiology and rate limitations’, *The Botanical Review*, 51(1), pp. 53–105. doi: 10.1007/BF02861058.

Sharkey, T. D. and Raschke, K. (1981) ‘Effect of Light Quality on Stomatal Opening in Leaves of Xanthium strumarium L.’, *Plant Physiology*, 68(5), pp. 1170–1174. doi: 10.1104/pp.68.5.1170.

Sharma, A. *et al.* (2003) ‘Plant growth-promoting bacterium Pseudomonas sp. strain GRP 3 influences iron acquisition in mung bean (Vigna radiata L. Wilzeck)’, *Soil Biology and Biochemistry*, 35(7), pp. 887–894. doi: 10.1016/S0038-0717(03)00119-6.

Shewry, P. R. (2009) ‘Wheat’, *Journal of Experimental Botany*, pp. 1537–1553. doi: 10.1093/jxb/erp058.

Shiferaw, B. *et al.* (2013) ‘Crops that feed the world 10. Past successes and future challenges to the role played by wheat in global food security’, *Food Security*, 5(3), pp. 291–317. doi: 10.1007/s12571-013-0263-y.

Shih, F. F. (2003) ‘An update on the processing of high-protein rice products’, *Nahrung - Food*, pp. 420–424. doi: 10.1002/food.200390093.

Simmonds, J. *et al.* (2014) ‘Identification and independent validation of a stable yield and thousand grain weight QTL on chromosome 6A of hexaploid wheat (Triticum aestivum L.)’, *BMC Plant Biology*, 14(1). doi: 10.1186/s12870-014-0191-9.

Sinclair, T. R. and Muchow, R. C. (1999) ‘Radiation Use Efficiency’, *Advances in Agronomy*, 65(C), pp. 215–265. doi: 10.1016/S0065-2113(08)60914-1.

Sinclair, T. R., Purcell, L. C. and Sneller, C. H. (2004) ‘Crop transformation and the challenge to increase yield potential’, *Trends in Plant Science*, 9(2), pp. 70–75. doi: 10.1016/j.tplants.2003.12.008.

Sinclair, T. R., Rufty, T. W. and Lewis, R. S. (2019) ‘Increasing Photosynthesis: Unlikely Solution For World Food Problem’, *Trends in Plant Science*. doi: 10.1016/j.tplants.2019.07.008.

Singh, J. *et al.* (2014) ‘Enhancing C3 photosynthesis: An outlook on feasible interventions for crop improvement’, *Plant Biotechnology Journal*, pp. 1217–1230. doi: 10.1111/pbi.12246.

Slattery, R. A. *et al.* (2018) ‘The impacts of fluctuating light on crop performance’, *Plant Physiology*, 176(2), pp. 990–1003. doi: 10.1104/pp.17.01234.

Smale, M. *et al.* (2002) ‘Dimensions of diversity in modern spring bread wheat

in developing countries from 1965', *Crop Science*, pp. 1766–1779. doi: 10.2135/cropsci2002.1766.

Smart, R. E. and Bingham, G. E. (1974) 'Rapid Estimates of Relative Water Content', *Plant Physiology*. American Society of Plant Biologists (ASPB), 53(2), pp. 258–260. doi: 10.1104/pp.53.2.258.

Soll, J. and Schleiff, E. (2004) 'Protein import into chloroplasts', *Nature Reviews Molecular Cell Biology*, pp. 198–208. doi: 10.1038/nrm1333.

Song, Q., Zhang, G. and Zhu, X. G. (2013) 'Optimal crop canopy architecture to maximise canopy photosynthetic CO 2 uptake under elevated CO2-A theoretical study using a mechanistic model of canopy photosynthesis', *Functional Plant Biology*, 40(2), pp. 109–124. doi: 10.1071/FP12056.

Song, Y., Jiang, C. and Gao, L. (2016) 'Polychromatic supplemental lighting from underneath canopy is more effective to enhance tomato plant development by improving leaf photosynthesis and stomatal regulation', *Frontiers in Plant Science*, 7(DECEMBER2016). doi: 10.3389/fpls.2016.01832.

Sonoike, K. (1996) 'Photoinhibition of photosystem I: Its physiological significance in the chilling sensitivity of plants', *Plant and Cell Physiology*, pp. 239–247. doi: 10.1093/oxfordjournals.pcp.a028938.

Sonoike, K. (2011) 'Photoinhibition of photosystem I', *Physiologia Plantarum*, 142(1), pp. 56–64. doi: 10.1111/j.1399-3054.2010.01437.x.

South, P. F. *et al.* (2018) 'Optimizing photorespiration for improved crop productivity', *Journal of Integrative Plant Biology*, pp. 1217–1230. doi: 10.1111/jipb.12709.

Souza, P. J. de O. P. de *et al.* (2009) 'Solar radiation use efficiency by soybean under field conditions in the Amazon region', *Pesquisa Agropecuária Brasileira*, 44(10), pp. 1211–1218. doi: 10.1590/s0100-204x2009001000001.

Spreitzer, R. J. and Salvucci, M. E. (2002) 'RUBISCO : Structure, Regulatory Interactions, and Possibilities for a Better Enzyme', *Annual Review of Plant Biology*, 53(1), pp. 449–475. doi: 10.1146/annurev.arplant.53.100301.135233.

Stephan, M. P. *et al.* (1991) 'Physiology and dinitrogen fixation of *Acetobacter diazotrophicus*', *FEMS Microbiology Letters*, 77(1), pp. 67–72. doi: 10.1111/j.1574-6968.1991.tb04323.x.

Stewart, D. W. *et al.* (2003) 'Canopy Structure, Light Interception, and Photosynthesis in Maize', *Agronomy Journal*. 95(6), pp. 1465–1474. doi: 10.2134/agronj2003.1465.

Stoger, E. *et al.* (1998) 'Molecular characteristics of transgenic wheat and the effect on transgene expression', *Transgenic Research*, 7(6), pp. 463–471. doi: 10.1023/A:1008833324193.

Suman, A. *et al.* (2005) 'Improving sugarcane growth and nutrient uptake by inoculating Gluconacetobacter diazotrophicus', *Plant Growth Regulation*, 47(2–3), pp. 155–162. doi: 10.1007/s10725-005-2847-9.

Takahashi, S. and Badger, M. R. (2011) 'Photoprotection in plants: A new light on photosystem II damage', *Trends in Plant Science*, 16(1), pp. 53–60. doi: 10.1016/j.tplants.2010.10.001.

Takahashi, S. and Murata, N. (2005) 'Interruption of the Calvin cycle inhibits the repair of Photosystem II from photodamage', *Biochimica et Biophysica Acta - Bioenergetics*, 1708(3), pp. 352–361. doi: 10.1016/j.bbabio.2005.04.003.

Tambussi, E. A. *et al.* (2002) 'Photoprotection in water-stressed plants of durum wheat (Triticum turgidum var. durum): Changes in chlorophyll fluorescence, spectral signature and photosynthetic pigments', *Functional Plant Biology*, 29(1), pp. 35–44. doi: 10.1071/PP01104.

Tapia-Hernández, A. *et al.* (2000) 'Natural endophytic occurrence of Acetobacter diazotrophicus in pineapple plants', *Microbial Ecology*, 39(1), pp. 49–55. doi: 10.1007/s002489900190.

Thidholm, E. *et al.* (2002) 'Novel approach reveals localisation and assembly pathway of the PsbS and PsbW proteins into the photosystem II dimer', *FEBS Letters*, 513(2–3), pp. 217–222. doi: 10.1016/S0014-5793(02)02314-1.

Tietz, S. *et al.* (2017) 'NPQ $_{(T)}$: a chlorophyll fluorescence parameter for rapid estimation and imaging of non-photochemical quenching of excitons in

photosystem-II-associated antenna complexes', *Plant, Cell & Environment*, 40(8), pp. 1243–1255. doi: 10.1111/pce.12924.

Ting, I. P. (1985) 'Crassulacean Acid Metabolism', *Annual Review of Plant Physiology*, 36(1), pp. 595–622. doi: 10.1146/annurev.pp.36.060185.003115.

Tourneux, C. and Peltier, G. (1995) 'Effect of water deficit on photosynthetic oxygen exchange measured using 18O2 and mass spectrometry in Solanum tuberosum L. leaf discs', *Planta*, 195(4), pp. 570–577. doi: 10.1007/BF00195717.

Townsend, A. J. *et al.* (2018) 'Suboptimal acclimation of photosynthesis to light in wheat Canopies', *Plant Physiology*, 176(2), pp. 1233–1246. doi: 10.1104/pp.17.01213.

Townsend, A., Ware, M. and Ruban, A. (2018) 'Dynamic interplay between photodamage and photoprotection in photosystem II', *Plant Cell and Environment*, 41(5), pp. 1098–1112. doi: 10.1111/pce.13107.

Treangen, T. J. and Salzberg, S. L. (2012) 'Repetitive DNA and next-generation sequencing: Computational challenges and solutions', *Nature Reviews Genetics*, pp. 36–46. doi: 10.1038/nrg3117.

Trissl, H. W., Gao, Y. and Wulf, K. (1993) 'Theoretical fluorescence induction curves derived from coupled differential equations describing the primary photochemistry of photosystem II by an exciton-radical pair equilibrium', *Biophysical Journal*, 64(4), pp. 974–988. doi: 10.1016/S0006-3495(93)81463-2.

Ueda, T. *et al.* (1995) 'Remarkable N2-fixing bacterial diversity detected in rice roots by molecular evolutionary analysis of nifH gene sequences', *Journal of Bacteriology*, 177(5), pp. 1414–1417. doi: 10.1128/jb.177.5.1414-1417.1995.

Uehlein, N. *et al.* (2003) 'The tobacco aquaporin NtAQP1 is a membrane CO2 pore with physiological functions', *Nature*, 425(6959), pp. 734–737. doi: 10.1038/nature02027.

Uehlein, N. *et al.* (2008) 'Function of Nicotiana tabacum aquaporins as chloroplast gas pores challenges the concept of membrane CO2

permeability', *Plant Cell*, 20(3), pp. 648–657. doi: 10.1105/tpc.107.054023.

Uehlein, N. *et al.* (2012) 'The Arabidopsis aquaporin PIP1;2 rules cellular CO 2 uptake', *Plant, Cell and Environment*, 35(6), pp. 1077–1083. doi: 10.1111/j.1365-3040.2011.02473.x.

United Nations (2019) *World Population Prospects 2019: Highlights*. Available at: https://www.un.org/development/desa/publications/world-population-prospects-2019-highlights.html (Accessed: 14 November 2019).

Urban, J. *et al.* (2017) 'Increase in leaf temperature opens stomata and decouples net photosynthesis from stomatal conductance in Pinus taeda and Populus deltoides x nigra', *Journal of Experimental Botany*, 68(7), pp. 1757–1767. doi: 10.1093/jxb/erx052.

Venkataraman, G. S. (1981) 'Blue-Green-Algae - a Possible Remedy to Nitrogen Scarcity', *Current Science*, 50(6), pp. 253–256. doi: 10.2307/24083417.

Verhoeven, A. S., Demmig-Adams, B. and Adams, W. W. (1997) 'Enhanced employment of the xanthophyll cycle and thermal energy dissipation in spinach exposed to high light and N stress', *Plant Physiology*, 113(3), pp. 817–824. doi: 10.1104/pp.113.3.817.

Vitousek, P. M. *et al.* (1997) 'Human alteration of the global nitrogen cycle: Sources and consequences', *Ecological Applications*, 7(3), pp. 737–750.

Waddington, S. R. *et al.* (1986) 'Improvement in the Yield Potential of Bread Wheat Adapted to Northwest Mexico 1', *Crop Science*, 26(4), pp. 698–703. doi: 10.2135/cropsci1986.0011183x002600040012x.

Walker, B. J. *et al.* (2016) 'The Costs of Photorespiration to Food Production Now and in the Future', *Annual Review of Plant Biology*, 67(1), pp. 107–129. doi: 10.1146/annurev-arplant-043015-111709.

Ware, M. A., Belgio, E. and Ruban, A. V. (2015a) 'Comparison of the protective effectiveness of NPQ in Arabidopsis plants deficient in PsbS protein and zeaxanthin', *Journal of Experimental Botany*, 66(5), pp. 1259–1270. doi: 10.1093/jxb/eru477.

Ware, M. A., Belgio, E. and Ruban, A. V. (2015b) 'Photoprotective capacity of non-photochemical quenching in plants acclimated to different light intensities', *Photosynthesis Research*, 126(2–3), pp. 261–274. doi: 10.1007/s11120-015-0102-4.

Ware, M., Dall'Osto, L. and Ruban, A. (2016) 'An In Vivo Quantitative Comparison of Photoprotection in Arabidopsis Xanthophyll Mutants', *Frontiers in Plant Science*, 7, p. 841.

Wehr, R. *et al.* (2017) 'Dynamics of canopy stomatal conductance, transpiration, and evaporation in a temperate deciduous forest, validated by carbonyl sulfide uptake', *Biogeosciences*, 14(2), pp. 389–401. doi: 10.5194/bg-14-389-2017.

Wingler, A. *et al.* (1999) 'The role of photorespiration during drought stress: An analysis utilizing barley mutants with reduced activities of photorespiratory enzymes', *Plant, Cell and Environment*, 22(4), pp. 361–373. doi: 10.1046/j.1365-3040.1999.00410.x.

Wu, A. *et al.* (2019) 'Quantifying impacts of enhancing photosynthesis on crop yield', *Nature plants*, 5(4), pp. 380–388. doi: 10.1038/s41477-019-0398-8.

Xiao, Y. G. *et al.* (2012) 'Genetic gains in grain yield and physiological traits of winter wheat in Shandong province, China, from 1969 to 2006', *Crop Science*, 52(1), pp. 44–56. doi: 10.2135/cropsci2011.05.0246.

Xu, C.-C. *et al.* (1998) 'Possible Involvement of Reversible Phosphorylation in the Regulation of Zeaxanthin Epoxidation in Rice Leaves', in *Photosynthesis: Mechanisms and Effects*, pp. 1907–1910. doi: 10.1007/978-94-011-3953-3_444.

Xu, C. C. *et al.* (1999) 'Suppression of zeaxanthin epoxidation by chloroplast phosphatase inhibitors in rice leaves', *Plant Science*, 146(1), pp. 27–34. doi: 10.1016/S0168-9452(99)00084-9.

Xu, C. C. *et al.* (2000) 'D1 protein turnover and carotene synthesis in relation to zeaxanthin epoxidation in rice leaves during recovery from low temperature photoinhibition', *Australian Journal of Plant Physiology*, 27(3), pp. 239–244. doi: 10.1071/pp99170.

Yamori, W. (2015) ‘Photosynthesis and respiration’, in *Plant Factory: An Indoor Vertical Farming System for Efficient Quality Food Production*, pp. 141–150. doi: 10.1016/B978-0-12-801775-3.00009-3.

Yamori, W. *et al.* (2016) ‘Enhanced leaf photosynthesis as a target to increase grain yield: insights from transgenic rice lines with variable Rieske FeS protein content in the cytochrome b 6 / f complex’, *Plant, Cell & Environment*, 39(1), pp. 80–87. doi: 10.1111/pce.12594.

Yamori, W. and Shikanai, T. (2016) ‘Physiological Functions of Cyclic Electron Transport Around Photosystem I in Sustaining Photosynthesis and Plant Growth’, *Annu. Rev. Plant Biol*, 67, pp. 81–106. doi: 10.1146/annurev-arplant-043015-112002.

Yang, J. C. *et al.* (2013) ‘Deficiency of phytochrome B alleviates chilling-induced photoinhibition in rice’, *American Journal of Botany*, 100(9), pp. 1860–1870. doi: 10.3732/ajb.1200574.

Yanni, Y. G. *et al.* (1997) ‘Natural endophytic association between Rhizobium leguminosarum bv. trifolii and rice roots and assessment of its potential to promote rice growth’, in *Plant and Soil*. Dordrecht, pp. 99–114. doi: 10.1007/978-94-011-7113-7_10.

Yunusa, I. A. M. *et al.* (1993) ‘Effect of canopy structure on efficiency of radiation interception and use in spring wheat cultivars during the pre-anthesis period in a mediterranean-type environment’, *Field Crops Research*, 35(2), pp. 113–122. doi: 10.1016/0378-4290(93)90144-C.

Zaks, J. *et al.* (2012) ‘A kinetic model of rapidly reversible nonphotochemical quenching’, *Proceedings of the National Academy of Sciences*, 109(39), pp. 15757–15762. doi: 10.1073/pnas.1211017109.

Zanke, C. D. *et al.* (2015) ‘Analysis of main effect QTL for thousand grain weight in European winter wheat (Triticum aestivum L.) by genome-wide association mapping’, *Frontiers in Plant Science*, 6. doi: 10.3389/fpls.2015.00644.

Zeiger, E. *et al.* (2002) ‘The guard cell chloroplast: A perspective for the twenty-first century’, *New Phytologist*, pp. 415–424. doi: 10.1046/j.0028-646X.2001.NPH328.doc.x.

Zhong, S. *et al.* (2019) 'Nitrogen addition increases the sensitivity of photosynthesis to drought and re-watering differentially in C3 versus C4 grass species', *Frontiers in Plant Science*, 10. doi: 10.3389/fpls.2019.00815.

Zhou, B. *et al.* (2014) 'Physiological traits contributed to the recent increase in yield potential of winter wheat from Henan Province, China', *Journal of Integrative Plant Biology*, 56(5), pp. 492–504. doi: 10.1111/jipb.12148.

Zhu, X. G. *et al.* (2004) 'The slow reversibility of photosystem II thermal energy dissipation on transfer from high to low light may cause large losses in carbon gain by crop canopies: A theoretical analysis', *Journal of Experimental Botany*, 55(400), pp. 1167–1175. doi: 10.1093/jxb/erh141.

Zhu, X. G., Portis, A. R. and Long, S. P. (2004) 'Would transformation of C3 crop plants with foreign Rubisco increase productivity? A computational analysis extrapolating from kinetic properties to canopy photosynthesis', *Plant, Cell and Environment*, 27(2), pp. 155–165. doi: 10.1046/j.1365-3040.2004.01142.x.

Zhu, X. G., De Sturler, E. and Long, S. P. (2007) 'Optimizing the distribution of resources between enzymes of carbon metabolism can dramatically increase photosynthetic rate: A numerical simulation using an evolutionary algorithm', *Plant Physiology*, 145(2), pp. 513–526. doi: 10.1104/pp.107.103713.

Zulfugarov, I. S. *et al.* (2007) 'Dependence of reaction center-type energy-dependent quenching on photosystem II antenna size', *Biochimica et Biophysica Acta (BBA) - Bioenergetics*. Elsevier, 1767(6), pp. 773–780. doi: 10.1016/J.BBABIO.2007.02.021.